Università degli Studi della Tuscia di Viterbo
DIPARTIMENTO DI SCIENZE AGRARIE E FORESTALI – DAFNE

Corso di Dottorato di Ricerca in
Scienze delle Produzioni Vegetali ed Animali (SPVA) - XXXII ciclo

DECIPHERING SULFUR INTERACTION WITH ESSENTIAL AND NON-ESSENTIAL ELEMENTS IN THE RHIZOSPHERE

s.s.d. AGR/13

Tesi di dottorato di:
Dott.ssa Eleonora Coppa
Firma:

Coordinatore del corso
Prof.ssa Roberta Bernini
Firma:

Tutore
Prof.ssa Stefania Astolfi
Firma:

A.A. 2018/19

Ad Andrea, Thomas, Alice ed Alessia.

Abstract

Human world population is expected to increase to 10 billion by 2050 (UN 2015), and a key challenge is to provide food and feed in an equitable, healthy, and sustainable manner. Access to adequate and nutritious food is essential to human wellbeing, but to reach this objective global food production needs to increase by 70% by 2050. A healthy soil is the major factor for agriculture production, but soil resources are finite and non-renewable over the human time scale. Both natural forces and mostly anthropogenic activities (e.g., deforestation, drainage, tillage, ecc) led to soil degradation and consequently to limited access to high-quality soil for provisioning of essential ecosystem services. The scarcity of healthy soil to obtain the required food production will thus imply the exploitation of marginal agricultural land, characterized by depletion of organic matter and nutrients, elemental imbalance leading to deficiency or toxicity, salinization, water-air imbalance.

Over the last 50 years, the combined outcome of significant reductions in S emission from industrial sources, use of mineral fertilizers without S, decreases in use of organic fertilizers, and changes in cropping systems including the use of high yielding commercial coupled with intensive management practices have led to a widespread S deficiency in soils at the global scale.

Sulfur is not only essential for optimal plant growth, development and crop productivity, but also for its contribution to the mitigation of stressful conditions in plants and, more importantly, for its integration with other nutrient uptake and metabolic pathways. As a result, plant physiological responses to environmental stresses, such as nutrient deficiency or toxicity, could be modified and even hampered by S deficiency.

These evidences highlight the importance to discuss the interactions S has with other elements (essential or not) in the rhizosphere.

Depletion of nutrients, elemental toxicity and salinization represent common stress factors that plants commonly experience in their natural habitat and most important limiting factors for agricultural production. Therefore, in this thesis, S implications on physiological responses to soil Fe deficiency, Cu pollution and Na accumulation were studied.

Table of contents

Chapter 1

Context and objectives of the study

1.1 Introduction

Human world population is expected to increase to 9.7 billion by 2050 and 11.2 billion by 2100 (Fig. 1.1) (UN 2015), and a key challenge is to provide food and feed in an equitable, healthy, and sustainable manner (Beddington, 2010). Access to adequate and nutritious food is essential to human wellbeing, but to reach this objective global food production needs to increase by 70% by 2050. A healthy soil is the major factor for agriculture production, but soil resources are finite and non-renewable over the human time scale. Both natural forces and mostly anthropogenic activities (e.g., deforestation, drainage, tillage, ecc) led to soil degradation and consequently to limited access to high-quality soil for provisioning of essential ecosystem services.

Climate change will superimpose on these conditions in various regions of the world, including Europe, and in particular the Mediterranean area. Satisfying increased demands in agriculture with existing farming practices is likely to lead to more intense competition for natural resources, increased greenhouse gas emissions, and further deforestation and land degradation. This condition is even more dramatic by comparing agricultural productivity between high-income and low-income countries.

The dramatic climate changes have enhanced the agriculture challenges of increasing food production, mitigating climate change and restoring landscapes (Beddington, 2010). Between 1950 and 1970, world fertilizer consumption has increased fourfold to increase agricultural production to meet food demand for increasing populations (Tilman et al., 2002). However, it is time to realize that this approach to increase crop production is depleting our environment and ecosystem. Therefore, new strategies need to be investigated to increase plant growth and productivity, and meet the food security of the world.

It is also clear that crop production cannot be increased by increasing arable land, but rather by improving the crop productivity on existing arable lands.

Recent estimates report that the amount of land used for agricultural purposes has continued to decline over the past few years, and this trend will continue to 2030 (Report: EU agricultural outlook 2017-30). As a consequence, to maximize ecosystem services like food production, it is crucial to exploit marginal agricultural lands, in which existing environmental problems (nutrient depletion, water scarcity, acidity, salinization, depletion of organic matter, and poor drainage) due

to the combination of changes in land use increasing pollution and declining biodiversity (Scherr, 1999; Tilman et al, 2002) have been exacerbated by climate change. Therefore, novel crop management strategies are needed to improve crop productivity and quality under stressful climate conditions.

In this context, the exploitation of the potential and sustainable use of S nutrition in improving plant adaptation to marginal lands particularly vulnerable to climate change and characterized by natural resources limitation is particularly interesting.

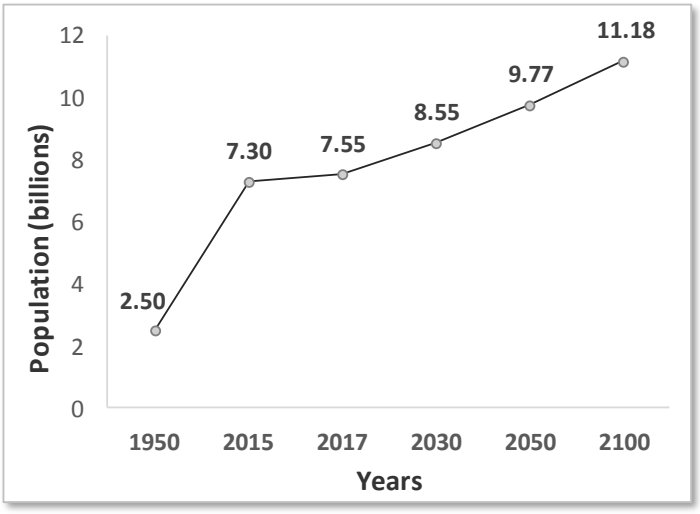

Fig. 1.1 The changing world population over 150 years. (Sources: UN and EEA)

1.2 Sulfur

Environmental policies at the beginning of the 1980s have drastically reduced SO_2 emissions with a further reduction in the 1990s (Fig. 1.2) (Haneklaus et al., 2008) causing a reduced S input to soil. This phenomenon has been worsened by the use of high-analysis low-S fertilizers and the declining use of S-containing fungicides with the final result of a widespread S deficiency for crops (McGrath and Zao., 1995; McGrath et al., 1996).

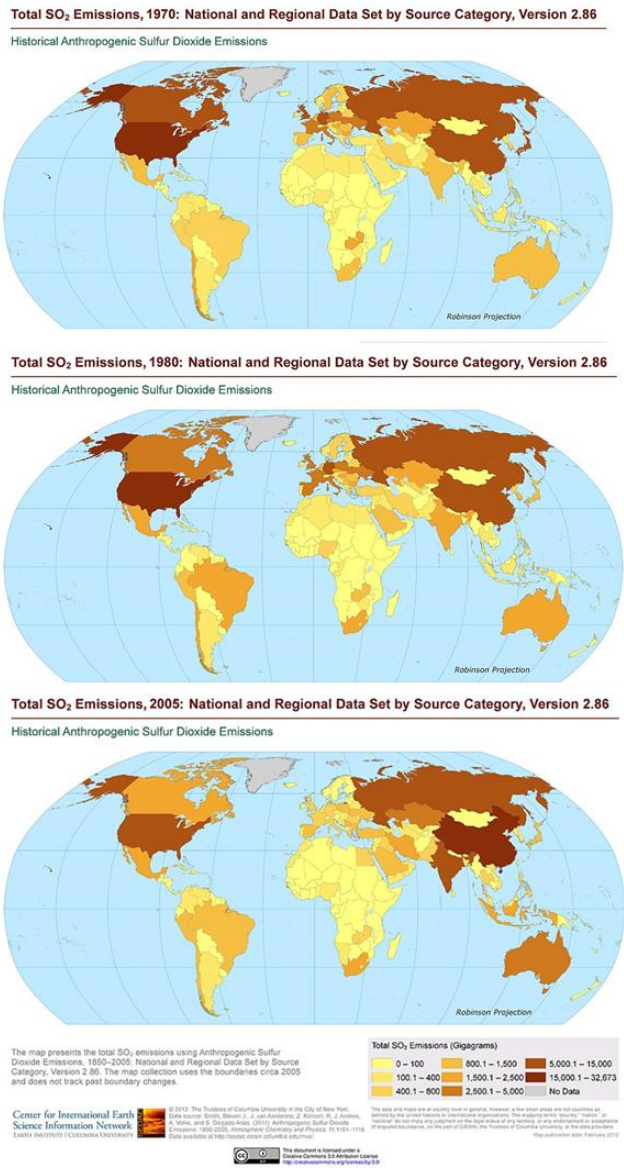

Fig. 1.2 Historical anthropogenic sulfur dioxide emissions (From: **https://sedac.ciesin.columbia.edu/data/collection/haso2/maps/gallery/search/1**)

1.2.1 Sulfur in soil

Sulfur is present in soils in different oxidation states (from -2 of sulfide S^{2-} to +6 of sulfate SO_4^{2-}) (Lewandowska and Sirko, 2008). Plants can use sulfur dioxide (SO_2) through open stomata but sulfate (SO_4^{2-}) taken up by roots represents the most important source of S for plants (Marschner, 2012). Sulfate in soils represents less than 5% of the total S amount, it can be found in soil as adsorbed or soluble form, but in calcareous soils SO_4^{2-} is also found co-precipitated with

magnesium and calcium as insoluble compounds (Scherer, 2009). Sulfate concentration in soil solution changes as a function of plant uptake, S input with fertilizers, mineralization and immobilization. In general, lower SO_4^{2-} concentration is found in winter and spring because of leaching and low mineralization rates. Adsorption of SO_4^{2-} is pH-dependent and occurs only with pH values lower than 6.5 reaching the maximum at pH 3 (Scherer, 2009). In terrestrial ecosystems S content fluctuates from 0.002 to 10% and several factors such as topography, climate and vegetation influence the S pools in terms of nature, and quantities (Germida et al., 1992). The main S fraction in soil is represented by organic S (Scherer, 2009) and, being S an essential component of soil organic matter, as well as carbon (C) and nitrogen (N), it is associated with these two macronutrients in soils. However the C:N:S ratio is not stable but very variable among individual soils from different regions of the word (Tab. 1.1) (Freney and Williams, 1983; Germida et al., 1992).

The organic S pool can be divided into two groups, organic sulfates and C-bounded S (C-S). The organic sulfates include esters (C-O-S-), sulfamates (C-N-S), and sulfated thioglycosides (N-O-S); while the C-S includes amino acids (up than 30% of total organic S in soils), proteins, polypeptides, heterocyclic compounds, sulfinates, sulfones, sulfonates, and sulfoxides (Germida et al., 1992). The C-S pool is important for the biological mineralization of S (long-term mineralization), mediated by microbial organisms (Scherer, 2001; Scherer, 2009): they use organic C as a source of energy and release SO_4^{2-}, as by-product of C oxidation to CO_2. While the sulfate-ester pool are involved in biochemical mineralization of S (short-term mineralization), since they serve as a substrate for different microbial enzymes (Gemida et al., 1992; Haneklaus et al., 2007; Scherer, 2009) when SO_4^{2-} in the soil does not meet microbial S demand (Scherer, 2009). These enzymes are classified according to the S-ester that they hydrolyze to release SO_4^{2-} and are haryl, alkyl, steroid, gluco-, chondro-, and myco-sulfatases (Germida et al. 1992).

Thus, it is clear that the entire factors affecting microbial activity can also affect the mineralization of S (Haneklaus et al., 2007).

Sulfur in soil is also associated with minerals, we found S in sulfides- and sulfates -containing rocks. Sulfides are widespread transition metal compounds with S. The most important sulfides are pyrite (FeS_2), marcasite (FeS_2) and pyrrhotite (Fe_5S_6 – $Fe_{16}S_{17}$) (Haldar and Tišljar, 2014). However, other sulfides can be found in soils such as chalcopyrite ($CuFeS_2$,) pentlandite ($FeNiS_3$) and ornite (Cu_5FeS_4) sphalerite (ZnS), galena (PbS), molybdenite (MoS), argentite (Ag_2S), cinnabar (HgS), chalcocite (Cu_2S) and other sulfides are present only in limited amounts (Freney

and Williams, 1983). Sulfates are salt of sulfuric acid (H_2SO_4) and are mainly represented by gypsum ($CaSO_4 \cdot 2H_2O$), anhydrite ($CaSO_4$) and baryte ($BaSO_4$) (Haldar and Tišljar, 2014). However, S inputs provided by the mineral fraction are less than 1 kg ha^{-1} (Haneklaus and Bloem, 2000).

Region	C:N:S	Reference
Africa		
Tropical Africa	>100:10:1.00	Dabin (1972)
North America		
Minnesota	122:10:1.48	Evans and Rost (1945)
Iowa	109:10:1.54	Tabatabai and Bremmer (1972 a, b)
Oregon	145:10:1.01	Harward et al. (1962)
South America		
Brazil	194:10:1.6	Neptune et al. (1975)
Asia		
India	80:10:0.96	Bhardwaj and Pathak (1969)
Australiasia		
Eastern Australia	150:10:1.26	Williams and Steinbergs (1958)
Western Australia	118:10:1.20	Barrow (1969)
New Zeland	120:10:1.30	Walker and Adams (1958)
Europe		
Scotland	140:10:40	Willliams et al. (1960)
Mean worldwide		
Agricultural soils	130:10:1	Germida et al. (1991)
Native grassland and woodland soils	200:10:1	Germida et al. (1991)

Tab. 1.1 Carbon, nitrogen and sulfur relation in different regions of the world (Modified from Freney and Williams, 1983)

1.2.2 Sulfur in plants: uptake transport and assimilation

Sulfate transport across the plasma membrane into the root cells is an active process against concentration gradient (S concentration into the root cells is 100-1000 times higher than in soil solution), and chemical gradient (being sulfate negatively charged). The transport of sulfate is a secondary active transport with energy consumption (obtained from ATP hydrolysis) and coupled with protons ($3H^+/SO_4^{2-}$) (Clarkson et al., 1993; Hawkesford et al., 2004). Both sulfate uptake from soil and its distribution within plant requires specific transporters. Smith et al. (1995) have

identified the first sulfur transporter (SULTR) in *Stylosanthes hamata* (L.) and in the following years many genes coding for proteins responsible for sulfate transport into the root cell and within the plant have been isolated, characterized and divided into 5 groups (Fig. 1.3) (Hawkesford and De Kok, 2007):

- *Group 1*: high-affinity transporters (mainly expressed in roots) that operate at sulfate concentration < 0.1 mM.
- *Group 2*: low-affinity transporters (expressed in vascular tissue, may be involved in the sulfate tissue distribution) which operate at sulfate concentration ≥ 0.1 mM.
- *Group 3*: the enigmatic group, called "*leaf group*" (these transporters may be peculiar of leaf tissues), but the information about these transporters is still scarce.
- *Group 4*: tonoplast transporters (involved in S outflow from the vacuole, are up-regulated by S deficiency).
- *Group 5*: tonoplast transporter (the specific function has not been yet identified).

Sulfur transporters (SULTRs) are integrated into membranes by 12 transmembrane domains (TMDs). They also have a STAS domain (sulfate transporters and antisigma factor antagonists) in the C-terminus, which is important for localization in the membrane, for their activity and for interaction with other proteins (Hawkesford, 2003; Buchner et al., 2004; Takahashi et al., 2011; Huang et al., 2018). Interestingly, the *Group 5* transporters are lacking the STAS domain (Hawkesford, 2003)

The SULTR family is well characterized in *Arabidopsis* (Takahashi et al., 2000; Hawkesford, 2003). *Group 1* includes three genes, *SULTR1;1, SULTR1;2* and *SULTR1;3*. The first two are involved in sulfate transport into the root cells (Gigolashvili and Kopriva 2014), but *SULTR1;1* is more specifically and strongly up-regulated by S starvation (Hawkesford, 2003) than *SULTR1;2,* which works mainly under S-sufficient condition (Shibagaki et al., 2002; Rouached et al., 2008; Gigolashvili and Kopriva, 2014; Huang et al., 2018) and it is suggested to play a role as S-plant status sensor (Takahashi et al., 2011; Gigolashvili and Kopriva, 2014). *SULTR1;3* is localized in the phloem and it is involved in S distribution within plant (Yoshimoto et al., 2003; Gigolashvili and Kopriva, 2014; Huang et al., 2018.). Transporters included in *Group 2,* such as *SULTR2;1* and *SULTR2;2,* are responsible for the long-distance distribution of sulfate. *Group 3* comprises five transporters, *SULTR3;1, 3;2, 3;3, 3;4* and *3;5*, expressed in the plastid envelope whose function has not been well defined, even if it has been suggested that *SULTR3;5* could act modulating the activity of *SULTR2;1* thus enhancing root to shoot transport of sulfate (Huang et

al., 2018). *Group 4* includes two transporters, *SULTR4;1* and *SULTR4;2*, involved in the outflow of sulfate from vacuoles through tonoplasts (Kataoka et al., 2004.), and particularly up-regulated under S deficiency (Takahashi et al., 2011). Finally, *Group 5* includes two transporters, *MOT1* and *MOT2,* lacking the STAS domain and most likely involved in Mo uptake (Hawkesford, 2017).

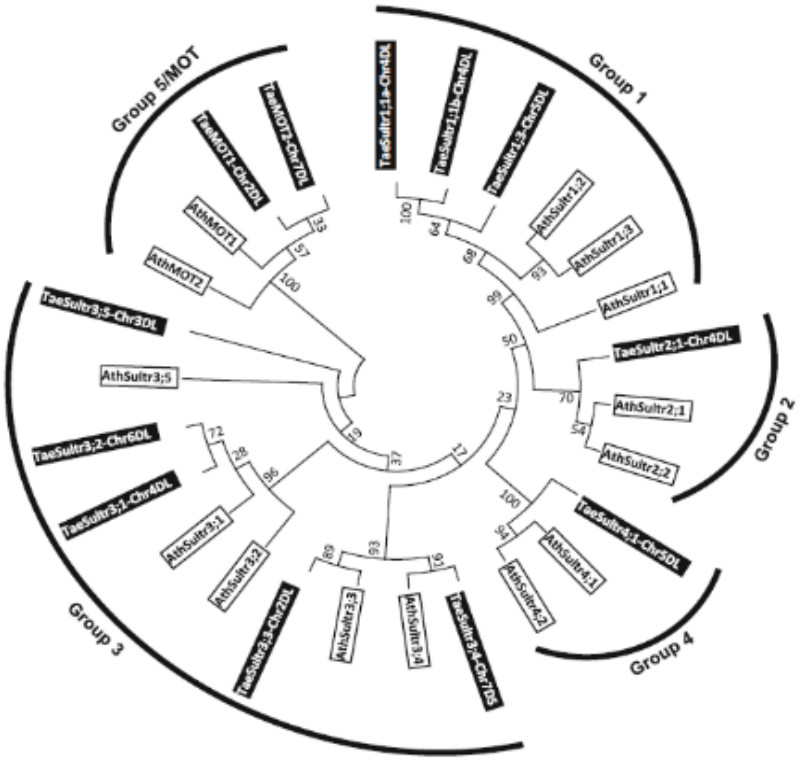

Fig.1.3 Phylogenetic relationship of the wheat (black highlighted) and Arabidopsis (white highlighted) sulfate transporter gene families (From: Hawkesford 2017).

Sulfate uptake and translocation requires a tight and coordinated regulation to guarantee balanced S levels in the cytoplasm, avoiding excess or deficiency. Regulation is achieved by both induction and repression: S deficiency in the growth medium commonly causes an increase in uptake rate, by upregulation of transporters; on the other hand, the accumulation of sulfur compounds in plant cells, inhibits uptake rate by downregulation of sulfate transporters (Hawkesford, 2003).

Once inside root, sulfate is first reduced and then incorporated into organic compounds (Fig. 1.4) (Leustek et al., 2000; Hawkesford et al., 2000). Both reduction and assimilation mainly occur in leaf tissues since the enzymes involved in these processes are localized in chloroplasts (and to a lesser extent in root plastids) (Lewandowska and Sirko, 2008). The assimilatory pathway of sulfate

starts with sulfate activation, catalyzed by the enzyme ATP sulfurylase (ATPS) which produces adenosine 5'-phosphosulfate (APS), which in turn is reduced to sulfite (SO_3^{2-}) by the activity of APS reductase (APR) with glutathione (GSH) as electron donor. Sulfite is then reduced to sulfide (S^{2-}) in the reaction catalyzed by the enzyme sulfite reductase (SiR). The first stable compound of S assimilation pathway is the amino acid cysteine (Cys) synthesized by condensation of *O*-acetylserine (OAS) (produced by the activity of serine acetyl-transferase, SERAT) and S^{2-} in the reaction catalyzed by O-acetylserine-(thiol)lyase (OAS-TL) (Leustek et al., 2000; Kopriva, 2006; Lewandowska e Sirko, 2008; Kopriva, 2017).

The second S-containing amino acid, methionine (Met), is synthesized in three steps from Cys. In the first step, the enzyme cystathionine-γ-synthase (CGL) catalyzes cystathionine production from Cys and *O*-phosphomoserine (OPH), which derived from aspartate. An α, β-elimination of cystathionine is determined by the subsequent activity of cystathionine-β-lyase (CBL) that catalyses the penultimate step in the biosynthesis of Met, in which cystathionine is cleaved to produce homocysteine (homo-Cys), pyruvate and ammonia (Ravanel et al., 1998; Saito, 2000). In the last step, a methyl group from N^5-methyl-tetrahydrofolate (5-$CH_3H_4PteGlu_n$) is transferred to homo-Cys by the cobalamin-independent methionine synthase (MS) producing tetrahydrofolate and methionine (Ravanel et al., 1998). Methionine is incorporated into protein or converted to S-adenosylmethionine (SAM) by SAM synthetase (SAMS) (Hoefgen and Hesse, 2007; Amir, 2010). S-adenosylmethionine is the precursor of ethylene (ET), biotin, polyamines (PAs), nicotianammine (NA), and many other secondary metabolites, such as phytosiderophores (PS). Moreover, SAM is the key substrate of different enzymes and the methyl donor in RNA and DNA modification.

Cysteine is also the precursor of the tripeptide glutathione (γ-glutamylcysteinglycin, GSH), which is synthesized in two ATP-dependent steps (Hoefgen and Hesse, 2007; North and Kopriva., 2007; Takahashi et al., 2011). Firstly, γ-glutamilcysteine synthetase (ECS) catalyzes the synthesis of γ-glutamilcysteine (γ-EC) from L-glutamate and L-Cys, then GSH synthetase (GSHS) catalyzes the addition of glycine to the C-terminus to form GSH, which is the main form of reduced sulfur in the phloem.

Finally, Cys seems to be also the S-donor for Fe-S cluster synthesis (Balk and Lobréaux, 2005).

Other S-containing compounds are produced through an alternative pattern in which APS can be phosphorylated by the APS kinase (APSK) with the formation of adenosine 3'-phosphate 5'-phosphosulfate (PAPS) that is used as precursor, by the multiprotein family of sulfotransferases (SOTs), for the synthesis of coumarins, glucosinolates, flavonoids, gibberellic acids,

hydroxyjasmonates, phenolic acids, steroids or sulfate esters. (Klein and Papenbrock., 2004; Lewandowska e Sirko, 2008; Kopriva, 2017).

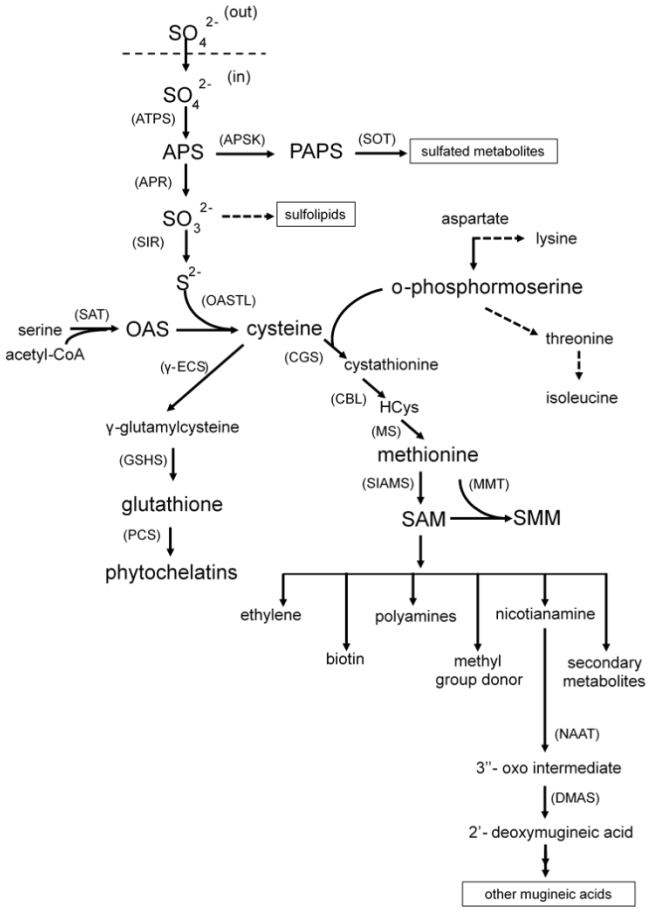

Fig.1.4 Schematic representation of S reduction and assimilation in plants (Modified from: Lewandowska and Sirko, 2008).

As previously described for uptake, also S assimilation process is strongly regulated, for both the importance of S compounds for plants and the toxicity of intermediates compounds of S assimilation pathway (such as H_2S) (Rennenberg 1984). In particular, APS reduction is the main regulation step of the S assimilation pathway (Davidian and Kopriva, 2010). This enzyme is regulated in different ways by sulfate, but also by Cys and GSH (Lewandowska and Sirko, 2008). In particular, S deficiency induces APR and ATPS activity and this process is controlled at transcriptional level (with increased expression of genes encoding for APR and ATPS)

(Lewandowska and Sirko, 2008). On the contrary, it has been shown that ATPS activity is repressed by accumulation of S-compounds, such as thiols (Hesse et al., 2004).

Similarly to transporters, also the enzymes of the assimilatory pathway, except sulfite reductase (SiR), are encoded by multiple genes. For example, in *Arabidopsis* there are four isoforms of ATPS (*ATPS1, ATPS2, ATPS3* and *ATPS4*) (Lewandowska and Sirko, 2008; Kopriva et al., 2009), three for APR (*APR1, APR2* and *APR3*), four for APK (*APK1, APK2, APK3* and *APK4*) (Kopriva et al., 2009) and nine isoforms of OASTL (*OAS-TL-A1; OAS-TL-A2; OAS-TL-B; OAS-TL-C; CS26: CS-like protein; Atcys-D1: Atcys-D2*) (Fig. 1.5) (Wirtz et al., 2004; Kopriva et al., 2009).

It has been shown that S deficiency inducible microRNA (miRNA395) regulates three *ATPS* genes (*ATPS1, -3* and *-4*), but its functional significance is still unclear (Lewandowska and Sirko, 2008; Kopriva et al., 2009). The accumulation of miRNA395 under S deficiency condition is induced by SLIM1 (Sulfur Limitation1), a transcription factor belonging to the Ethylene-Insensitive-3-like amily (EIL3). Moreover, SLIM1 under S deficiency condition also controls MYB transcription factors that regulate *ATPS, APK1, APK2, APR* and *SIR*

(Davidian and Kopriva, 2010). However, S deficiency does not affect the expression of SLIM1 (Kawashima et al., 2011).

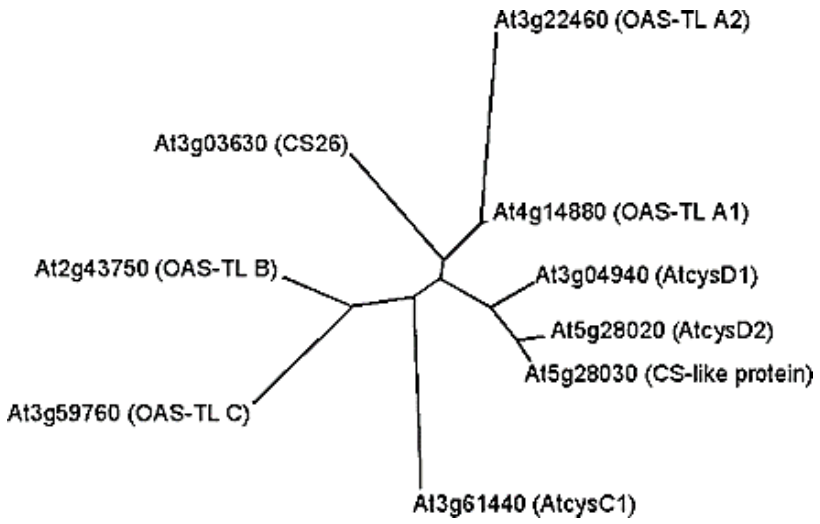

Fig. 1.5 Sequence relationship of OAS-TL-like proteins in *A. thaliana* (from Wirtz et al., 2004)

1.3 The importance of sulfur in plant nutrition

Sulfur is an essential macronutrient for plants, being crucial for many fundamental metabolic processes. As previously described, it is a component of two amino acids, methionine (Met) and cysteine (Cys), and therefore essential for protein synthesis, protein structures and enzymes function. Moreover, S is fundamental for the synthesis of many other S compounds important for plant growth and development (Fig. 1.6).

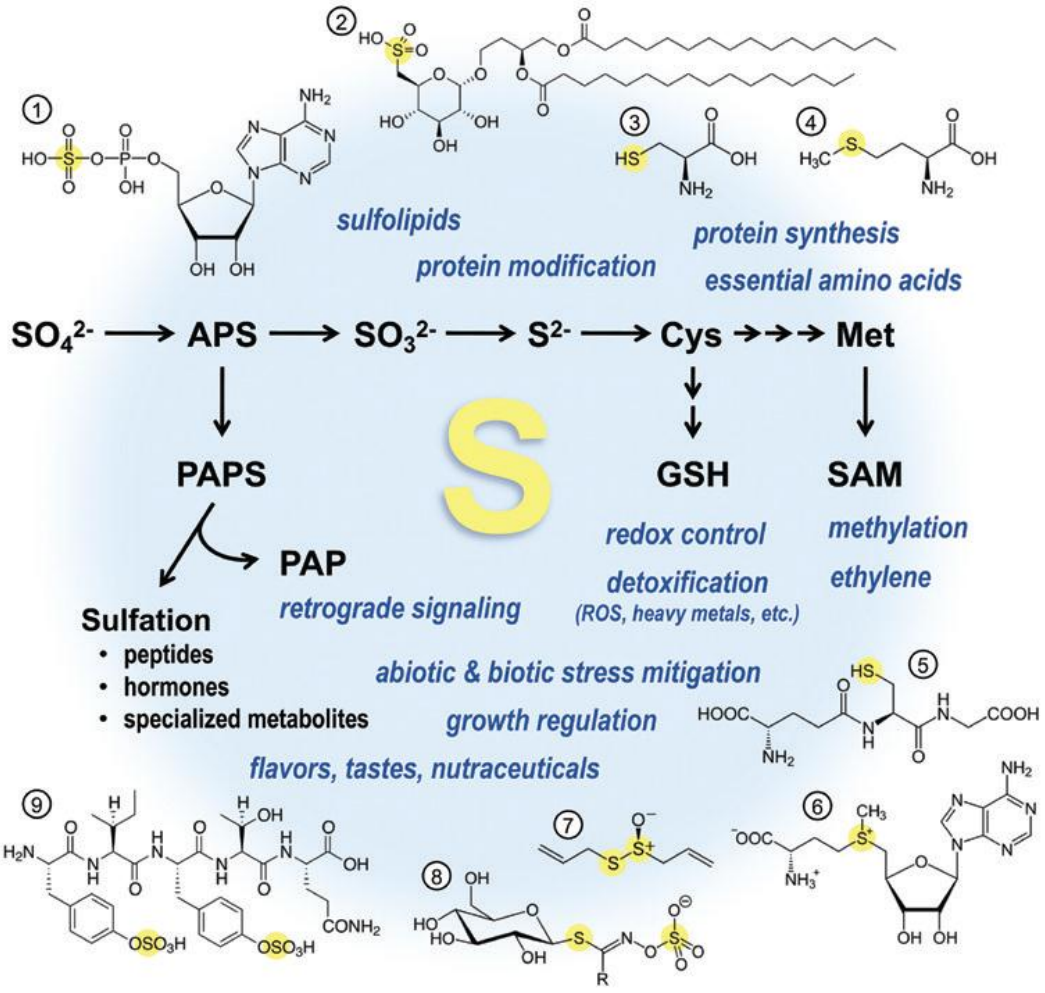

Fig. 1.6: Representation of physiological functions of S drived metabolites in plants (From: Kopriva et al., 2019)

Plants exposed to S deficiency show typical symptoms, such as a reduction of shoot biomass, often associated to an increase of root development, and the onset of leaf chlorosis, mainly involving young leaves being S mobility within plant quite low (Fig. 1.7). The unbalanced plant growth is due to the need to increase soil exploration to find the nutrient, and causes the reduction of plant shoot/root ratio (Robinson, 1994).

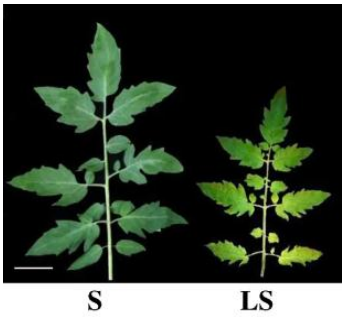

Fig. 1.7: Morphological effects of S deficiency. Decreased growth of the aerial part of the plant and leaf chlorosis. S indicates S sufficiency while LS low S supply (Modified from: Hasan et al., 2018).

On the other hand, the lack of Cys biosynthesis under S deficiency condition not only impairs the synthesis of other compounds that starts with Cys, such as GSH and Met (Hoefgen and Hesse, 2007), but also negatively affects protein structure and function. Cys is fundamental for the formation of disulfide-bridges, which are in turn fundamental for the tertiary structures of proteins. Therefore, S-starvation not only affects crop productivity (Barker and Pilbeam, 2007) but also crop quality. For example, it has been recognized that the biological quality of proteins is negatively affected in potatoes, kales, and beans (Eppendorfer and Eggum, 1992 and 1994) and the baking quality of wheat is negatively affected since disulfide-bridges are responsible of the glutenin fraction polymerization (Zhao et al., 1999; Barker and Pilbeam, 2007).

On the other hand, GSH has an important role in plant antioxidant response, being the most abundant antioxidant compound in plant tissues (North and Kopriva., 2007). It can directly detoxify reactive oxygen species (ROS) and it has been demonstrated that under stress conditions plants increase the synthesis of GSH by inducing the activity of APR and OASTL, and also the abundance of *APR* mRNA. The involvement of GSH in stress responses was confirmed by higher level of GSH and GSH reductase (GR) activity in plants exposed to salicylic acid (SA) and abscisic acid (ABA). SA is important for plant stress tolerance, while ABA is related to plant adaptation under stress conditions (Capaldi et al., 2015).

GSH is also the precursor of phytochelatins (PC), which play an important role in the metal detoxification in plants exposed to high levels of Cd, Cu, and Zn (Rauser, 1995; Cobbett, 2000; Heiss et al., 2003).

Due to the role of S compounds in plant responses to abiotic and biotic stresses, S deficiency most likely impairs plant's ability to cope with stress conditions as well as excess of S supply improves plant photosynthesis and growth under stresses conditions by increasing GSH synthesis (Fatma et al., 2014).

Methionine is directly involved in protein synthesis, being AUG the codon used for translation initiation (Sasaki and Nakashima, 2000), therefore S deficiency reduces the protein synthesis rate, with consequent accumulation of N compounds in plant cells (Barker and Pilbeam, 2007). Moreover, being the precursor of SAM, Met is also involved in the synthesis of ethylene (ET), an important hormone for plant growth and development. The enzymes involved in ET synthesis are ACC synthase (ACS) and ACC oxidase (ACO). The first one catalyzes the synthesis of 1-aminocyclopropane-1-carboxylic acid (ACC) from SAM, while the second one catalyzes the synthesis of ET from ACC (Wang et al., 2002). In particular, ET plays a key role in many processes, such as root hairs development, fruit ripening and seed germination (Wang et al., 2002). Furthermore, together with jasmonic acid (JA) and SA, it seems to be involved in abiotic and biotic stress responses (Wang et al., 2002; Yang et al., 2019). Being SAM the precursor not only of ET but also of PAs, the synthesis of ET competes with the one of PAs (Fig. 1.8) (Chen et al., 2019). Polyamines are present in the plant mainly in three free forms, putrescine (Put), spermidine (Spd), and spermine (Spm) and are involved in stress responses, fruit maturation, flowering, and other important processes.

Finally, S is an essential component of Fe-S clusters, the most ubiquitous and versatile prosthetic groups (Pala et al., 2018). The biogenesis of these clusters involves three different assembly machineries: SUF machinery located in chloroplast, the Fe-S cluster (ISC) assembly machinery in mitochondria and the cytosolic Fe-S protein assembly (CIA) machinery located in cytosol (Balk and Schaedler, 2014). In particular mitochondria and the ISC has a central role, since this machinery mature all organellar Fe-S protein and provides an unknown sulfur-containing compound, translocated by an ABC transporter into the cytosol, that is necessary for the extramitochondrial Fe-S protein maturation (Stehling and and Lill, 2013). These clusters are involved in electron transfer, with a critical role in many enzymes involved in: S and N assimilation, DNA repair and replication, ribosome biogenesis, respiration and photosynthesis

(Balk and Pilon, 2011). Thus, S deficiency may negatively influence also the activity of enzymes that contain Fe-S clusters, with consequent negative effects on the processes in which these enzymes are involved.

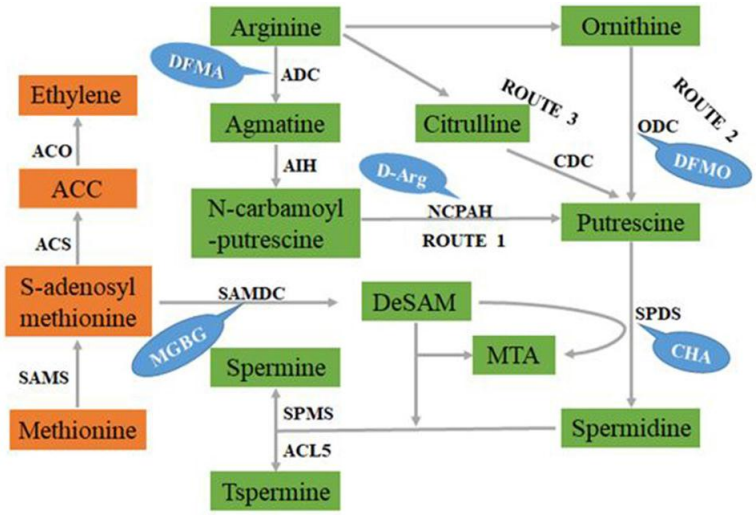

Fig. 1.8 The pathway of polyamines (PAs) and ethylene (ET) biosynthesis (from Chen et al., 2019)

1.4 **Sulfur interaction with essential and non-essential elements**

The availability of nutrients in different soils and how it influences the physiology of the plants has been widely described at the level of single nutrient. However, this picture is most likely confounded by nutrient interactions. It is recognized that the deficiency or excess of a single nutrient is typically coordinated with a change in the demand for other nutrients. In particular, the glossary of Soil Science Terms (2008) defines nutrient interaction as "*A term usually used to describe the response from two or more nutrients applied together that deviates from additive individual responses when applied separately. This term may also be used to describe metabolic or ion-uptake phenomenon*". In this context, we can distinguish between positive/synergic interaction (when plant grows better with combined nutrients with respect to the sum of their individual effects) and negative/antagonistic interaction (combining nutrients results in worsening plant growth with respect to the sum of their individual effects) (Marschner, 1995; Fageria, 2001). Therefore, multi-level interactions among the various mineral elements need to be investigated urgently in order to understand how the different sensing and signaling pathways activated in

response to changes in availability of one element are coordinately integrated with those of other elements. However, the consequences of nutrient interactions are largely unknown, even though such scenarios commonly occur in agroecosystems. In particular, excess or deficiency of one nutrient could modify the internal demand and consequently the uptake and assimilation rate of other nutrients.

Poor information is due to the fact that plant response to fluctuation of a single nutrient is different to that of multiple nutrients, and more importantly, it is not possible to predict plant response to multiple nutrients by taking into account plant response to the single element.

In particular, little is known concerning the physiological responses during S deficiency conditions in relation to how they are modified by the interactions S has with other elements (essential or not) in the rhizosphere.

Well known example of positive interaction is the one between N and S. It has been widely demonstrated that grain productivity increases with combined N and S fertilization (Kalmbacher et al., 2005; Habtegebrial and Singh, 2006; Mathot et al., 2008; Salvagiotti et al., 2009), most likely due to the involvement of both elements in protein synthesis (Crawford et al., 2000). In fact, N and S assimilatory pathways are coordinated and probably subjected to co-regulation mechanisms (Koprivova et al., 2000). The lack of one of these two elements represses the assimilation of the other one and induces physiological changes aiming to rebalance the two nutrients within the plant (Hawkesford e De Kok, 2006). Clear links have been also established between S and phosphorous (P) in the soil/plant system. Plants have developed tightly controlled mechanisms to coordinate S transport and homeostasis with photosynthesis and the carbon status, in a similar manner to the inorganic P transport system (Lejay et al., 2008). Plants maintain intracellular homeostasis of both elements in response to their respective external availability. For instance, plant cells operate a rapid replacement of sulfolipids by phospholipids under S deficiency, and vice versa during P deficiency (Sugimoto et al., 2010). Such a metabolic switch is an evidence of P/S nutritional interdependency.

Obviously S interaction with other elements is not only limited to N and P, and for different reasons, S has been reported to interact with other essential and non-essential elements, among which iron (Fe), copper (Cu) and sodium (Na).

1.4.1 Iron

Iron (Fe) is among the major nutrients responsible for the quality and quantity of crop yields and its fertilization management has been the focus of attention for the last decades (Kim and Guerinot, 2007; Briat, 2009).

It is crucial for the proper functioning of metabolic processes related to electron transport, such as respiration and photosynthesis, and for chlorophyll biosynthesis (Briat, 2007; Briat and Vert, 2004). Indeed, Fe deficiency firstly appears with a reduced growth and leaf chlorosis in young leaves and then on older ones associated with alteration of the main metabolic pathways. Fe deficiency provokes serious imbalances in the ultrastructure and functionality of chloroplast, being the 90% of leaf-Fe present in chloroplasts (López-Millán et al., 2016; Morrissey and Guerinot, 2009).

The main sink of Fe within the plant is represented by Fe-S clusters, in which Fe is linked with S (Balk and Pilon 2011). The main form is represented by [2Fe-2S] and [4Fe-4S], but they exist also in the form [3Fe-3S] (Stehling and Lill, 2013)**.**

Fe is also bound with N in hemeproteins, such as cytochromes, performing electron transport in the respiratory chain (Rout and Sahoo, 2015), catalase, peroxidase and leg-hemoglobin, which is involved in N_2 biological fixation (Marschner, 1995).

In soils, Fe is present in huge amount, being the fourth element in the earth's crust in percentage after oxygen, silicon, and aluminum. Therefore, widespread limited availability of Fe for plant nutrition is not related to its low absolute content into the soil, but rather to its limited solubility. In particular, Fe deficiency is a typical features of alkaline soils (Marschner, 1995), which cover more than 25% of the earth's surface (FAO and ITPS, 2015).

Low Fe availability in calcareous soils can be ascribed to an extremely low solubility of soil Fe, which is essentially in ferric oxide form at high pH values. However, alkaline conditions may also depress or even block Fe uptake from the apoplast into the symplast, which can be related to the pH of the former (Mengel, 1994, Nikolic and Kastori, 2000).

When Fe is limited in the substrate, roots rely on two main strategies to acquire it, Strategy I and Strategy II, based on Fe^{3+}-reduction and Fe^{3+}-chelation, respectively (Fig. 1.9) (Kobayashi and Nishizawa, 2012).

The Strategy I is used by all plants except grasses, while Strategy II is only typical of grasses (Marschner et al., 1986; Kobayashi and Nishizawa, 2012).

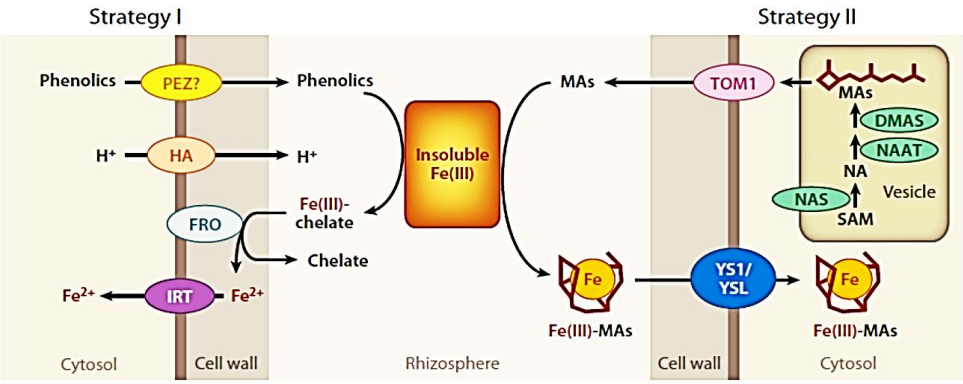

Fig. 1.9: Representation of Strategy I and Strategy II mechanisms (From: Kobayashi and Nishizawa, 2012)

The Strategy I mechanism starts by inducing the activity of plasma membrane H^+ATPase which increases proton extrusion rate to solubilize Fe^{3+} in the soil (Santi et al., 2005; Kim and Guerinot, 2007; Morrissey and Guerinot, 2009). In particular, Fe^{3+} is 1000 times more soluble with pH decreasing of one unit (Kim and Guerinot, 2007). The release of organic acids by roots also contributes to Fe solubilization in the rhizosphere (Fourcroy et al., 2014). Solubilized Fe^{3+} is then reduced to Fe^{2+} by the increased activity of a membrane-bound Fe^{3+}-chelate reductase and the resulting Fe^{2+} in transported into the plant root cell by a Fe^{2+}-transporter (Eide et al., 1996; Morrissey and Guerinot, 2009). The genes encoding for the Fe^{3+}-chelate reductase (*FRO*, ferric reductase oxidase) and for the Fe^{2+}-transporter (*IRT*, iron-regulated transporter), have been identified first in *Arabidopsis* and then in tomato (Eide et al., 1996; Robinson et al., 1999; Eckhardt et al., 2001; Li et al., 2004). The main regulator of these genes seems to be *FIT*, Fe deficiency-Induced Transcription factor (*FER* in tomato), which is a basic Helix-Loop-Helix (bHLH) transcription factor (Lingam et al., 2011; Lucena et al., 2015). Moreover, *FIT* (*FER*) seems to be involved also in the regulation of plasma membrane H^+ATPase (Kim and Guerinot, 2007).

Under Fe deficiency, the induction of all components of Strategy I at root level is accompanied by root morphological changes, and a concomitant increase of ET synthesis it has been observed (Römheld and Marschner, 1986; Romera and Alcántara, 2004; Garcia et al., 2015). Thus, it has been hypothesized the involvement of this hormone in inducing physiological and morphological changes under Fe deficiency. Indeed, ET seems to stimulate the development of root hairs, cluster cells and root epidermal transfer cells, suggesting its involvement in the development of root morphological modifications (Römheld, 1978). Ethylene seems to stimulate also the components

of the Fe deficiency response: the expression of *FIT* (*FER*), the ability to acidify the external medium with regulation of plasma membrane H^+ATPase (Lucena et alt., 2015) and the reduction of ferric iron (Romera and Alcántara, 2004), suggesting its involvement also at physiological level. The link between *FIT* and ET signaling comes from the evidence that *FIT* interact with *EIN3* (ETHYLENE INSENSITIVE 3) and *EIL1* (ETHYLENE INSENSITIVE3-LIKE) transcription factors, and this interaction is fundamental to prevent *FIT* proteasomal degradation, with increased stability of *FIT* and control of Fe deficiency response by ET signaling (Lingam et al., 2011). Moreover, *FIT* (*FER)* has been also reported to interact physically with others bHLH family members (bHLH38 and bHLH39) to induce the response of the plant under Fe deficiency condition (Wang et al., 2007).

Another typical response of plants under Fe deficiency conditions is the release by roots of phenolic compounds (Römheld e Marschner, 1986; El-Baz et al., 2004), such as caffeic acid. The release of phenolic compounds depends on the activity of some genes that are controlled by the *MYB72* gene, which is also controlled by *FIT* (*FER*) and then by ET (Fig. 1.10) (Lucena et al., 2015). Interestingly, MYB72 interacts also with SLIM 1 transcription factor, a central regulator of S starvation responses (Wawrzyńska and Sirko, 2014; Kopriva, 2017).

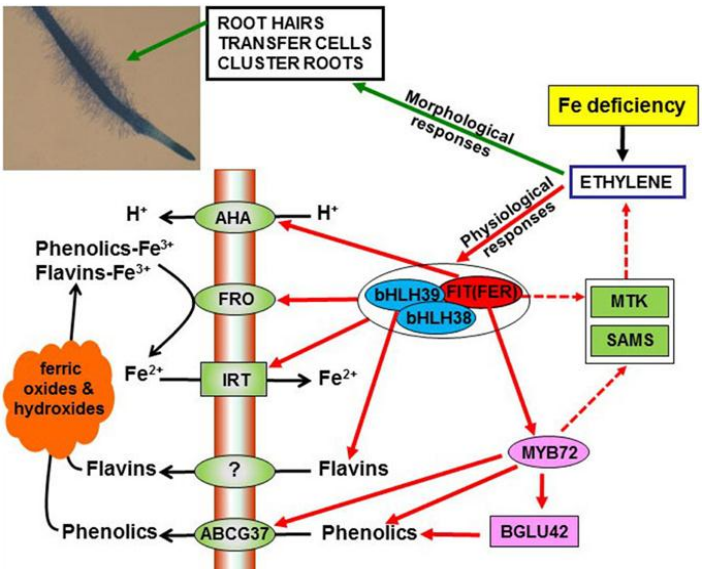

Fig. 1.10: Role of Ethylene (ET) in the regulation of morphological and physiological responses to Fe deficiency in Strategy I plants (From: Lucena et al., 2015).

The Strategy II mechanism, used only by grasses, is called chelation-strategy because it is characterized by the release of low molecular weight non-proteinogenic amino acid named phytosiderophores (PS), which are able to chelate Fe^{3+} in the rhizosphere (Marschner, 1995). Phytosiderophores, belong to the mugineic acid (MA) family, and are synthesized from Met as precursor (Fig. 1.4), (Mori and Nishizawa, 1987). Met is converted to SAM (as described in paragraph 1.2)**.** Fe deficiency condition specifically induces the biosynthesis and release of PS by the root specific transporter *TOM1* (Transporter of MA 1). Once in the rhizosphere, PS are able to create stable complexes with Fe^{3+} and the whole Fe^{3+}-PS complex is taken up by roots through the activity of the specific transporter *YS1* (Yellow stripe 1) (Morrissey and Guerinot, 2009). Plant ability to release PS is related to its ability to tolerate Fe deficiency conditions, and among grasses barley is the most efficient, whereas rice the less one (Römheld, 1987).

Once Fe enter in the root cells is transported to shoot preferentially to youngest leaves, but for its translocation, Fe needs to be chelated, since in the free form it tends to create free radicals in redox reactions in the presence of oxygen (Lobreaux and Briat, 1991).

Besides NA, which is the main chelator of simplastic Fe in both Strategy I and Strategy II plants, other compounds are responsible for Fe chelation within the plant and they are represented by various organic acids, including citrate (Hell and Stephan, 2003). In particular when Fe enters into the xilem seems to be complexed with citrate (Morrissey and Guerinot, 2009; Kobayashi et al., 2019), this organic acids is effluxed into the xilem by the citrate transporter FRD3. Interestingly, under Fe deficiencny *FRD3* is up-reguated, while *Arabidopsis frd3* mutant shows Fe deficiency symptoms accompanied by the activation of Fe deficiency response also under iron sufficiency (Rogers and Guerinot, 2002)

The description of both Strategy I and Strategy II mechanisms indicates that the amino acid Met, playing an important role in both strategies as precursor of ET (Strategy I) and PS (Strategy II), represents the first connection between Fe and S.

Within the last years, extensive information has been accumulated on the reciprocal influence between S and Fe nutrition at both physiological and molecular level in several plant species. In particular, it has been clearly demonstrated that plant capability to take up and accumulate Fe is strongly dependent on S availability in the growth medium in both grasses (Bouranis et al., 2003; Astolfi et al., 2006; Zuchi et al., 2012: Celletti et al., 2016) and dicots (Paolacci et al., 2014; Zuchi et al., 2009, 2015). Moreover, it has been demonstrated in wheat that providing S above adequate concentrations may result in the improvement of Fe use efficiency (Hawkesford et al., 2014) and

this S nutritional effect seems to be especially advantageous for plants grown under severe Fe limitation (Zuchi et al., 2012). On the other hand, it has been demonstrated that Fe deficiency adaptation requires the adjustment of S uptake and assimilation rate (Astolfi et al., 2006; Ciaffi et al., 2013; Paolacci et al., 2014).

It has been suggested that limited availability of S could impact on the Fe metabolism for its effect on Met synthesis. Under Fe deficiency, Strategy I plants increase ET and NA synthesis (Li and Li, 2004; Molassiotis et al., 2005; Zuchi et al., 2009) with relevant consumption of Met, which represents the precursor of both compounds (Hesse and Hoefgen, 2003) and the same could occur in Strategy II plants, in which Met is the precursor of PS (Guerinot and Yi, 1994). As a consequence, the observed regulation of S uptake by roots and root-to-shoot translocation rate might be explained by the need to meet the increased demand for methionine and its derivatives in response to Fe starvation (Paolacci et al., 2014; Zuchi et al., 2009, 2015).

Furthermore, a second link between S and Fe is represented by Fe–S clusters (Balk and Pilon, 2011; Mapolelo et al., 2013; Balk and Schaedler 2014). However, there are no information about the coordination between the assembly of Fe-S clusters and the assimilation pathways of S and Fe.

Taken together, these evidences clearly indicate that S is a limiting factor not only for plant growth and development but also for plant response to Fe deficiency.

It has been demonstrated that S deficiency modulates the expression of several genes involved in Fe homeostasis. In tomato, it has been demonstrated that S deficiency virtually abolished the expression of the NA synthase (*LeNAS*) gene and limited the expression of both *LeIRT1* and *LeFRO1* gene (Zuchi et al., 2009), while in barley the expression of *HvYS1*, the specific transporter of Fe-PS complexes, is modulated by S supply (Astolfi et al., 2010). On the other hand, there are some indications that Fe deficiency induces a significant increase in the demand for S, and thus activates S uptake and assimilation rate similarly to S deficiency condition. The purpose of this response could be the improvement of plant capability to cope with Fe deficiency, as demonstrated in tomato (Paolacci et al., 2014) and in wheat (Celletti et al., 2016). In tomato, with increasing S and thiols concentration, *FRO1* expression and Fe(III)-chelate reductase activity increased (Paolacci et al., 2014), as also PS release in wheat (Celletti et al., 2016).

However, higher S needs to sustain the activation of Strategy I and II mechanisms cannot fully account for the observed link between the flow of these two essential nutrients in plant, but presumably reflect a direct interference of Fe with the signal transduction pathway involved in S metabolism (and *vice versa*), and with the activation of different acquisition strategies. These

findings support a model in which Fe and S metabolism need to be coordinated to a certain extent as for the maintenance of Fe-S-cluster formation and, on the other hand, being S metabolism additionally involved in multiple processes of primary and secondary metabolism, they need to be also independently modulated. In part, this is mirrored by the intensive overlap, but also distinct responses observed by using metabolome (in tomato, Zuchi et al., 2015) and transcriptome-wide (in wheat, Zamboni et al., 2017) approaches to study the interplay between S and Fe.

1.4.2 Copper

Copper (Cu) is an essential element, associated with proteins and enzymes involved in electron transfer and redox reactions (Brunetto et al., 2016; Printz et al., 2016), such as superoxide dismutase (SOD), cytochrome oxidase (CcO), ascorbate oxidase, diamine oxidase and polyphenol oxidase (Marschner, 2012), and more than 50% of Cu is in the chloroplasts, bound to plastocyanin (Marschner, 2012).

Recently, progresses have been done in the understanding of Cu transport into cells and organelles. A family of high ffinity Copper Transport Proteins (COPT) has been identified, with specialized functions in Cu homeostasis (Sancenon et al., 2003; Wintz et al., 2003; Puig, 2014). In particular, COPT1 is involved in root Cu uptake. Under Cu limitation the expression of *COPT 1* is regulated by SPL7 (SQUAMOSA promoter-binding protein-like 7), the master regulator of Cu homeostasis in *Arabidopsis* (Puig, 2014). SPL7 activates also the expression of Cu^{2+} reductase (*FRO4* and *FRO5*), and it has been suggested that first Cu^{2+} is reduced to Cu^{+} by these Cu^{2+} reductases and then Cu^{+} is taken up by COPT1 (Puig, 2014).

Despite Cu essentiality, plant exposure to high Cu concentrations finally results in adverse effects on plant growth, by disturbing a wide range of biochemical and physiological processes, such as photosynthesis, pigment synthesis, nitrogen and protein metabolism, and membrane integrity (Luna et al., 1994; Shen et al., 1998; Nielsen et al., 2003; Demirevska-Kepova et al., 2004).

Toxic Cu accumulation can originate from the use of Cu in agriculture, e.g. as the “Bordeaux Mixture” for vine downy mildew disease as well as in other pesticides. In vineyards, Cu-accumulation can reach very high levels (often higher than 200 mg kg^{-1}) (Fig. 1.11) (Komarek et al., 2010).

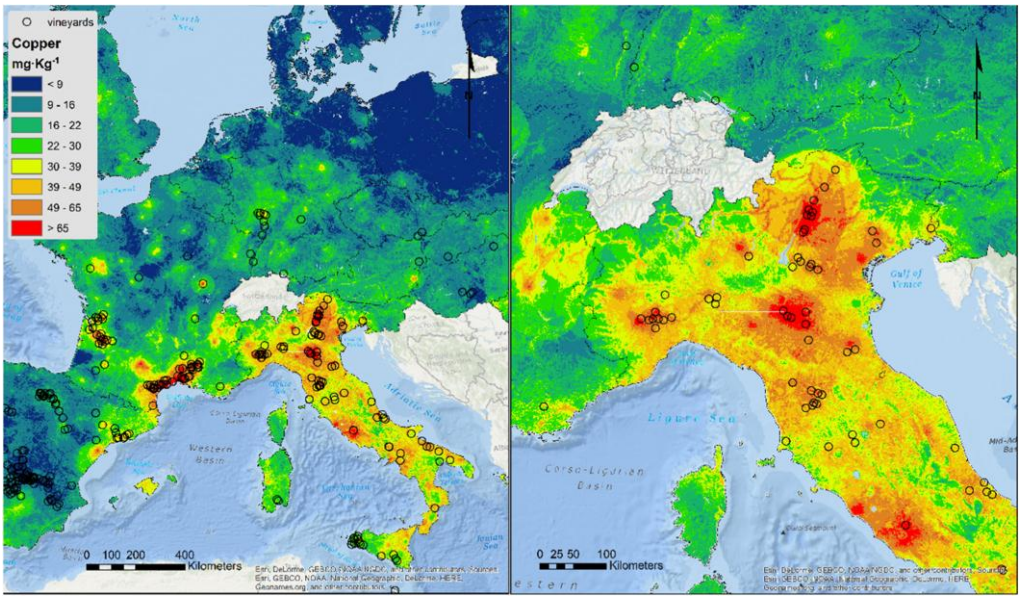

Fig. 1.11: Map of topsoil copper concentration (mg kg^{-1}) and vineyard distribution (black circles) (From: Ballabio et al., 2018).

Runoff from agricultural fields can reach several micromolar Cu (Zhang et al., 2003; He et al., 2009), a concentration that is lethal for many aquatic plants (review by Küpper and Kroneck, 2005). Copper pollution can also result from industrial activities such as Cu mining and waste deposition (Ke et al., 2007). As the result of a long-term field application, Cu residues can cause impacts on soil biota by reducing soil microbial biomass and earthworms in the orchard (Van-Zwieten et al., 2004).

Cu accumulation in vineyards does not represent a problem for vine growth and development and wine quality, since the root apparatus of vine develops below the contaminated layer, and furthermore the translocation of the metal to the shoot is very low. However, Cu-contaminated soils are not suitable for other crops, since excess copper in substrate could lead to growth reduction and may even be lethal for plants, for food security and human health.

Even low Cu concentrations result in photosynthesis inhibition by the formation of Cu-chlorophylls, which are unsuitable for photosynthesis (Küpper et al., 2006). Copper impairs cellular transport processes and for example, significant reductions of root calcium and iron contents, as well as extensive damage to root epidermal cells in maize plants were observed (Ouzounidou et al., 1995). Finally, due to its redox properties, Cu induces oxidative stress and the related production of highly reactive hydroxyl radicals leads to the corruption of lipids, proteins,

DNA and other biomolecules. This injury to biomolecules is a consequence of the oxidative stress induced by Cu (Yruela, 2005; Nagajyoti et al., 2010; Sytar et al., 2013).

These evidences support the hypothesis that the mitigation of Cu toxicity in plants is achieved by increasing production of antioxidant enzymes or compounds, as protection against oxidative damage, and/or chelating compounds.

Since GSH is the major antioxidant compound within the plant, and the precursor of PC (important for metal detoxification), plant exposure to toxic Cu concentrations could result in higher S nutritional requirement to activate the antioxidant responses as previously described, or to synthesize metal-binding S compounds, but, despite this, the mechanisms by which S nutrition could improve plant tolerance to Cu stress have received little attention.

Recently, Gilabel et al., (2013) reported that in *Panicum maximum* grown under different combination of three S concentrations and four Cu concentrations, a sufficient S supply was useful to reduce the Cu phytotoxic effects. Moreover, it has been reported that the exposure of *Brassica pekinensis* to high concentration of Cu resulted in an increase of total S and non-protein thiols content within the plant, associated with a stimulated activity and expression of *SULTR1;2*, *SULTR4;1* and *SULTR4;2* (Shahbaz et al., 2009). The modulation of sulfate transporters expression and activity was attributed to higher S demand generated by Cu exposure or probably to a direct interference of Cu with signal compounds involved in the regulation of S uptake and transport within the plant (Shahbaz et al., 2009).

Thus, it is clear that the understanding of Cu acquisition mechanisms together with the role of S metabolism in Cu-tolerance will be important for the development of strategies aimed at limiting the toxic effect of the metal.

1.4.3 *Sodium*

Sodium (Na) is not considered an essential element, except for *Atriplex vesicaria* (Marschner, 2012), *Kochia childsii* (Maathuis., 2014) and for some of C4 species.

Salinity is one of the major constraints for agriculture, affecting crop yield and food production worldwide, and it is a direct consequence of global warming. Indeed, drought due to both, water scarcity and high evaporation rates, causes water to rise up into the soil by capillarity, dragging the dissolved salts with it, thus determining their accumulation in the upper layers of soils, increasing the phenomenon of salinization. Water resources are rapidly depleting for the large water use in

agricultural and industrial activities. Moreover, the intrusion of salt water compromises the underground aquifers, contributing to freshwater scarcity with a very negative effects on crop production mainly in coastal zone, particularly vulnerable to climate change (FAO and ITPS 2015; McFarlane et al., 2016; Rahman et al., 2018). More than 800 million ha of cultivates soils are affected by salinity, of these 397 million ha are saline soils, while 434 million ha are sodic soils (based on 1974 FAO/UNESCO soil map of the world). In particular, soils are defined sodic, when the percentage of exchangeable Na exceeds 15%.

Although NaCl is a major salt present in saline soils, most crops suffer toxicity of sodium more and before that of chloride (White and Broadley, 2001).

Saline stress has adverse effects on plant growth and productivity (Tester and Devenport, 2003; Khan et al., 2009; Syeed et al., 2011). The physiological processes mainly affected by high Na^+ concentration include impairment of osmotic homeostasis, nutrient imbalance affecting other ions and oxidative stress as a secondary problem (Zhu, 2001). As example,

Na^+ can substitute K^+, indeed its beneficial effect have been observed under K-deficiency (Subbarao et al., 2003). It happens because Na^+ and K^+ are very similar form a chemical and structural point of view (Amtmann and Sanders, 1999). Na^+ uptake is mediated by many different K^+ carriers, such as, AKT1, HKT1, NORC and voltage-independent channels (VIC), and Na^+ toxicity/tolerance is correlate with the low-affinity Na^+ transport by the transporter HKT1 (high-affinity potassium transporter 1), and with Na^+/K^+ competition for the same transporters (Rubio et al., 1995). Indeed, under salt stress the balance between Na^+ and K^+ is mediate by the transporters of HKT1-family (Ali et al., 2019).

Therefore, under conditions of saline stress, plants ability to activate physiological responses to minimize the oxidative stress could be crucial to survive.

It is widely documented, and previously described also for Cu stress, that in the face of different types of stress, the production of free radicals and reactive oxygen species (ROS) increases, with consequent damage to macromolecules and cell integrity (Khan et al., 2014). Lipid peroxidation and protein carbonylation are among the first physiological "symptoms" of oxidative stress.

Under salt stress, plant increases the activity of antioxidant enzymes and the synthesis of proline and GSH (Giraud et al., 2008; Nazar et al., 2011; Ashfaque et al., 2014). In particular, salinity tolerance is correlated with plant ability to produce GSH (Noctor et al., 1998; Ruiz and Blumwald, 2002; Kocsy et al., 2004). Being GSH directly synthesized from Cys, it was also reported an increased synthesis of Cys in response to salt stress (Nazar et al., 2011). The accumulation of GSH

determined by salt stress condition was associated with an up regulation of chloroplast APR and SAT (Queval et al., 2009). Moreover, in *Brassica juncea* L. it has been observed that a higher ATPS activity, resulting in an increased GSH synthesis, resulted in a less sensitivity to salt tress (Khan et al., 2009). Finally, it has been hypothesized a role for OASTL proteins under salt stress condition. In particular, transcription and translation of *OASTL* genes was induced under salt stress condition in *Arabidopsis*, and the expression of *Arabidopsis* cytosolic OASTL confers the salt stress resistance to yeast , even if the effects of the stress condition on S assimilatory pathway were different in plant and yeast (Romero et al., 2001). The increased transcription and translation of OASTL genes in plants may be related to the increased need of Cys to synthesized GSH to overcome the oxidative stress generated by salt toxicity, and thus to the central role of S metabolism in these responses (Fig.1.12).

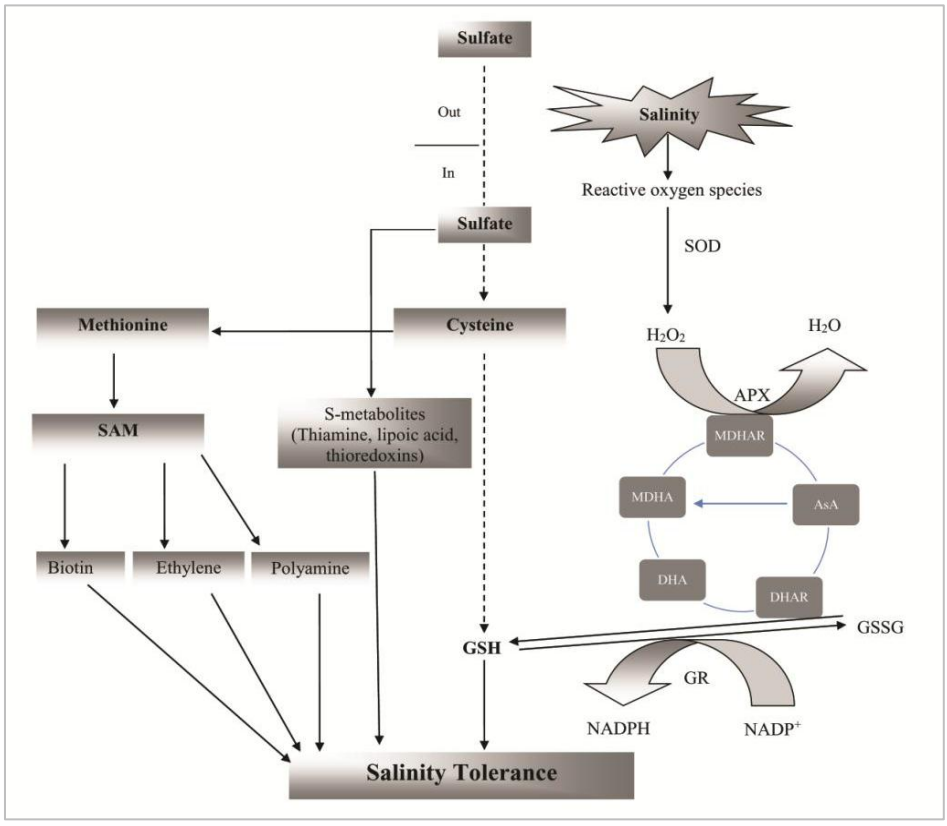

Fig. 1.12: Schematic representation of S metabolites involvement in salinity tolerance. (From: Khan et al., 2014).

1.5 Objectives

Sulfur deficiency in crops has become a constraint to yields over the last 50-60 years (Scherer, 2001), not only for high S requiring crops, such as Brassicaceae, but also for other crop species, such as wheat or maize (Zhao et al., 1999; Blake-Kalff et al., 2001).

Until then, S nutrition received only little attention, whereas most of published literature was devoted to nitrogen (N), phosphorus (P) and potassium (K) and their roles in crop production.

Today, the situation is even worsened: S deficiency is widespread in many cropping systems throughout the world and supplemental S through fertilizers is needed to sustain optimum crop yields (McGrath and Zhao 1995; McGrath et al. 1996).

The limited S availability in soil can be explained by several factors, first of all the decreased S deposition from rain and air resulting from reduced emissions of sulfur dioxide because of environmental policies. Moreover, changes in fertilization practices, and in particular the use of high-analysis type fertilizers, containing little or no S (Zhao et al., 1997, 1999), and reduced use of manure contributed to add less S to soils. Finally, the use of high yielding commercial varieties, coupled with intensive management practices, dramatically increased crop removal, resulting in more rapid depletion of S from soils.

Even if plant tissues are characterized by a low S content, which constitutes 0.3-0.5% of the total dry weight of plants, S plays a key role for plant growth and development.

In fact, it is a component of amino acids (cysteine and methionine) and proteins and thus plays an important role in many metabolic processes, such as photosynthesis, respiration and nitrogen assimilation. The importance of cysteine in plants is mainly defined by its role in the formation of disulfide bridges, which are determinants of the structure and folding of proteins and, consequently, of their stability and function (Haag et al., 2012). However, it also plays a role as a precursor for a large number of essential metabolites, such as glutathione (GSH) (Hoefgen and Hesse, 2007). On the other hand, methionine is crucial for the formation of proteins (Sasaki and Nakashima, 2000), but it plays additional roles through its first metabolite, S-adenosylmethionine (SAM), which is the major methyl-group donor in transmethylation reactions and an intermediate in the biosynthesis of polyamines, biotin and ethylene (Bürstenbinder et al., 2007).

Furthermore, being required for the synthesis of various other compounds, such as thiols (glutathione), sulfolipids and secondary S compounds (alliins, glucosinolates, phytochelatins), S

plays a crucial role in redox control of cellular processes (Foyer and Noctor, 2009) and in plant defence mechanisms (Rausch and Wachter, 2005; Noctor, 2006).

Considering the above described functions of S nutrition in plant metabolic processes, it is expected that plants have to be able to adjust their S uptake and assimilation rate not only to their growth rate and to changing S availability in soil but also in response to other both essential and not essential elements which increase the S demand for the plant.

Therefore, aim of this thesis was to address the following research questions:

1) Which are the reasons of the crosstalk between S and Fe nutrition? Are there common signals involved in their homeostasis?
2) Does S play a defensive role against phytotoxic effects of copper?
3) Does Na tolerance mechanisms require a higher S availability?

1) Iron deficiency is a constraint to yields in many cropping systems throughout the world, related to the limited availability of assimilable Fe forms. This issue is even more severe in calcareous soils, covering more than 30% of the earth's crust soils, in which high pH values favor Fe precipitation (Marschner, 1995).

During the past two decades, a close relation between S and Fe has been highlighted and demonstrated in both Strategy I and Strategy II plants (Astolfi et al., 2006; Zuchi et al., 2009; Zuchi et al., 2012; Paolacci et al., 2014; Forieri et al., 2013; Zuchi et al., 2015; Celletti et al., 2016; Zamboni et al., 2017; Vigani et al., 2018). Nevertheless, it remains unclear which are the mechanisms involved in the regulation of this interaction.

It is well known that Fe deficiency condition induces a significant increase in the demand for S resulting in increased S uptake and assimilation rate, similarly to what happens under S deficiency condition (Paolacci et al., 2014; Celletti et al., 2016). *Vice versa*, S deficiency significantly impairs plant capability to cope with Fe deficiency in both Strategy I and Strategy II plants (Astolfi et al., 2006; Zuchi et al., 2009).

These results were ascribed to methionine (Met) involvement in both Fe acquisition systems, since both ET and PS biosynthesis feed on a common precursor, SAM (Hesse and Hoefgen 2003).

However, the overall effects of combined S and Fe deficiency on plant metabolome are multi-faceted and cannot simply be explained by assuming the role of Met in both strategies (Zuchi et al., 2015). Furthermore, the evidence that both nutrients are needed for Fe-S cluster biosynthesis,

even explaining reduced Fe uptake under S deficiency, does not explain increased S uptake and assimilation under Fe deficiency, suggesting the existence of unknown regulation/signalling mechanisms involved in their close interplay.

The larger part of this thesis was therefore devoted on clarifying the regulatory mechanisms underlying S and Fe interaction in tomato (*Solanum lycopersicum* L.), as it is well known as Strategy I model plant.

Firstly, to gain better insight into the relation between S and Fe, changes in the exudate composition from roots of tomato plants exposed to single and combined S and Fe deficiency were evaluated. Rhizodeposition represents a sophisticated strategy that plants have developed to mobilize nutrients, including Fe, from soil and thus improving their acquisition by roots (Dakora and Phillips, 2002). It has been demonstrated that the release of root exudates is involved in both Fe acquisition systems (Strategy I and II) (Kobayashi and Nishizawa, 2012; Bocchini et al., 2015; Pii et al., 2015; Valentinuzzi et al., 2015; Celletti et al., 2016). However, to our knowledge, the effect of S deficiency, alone or in combination with Fe deficiency, on exudates' composition had not yet been explored.

Next, following previous studies showing that reductions in S availability can worsen Fe deficiency impact on tomato plants (Zuchi et al., 2009), we wondered whether plant S status and/or S external concentration could modify the capability to take-up and accumulate Fe.

We conducted an experiment by using a split-root system. The split-root system allows us to separate and evaluate systemic and local effects because this particular hydroponics system allowed the root system of each tomato plant to grow in two different compartments, both Fe-deficient, but one S-sufficient, and the other one S-deficient. Plant capability to cope with Fe deficiency was evaluated by analyzing changes in key components of the Strategy I (the FeIII-reducing activity and the expression of the *SlFRO1*, *SlIRT1* and *SlFER* genes), whereas changes in plant S uptake and assimilation rate were investigated by analyzing the expression of a high affinity sulfate transporter gene (*SlST1.1)* and the activity of the first (ATPsulfurylase, ATPS) and the last (O-acetylserine(thiol)lyase, OASTL) S pathway-related enzymes. Since it has been recently hypothesized a role for citric acid in the regulation mechanisms underlining Fe and S interplay (Vigani et al., 2018), also changes in citric acid accumulation between the two half of the root system were investigated.

Overall, our study suggested the potential role of citric acid in plant-adaptation to Fe deficiency and combined S and Fe deficiency (Vigani et al., 2018, Coppa et al 2018) and the rationale for such

explanation has been that citric acid is produced in mitochondria, where the assembly of Fe–S clusters also occurs (Balk and Pilon, 2011).

In addition to the aforementioned observation, it is known that an impaired organic acid metabolism (TCA cycle) in cells may stimulate a retrograde response (from mitochondria to the nucleus) (Butow and Avadhani, 2004) and it is also recognized that Target of Rapamicin (TOR) signaling pathway was found to be associated with retrograde signaling pathway in yeast and mammalian cells (Butow and Avadhani, 2004). Interestingly, in *Arabidopsis* it has been demonstrated that S deficiency results in a decreased TOR activity, with no phosphorylation of S6K protein (TOR target) (Dong et al., 2017). TOR mediated response to S deficiency includes the development of responses that are considered to occur also under other nutrients starvation, suggesting an overall role of TOR in nutrient sensing. Such responses are autophagy, lowered translation, and meristem activity inhibition (Dong et al., 2017). On these bases, we hypothesized that TOR may be involved also in plant adaptation to Fe deficiency as well as play a role in the regulation of S/Fe interplay.

Therefore, TOR activity was determined in root and shoot of tomato plants grown under single and combined deficiency of S and Fe. Moreover, TOR activity was correlated with glucose content, since reduced TOR activity under S deficiency is tightly associated with decrement of glucose content (Dong et.al 2017), and citric acid, since an endogenous variation in citric acid concentration might be involved in the regulation of Fe/S interplay (Coppa et al., 2018).

2) In order to tackle the increase of greenhouse gas emission, growing interest has been pointed on renewable energy sources and in particular to bioenergies, as an alternative to fossil fuels (DIRECTIVE 2009/28/EC). However, to satisfy the increased demand of biomasses for energy will imply to use thousands of hectares for their cultivation, generating a competition between food crops and no-food energy crops on land use (Baffes and Haniotis, 2010) and considering that, agricultural production needs to be increased in order to provide food to a growing population, the use of land for energy no-food crops, rather than for food crops, should be absolutely avoided. A suitable solution could be the use of low productive, marginal or abandoned lands for energy crops cultivation, such as soils characterized by high concentration of Cu that cannot be used for agricultural food production (Fagnano et al., 2012). However, to do that it is important to use Cu-tolerant crops and to understand the base mechanisms related to Cu-tolerance.

Plants require copper (Cu) as an essential element, being a cofactor in proteins and enzymes, but high Cu levels may be lethal or led to a drastically reduced plant growth and development, by affecting a wide range of biochemical and physiological processes, such as photosynthesis, pigment synthesis, nitrogen and protein metabolism, and membrane integrity (Luna et al., 1994; Shen et al., 1998; Nielsen et al., 2003; Demirevska-Kepova et al., 2004).

Copper accumulates in the ecosystems through natural and anthropogenic activities, but latter, mainly agricultural practices, are majorly contributing in Cu contamination of soil, being widely used as Bordeaux mixture (copper sulfate) to fight mildew in vineyards. In unpolluted soils, Cu concentration ranges between 20 and 100 mg kg^{-1} (Cao and Hu, 2000; Pietrzak and Uren, 2011), whereas in vineyards soils have been reported to range between 200 and 1000 mg kg^{-1} (Komarek et al., 2010; Pietrzak and Uren, 2011).

For vine growth and development, Cu accumulation does not represent a problem, since the root apparatus develops below the contaminated layer, and the translocation of the metal to the shoot is very low. Furthermore, Cu is commonly bound to organic matter, thus soils rich in organic matter result in a noteworthy increase of Cu adsorption, preventing plant uptake (Parat et al., 2002; Karlsson et al., 2006).

However, the pollution poses a risk to the environment or humans and, thus, these contaminated soils have to be abandoned and their use restricted to non agricultural purposes.

One of the most common effect of metal toxicity is the generation of excess reactive oxygen species (ROS). It is well known that to cope with oxidative stress, plants rely on non-enzymatic systems, other than enzymatic ROS scavengers. These comprise the antioxidants such as glutathione and cysteine (Foyer and Noctor, 2011; Sharma et al., 2019).

Thus, it is conceivable that Cu accumulation in soils may result in higher S nutritional needs for plant, and the modulation of sulfate metabolism may be involved in the Cu tolerance mechanisms. With this background, the second part of this thesis was dedicated to study the relation between S and Cu. These experiments were carried out by using as model species giant reed (*Arundo donax*, L.) plants. The rationale behind this choice was that we looked for a crop characterized by high biomass production as well as by good ability to grow in marginal lands. *Arundo donax* is a promising energy crop because of its high biomass production and its capacity to grow vigorously in marginal lands. It is indeed considered as a dangerous weed plant. Furthermore, it is the only biomass crop that has positive energy balance (assessed considering the energy costs of production

inputs and the energy output obtained by the transformation of the final product) when used for energy production (Angelini et al., 2005).

Finally, previous report showed that *Arundo donax* seems to be able to grow on Cu-contaminated soils (Elhawat et al., 2014, 2015). Thus, to evaluate the adaptive capacity and to characterize the physiological response of *Arundo donax* to artificial soil Cu-contamination, plants were grown with three different Cu levels (200, 400 and 800 ppm), and changes in S assimilation rate during the stress were recorded.

3) Salinity is considered one of the most important limiting factors for agricultural production and according to recent estimates (FAO, 2000) it currently affects 19.5% of the world's irrigated area, even if it also occurs on non-irrigated croplands. Moreover, salinity-affected areas are rapidly increasing, due to global warming, which results in both water scarcity and high evaporation rates, causing water to rise up into the soil by capillarity, dragging the dissolved salts with it, thus determining their accumulation in the upper layers of soils.

In particular, an excess of Na can limit plant growth and development by generating osmotic stress, and consequently a water deficit, and/or directly with toxic effects on biochemical processes.

One of the first consequences of plant exposure to high saline concentrations is the formation of reactive oxygen species (ROS). In order to balance the oxidized and reduced states of the cells, thereby avoiding adverse conditions, plants activate antioxidative system, which includes the S-containing metabolite glutathione (GSH), as above described for metal toxicity (Khan et al., 2014), most likely resulting in higher S nutritional requirements in plants.

On these bases, in the last part of the thesis, it has been tested the hypothesis that a close relationship might exist between Na tolerance and S assimilation rate. These experiments were carried out by using as model species olive (*Olea europaea* L.) crop and, in particular, a salt-tolerant (cv. Canino) and two its transgenic lines (Canino *At17-1* and Canino *At17-2*), overexpressing tobacco osmotin gene, and a salt-sensitive (cv. Sirole) olive cultivar. Osmotin gene could provide the salinity stress tolerance by favoring the accumulation of osmolytes, such as proline and glycine betaine (Barthakur et al. 2001; Singh et al. 1987; Subramanyam et al. 2011), which facilitate the compartmentalization of solutes reducing toxicity under salinity stress conditions (Husaini and Abdin 2008).

Olive is a typical crop of the Mediterranean basin, where soil salinization is projected to worsen as a consequence of global climate change and the availability of transgenic lines could represent a

potential and promising resource to face the challenge of climate change and higher food needs. Therefore, we compared the response of the four olive genotypes to different NaCl solutions (ranging from 0 to 200 mM).

In particular, we investigated whether the presence of osmotin gene triggered changes in proline accumulation and on lipid peroxidation (as an estimate of oxidative damage).

Furthermore, since GSH plays an active role in the process of response to salinity, we tested the hypothesis that a close relationship might exist between salt tolerance and S assimilation rate. Thus, changes in thiols levels as well as in extractable activities of ATPS and OASTL, the first and the last enzyme of S assimilation pathway, respectively, have been estimated in plants exposed to salt stress.

Chapter 2

Single and combined Fe and S deficiency differentially modulate exudomic profile in tomato: a double strategy for Fe acquisition?

In submission to International Journal of Molecular Sciences as "*Single and combined Fe and S deficiency differentially modulate exudomic profile in tomato: a double strategy for Fe acquisition?*", S. Astolfi, Y. Pii, T. Mimmo, L. Lucini, B. Miras-Moreno, M. Trevisan, E. Coppa, S. Violino, S. Celletti, S. Cesco.

Abstract

Fe chlorosis is considered one of the major constraints to crop growth and yield worldwide, being particularly worse when associated with S shortage since Fe and S nutrition are tightly linked. Plant adaptation to an inadequate nutrient availability often relies on the release of root exudates that enhance nutrients mobilization from soil colloids and favour their uptake by roots. This work aims at characterizing the exudomic profile of hydroponically grown tomato plants subjected to single or combined Fe and S deficiency, as well as at shedding light on the regulation mechanisms underlying Fe and S acquisition processes by plants.

Root exudates have been analysed by untargeted metabolomics, through liquid chromatography mass spectrometry as well as gas chromatography mass spectrometry following derivatization.

More than 200 metabolites could be putatively annotated. Venn diagrams show that 23%, 10% and 21% of differential metabolites are distinctively modulated by single Fe deficiency, single S deficiency or combined Fe-S deficiency, respectively. Interestingly, for the first time, a mugineic acid derivative is detected in dicot plants root exudates.

Results seem to support the hypothesis of a co-existence of the two Fe acquisition strategies in tomato plants.

Keywords: metabolomics; mugineic acid; iron; nutrient deficiency; nutrient interaction; phytosiderophores; root exudates, sulfur; strategy I; strategy II.

2.1. Introduction

Nowadays, in order to meet the challenge of a food safety in a context of an ever growing human population and of an ever decreasing global arable-land surface (also as a consequence of the climate change), the use of marginal agricultural land (characterized by unfavourable soil mineral

composition, nutrients unbalance, water scarcity, acidity, salinization, etc. [1], could be particularly strategic. In this respect, it should be highlighted that nutrients availability is often one of the major limitations to the expression of the best productive capacity of the cultivated plants species; unfortunately, this phenomenon is often evident also in the so-called fertile soils [2]. In these limiting conditions the agronomical practice of fertilization is essentially the only strategy usable to cope with the problem. However, the decline in the availability of the natural resources at the base of the fertilizers production [3] is becoming increasingly worrying from a long-term point of view. This context is made even more complicated by the growing global demand for fertilizers due to the agricultural progress of the developing countries [4]. All these aspects clearly show how much could be unsustainable in a long period a form of agriculture as implemented today. For these reasons, the possibility of cultivating plant species particularly efficient in the exploitation of the nutritional resources already present in the soils, appears particularly strategic and urgent. In fact, the limitation of the environmental [5] as well as the economic [4] impact of agriculture related to a massive use of fertilizers appears to be one of the priorities. However, in order to meet this challenge, the understanding of the mechanisms underlying the acquisition processes of each single nutrient by roots is surely of pivotal role. In this context, it should be also noted that in this last decade a sort of interconnection between nutrients affecting the whole mineral nutrition process of a crop has been clearly well demonstrated (see also Sambo et al., [6]). In particular, the lack (deficiency) or excessive (toxicity) availability of a single nutrient is typically coordinated with the demand levels of other nutrients [7-10]. For this reason, it appears clear that the use efficiency of a single nutrient does not depend exclusively on its own levels of availability in the growth medium. At the field scale this aspect is particularly crucial for the efficacy of a fertilization plan of a crop. Therefore, the adoption of an approach that considers the availability of nutrients as a whole becomes essential for a more complete understanding of the plant mineral nutrition process of crops as well as for the exploitation of this agronomic practice in a contest of a smart and more sustainable agriculture. Moreover, the identification/characterization of the sensing and signalling pathways activated in crops (as a consequence of the nutrients availability fluctuations in a context of coordinated levels on nutrients demand) is equally fundamental. In this respect, it should be noted that in the last decade a specific mutual interaction between Fe and S has been clearly demonstrated in a wide variety of crops [11-15] having an impact not only at the level of acquisition processes of the two nutrients but also affecting reciprocally their assimilation pathways. Regarding this latter aspect, it is illustrative to mention the Fe biofortification of wheat grain gained through an over

sulfate fertilization [16]. In this context, the recent environmental policies that have led to the reduction of S-rich industrial emissions, decreasing therefore the free S deposition at the soil with a consequent and progressive S depletion in the arable soil [17], have aroused even more interest in this mutual Fe/S interaction. The expected further decrease in soil S contents in the next future will further contribute to stimulate interest in this regard. This aspect is even more intriguing if we consider that, differently from S, Fe is abundantly present in soils, although its available fraction is very often insufficient to guarantee a balanced growth of the crop [18,19].

Plant adaptation to an environment characterized by an inadequate nutrient availability is a process relying on several and often sophisticated strategies aimed at enhancing the nutrients mobilization from soil minerals and at favouring their acquisition by roots. These strategies include also the release of root exudates (a mixture of organic acids, phenolic compounds, sugars, vitamins, amino acids, inorganic molecules, enzymes, and root border cells, [19,20] directly involved in the biogeochemical cycles of nutrients in soils [21]. Once synthesized inside the plant cells, they are then released by roots into the rhizosphere through diversified root exudation mechanisms [22,23]. From the agronomic point of view an example of their function is represented by the root secretion of extracellular enzymes that, via the *mineralization* process within the organic matter cycle, can significantly increase the rhizosphere availability of nutrients like N, P, S and metals previously preserved in the organic matrix [23]. Differently, based on the different solubility of nutrients in soil minerals, the acidification or alkalinisation of the rhizosphere as a consequence of the root release of exudates like H^+, HCO_3^-, organic acids, etc. can considerably favour or hinder the mobilization process of different nutrients/elements like P, K, Fe, Zn, etc. [24,25]. In this respect, also the enhanced exudation of organic ligands like phytosiderophores and organic acids with high affinity for elements/metals (such as Fe) can have a very positive impact on the metal mobilization (mineral weathering) [19,26-28]. With respect to the organic acids, it should be mentioned that they can also impact on the rhizosphere processes and the fertility levels of this soil volume through their direct effect on the microbial biomass and its activity [29,30].

In particular with respect to Fe, it has been clearly shown that root exudates are involved in both adaptative mechanisms (FeIII-reduction-based *Strategy I* of dicots and FeIII-phytosiderophore complexes-based *Strategy II* of grasses*)* developed by plants in order to guarantee the Fe homeostasis in the different tissues [31] and some studies have shown that the composition of root exudates can change significantly as a function of the diverse levels of Fe availability [32-35]. However, despite the mutual interaction between Fe and S is well documented for the uptake

mechanisms of the respective nutrients [11-15] , to our knowledge there are still no indications regarding the role of this phenomenon in the exudate composition. From a general point of view, it is reasonable to hypothesize an effect of the variable S availability on the exudative pattern of roots with consequent adjustments of the organic compound fluxes in the soil. This aspect is particularly relevant considering that the potential capacity of the roots to modify effectively the rhizosphere to their own advantage depends on the quali-quantitative composition of exudates [20,22,23]. Moreover, considering that at the field level the onset of S deficiency symptoms is not only increasingly likely in the next future but also, when present, at greater gravity extent, it appears evident how crucial is the characterization and comprehension of this phenomenon.

Therefore, on the basis of these premises, in the present work the root exudation pattern as well as the chemical composition of these exudates have been evaluated using tomato plants exposed to different levels of nutrient availability, i.e. single Fe, single S, or combined Fe-S deficiency. Results suggest that the pool of metabolites released in the rhizosphere, belonging to the primary and secondary metabolism, is considerably adapted to the diverse external nutrient conditions, i.e. the single deficiency of Fe or S, or the combination of both Fe-S deficiencies.

2.2 Materials and methods

2.2.1 Experimental conditions and treatments

The experiment was conducted with hydroponically grown tomato (*Solanum lycopersicum* L. cv. Marmande) plants. Seeds were germinated for six days in darkness at 28°C and, after germination, uniform seedlings were transferred to plastic pots (6 seedlings per pot) containing 2.2 L of nutrient solution [73] for seven days, being exposed to 1.2 mM sulfate and 40 μM Fe^{III}-EDTA. Plants were then transferred for further nine days to four different nutritional conditions (control, C, 1.2 mM sulfate and 40 μM FeIII-EDTA; Fe deficiency, F, 1.2 mM sulfate and 0 μM FeIII-EDTA; S deficiency, S, 0 mM sulfate and 40 μM FeIII-EDTA; dual deficiency, D, 0 mM sulfate and 0 μM FeIII-EDTA).

In S-free nutrient solution, sulphate salts (K^+, Mn^{2+}, Zn^{2+}, Cu^{2+}) were replaced by appropriate amounts of the corresponding chloride salts (K^+, Mn^{2+}, Zn^{2+}, Cu^{2+}). Nutrient solution was continuously aerated and changed every 3 days. Plants were grown in a growth chamber under 200 μmol photons m^{-2} s^{-1} PPF and 14h/10h day/night regime (27/20 °C day/night temperature cycling; 80% relative humidity). Both leaves and roots were harvested 16 days after transfer in nutrient solution.

2.2.2 Collection of root exudates

Root exudates were collected nine days after imposition of various treatments (C, F, S and D). Briefly, tomato plants were removed from the nutrient solution and the roots were carefully washed for 30 min in 2 L of deionised water. Then, root systems of four plants from each condition (about 0.5 g root fresh weight) were immersed into 10 mL deionised water for 6 hours under continuous aeration. Thereafter, Micropur (10 mg l^{-1}) (Roth, Karlsruhe, Germany) was added to prevent microbial degradation of organic compounds.

2.2.3 Metabolomic profiling by UHPLC/QTOF-MS

Root exudates were filtered through a 0.22 μm cellulose membrane into an amber vial for analysis. The profile of metabolites was determined through UHPLC liquid chromatography with quadrupole-time-of-flight mass spectrometry (UHPLC/QTOF-MS). In more detail, a 1290 series LC system equipped with a binary pump, an JetStream Electrospray source and a G6550 iFunnel QTOF mass spectrometer (Agilent technologies, Santa Clara, CA, USA) were used as previously reported [74]. Briefly, the QTOF acquisition was carried out in positive SCAN mode (100–1200 m/z range) and a chromatographic gradient reverse phase separation was achieved using water and methanol as eluents on an Agilent Zorbax Eclipse-plus column (75 × 2.1 mm i.d., 1.8 μm). The injection volume was 3.5 μL and flow rate was 220 μL min^{-1} [75]. Features deconvolution as well as the following mass and retention time alignment were carried out in Profinder B.06 (from Agilent Technologies). Compound annotation was based on accurate mass (mass accuracy < 5 ppm), isotope spacing and isotope ratio, against a custom database produced by combining compounds exported from PlantCyc 9.6 (Plant Metabolic Network, http://www.plantcyc.org; accessed April 2017), Phenol-Explorer 3.6 (http://www.phenol-explorer.eu; accessed April 2017), as well as additional compounds taken from literature and that might be present in root exudates. Based on the approach used, the annotation level corresponded to Level 2 (putatively annotated compounds) of COSMOS Metabolomics Standards Initiative (http://cosmos-fp7.eu/msi.html).

2.2.4 Metabolomic profiling by GC/MS

A further gas chromatography mass spectrometry (GC/MS) analysis [76] was also applied to achieve complementary information about chemical profiles in root exudates. Briefly, an aliquot (200 μL) of root exudate was dried overnight in a speed vacuum concentrator. Thereafter, 60 μL

of 2% methoxyamine hydrochloride (Sigma-Aldrich, St Louis, MO, USA) in pyridine, 90 µL of N-Methyl-N-(trimethylsilyl)trifluoroacetamide and 1% trimethylchlorosilane (Sigma-Aldrich) were added for derivatization purposes [77]. Finally, the samples were transferred into vials to be analysed.

An Agilent 6890 gas chromatograph coupled to an Agilent 5977 quadrupole mass spectrometer were used for GC/MS analysis. Chromatographic separation was done on a 30 m DB-5MS capillary column. Derivatized extracts were injected in splitless mode (250 °C), and helium (1 ml/min) was used as carrier gas. The oven temperature program started from 100 °C (maintained for 2 min) up to 325 °C at 10 °C min^{-1}. A fatty acid methyl ester mixture (FAME mix, Agilent Technologies) was used to calculate retention indexes. Deconvolution was done using the software 'Unknown Analysis' (Agilent Technologies) and identification was based on spectral comparison against the 'Fiehn Library' (Agilent Technologies, released May 2016).

2.2.5 Bioinformatics analysis

The *TOM* sequences of *Hordeum vulgare* (*HvTOM1*) and *Oryza sativa* (*OsTOM1*, *OsTOM2* and *OsTOM3*) were used to obtain *SlTOM* homologues by an amino acids sequence BLAST analysis, using the *Solanum lycopersicum iTAG2.4* genome provided by Phytozome (http://phytozome.jgi.doe.gov/pz/portal.html). Similarly, the Yellow Stripe-like (YSL) protein sequences from *Hordeum vulgare*, Zea mays, *Oryza sativa and Arachis hypogea* were used to obtain *SlYSL* homologues by an amino acids sequence BLAST analysis, using the *Solanum lycopersicum iTAG2.4* genome. Subsequently, multiple sequence alignments were run by CLUSTALW algorithm (http://clustalw.ddbj.nig.ac.jp/) and the phylogenetic trees were obtained using FigTree (http://taxonomy.zoology.gla.ac.uk/rod/treeview.html) for both TOM and YSL transporters.

2.2.6 Extraction of total RNA, cDNA preparation and expression analyses

Total RNA was extracted from frozen tomato root tissues using the Spectrum Plant Total RNA Kit (Sigma Aldirch). Then, 1 µg of RNA was treated with 1u of DNAse RQ1 (Promega, Madison, WI, USA). The cDNA synthesis was performed using ImProm-II Reverse Transcription System (Promega, Madison, WI, USA). Quantitative Real-Time RT-PCR was performed using gene-specific primers (approximately 20 nt-long), amplifying fragments of about 100 bp (Supplementary Table 1). The specificity of each primer was tested firstly performing a BLAST directly on the

tomato genome mRNA prediction and subsequently carrying out the melting curve. The elongation factor and the ubiquitin primers were obtained by Vigani *et al.*, [14] . The Real-Time RT PCR was performed using SsoFast EvaGreen Supermix (Bio-Rad), the Qiagen Rotor Gene Q Real-Time PCR. The amplification efficiency was obtained through LinReg PCR [78] and the relative expression and the standard error was calculated according to Paffl, Horgan and Dempfle [79].

2.2.7 Other measurements

The measurements of chlorophyll levels per unit area were estimated in attached leaves with a non-destructive portable apparatus, the SPAD chlorophyll meter (Minolta Co.), using the youngest fully expanded leaf from the top of each plant and presented as SPAD units.

2.2.8 Statistical analysis

Each reported value represents the mean ± SD of measurements carried out in triplicate and obtained from four independent experiments. Statistical analyses of data were carried out by ANOVA with the GraphPad InStat Program (version 3.06). Significant differences were established by posthoc comparisons (HSD test of Tukey) at $P < 0.01$.

Both GC/MS and UHPLC/QTOF-MS metabolomics data were interpreted in Agilent Mass Profiler Professional B.12.06 (from Agilent Technologies). Post-acquisition processing included normalization at the 75th percentile and baselining to the median of the control. Unsupervised hierarchical cluster analysis (Euclidean similarity, 'Wards' linkage rule) was formerly carried out on the basis heatmaps generated from fold-change values. Thereafter, Partial Least Squares Discriminant Analysis (PLS-DA) supervised modelling was also done. The metabolites having the highest discrimination potential, based on model prediction scores on first and second latent vectors, were identified. Analysis of variance (one-way ANOVA, Benjamini-Hochberg multiple testing correction) and fold-change analysis (cut-off: 3-folds) were finally done in Mass Profiler Professional.

Chemical Similarity Enrichment Analysis (ChemRICH) was performed, as previously described [37]. The online web-app tool (http://chemrich.fiehnlab.ucdavis.edu) was used for this purpose. Therein, Tanimoto substructure chemical similarity coefficients were used to cluster metabolites into non-overlapping chemical groups.

2.3 Results

2.3.1 Plant growth features

All nutrient deficiency treatments significantly affected the growth features of tomato seedlings (Fig. 1 and 2). Single Fe deficiency (F) did not affect plant growth, but resulted in strong decrease of chlorophyll content, estimated as SPAD units (-45%, with respect of control condition). Single S deficiency (D) resulted in notable increase of root apparatus development (+33% with respect of control condition). On the other hand, the variables affected by combined Fe and S deficiency (D condition) included root growth, that was increased by 42% and chlorophyll content, that was reduced by 24%.

2.3.2 Metabolomic profiling of root exudates

Root exudates of tomato plants were collected 9 days after the treatments, by submerging roots in a water-based trap solution, as previously described [34,36]. Root exudates were thereafter subjected to untargeted metabolomic analyses through complementary GC-MS and UHPLC/QTOF-MS approaches. The PLS-DA multivariate modelling carried on the dataset obtained through GC-MS technique highlighted four independent clusters (Fig. 3a). A similar clustering pattern was also obtained from UHPLC/QTOF-MS profiles, even though in this case S and C conditions were partially overlapping (Fig. 3b). PLS-DA accuracy, following N-fold validation (N=3) was 100% for both GC-MS and UHPLC/QTOF-MS modelling.

The Volcano Plot statistical analysis carried out on GC-MS data highlighted 124, 124 and 124 differentially represented metabolites in the root exudates of F, S and D plants, respectively, as compared to C plants (Supplementary Table 2). The complete list of metabolites is provided as supplementary material (Supplementary Table 3). Within the metabolites differentially represented in the exudates of F plants, 58 were up-accumulated and 66 down-accumulated as compared to C plants (Supplementary Table 2). In the case of S and D plants, the majority of the differentially regulated metabolites were down-accumulated (89 and 83, respectively), whilst only 35 and 41 were over-represented as compared to control plants (Supplementary Table 2). Among the up-accumulated metabolites, 14 were released in all the physiological conditions, whereas 23, 2 and 11 were characteristic for F, S and D plants, respectively (Fig. 4a). On the hand, 46 metabolites were commonly down-accumulated in all the stress conditions imposed, whilst the lack of 7, 9 and 12 metabolites was a distinctive feature of F, S and D plants, respectively (Fig. 4b).

The UHPLC/QTOF-MS technique allowed the identification of 93, 93 and 83 differentially represented metabolites in the root exudates of F, S and D plants, respectively, as compared to C plants (Supplementary Table 4). The profile of differentially represented metabolites in F and D conditions was similar; in fact, we observed 44 and 49 up-accumulated metabolites and 49 and 44 down-accumulated metabolites, as compared to control, in F and S plants, respectively). In the case of D condition, 47 and 36 metabolites were up- and down-accumulated, respectively. Within the group of up-accumulated metabolites, 22 were over-represented in all the physiological conditions with respect to control, whereas 11, 8 and 13 were characteristic for F, S and D plants, respectively (Fig. 4c). On the contrary, 18 metabolites were commonly down-accumulated in all the nutritional conditions as compared to controls, whilst the reduction of 10, 2 and 9 metabolites was a distinctive feature of F, S and D plants, respectively (Fig. 4b).

2.3.3 ChemRICH set enrichment analysis

Due to the large data set provides by metabolomics approach, clustering metabolites is a method to obtain a deeper insight in the biological processes. In this study, encoded chemical structures were used to clusterized and define the metabolites. Since some compounds are not yet classified in chemical ontologies, chemical similarity to clustering the principal classes of metabolites is emerging as a powerful tool.

In these sense, Tanimoto substructure chemical similarity coefficients were used to cluster metabolites into non-overlapping chemical groups to better understand the complexity of the metabolite signatures [37] . ChemRICH set enrichment statistics plot identified different chemical clusters being phenols, coumaric acids and amino acids the most represented cluster in root exudates under all conditions (Fig. 5). All the treatment showed a similar profile of characteristic metabolites (Supplementary Table 5), in terms of abundance and statistical significance. Nevertheless, different accumulation patterns of the represented chemical classes could be described. In particular, flavones were over-represented in F and S plants (Fig. 5a, b) and down-accumulated in the double deficiency (D) condition (Fig. 5c), whereas carotenoids increased in the root exudates of Fe deficient plants (F) and decreased in those of S deficient and double deficient plants (Fig. 5). In the root exudates of F and D plants, an increase in the concentration of caffeic acids was also detected, while saturated fatty acids decreased in F condition and increased in S and D (Fig. 5). Phenols, coumaric acids, flavonoids, amino acids, and coumarins resulted always up-accumulated in all the nutritional conditions considered (*i.e.* F, S and D) as compared to C

conditions (Fig. 5), albeit to a different extent. Interestingly, the secretion of coumarins by roots of D plants was enhanced than under F and S condition, whereas total free amino acid concentration increased in F and S plants with respect to the D ones (Fig. 5). In particular, 11 amino acids were identified in root exudates of tomato plants, and changes associated with single or combined Fe and S deficiency were detected (Fig. 6). Up-accumulation was recorded for serine, allothreonine and isoleucine, whereas down-accumulation was observed for norleucine and leucine, irrespective of the nutritional teatment (Fig. 6). The main change in plants grown in Fe-deficient medium, relative to plants grown in S and D condition, was the up-accumulation of the amino acids GABA, beta-glutamic acid and glycine (with increases of 6.7-, 5.1- and 16.3-folds than control, respectively) (Fig. 6). On the other hand, the main change in plants grown in S-deficient medium, relative to plants grown in F and D condition, was the up-accumulation of the amino acids homoserine and glutamic acid, with 2.1-fold and 8-fold increases as compared to control, respectively (Fig. 6). Interestingly, in tomato root exudates, hydroxymugineic acid was found and, more importantly, it was found to be down-regulated under both F and S condition, with 4-fold lower concentrations than control (Fig. 6). Finally, changes associated with combined deficiency (D) followed F or S pattern, even if at different extent, but the abundance of hydroxymugineic acid was similar to that of control (Fig. 6).

2.3.4 Bioinformatics and gene expression analysis

Genes putatively encoding orthologous *TOM1* transporters in *Solanum lycopersicum* genome were identified on the base of amino acid sequence similarity with members of TOM1 transporters family in other organisms, like *Hordeum vulgare* and *Oryza sativa*, by running a Blastp analysis [38] in the *Solanum lycopersicum iTAG2.4* genome provided by Phytozome (http://phytozome.jgi.doe.gov/pz/portal.html). This approach allowed the retrieval of four transcripts, namely *Solyc01g096730.2.1*, *Solyc01g096720.2.1*, *Solyc01g096740.2.1* and *Solyc10g076940.1.1* (Supplemental Fig. 1). The phylogenetic analysis and a pairwise alignment highlighted that the sequences *Solyc01g096730.2.1* and *Solyc01g096720.2.1* identified the same transcript, therefore only *Solyc01g096730.2.1* was considered for the further molecular analyses (Supplemental Fig. 1). In order to understand whether the transcripts putatively encoding *SlTOM1* orthologous genes, *Solyc01g096730.2.1, Solyc01g096740.2.1* and *Solyc10g076940.1.1* (hereafter referred to as *SlTOM1.1, SlTOM1.2* and *SlTOM1.3*, respectively), might be involved in the plant responses to the different nutritional regimes, quantitative real time RT-PCR analyses were run.

The expression of both *SlTOM1.1* and *SlTOM1.3* was significantly upregulated by about three to four times in S and D nutritional regimes (Fig. 7a, c). On the contrary, the expression of *SlTOM1.2* was strongly reduced by the lack of sulfur in the growth medium (S condition), whilst the double deficiency did not modulate the gene transcription (Fig. 7b). Noteworthy, the Fe deficiency condition did not induce the transcriptional regulation of any of the three *SlTOM1* genes (Fig. 7).

The Yellow Stripe-like (YSL) protein sequences of *A. thaliana*, *O. sativa*, *Z. mays* and *Arachis hypogaea* have been used to isolate putative *YSL* orthologous transcript in the tomato *iTAG2.4* genome by running a Blastp analysis [38]. The analysis allowed the isolation of nine transcripts, namely *Solyc08g083060.2.1*, *Solyc09g074960.1.1*, *Solyc03g031920.2.1*, *Solyc02g005340.2.1*, *Solyc05g053110.1.1*, *Solyc03g082620.2.1*, *Solyc05g053110.1.1*, *Solyc02g094280.2.1* and *Solyc02g081570.2.1*, which have been subjected to multiple alignment and phylogenetic analysis. The phylogenetic tree displayed that one member (*i.e. Solyc08g083060.2.1,* hereafter referred to as *SlYSL1*) of this multigenic family of tomato had a high similarity with *AhYSL1* (Supplemental Fig. 2), which has already been characterized for its expression in the root tissues (epidermis/exodermis) of Fe deficient peanut plants [39]. In addition, *AhYSL1* was also hypothesized to transport the Fe-DMA complexes inside peanut roots [39]. The quantitative real time RT-PCR analyses showed that *SlYSL1* expression was not modulated in S and D conditions in comparison with control roots (Fig. 7d). On the other hand, a significant downregulation (about 50% reduction) was observed in plants grown in a Fe deficient nutritional regime (F) when compared to control plants (Fig. 7d).

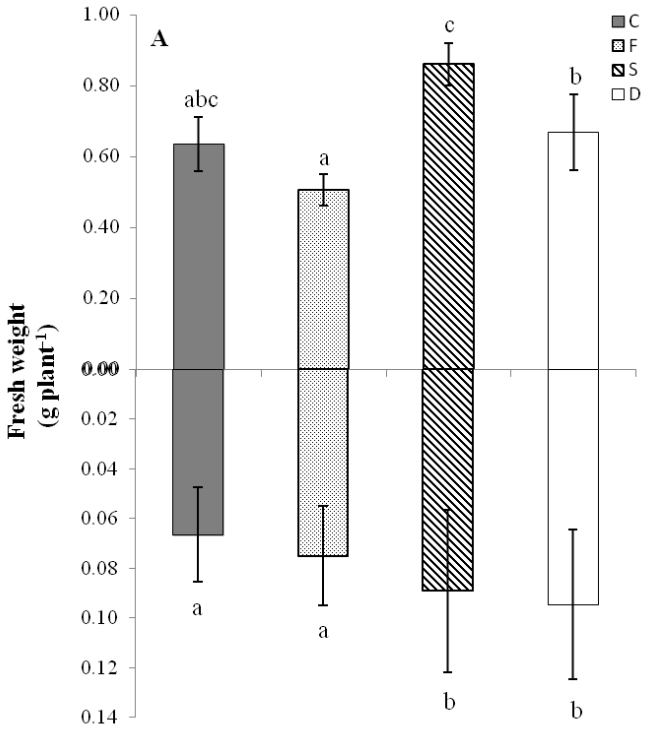

Figure 1. Biomass accumulation of tomato plants. Shoot (**a**) and root (**b**) fresh weight (g plant^{-1}) of tomato plants subjected to different nutritional treatments (C=control, F=Fe deficiency, S=S deficiency, D=dual deficiency). Data are means ±SD of six independent replicates run in triplicate. The statistical significance has been tested by a one-way ANOVA test with Tukey post-test. Significant differences between samples are indicated by different letters (p<0.01).

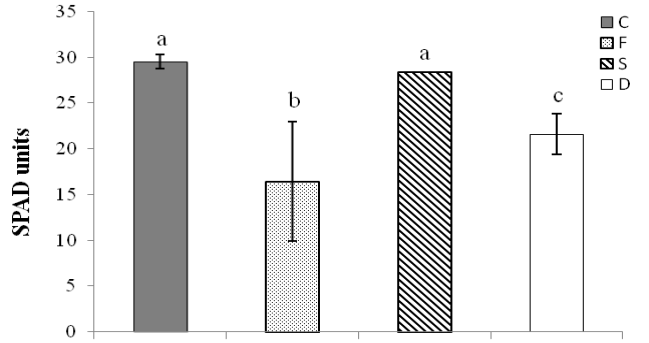

Figure 2. Chlorophyll content in tomato leaves. Changes in chlorophyll levels, evaluated as SPAD units, in leaves of tomato plants subjected to different nutritional treatments (C=control, F=Fe deficiency, S=S deficiency, D=dual deficiency). Data are means ±SD of six independent replicates run in triplicate. The statistical significance has been tested by a one-way ANOVA test with Tukey post-test. Significant differences between samples are indicated by different letters (p<0.01).

A

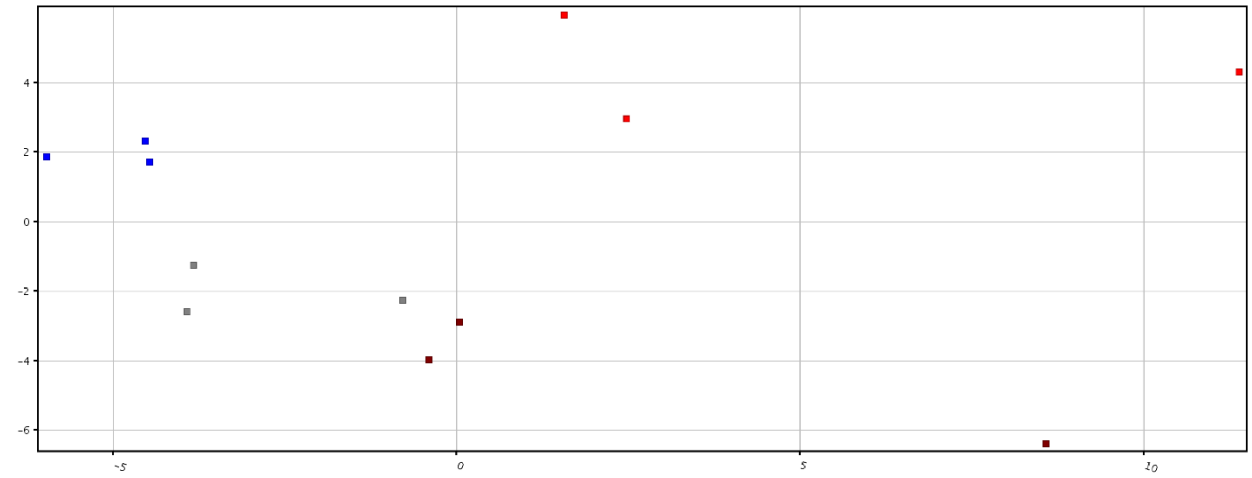

B

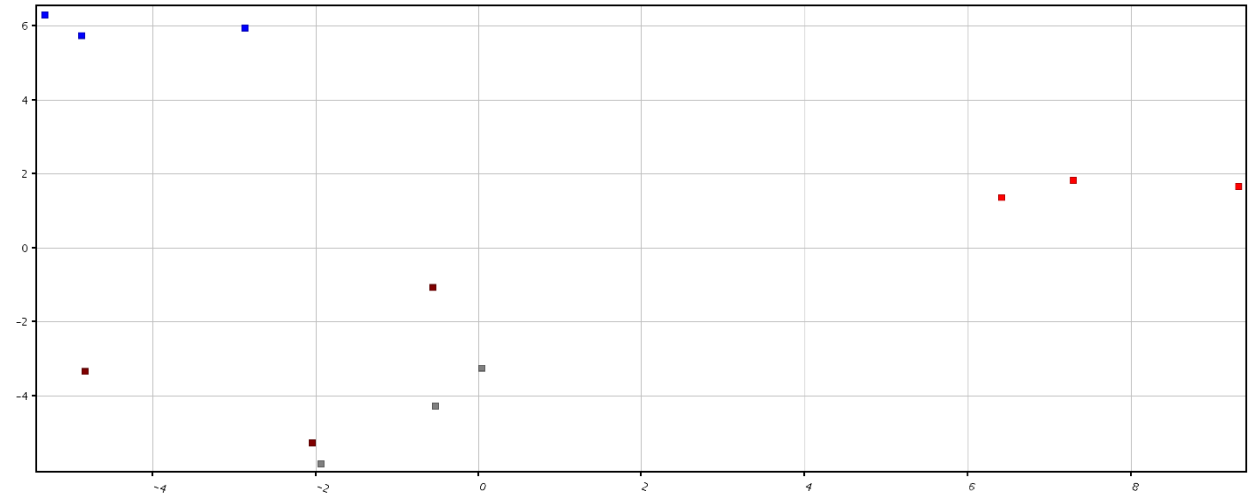

Figure 3. Partial Least Squares Discriminant (PLS-DA) multivariate modelling from the dataset obtained through GC-MS (A) and UHPLC/QTOF-MS (B) analysis in the root exudates of plants exposed to the different nutritional conditions (Grey=Control, Blue=Fe deficiency, Brown=S deficiency, Red=dual deficiency).

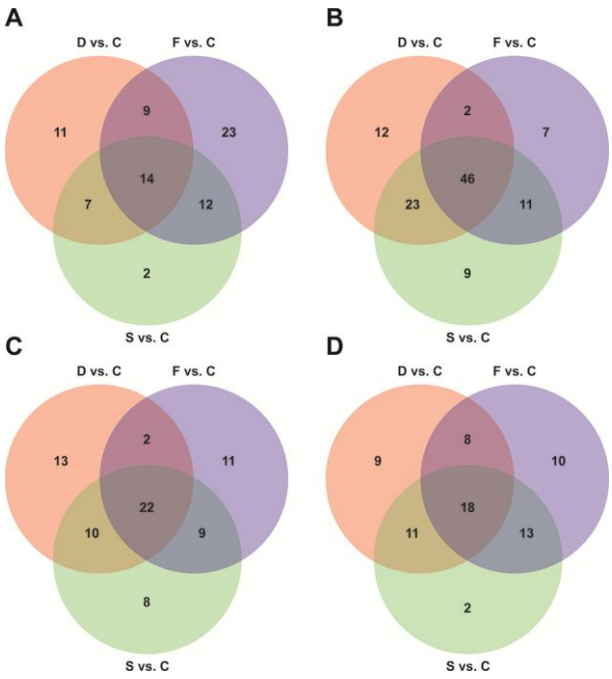

Figure 4. Venn diagrams representing the differentially represented metabolites detected in the root exudates of plants exposed to the different nutritional conditions. **A**. Number of up-regulated metabolites detected by GC-MS techniques and normalized on control samples. **B**. Number of down-regulated metabolites detected by GC-MS techniques and normalized on control samples. **C**. Number of up-regulated metabolites detected by HPLC-MS techniques and normalized on control samples. **D**. Number of down-regulated metabolites detected by HPLC-MS techniques and normalized on control samples.

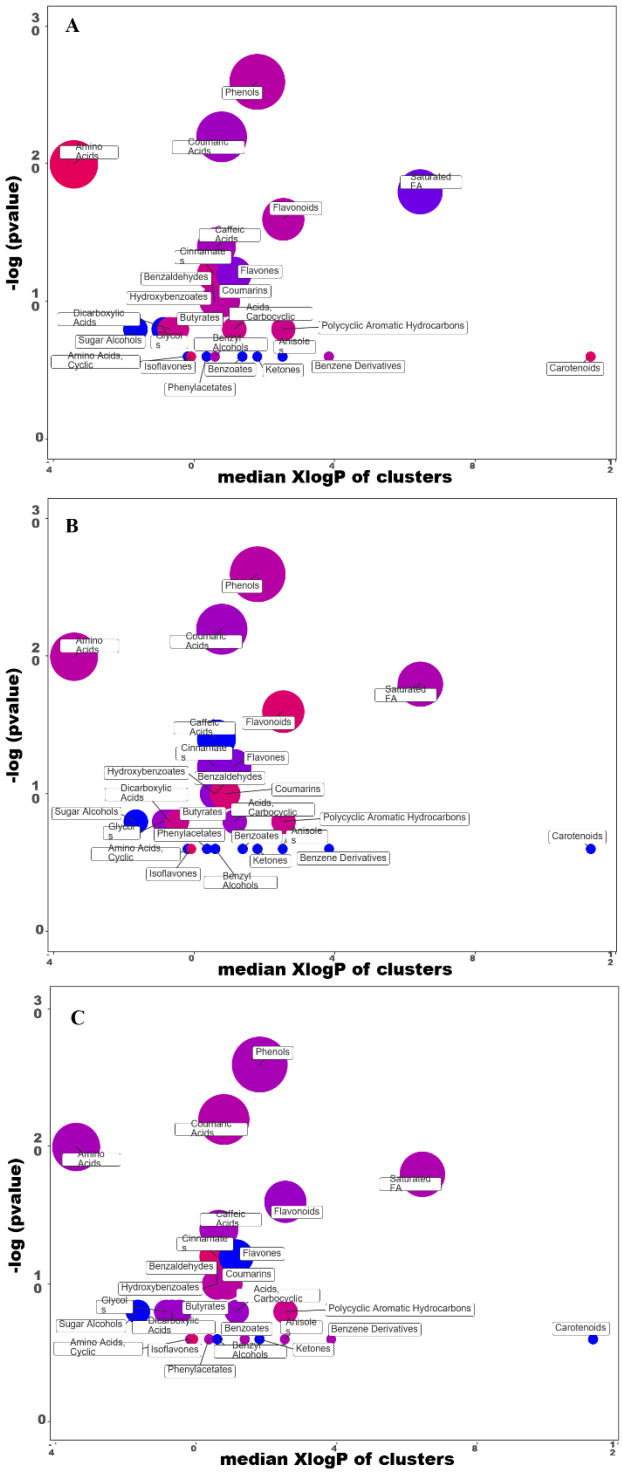

Figure 5. Chemical similarity enrichment analysis (ChemRICH diagrams) of the metabolites found in plants under Fe deficiency (**A**), S deficiency (**B**) and dual deficiency (**C**), as obtained by UHPLC/QTOF-MS and GC-MS. Color is according to proportion of increased or decreased compounds (red = increased, blue = decreased, pink = mixed) within each cluster.

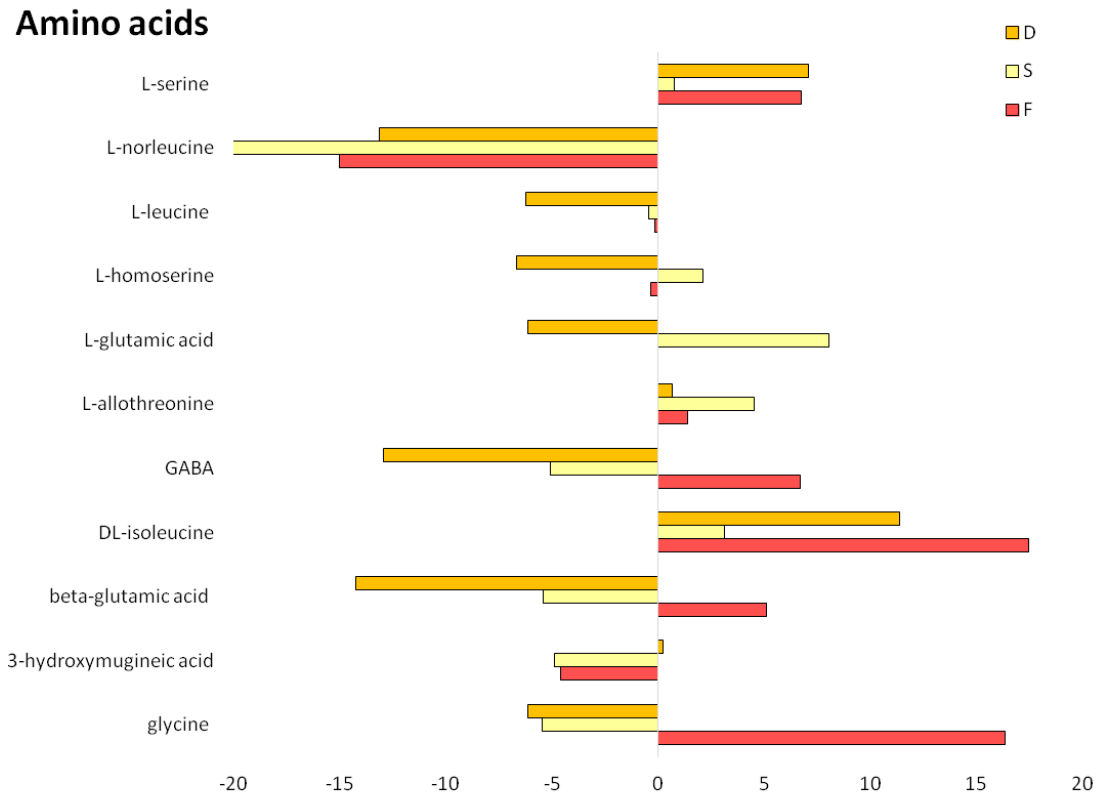

Figure 6. Changes in amino acids release induced by different nutritional regimes
Amino acids in root exudates from tomato plants subjected to different nutritional treatments (C=control, F=Fe deficiency, S=S deficiency, D=dual deficiency). The figure shows metabolites that change significantly in F, S or D condition with respect to control samples (*P<0.001) and changes are expressed as fold changes (treatment/control ratio).

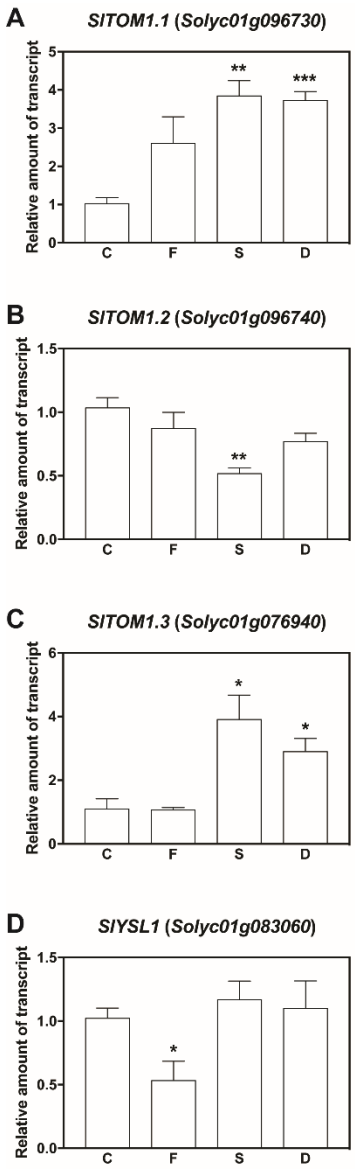

Figure 7. Gene expression analyses in the root tissue of tomato plants subjected to different nutritional regimes. The levels of expression of *SlTOM1.1* (**A**), *SlTOM1.2* (**B**), *SlTOM1.3* (**C**) and *SlYSL1* (**D**) were assessed by quantitative Real Time RT–PCR. The data were normalised to two internal controls, Tomato *LeEF-1* mRNA for elongation factor 1 alpha and Tomato *ubi3* gene for ubiquitin. The relative expression ratios were calculated using C plants as a calibrator sample. The values reported are means ± SE (n = 3). The statistical significance was tested by means Student's t test (*, $p<0.05$; **, $p<0.01$; ***, $p<0.001$).

2.4 Discussion

The root acquisition of both iron (Fe) and sulfur (S) has been extensively studied in crops, being these two nutrients crucial for the vegetative development of the plants and fundamental for the qualitative and quantitative features of their edible parts [40]. Considering the progressive depletion of S in the arable soil, ascribable to the reduction of S-rich industrial emissions [17,41], this topic is attracting a very high attention. Interestingly, studies in the literature have also provided evidence that Fe and S nutrition are tightly linked; in fact, S is required for the biosynthesis, among other compounds, of the amino acid methionine, which is the precursor of both nicotianamine (NA) and mugineic acid (MA) [42]. Indeed, this latter, together with its derivatives (*i.e.* phytosiderophores - PS), is a key elements in the Fe acquisition mechanism in Strategy II plants [31], whereas NA, along with citric acid, is required in both monocots and dicots for the chelation and the translocation, of Fe within plant tissues [43]. Furthermore, S shortage has been also shown to limit the onset of Fe deficiency response in dicot plants as tomato [44]. Consistently, it has been demonstrated that a super-optimal S provision can help recovering the Fe deficiency symptoms in wheat, *i.e.* a monocot plant species, *via* an improved Fe use efficiency within the plant [45].

Results here presented show that imposition of Fe shortage significantly reduced the levels of chlorophyll content (Fig. 2), whereas single S deficiency both in single and combined (S and Fe) condition (S and D condition, respectively) increased root growth (Fig. 1). Leaf chlorosis is a typical phenomenon associated with Fe deficiency [40], whereas the increased development of root apparatus reflects a classical response to S limitation, as extensively reported in literature [46]. Moreover, Fe deficiency (F condition) also limited the biomass accumulation at the shoot level (Fig. 1), as previously described [44].

Despite previous studies have widely demonstrated that root exudation is a fundamental tool adopted by plants to directly shape the rhizosphere favoring the root Fe acquisition [34,47,48], the knowledge about the root exudation pattern of S deficient plants is rather limited. Furthermore, although the relationship between Fe and S uptake has been clearly demonstrated [11-15], to the best of our knowledge information concerning the exudation profiles of plants exposed to single S deficiency or combined Fe and S deficiency is still missing. Interestingly, Astolfi *et al.* [49] demonstrated that S starvation strongly limits the release of PSs in Fe deficient barley plants,

suggesting that the intracellular S levels most likely have an impact on the qualitative and quantitative root exudation pattern.

An untargeted metabolomic approach was undertaken using the complementary GC-MS and UHPLC/QTOF-MS techniques combined with multivariate statistical analysis methods, to acquire and analyze the exudomic profile of tomato plants subjected to Fe and S deficiency, alone or in combination. Interestingly, the PLS-DA score plots described 4 independent clusters, according with the different nutritional regimes: control (C), single Fe (F) and S deficiency (S) and combined Fe and S deficiency (D) (Fig. 3). However, exudate profile of S condition was similar to that of control (Fig. 3). These results strengthened the finding that both single Fe and S, and combined Fe-S starvations induced a clearly distinct response, as previously reported at transcriptomic [50-51] and metabolomics [12] levels. Venn diagrams following Volcano analysis ($P< 0.001$, fold-change cut-off=3) showed that the majority of the differentially represented metabolites were shared between the nutritional condition imposed (100 metabolites) (Fig. 4). Furthermore, it revealed that 23% (51), 10% (21) and 21% (45) of differential metabolites were distinctively and significantly modulated by single Fe, single S and combined Fe-S deficiency, respectively (Fig. 4). This study clearly confirms that plant roots secrete a wide range of compounds when exposed to a nutritional stress, improving the edaphic conditions (e.g. nutrient availability) in the rhizosphere. However, the types and the concentrations of the compounds released by the roots are considerably different between the four treatments. In this respect, it is intriguing to note that single Fe deficiency had a more pronounced impact on exudomic profile than that induced by S or the combined Fe-S deficiency.

Due to the large data set provided by the metabolomic study, an approach of data reduction based on the clustering by classes has been used in this work. Therefore, the encoded chemical structures were used to clusterized and define the different metabolites. Since some compounds are not yet classified into chemical ontologies, chemical similarity enrichment has been selected to cluster the principal classes of metabolites. With this regard, Tanimoto substructure chemical similarity coefficients were used to cluster metabolites into non-overlapping chemical groups in order to better understand the complexity of the metabolite signatures. Statistical significance was evaluated by the Kolmogorov-Smirnov test [37]. ChemRICH set enrichment statistics plot identified different chemical clusters, being phenols, coumaric acids and amino acids the most represented chemical clusters in tomato root exudates. This pattern was independent from the growing condition, albeit showing different variations according to the starvations (Fig. 5). In

particular, phenols and coumaric acids showed a general increase in all the conditions; indeed, the exudation of phenols has already been shown to be involved in the response to Fe starvation, possibly for the mobilization of sparingly soluble Fe sources [52-55]. Moreover, phenolics can increase the solubility and the uptake of metals such as Fe by chelation or reduction [52,54-56]. Similar results were found by other authors who showed that *Arabidopsis* phenylpropanoid pathway is stimulated in roots by Fe deficiency [54,57]. Also coumarins have aready been shown to be part of the Fe deficiency response in plants. In particular, the biosynthesis and the release of catechol-type coumarins have been demonstrated to contribute to Fe acquisition under limiting conditions [58-66]. Interestingly, both phenolic compounds and coumarins were also released in S and D conditions, possibly highlighting that this mechanism of the Fe deficiency response is not affected by the inhibitory effect induced by S shortage on the Fe nutrient acquisition process.

On the contrary, the class of amino acids increased only in the root exudates of F plants. At present, very little is known about the role of these compounds in root exudates as a response to nutrients starvation; to date, the release of amino acids has been observed in P-deficient soybean and strawberry plants [34,67] and in cucumber plants subjected to Fe deficiency[33]. Among the overrepresented amino acids, glycine and glutamic acid were the only two compounds specifically overaccumulated in the root exudates of F plants, as also previously reported by [33]. These pieces of evidence further strengthen the hypothesis that glycine might participate in the Fe mobilization from barely available sources *via* a complexation process. In fact, the stability constant of the complex Fe(III)-glycine is very similar to that of Fe(III)-citrate [33]. On the other hand, glutamic acid has been described as a strong chemoattreactant for bacteria at rhizosphere level [48,68]; therefore, its presence in the root exudates might suggest that Fe-starved tomato plants are actively recruiting the rhizosphere microbiota in favor of useful associations , *i.e.* with plant growth-promoting rhizobacteria, to cope more efficiently with the nutrient disorder [69].

A particularly intriguing aspect of this study is represented by the results obtained analyzing the root exudation profiles of tomato plants grown in condition of adequate availability of Fe and S (C condition). In fact, in this case, the presence of 3-hydroxymugineic acid, an organic compound belonging to the class of PSs, has been detected. Moreover, its amount is considerably decreased (4-folds decrease) when the plants have been exposed only to the single Fe or single S deficiency. No changes have been measured in its levels in exudates of dual (Fe-S) deficient plants, compared to control (Fig. 6). Concerning this specific result, it is well known that Fe-starved plants secrete in the rhizosphere a diversity of compounds playing an important role in the biogeochemical cycle

of this element. In fact, thanks to the Fe mobilization process, the extent of the nutrient solubilization from soil minerals and the magnitude of its uptake by roots can be significantly increased. In particular, it has been shown that Strategy I plants release phenolics from roots under Fe deficiency [34,56,70], whereas the secretion of phytosiderophores (PS) is typical of Strategy II plants (only grasses). Our finding strongly support the hypothesis that the distinction between the two mechanisms/strategies could not be so sharp [71]. The results of this study emphasize that the two strategies are not mutually exclusive and report that a MA derivative was actually detected in root exudates of dicot plants. Therefore, such information suggest the existence, also in tomato, of a double strategy for Fe acquisition, as already demonstrated in rice plants [31]. Indeed, recent pieces of research showed that Fe deficiency symptoms in *Arachis hypogea* plants could be alleviated by the intercropping with maize plants [39]. In particular, these authors demonstrated that the deoxymugineic acid (DMA) released by maize plants could bind Fe(III) in the soil and the complex DMA-Fe(III) could be taken up by peanut plants through AhYSL1 transporters [39]. The phylogenetic analyses tomato genome highlighted the presence of at least three *TOM1* gene putative isoforms (*SlTOM1.1*, *SlTOM1.2* and *SlTOM1.3*) for the release of PSs and one *SlYSL1* gene homologous to *AhYSL1*, putatively involved in the uptake of the Fe(III)-PSs complexes. The gene expression analyses showed that *SlTOM1.2* was the most expressed genes among the *TOM1* homologs (Supplementary Fig. 3) and its expression was highest in control. On the contrary, the expression of this gene was significantly downregulated in single Fe, single S and combined Fe-S deficiency, supporting the decrease of 3-hydroxymugineic acid contents measured at the metabolomic level (Fig. 6 and Fig. 7). Noteworthy, *SlYSL1* was significantly down-regulated in F plants (Fig. 7d).

These data might suggest that in tomato plants both strategy I and II are encoded at genomic level and expressed concurrently only when the availability of the two nutrients (*i.e.* Fe and S) is not limited. On the contrary, when Fe is lacking, tomato plants showed to rely just on one mechanism (Strategy I), probably the most efficient to acquire the micronutrient from the external environment. As a consequence, the molecular entities involved in the Strategy II are then shut down (*i.e.* synthesis of 3-hydroxymugineic acid and restraint of the *SlTOM1.2* and *SlYSL1* gene expression). In conclusion, the evidence here reported seems to support the hypothesis of a co-existence of the two Fe acquisition strategies in tomato plants (Fig. 8). However, these data do not rule out a specificity of the response to the nutritional disorder in tomato. In fact, while the exposure of tomato plants to the single Fe deficiency is associated to a decreased secretion of 3-

hydroxymugineic acid (Fig. 6 and Fig. 8), this compound is considerably accumulated in Strategy II plants as a consequence of the same nutritional stress [72]. It can be postulated that a strategy shift, towards the more efficient one in coping with the Fe shortage (*i.e.* Strategy I in tomato plants), could be at the basis of this behavior. Moreover, the strongly reduced secretion of hydroxymugineic acid by tomato roots under S deficient conditions confirms the crucial role played by the intracellular S pools in its synthesis [49] and, more in general, in the biogeochemical cycle of Fe in the rhizosphere.

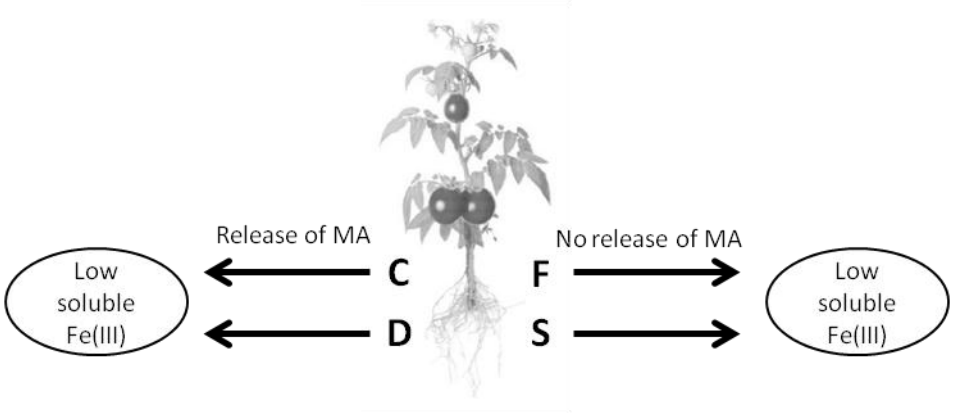

Figure 8. Scheme showing suggested Fe-solubilizing mechanisms occurring in rhizosphere when tomato plants were grown in complete nutrient solution (control, C) or under Fe (F), sulfur (S) and combined Fe+S deficiency (D).

Supplementary materials

Supplementary Figure 1. Phylogenetic tree obtained by aligning TOM protein from *S. lycopericum*, *H. vulgare* and *O. sativa*.

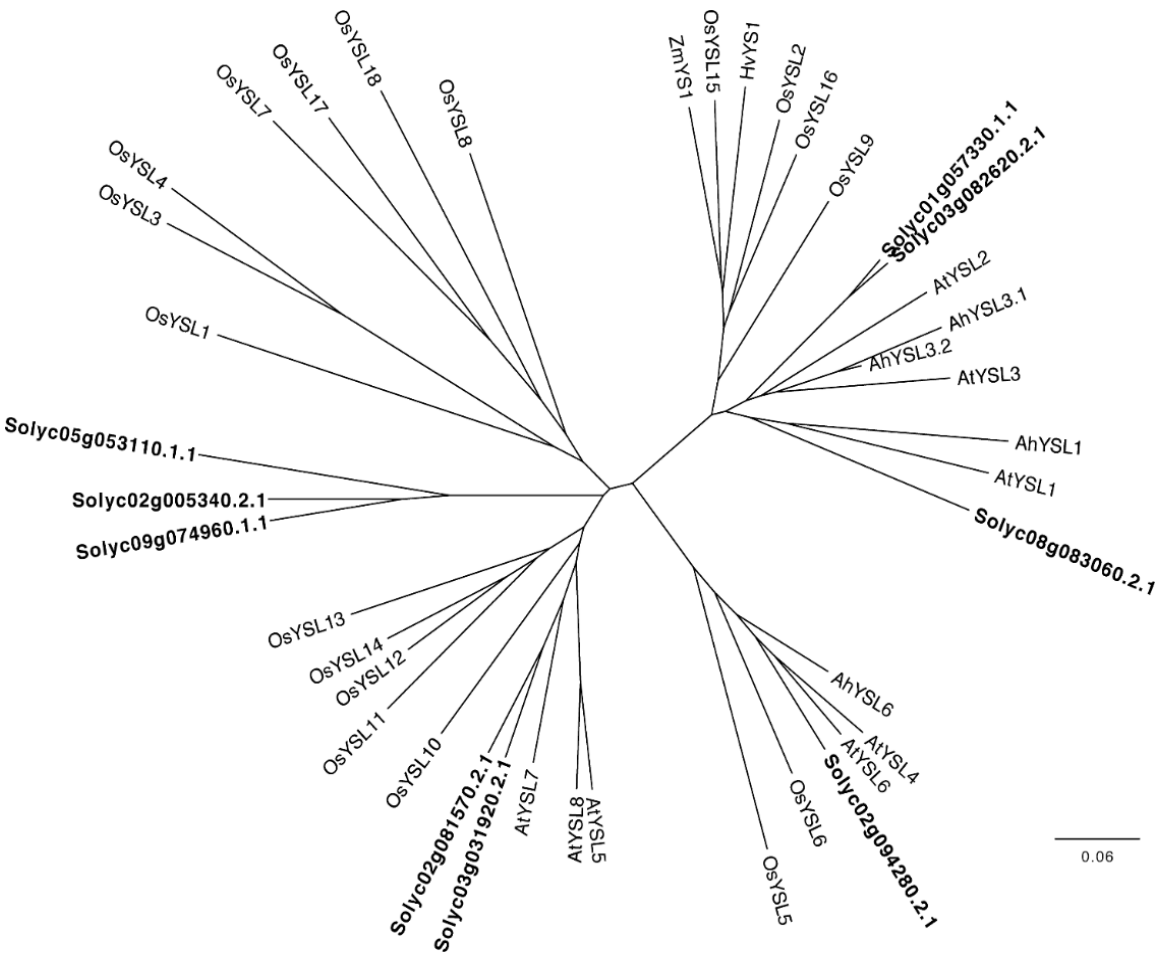

Supplementary Figure 2. Phylogenetic tree obtained by aligning YSL protein from *S. lycopericum*, *A. hypogea*, *H. vulgare*, *Z. mays* and *O. sativa*.

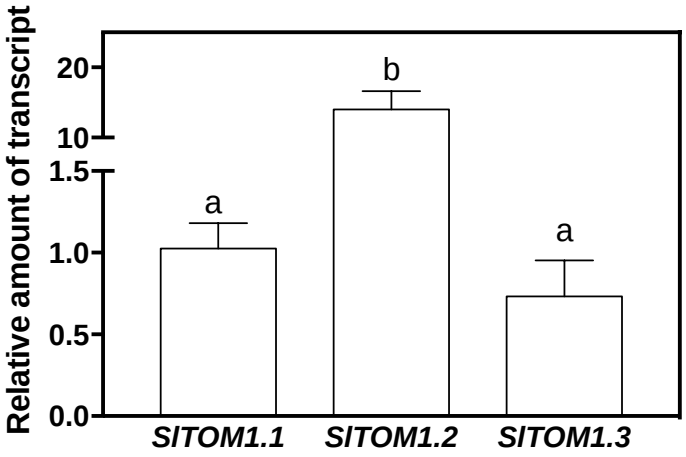

Supplementary Figure 3. Gene expression analyses in the root tissue of tomato plants grown in full nutrient solution. The levels of expression of *SlTOM1.1, SlTOM1.2* and *SlTOM1.3* were assessed by quantitative Real Time RT–PCR. The data were normalised to two internal controls, Tomato *LeEF-1* mRNA for elongation factor 1 alpha and Tomato *ubi3* gene for ubiquitin. The relative expression ratios were calculated using *SlTOM1.1* gene expression as a calibrator. The values reported are means ± SE (n = 3). The statistical significance was tested by means Student's t test (*, $p<0.05$; **, $p<0.01$; ***, $p<0.001$).

Supplementary Table 1. Quantitative Real-Time RT-PCR performed using gene-specific primers (approximately 20 nt-long), amplifying fragments of about 100 bp .

Gene Name	Gene ID	Primer Forward (5'-3')	Primer Reverse (5'-3')
SlTOM1.1	*Solyc01g096730*	TCAGACAAGAACTTATGATCGT	TCACCCTGTTTCCCGACTAA
SlTOM1.2	*Solyc01g096740*	CTGACTTTCAAACCATTCCTTG	CACGTAAAATAGAATATTAAAAAAAT
SlTOM1.3	*Solyc10g076940*	TACTTCTGACCCTCAGACCC	CACGAGCCTCTCTTGCATT
SlYSL1	*Solyc08g083060*	CAGTTGCTTCTGGTTTGATCT	TCAAGAAGCCAAGAATTTCATG

Supplementary Table 2. Volcano analysis of metabolites obtained through GC-MS in the root exudates of plants exposed to the different nutritional conditions.

			[Fe+S_deficiency] vs [control]				[Fe_deficiency] vs [control]				[S_deficiency] vs [control]			
Compound	p	p (Corr)	FC	Log FC	FC (abs)	Regulation	FC	Log FC	FC (abs)	Regulation	FC	Log FC	FC (abs)	Regulation
[69217] 1-methylhydantoin 1 [10.578]	0	0	11,4703	3,519831	11,4703	up	135,716	7,084451	135,716	up	2,4016	1,264	2,4016	up
[2341] Benzphetamine [16.991]	0	0	8366,579	13,03042	8366,58	up	45,8127	5,517676	45,8127	up	2,38563	1,25437	2,38563	up
[12290] 4-hydroxypyridine [8.204]	0	0	40,1455	5,327167	40,1455	up	-1	0	1	down	-44,5321	-5,47677	44,5321	down
[12364] adipamide 2 [16.344]	0	0	827,2577	9,692193	827,258	up	255,756	7,998622	255,756	up	-44,5321	-5,47677	44,5321	down
[938] nicotinic acid [10.27]	0	0	123,0137	6,942675	123,014	up	1916,06	10,90393	1916,06	up	1,55912	0,64073	1,55912	up
[867] malonic acid 1 [8.919]	0	0	799,7393	9,643386	799,739	up	302,098	8,238873	302,098	up	6,73179	2,75099	6,73179	up
[8897] iminodiacetic acid 1 [12.487]	0	0	2,589859	1,372873	2,58986	up	-425,858	-8,734229	425,858	down	-18964,3	-14,211	18964,3	down
[8217] 1-octadecene [16.36]	0	0	364,9106	8,511399	364,911	up	-1	0	1	down	1,39069	0,4758	1,39069	up
[675] 5,6 - dimethylbenzimidazole 1 [15.6311]	0	0	4,710074	2,23575	4,71007	up	-92,1868	-6,526489	92,1868	down	-4105,27	-12,0033	4105,27	down
[439232] N-acetyl-ornithine 2 [18.409]	0	0	139,1836	7,120845	139,184	up	77,9631	6,28472	77,9631	up	-44,5321	-5,47677	44,5321	down
[107689] L-(+) lactic acid [6.851]	0	0	290,7651	8,18371	290,765	up	245,229	7,937983	245,229	up	-26,0095	-4,70096	26,0095	down
[1176] urea [9.599]	0	0	1,506813	0,591501	1,50681	up	283,906	8,149267	283,906	up	4,11461	2,04076	4,11461	up
[10442] 1,3-propanediol [6.777]	0	0	217,1837	7,762772	217,184	up	-1	0	1	down	366,739	8,51861	366,739	up
[18189] 4-acetamidobutyric acid 2 [13.058]	0	0	451,9591	8,820048	451,959	up	-1	0	1	down	3,34495	1,74198	3,34495	up
[126] 4-hydroxybenzaldehyde 2 [13.005]	0	0	-617,249	-9,269709	617,249	down	-839,034	-9,712585	839,034	down	-37363,9	-15,1894	37363,9	down
[7152] N-(2-hydroxyethyl)iminodiacetic acid 2 [16.659]	0	0	293,5979	8,197698	293,598	up	168,34	7,395237	168,34	up	7,46225	2,89961	7,46225	up
[42953] diglycerol 2 [15.958]	0	0	1,507132	0,591806	1,50713	up	1,23911	0,3093	1,23911	up	-7702,41	-12,9111	7702,41	down
[6853] fluorene [14.182]	0	0	-2,31686	-1,212169	2,31686	down	11,0349	3,463996	11,0349	up	-125,977	-6,97701	125,977	down
[262] 2,3-butanediol 1 [6.42]	0	0	-36,4856	-5,189256	36,4856	down	-204,823	-7,678234	204,823	down	-4209,55	-12,0395	4209,55	down
[10436] orcinol [12.28]	0	0	-1522,42	-10,57215	1522,42	down	117,968	6,882248	117,968	up	-36,7174	-5,19839	36,7174	down
[325] 4-isopropylbenzyl alcohol [11.659]	0	0	-1,70879	-0,772975	1,70879	down	-78,8664	-6,301338	78,8664	down	1,36387	0,4477	1,36387	up
[62453] 4-vinylphenol 2 [22.488]	0	0	7691,499	12,90905	7691,5	up	54,4975	5,768119	54,4975	up	1,38314	0,46795	1,38314	up
[20393] mono(2-ethylhexyl)phthalate [19.512]	0	0	21475,72	14,39042	21475,7	up	32,912	5,04054	32,912	up	-1,12921	-0,17531	1,12921	down
[5641] carbamic acid ethyl ester (urethane) [6.361]	0	0	8,670772	3,11616	8,67077	up	173999	17,40872	173999	up	-114,803	-6,84301	114,803	down
[892] allo-inositol [17.245]	0	0	-35,7111	-5,1583	35,7111	down	-78,7119	-6,29851	78,7119	down	2,88082	1,52648	2,88082	up
[443586] 3,5-dihydroxyphenylglycine 2 [18.124]	0	0	-348047	-18,40892	348047	down	-191,418	-7,580585	191,418	down	-14395,5	-13,8133	14395,5	down
[5570] trigonelline [13.039]	0	0	-1498,06	-10,54888	1498,06	down	1,06424	0,08982	1,06424	up	-1062,74	-10,0536	1062,74	down
[4114] xanthotoxin 2 [20.715]	0	0	5,342397	2,417487	5,3424	up	4,17412	2,061472	4,17412	up	-2024,16	-10,9831	2024,16	down
[12647] L-homoserine 1 [11.141]	0	0	-101,87	-6,670592	101,87	down	-1,28015	-0,356315	1,28015	down	4,36825	2,12705	4,36825	up
[49] 3-methyl-2-oxobutanoic acid 1 [7.562]	0	0	103561,1	16,66012	103561	up	67,7071	6,081235	67,7071	up	-44,5321	-5,47677	44,5321	down
[791] DL-isoleucine 1 [8.576]	0	0	2662,658	11,37865	2662,66	up	178094	17,44228	178094	up	8,65902	3,1142	8,65902	up
[244] benzyl alcohol [8.264]	0	0	1,439192	0,525259	1,43919	up	-44,7433	-5,483601	44,7433	down	-1992,51	-10,9604	1992,51	down
[99289] L-allothreonine 2 [16.365]	0	0	1,576231	0,656479	1,57623	up	2,59082	1,373409	2,59082	up	22,8743	4,51566	22,8743	up
[5146] 2-hydroxybenzyl alcohol [12.068]	0	0	1,525235	0,609032	1,52524	up	-2,0312	-1,022336	2,0312	down	-3097,67	-11,597	3097,67	down
[1004] phosphoric acid [9.966]	0	0	364,6902	8,510528	364,69	up	8844945	23,07642	8844945	up	52,6242	5,71765	52,6242	up
[240] benzaldehyde [7.616]	0	0	-960,102	-9,907043	960,102	down	-1,02389	-0,034054	1,02389	down	-228242	-17,8002	228242	down
[521171] 3,4',5,6,7-Pentamethoxyflavone [27.459]	0	0	-18,7115	-4,225854	18,7115	down	43,2965	5,436177	43,2965	up	-24,3175	-4,60392	24,3175	down
[8215] behenic acid [23.897]	0	0	-18563,5	-14,18018	18563,5	down	157,177	7,296243	157,177	up	-1707910	-20,7038	1707910	down
[] L-Ascorbic Acid-13C6 2 [17.144]	0	0	-188,048	-7,554955	188,048	down	-4,91318	-2,296658	4,91318	down	-10047,5	-13,2946	10047,5	down
[74318] 9-hydroxyfluorene [16.564]	0	0	-1,81539	-0,860277	1,81539	down	1023,64	9,999498	1023,64	up	79,4013	6,31109	79,4013	up
[5984] fructose 1 [17.18]	0	0	-4,4123	-2,14153	4,4123	down	715,289	9,482382	715,289	up	-7,55546	-2,91752	7,55546	down
[69362] beta-hydroxyisovalerate [9.084]	0	0	3,012419	1,590922	3,01242	up	146,545	7,195202	146,545	up	6,71608	2,74762	6,71608	up
[5281] stearic acid [20.675]	0	0	192447,8	17,55411	192448	up	6526390	22,63785	6526390	up	885,792	9,79082	885,792	up
[7222] benzothiazole [9.574]	0	0	6,381159	2,673819	6,38116	up	-3,45493	-1,788657	3,45493	down	-80,8987	-6,33804	80,8987	down
[1647] 3-aminopropionitrile 1 [6.478]	0	0	-67,8279	-6,083806	67,8279	down	503,751	8,976567	503,751	up	-14457,3	-13,8195	14457,3	down
[96] acetoacetate 1 [7.603]	0	0	-55,102	-5,784032	55,102	down	-14864,7	-13,8596	14864,7	down	-1644,92	-10,6838	1644,92	down
[122121] phytosphingosine 2 [23.812]	0	0	-983,588	-9,941911	983,588	down	-27,2377	-4,767534	27,2377	down	-124904	-16,9305	124904	down
[970] oxalacetic acid [12.45]	0	0	1162,036	10,18244	1162,04	up	-1	0	1	down	2,21454	1,14701	2,21454	up
[3393] Flurazepam [25.225]	0	0	2,269066	1,182098	2,26907	up	-102902	-16,65091	102902	down	-122,297	-6,93425	122,297	down
[439227] pipecolic acid 2 [11.22]	0	0	3,547471	1,826791	3,54747	up	-52,7162	-5,720175	52,7162	down	-2347,56	-11,1969	2347,56	down
[5801] 2-aminophenol 3 [13.489]	0	0	602,9132	9,235806	602,913	up	-1	0	1	down	-44,5321	-5,47677	44,5321	down
[700] ethanolamine [9.879]	0	0	168,4171	7,395895	168,417	up	138,889	7,117787	138,889	up	-44,5321	-5,47677	44,5321	down
[6054] phenylethyl alcohol [9.328]	0	0	143,1406	7,161289	143,141	up	54,7245	5,774116	54,7245	up	-44,5321	-5,47677	44,5321	down
[254] 2,3-dihydroxybiphenyl [16.889]	0	0	-13496,5	-13,7203	13496,5	down	-4,3444	-2,119158	4,3444	down	-8198,4	-13,0011	8198,4	down
[5951] L-serine 2 [11.174]	0	0	135,2441	7,079422	135,244	up	107,908	6,753657	107,908	up	1,68209	0,75025	1,68209	up
[4646739] 12a-Hydroxy-9-Demethylmunduserone-8-Carboxylic Acid [26.831]	0	0	-1,02007	-0,028662	1,02007	down	-1,0784	-0,108888	1,0784	down	1,30219	0,38094	1,30219	up
[119054] conduritol epoxide 2 [18.004]	0	0	1,102325	0,14055	1,10233	up	119,241	6,897742	119,241	up	163,298	7,35136	163,298	up
[2266] azelaic acid [16.359]	0	0	-70,912	-6,147957	70,912	down	5862,96	12,51741	5862,96	up	2,51493	1,33052	2,51493	up
[12298] valeramide 2 [7.214]	0	0	-24908,1	-14,60433	24908,1	down	-351,254	-8,456369	351,254	down	2,69835	1,43208	2,69835	up
[439196] L-dithiothreitol 2 [17.086]	0	0	-101,779	-6,669295	101,779	down	-229,987	-7,84541	229,987	down	1,16492	0,22023	1,16492	up
[688664] 3,7-Dimethoxyflavone [23.334]	0	0	-70,912	-6,147957	70,912	down	57,7699	5,852245	57,7699	up	52,3428	5,70992	52,3428	up
[7095] biphenyl [11.505]	0	0	-2416,4	-11,23864	2416,4	down	-34,076	-5,090684	34,076	down	112,92	6,81916	112,92	up
[6106] L-leucine 1 [8.298]	0	0	-74,9953	-6,228728	74,9953	down	-1,1361	-0,184085	1,1361	down	-1,37305	-0,45739	1,37305	down
[65166] 2', 5'-Dideoxyadenosine [22.114]	0	0	-44,416	-5,473006	44,416	down	-6579,32	-12,68372	6579,32	down	-2988,13	-11,545	2988,13	down
[985] palmitic acid [18.846]	0	0	694,4513	9,43973	694,451	up	-1	0	1	down	102002	16,6382	102002	up
[101] 3-hydroxybenzaldehyde [12.313]	0	0	-3832,37	-11,90402	3832,37	down	-58,8426	-5,878788	58,8426	down	1,33414	0,41591	1,33414	up
[8222] eicosane [18.464]	0	0	-1,02412	-0,03439	1,02412	down	-30,1083	-4,91209	30,1083	down	-28,7394	-4,84496	28,7394	down
[8697] 2-ethylcaproic acid [8.5301]	0	0	-1,17581	-0,233657	1,17581	down	54,2393	5,761266	54,2393	up	99,476	6,63628	99,476	up
[] L-Ascorbic Acid-13C6 3 [17.489]	0	0	-1579497	-20,59103	1579497	down	-241,14	-7,91373	241,14	down	-41737,1	-15,349	41737,1	down
[675] 5,6 - dimethylbenzimidazole 2 [16.587]	0	0	-9596,85	-13,22835	9596,85	down	-4,61984	-2,207842	4,61984	down	1,91403	0,93661	1,91403	up
[1133] thioglycolic acid [9.725]	0	0	4,192545	2,067826	4,19254	up	-1	0	1	down	1187,37	10,2136	1187,37	up
[9862] 6-methyl-5-hepten-2-one [7.322]	0	0	-2350,75	-11,1989	2350,75	down	1,19993	0,262955	1,19993	up	-1,11859	-0,16168	1,11859	down
[5280442] Acacetin [13.1191]	0	0	-1,76E+07	-24,07008	1,76E+07	down	-4096,62	-12,00022	4096,62	down	-3805,5	-11,8939	3805,5	down
[11349] 3-hydroxyflavone [21.139]	0	0	8,549159	3,095783	8,54916	up	74,3315	6,215901	74,3315	up	405,043	8,66193	405,043	up
[33032] L-glutamic acid 3 (dehydrated) [13.232]	0	0	-70,912	-6,147957	70,912	down	-1	0	1	down	264,692	8,04817	264,692	up
ethylene-5-(2,5-Dioxotetrahydrofuran-3-YL)-6-OXO--10, 10-Dimethylbicyclo[7:2:0]Unde	0	0	-1,49228	-0,57752	1,49228	down	57,2213	5,83848	57,2213	up	117,07	6,87123	117,07	up
[1136] 4-methyl-5-thiazoleethanol [11.256]	0	0	-5468,41	-12,4169	5468,41	down	-2,02214	-1,015882	2,02214	down	-7852,52	-12,9389	7852,52	down
[8066] 2-butyne-1,4-diol [9.446]	0	0	-1,46026	-0,546222	1,46026	down	-3,08936	-1,627307	3,08936	down	1,55415	0,63612	1,55415	up
[73064] beta-glutamic acid [13.279]	0	0	-19537,9	-14,25398	19537,9	down	34,734	5,118277	34,734	up	-43,6032	-5,44636	43,6032	down
[3015189] Avocadyne [21.805]	0	0	-445027	-18,76353	445027	down	-6275,77	-12,61558	6275,77	down	-1863,49	-10,8638	1863,49	down
[7418] m-toluic acid [11.006]	0	0	-4621,57	-12,17417	4621,57	down	1,11493	0,156948	1,11493	up	-50,2789	-5,65188	50,2789	down
[10820] 4-isopropylbenzoic acid [13.247]	0	0	-53,6553	-5,745649	53,6553	down	-2,18699	-1,128947	2,18699	down	-1,66171	-0,73267	1,66171	down
[3744] indole 3-propionic acid 1 [18.758]	0	0	-23,0747	-4,528242	23,0747	down	-69,755	-6,124226	69,755	down	5,12667	2,35802	5,12667	up
[119] gamma-aminobutyric acid (GABA) [13.326]	0	0	-7870,56	-12,94225	7870,56	down	102,869	6,684671	102,869	up	-34,0845	-5,09104	34,0845	down
[24135] 4-O-Methylphloracetophenone 1 [15.588]	0	0	-5154,07	-12,3315	5154,07	down	-72,6826	-6,183538	72,6826	down	47,3274	5,5646	47,3274	up
[440917] limonene [6.621]	0	0	-3964,34	-11,95287	3964,34	down	-55,9051	-5,804909	55,9051	down	-1,44821	-0,53427	1,44821	down
[753] glycerol [9.941]	0	0	1,463349	0,549274	1,46335	up	50946	15,63668	50946	up	-38,5389	-5,26824	38,5389	down
[7463] p-cymene [6.529]	0	0	-5720,81	-12,482	5720,81	down	-68,2522	-6,092804	68,2522	down	-14,0797	-3,81555	14,0797	down
[243] benzoic acid [9.594]	0	0	-6,32E+07	-25,91396	6,32E+07	down	-737,853	-9,52719	737,853	down	-416902	-18,6693	416902	down
[5280335] D-sphingosine 1 [22.326]	0	0	-70,912	-6,147957	70,912	down	31233,2	14,93079	31233,2	up	489,242	8,9344	489,242	up
[5367146] 2-hydroxychalcone 2 [20.305]	0	0	-85,776	-6,422502	85,776	down	56,0279	5,808075	56,0279	up	-3593,1	-11,811	3593,1	down
[995] phenanthrene [16.541]	0	0	-2,65191	-1,40703	2,65191	down	19,1779	4,26137	19,1779	up	42,658	5,41474	42,658	up
[RTL] Myristic Acid d27 [16.727]	0	0	-5132,12	-12,32534	5132,12	down	1,307	0,386261	1,307	up	-82,7454	-6,37061	82,7454	down
[62453] 4-vinylphenol 1 [10.051]	0	0	-240919	-17,87819	240919	down	-2,55286	-1,352115	2,55286	down	-6141,87	-12,5845	6141,87	down
[10241] 9-fluorenone [17.583]	0	0	-4210,26	-12,03969	4210,26	down	-1,44522	-0,531289	1,44522	down	-4604,87	-12,1689	4604,87	down
[21236] L-norleucine 1 [8.945]	0	0	-9011,73	-13,13759	9011,73	down	-33874,7	-15,04792	33874,7	down	-1508514	-20,5247	1508514	down
[338] salicylic acid [13.075]	0	0	-912,247	-9,833281	912,247	down	-1099,26	-10,10231	1099,26	down	-703,32	-9,45804	703,32	down
[736228] 3-Methylorsellinic Acid 1 [12.918]	0	0	-3346,46	-11,70842	3346,46	down	1,16227	0,216949	1,16227	up	-1419,11	-10,4708	1419,11	down
[1531] 2-amino-2-methyl-1,3-propanediol 2 [10.56]	0	0	-70,912	-6,147957	70,912	down	3628,22	11,82505	3628,22	up	-44,5321	-5,47677	44,5321	down
[3848] 3-phenyllactic acid [13.981]	0	0	1,154412	0,207158	1,15441	up	981,516	9,938868	981,516	up	-44,5321	-5,47677	44,5321	down
[1110] succinic acid [10.509]	0	0	-7151,27	-12,80398	7151,27	down	94,9265	6,568739	94,9265	up	-4490,93	-12,1328	4490,93	down
[637517] elaidic acid [20.508]	0	0	-70,912	-6,147957	70,912	down	5117,13	12,32112	5117,13	up	-44,5321	-5,47677	44,5321	down
[24154] galactosamine 4 [17.797]	0	0	-23363,6	-14,51198	23363,6	down	101577	16,63222	101577	up	-14672,1	-13,8408	14672,1	down
[2346] benzyl isothiocyanate [11.361]	0	0	-70,912	-6,147957	70,912	down	1016,36	9,989192	1016,36	up	-44,5321	-5,47677	44,5321	down
[750] glycine [10.456]	0	0	-70,912	-6,147957	70,912	down	82872,9	16,33861	82872,9	up	-44,5321	-5,47677	44,5321	down

[440294] cis-1,2-dihydro-1,2-naphthalenediol [14.877]	0	0	1,134945	0,182623	1,13495	up	65,6777	6,037332	65,6777	up	59,05491	5,883985	59,0549	up
[660] dihydrocoumarin 4 [15.666]	0	0	-70,912	-6,147957	70,912	down	5969,08	12,54329	5969,08	up	164,2964	7,360157	164,296	up
[3126] DL-dihydrosphingosine 2 [22.602]	0	0	-5978,68	-12,54561	5978,68	down	1,60147	0,679394	1,60147	up	5,591106	2,483134	5,59111	up
[7478] p-anisic acid [13.2267]	0	0	-3408,99	-11,73513	3408,99	down	13,2459	3,727469	13,2459	up	-81,9727	-6,35707	81,9727	down
[31404] 2,6-ditert-butyl-4-methylphenol 1 [13.049]	0	0	-70,912	-6,147957	70,912	down	821489	19,64788	821489	up	1,753878	0,810548	1,75388	up
[4771] Phentermine 2 [11.286]	0	0	-70,912	-6,147957	70,912	down	290,348	8,18164	290,348	up	735,9482	9,52346	735,948	up
[11266] 2-hydroxybutyric acid [7.852]	0	0	-70,912	-6,147957	70,912	down	4377,7	12,09596	4377,7	up	3,869814	1,952264	3,86981	up
[9958] 4-methylcatechol [11.51]	0	0	-6244,09	-12,60828	6244,09	down	-1,05921	-0,082994	1,05921	down	1,432106	0,518138	1,43211	up
[16217112] D-glucose-C-d7 1 [17.411]	0	0	-10691,1	-13,38413	10691,1	down	-1,10396	-0,142689	1,10396	down	-81,5669	-6,34991	81,5669	down
[64956] DL-3-aminoisobutyric acid 1 [9.066]	0	0	-70,912	-6,147957	70,912	down	5398,83	12,39843	5398,83	up	1,385517	0,470424	1,38552	up
[351795] 3-indoleacetonitrile [17.214]	0	0	-566887	-19,1127	566887	down	-67,6354	-6,079708	67,6354	down	-355999	-18,4415	355999	down
[10918] L-carnitine 1 [15.426]	0	0	-211946	-17,69334	211946	down	-66,5798	-6,057012	66,5798	down	-133100	-17,0221	133100	down
[5801] 2-aminophenol 2 [12.039]	0	0	-325987	-18,31446	325987	down	-6495,96	-12,66533	6495,96	down	-1,74E+07	-24,05	1,74E+07	down
[68152] 3-hydroxypropanoic acid 3 [18.459]	0	0	-1022514	-19,96369	1022514	down	1,70034	0,765822	1,70034	up	-642129	-19,2925	642129	down
[379] caprylic acid [9.81]	0	0	-10146,6	-13,30872	10146,6	down	146,993	7,199608	146,993	up	-6372	-12,6375	6372	down
[997] phenylpyruvate [13.964]	0	0	-1142243	-20,12344	1142243	down	-16107,9	-13,97548	16107,9	down	-21456,3	-14,3891	21456,3	down
[8163] 2-undecanone 1 [11.323]	0	0	-270812	-18,04693	270812	down	-3818,99	-11,89898	3818,99	down	-170068	-17,3758	170068	down
[11915] benzoylformic acid 2 [13.386]	0	0	-390871	-18,57633	390871	down	-5512,06	-12,42838	5512,06	down	-2909,45	-11,5065	2909,45	down
[1548943] capsaicin [22.788]	0	0	-373564	-18,511	373564	down	-5268	-12,36304	5268	down	-4520,77	-12,1424	4520,77	down

Supplementary Table 3. Dataset of metabolites obtained through GC-MS (A) and UHPLC/QTOF-MS (B) analysis in the root exudates of plants exposed to the different nutritional conditions

A

	control			Fe-deficiency			S-deficincy			Fe+S-deficiency		
Compound	xud_1-AllHit	xud_2-AllHit	ud_3-AllH	ud_4-AllH	ud_5-AllH	xud_6-AllHit	xud_7-AllHit	ud_8-AllH	ud_9-AllH	d_10-AllH	d_11-AllH	d_12-AllH
[24154] galactosamine 1 [17.244]	1	1	1	1	1	1	1	1	1	1	65802	1
[69217] 1-methylhydantoin 1 [10.578]	1	1	38720,9	1	1501661	64456,88	4807997	9851,53	1	1	8912402	2337935
[10465] heptadecanoic acid [19.8]	1	1	1	1	1	1	1	1534662	1	1	74360,8	1
[971] oxalic acid [7.883]	1	412512,7	6913287	888413	9844003	1904645,9	1	102777	1659886	1	4103635	3369469
[2341] Benzphetamine [16.991]	1	1	1	1	96152	1	1	1	1199019	2723175	413519	185452
[12290] 4-hydroxypyridine [8.204]	1	1	1	1	1	1	1	1	1	1	2664224	8659,61
[8343] dioctyl phthalate [23.163]	1	80175,64	1	1	1	1	1	1	1319341	1	334766	1
[12364] adipamide 2 [16.344]	1	1	1	1,67E+07	1	1	1	1	1	1,75E+07	1,15E+07	1
[2723970] glycine-d5 deuterated [10.446]	1	1	1	1	1	1	1	1	1	1	4424813	1
[8406] 2-carboxybenzaldehyde 1 [13.826]	1	1	1	1	1	1	1	1	1	1	850763	1
[90008] psicose 1 [17.059]	1	1	1	1	1	1	1	1	1	1	5,73E+07	1
[938] nicotinic acid [10.27]	1	1	1	162511	43285,5	1	1	1	334701	1	220032	3016704
[6058] 2-aminoethanethiol 1 [20.388]	1	1	1	1	3540883	1	1	1	1,18E+07	1	7810846	1
[867] malonic acid 1 [8.919]	1	1	1	1	2,76E+07	1	1	1	2,69E+07	1,10E+08	1661791	1
[8897] iminodiacetic acid 1 [12.487]	1	1	7,72E+07	1	1	1	1	1	1	1	1,50E+07	3,19E+07
[8158] pelargonic acid (nonanoic acid) [11.129]	1	1	1	1	1	1	1	38204,5	1	1	271058	1
[1060] pyruvic acid [6.714]	1	1	1	1	1	1	1	1	1	1	5263996	1
[70914] N-acetyl-L-glutamic acid 1 [13.063]	1	1	1	1	1	1	1	1	1	1	387892	1
[673] N,N-dimethylglycine [6.332]	1	1	1	1,39E+07	1	1	1	1	1	1	3,01E+07	1
[92824] D-malic acid [12.794]	1	1	1	366376	1	1	1	1	5108970	1	1591515	1
[8217] 1-octadecene [16.36]	1	1	1	1	1	1	1	1	237525	1	3210112	5397570
[439665] threose 2 [12.371]	1	1	1	1	3855388	1	1	1	1	1	4,30E+07	1
[311] citric acid [16.615]	1	1	1	572294	1	1	1	1	273488	1	932856	1
[675] 5,6 - dimethylbenzimidazole 1 [15.6311]	1	1	783441	1	1	1	1	1	1	1	1908507	1,53E+07
[12665] 2-piperidone 1 [8.057]	1	1	1	1	396714	1	1	1	1	1	73779,5	1
[614] L-proline 1 [8.58]	1	1	1	1	1	1	1	1	1	1	2965144	1
[1990] acetohydroxamic acid [7.72]	1354219,8	4396074,5	8187300	6769578	329056	3451654,2	2298008,2	193557	6,36E+07	4097902	1,46E+07	7558846
[439232] N-acetyl-ornithine 2 [18.409]	1	1	1	1	1	473878,75	1	1	1	1	2273094	422966
[642609] trans caftaric acid 2 [25.529]	1	1	1	1	1	1	1	1	1	1	349482	1
[736] gluconic acid lactone 1 [17.303]	1	1	1	1	1	1	1	1	72179,5	1	1,59E+07	1
[107689] L-(+) lactic acid [6.851]	1	1284697	1	2236022	8473014	1	1	1	6448003	246805	2,53E+07	1805674
[1176] urea [9.599]	1	1	1158215	1	1,79E+07	1478311,1	433462,84	1	1,64E+07	29941,3	4,72E+07	1
[594] L-cysteine 2 [13.582]	1	1	1	1	1	1	1	1	1	1	35800,5	1
[10442] 1,3-propanediol [6.777]	1	1	1	1	1	1	180488,3	2,41E+07	1	68603	5,32E+07	1
[18189] 4-acetamidobutyric acid 2 [13.058]	1	1	1	1	1	1	3305110,2	1	1	1	1,78E+07	1844795
[126] 4-hydroxybenzaldehyde 2 [13.005]	120781,61	4890,32	1	1	1	1	1	1	1	1	895604	1
[5959] chloramphenicol 1 [22.438]	1	1	1	1	1	1	1	1	124862	1	43705,4	1
[7152] N-(2-hydroxyethyl)iminodiacetic acid 2 [16.659]	1	1	1	1	1	4770506,5	1	1	3,67E+07	4326913	2085637	1
[2164] Amobarbital 1 [15.992]	1	1	1	12652,9	1	1	1	1	1	1	14916,4	1
[206] D (+) galactose 2 [17.662]	1	1	1	1	3527227	1	1	1	1	1	2023698	1
[42953] diglycerol 2 [15.958]	1	5174423	1	9844368	1	1	1	1	1	349814	1,81E+07	1
[6853] fluorene [14.182]	270010,7	1	1	32117,3	11296,5	1	1	11926,9	1	34329,1	225517	1
[262] 2,3-butanediol 1 [6.42]	1	2493437,8	8259331	1	2396659	1	1	1	2,44E+07	1	7,43E+07	2033934
[5556] Triazolam [27.243]	1	1	1	1	1	263019,9	1	1	1	1	15271,3	1
[10436] orcinol [12.28]	1	25135,07	182127	164862	157959	288588,6	1	144677	56449,1	1	462604	1
[11915] benzoylformic acid 1 [12.733]	1	1	165101	1	1	1	8706,86	1	1	1	2876503	1
[4763] Phenobarbital [18.17]	1	1	5,11E+07	1	1	1	1	1	1	1	1,53E+07	1
[325] 4-isopropylbenzyl alcohol [11.659]	1	1,65E+07	304304	1	1,02E+07	1	1,57E+07	502881	142485	222307	1601246	1008744
[62453] 4-vinylphenol 2 [22.488]	1	1	1	1	1	161856,8	233677,08	1	1	681088	544504	437509
[444539] cinnamic acid [13.562]	1	1	1	1	1	1	1	1	1	1	1,06E+07	1
[6989] thymol [10.475]	3864001,8	3334313,8	1	1,76E+07	1160089	942021,8	3873321,2	1	8515382	1	4,70E+07	1376266
[10229] 9-phenanthrenol [19.551]	1	1	1	1	1	33166,82	1	1	1	1	13045,1	1
[20393] mono(2-ethylhexyl)phthalate [19.512]	1	1	1	1	35650,2	1	1	61333,6	1	42472,7	1,49E+07	5577202
[5641] carbamic acid ethyl ester (urethane) [6.361]	1	6,23E+07	1	6,00E+07	1,18E+08	4,65E+07	1	3636800	1	1	9,75E+07	1,49E+08
[892] allo-inositol [17.245]	1	1	487665	1	1	1	186767,06	1	5512977	1	3818301	1
[6537496] chlorogenic acid 1 [26.37]	1	1	1	1	1	1	1	1	1	1	332572	1
[443586] 3,5-dihydroxyphenylglycine 2 [18.124]	338329,5	820576	258272	1	241369	42354,98	174174,53	12186,9	1	1	606431	1
[6288] L-threonine 2 [11.464]	1	1	1	1	1	1	1	1	1	1	5,65E+07	1
[446284] eicosapentaenoic acid [24.013]	1	1	1	27122,3	1	1	1	1	1	1	4020659	1
[5570] trigonelline [13.039]	1	13863,03	56992,8	1	19020,8	50068,51	58131,49	1	1	1	83801,2	1
[3294434] digalacturonic acid 2 [24.912]	1	1	1	1	68044,5	1	1	1	130906	1	8968843	1
[439616] mandelic acid [12.588]	1	1	1	1	1	1	1	1	1	1	1,53E+07	1
[4114] xanthotoxin 2 [20.715]	1	93911,03	1	6829858	1	1	1	1	1	1	306517	1,67E+07
[12647] L-homoserine 1 [11.141]	1	1	1,52E+08	7,24E+07	1	1	4,52E+07	1	2,47E+07	1	5,12E+07	1
[5280370] squalene [25.251]	1	1	1	1	1	1	1	965778	1	1	1003298	1
[11005] myristic acid [16.887]	1	1	1	1	1	388494,78	1	8070419	1	1	1714525	1
[49] 3-methyl-2-oxobutanoic acid 1 [7.562]	1	1	1	1	310386	1	1	1	1	3239161	3978834	3,07E+07
[791] DL-isoleucine 1 [8.576]	1	1	2,98E+08	9,03E+07	1,57E+08	1,18E+08	2,06E+08	1	8,27E+07	7,12E+07	1,66E+08	1,70E+08
[26879] levamisole [18.583]	1	1	1	1	1	106352,81	1	1	1	1	1199591	1
[244] benzyl alcohol [8.264]	1	89574,58	1	1	1	1	1	1	1	1	534315	178197
[7911] malonamide 3 [12.993]	1	1	1	1	1	1	1	1	1	1	2487940	1
[448388] D-allose 1 [17.278]	1	1	1	70448,2	1	1	1	1	1	1	7,06E+07	1
[1101] L- sorbose 2 [17.235]	1	1	1	1	1	1	27088,9	1	1	1	4,30E+07	1
[24749] D-glucose 1 [17.426]	1	1	1	1	1	1	1	1	1	1	4702792	1
[99289] L-allothreonine 2 [16.365]	839215,4	1	1	1	1	1,46E+07	2,13E+08	1	4171904	386348	3033290	1
[5146] 2-hydroxybenzyl alcohol [12.068]	1	336578,6	1	40163	1	1	1	1	1	1	823404	517181
[1004] phosphoric acid [9.966]	1	1	1	7108928	9451929	1,03E+07	280517,78	1	45879	1	4961333	3486038
[66868] porphine 1 [10.77]	1	1	1	1	1	1	1	1	1	1	1551474	1
[5460673] D-saccharic acid [18.614]	1	1	1	1	58491,6	1	56354,17	1	1	1	438784	1
[240] benzaldehyde [7.616]	399538,47	509423,8	116046	543607	120666	335462,56	175428,64	1	1	1	1,10E+07	861918
[3661] hyoscyamine (atropine) [21.001]	1	1	1	1	1	1	1	1	1	1	32771,7	1
[74840] N- carbobenzoxy-L-leucine 3 [23.649]	1	1	11018,7	1	1	1	1	1	1	1	132751	1
[92817] D-(+)-melezitose [29.952]	1	1	1	1	1	1	1	1	1	1	3871245	1
[18950] D-mannose 2 [17.435]	1	1	32161	1	1	1	1	1	1	1	2,95E+07	1
[638014] beta-ionone 1 [13.529]	1	1	1	1	1	1	1	1	704077	1	589072	1
[521171] 3,4',5,6,7-Pentamethoxyflavone [27.459]	1	1	9477,57	123867	6210,09	1	1	58205	1	1	515856	1
[6262] L-ornithine 2 [16.632]	1	1	1	1	1	1	1	1	1	1	1536468	1
[10467] arachidic acid [22.367]	1	1	1	1	1	1	1	1	1	1	190352	1
[150923] 3-methyloxyindole 1 [12.949]	1	1	1	1	1	1	2,97E+07	1	1	1	1,16E+07	1
[8215] behenic acid [23.897]	1	7283933,5	7744847	4010799	1,46E+07	3732692,8	1	1	1	1	3144535	1
[69505] Antiarol [14.156]	1	1	1	1	1	1	1	1	1	1	142811	1
[785] benzoquinone [11.7]	1	1	1	1	1	1	1	1	1	1	399375	1
[892] myo-inositol [19.354]	1	1	1	1	1	1	1	1	1	1	614381	1
[] L-Ascorbic Acid-13C6 2 [17.144]	557418,44	1	1,04E+07	1	19302	2535448,8	505340,22	1	1	517334	601630	1
[65553] tetrahydrocorticosterone 4 [27.497]	1042164,6	1	1	1	1	1	1	1	1	1	1,74E+07	1
[74318] 9-hydroxyfluorene [16.564]	1	32767,92	1	14392,9	10445,1	233795,62	177521,8	51530,8	158354	133194	14662,7	1
[445070] trans-trans-farnesol [16.431]	1	1	1	1	1	1	1	1	1	1	1,78E+07	1
[5984] fructose 1 [17.18]	1	23530,58	1	582138	1,48E+07	1	1	1	4818017	1	9,77E+07	1
[111] 3-ureidopropionate 1 [14.091]	1	1	1419482	342799	1	1	1	1	1	1	453569	1
[69362] beta-hydroxyisovalerate [9.084]	1	1	2259952	2912949	1	2441633,2	3,29E+07	1	1836289	1	1,65E+07	1338954

[5281] stearic acid [20.675]	1	1	1	1,33E+07	1,10E+07	1896816,2	1	3775171	1,63E+07	1,07E+07	8670499	2,74E+07
[445639] oleic acid [20.504]	1	1	1	1	1	1	1	1	1	1	129118	1
[7222] benzothiazole [9.574]	1	1	188130	4561,85	1	1	31379,99	1	1	1	5777602	3016956
[1647] 3-aminopropionitrile 1 [6.478]	1	1	3,42E+07	5,80E+07	1	7,54E+07	1	1	1	1	3,91E+07	1
[8871] 2-hydroxypyridine [6.519]	1	1	2101588	1	1	838699,6	1	27431,3	1	1	268565	1
[45] tartronic acid [11.523]	1	1	1	1	1	1	1	1	1	1	1173549	1
[6781] diethyl phthalate [14.035]	100816,58	1	108467	1	312562	3400506,2	1	12158,5	147078	277558	1,37E+07	7503225
[443651] petunidin-3-glucoside 2 [34.412]	1	1	1	1	1	1	1	1	1	1	247781	1
[3744] indolepropionic acid [19.196]	1	1	1	1	1	1	1	1	1	1	6728897	1
[96] acetoacetate 1 [7.603]	564877,25	1	5814517	1	1	1	1	1	6,52E+07	476243	1,47E+07	1
[122121] phytosphingosine 2 [23.812]	1	110207,46	200216	1	1091939	1	1	1	1	1	8268537	1
[219984] 1,5-anhydro-D-sorbitol [16.967]	1	1	1	1	1	1	635111,44	1	1	1	1,18E+07	1
[6057] tyrosine 1 [17.354]	1	1	1	1	1	1	1	1	1	1	449245	1
[970] oxalacetic acid [12.45]	1	1	1	1	1	1	1	1	959117	1	9714022	5,76E+07
[3393] Flurazepam [25.225]	1	3,86E+07	2,82E+07	1	1	1	4,30E+07	1223499	1	9778055	7853620	5,91E+07
[979] 4-hydroxyphenylpyruvic acid 1 [16.939]	1	1	1	841715	1	1	1	1	1	1	1,21E+08	1
[5460005] 2-deoxy-D-ribose 1 [13.816]	1	1	1	1	1	1	1	1	1	1	2718643	1
[18407] 4-acetylbutyric acid 2 [10.806]	1	1	1	1	1	1	1	1	1	1	1,40E+07	1
[7427] D-(+) trehalose [24.752]	1	1	1	1	1	1	1	1	2786531	1	1418089	1
[C9] Methyl Pelargonate [9.248]	1	1	1	1	1	1	21165,5	1	1	1	1,28E+07	1
[439227] pipecolic acid 2 [11.22]	1	146498,56	1	1	1	1	1	1	1	889800	2620929	1
[1183] vanillin [14.707]	746287,6	1	90319,1	181557	156272	327176,66	231098,98	1	104630	54275,4	685694	328002
[92817] melezitose [29.884]	1	1	1	1	1	1	1	1	1	1	6128660	1
[91460] Ecgonine [14.66]	1	1	1	1	1	1276551,1	1	1	85133,1	1	110869	1
[5801] 2-aminophenol 3 [13.489]	1	1	1	1	1	1	1	1	1	1	2991847	2,61E+07
[1531] 2-amino-2-methyl-1,3-propanediol 1 [8.436]	1	9,22E+07	1,16E+08	1,02E+08	5,55E+07	8,31E+07	6,79E+07	1	9,48E+07	3,63E+07	1,44E+08	7,74E+07
[700] ethanolamine [9.879]	1	1	1	1	1	2679179,5	1	1	1	1	1356619	1255620
[451991] 1,4-dideoxy-1,4-imino-D-arabinitol 2 [13.906]	1	1	1	1	1	57139,28	1	1	1	1	363824	1
[6054] phenylethyl alcohol [9.328]	1	1	1	163888	1	1	1	1	1	114769	9112132	1
[254] 2,3-dihydroxybiphenyl [16.889]	1	4019240,5	6,42E+07	1,21E+07	260443	1	4,14E+07	1	1	1	3,74E+07	1
[5951] L-serine 2 [11.174]	1	1	1	1	1256493	1	1	420306	1	1	8967476	98365,5
[150923] 3-methyloxyindole 4 [17.013]	1	1	1	1	1	1	1	1	1	1	330532	1
ethylene-5-(2,5-Dioxotetrahydrofuran-3-YL)-6-OXO--10, 10-Dimethylbicyclo[7:2:0]Undeca	370048,5	283599,84	1	103105	1	226244,94	356126,97	213374	1	339454	744568	1
[439167] D-ribose-5-phosphate 2 [19.548]	1	1	1	1	1	1	1	1	1	1	97571,9	1
[13730] 2'-deoxyadenosine [23.781]	1	1	78643,9	1	1	1	1	1	1	1	2256285	1
[10394] 3-(4-hydroxyphenyl)propionic acid [15.979]	1	1	1	1	1	1	1	1	1	1	325039	1
[2724898] 1-octen-3-ol [7.217]	1	1	1	8380031	1	1	1	1	2852358	1	1,50E+08	1
[4646739] 12a-Hydroxy-9-Demethylmunduserone-8-Carboxylic Acid [26.831]	1	383063,97	1	305447	1	1	307343,25	1	243046	167565	768002	1
[188955] 2'-Deoxyadenosine 3' :5'-cyclic monophosphate [27.587]	1	1	1	1	1	1	1	28278,3	1	1	55029,6	1
[239] Beta- alanine 2 [14.555]	1	5,22E+07	2,95E+07	5,32E+07	1	1,78E+07	1	3,42E+07	8,01E+07	351560	1,22E+08	2,75E+07
[11903] 2-ethyltoluene [6.007]	1	1	1	1	1	1	1	1	11792,5	1	1135748	1
[440080] kestose [29.266]	1	18895,94	1	1	97668,9	1	1	1	18308,7	1	1	45846,1
[5950] L-alanine 1 [7.4748]	1	1	1	300540	1	1	1	1	1353407	1	1	1
[7413] cyclohexanecarboxylic acid [8.944]	1	1	1	1	1	1	1	1	227735	1	1	1
[439289] 5alpha-Androstan-3, 17-Dione 2 [24.357]	1	1	1	1	1	1	1	1	26947,6	7820,25	1	1
[740] alpha-D-glucosamine 1-phosphate [16.61]	1	1	1	1	1	1	1	1	1040849	1	1	1
[439194] glyceric acid [10.735]	1	1	1	1	1	1	1	1	3374013	1	1	1
[6131] cytindine-5'-monophosphate 1 [18.663]	1	1	1	1	1	1	1	1	18875,9	1	1	1
[439215] galacturonic acid 2 [18.111]	1	1	1	1	1	1	1	1	12508,3	1	1	1
[262] 2,3-butanediol 2 [6.55]	1	1	1	1	1	5886494	1	1	5548676	9196100	1	1
[867] malonic acid 2 [11.938]	1	1	1	1	1	1	1	1	2482592	1	1	1
[119054] conduritol epoxide 2 [18.004]	1	1	1	1695438	1	1	1	74532,3	5159558	1	1	477626
[2266] azelaic acid [16.359]	1	1	1	911066	1	221207,7	1	1	1404745	1	1	1
[403] 4-aminophenol 3 [14.031]	1	1	1	1	1	1	1	1	498446	1	1	1
[12298] valeramide 2 [7.214]	1	4,33E+07	1	1	1	1	1	2236742	3,36E+07	1	1	1
[439196] L-dithiothreitol 2 [17.086]	1	1	1,22E+07	1	1	1	499869,66	1	3397522	4114295	1	1
[65270] cysteinylglycine 2 [18.473]	1	1	1	1	1	1	1	1	2,23E+07	1	1	1
[5281855] ellagic acid [28.458]	1	1	1	1	1	1	1	1	6148516	1	1	1,50E+07
[791] DL-isoleucine 2 [10.225]	1	1	1	1	345250	1	1	1	499372	1	1	593047
[688664] 3,7-Dimethoxyflavone [23.334]	1	1	1	192798	1	1	259478,5	1	48807,8	1	1	1
[2682] 1-hexadecanol [18.045]	1	1	2012729	8357754	1	1	1	1	109260	1	1	1
[7095] biphenyl [11.505]	1	1	39568,2	1	1	1	89262,37	168264	334981	1	1	1
[7269] 1,2,4,5-tetramethylbenzene [7.804]	437383,94	1,16E+07	86860,2	5,98E+07	6524406	2,50E+07	722128,25	119268	1359769	8284388	1	1,53E+07
[9750] citrulline 1 [15.82]	1	1	1	230968	1	1	1	1	1307266	1	1	3384166
[6106] L-leucine 1 [8.298]	1	1	3,64E+07	1	1	2,48E+07	1	50875,9	2,44E+07	1	1	3,08E+07
[65166] 2', 5'-Dideoxyadenosine [22.114]	1	790436,7	360311	1	1	1	1	1	942682	225752	1	5133975
[985] palmitic acid [18.846]	1	1	1	1	1	1	1,49E+07	2364009	2660688	7996285	1	1,49E+07
[441035] talose 2 [17.584]	1	1	1	1	1	1	1	1	360030	1	1	1
[594] L-cysteine 1 [12.544]	1	1	1	1	1	1761214,6	1	1	8,18E+07	8081511	1	1
[101] 3-hydroxybenzaldehyde [12.313]	1	222479,3	306884	1	335112	1	223264,53	174692	367110	1	1	432536
[439766] citramalic acid [12.63]	1	1	1	1	1	1	1	1	1839802	1	1	1
[8222] eicosane [18.464]	1	27293,49	1	1	1	1	1	1	101542	29466,7	1	307488
[8697] 2-ethylcaproic acid [8.5301]	1	187786,05	1	142910	1	209672,38	321468,8	287846	176416	274611	1	150000
[128869] galactonic acid 2 [18.504]	1	1	1	1	1	1	1	1	131454	1	1	1
[69141] 4-hydroxyquinoline 1 [14.529]	1	1	1	1	1	1	1	1	26226,1	1	1	21030,2
[65550] D-lyxose 1 [14.741]	1	1	1	1	1	1	1	1	4887012	1	1	1
[] L-Ascorbic Acid-13C6 3 [17.489]	3133468	1029338,5	1,93E+07	1517714	2923772	1	1	437414	172784	1	1	5630482
[740] alpha-glucosamine 1-phosphate [16.631]	1	1	54333,3	1	1	1	1	1	232100	1	1	1
[675] 5,6 - dimethylbenzimidazole 2 [16.587]	1	2478721,5	1	25139	1	1	1	185976	8253423	1	1	1
[1133] thioglycolic acid [9.725]	1	1	1	1	1	1	4900116	1	3,02E+07	1	1	2,63E+07
[5280567] 4-methylumbelliferone [18.491]	1	1	1	1	1	1	1	1	57294,5	1	1	1
[9862] 6-methyl-5-hepten-2-one [7.322]	1	1	36430,1	62940,9	1	1	1	7689,89	298917	1	1	1
[10712] cellobiose 2 [24.7]	1	1	1	1	1	1	1	1	137897	1	1	1
[439232] N-acetyl-ornithine 1 [18.196]	1	1	1	1	1	1	1	1	349675	1	1	1
[69141] 4-hydroxyquinoline 2 [18.24]	1	6988586	2167807	69488,5	245205	1	1	1,18E+07	866338	9210190	1	1,00E+07
[8299] acetol 1 [13.293]	1	1	1	1	1	1	1	1	1,05E+07	1	1	1
[1615] 3,4-MDMA [15.444]	1	1	7212596	1	1	1	1	1	2,09E+07	1	1	1
[190] adenine 1 [17.066]	1	1	1	1	1	1	1	1	48379,5	1	1	1
[5280442] Acacetin [13.1191]	427049,78	195979,11	183063	1	1	222848,8	1	177020	138692	1	1	1
[757] glycolic acid [7.049]	1	1	1	1	1	1	1	1	870103	234770	1	1
[6844] 1-hydroxy-2-naphthoic acid [18.356]	1	1	1	1	1	1	1	1	23754,9	1	1	1
[439451] galactinol 2 [26.479]	1	1	1	1	1	1	1	1	771867	1	1	1
[94220] lactamide 1 [7.959]	1	1	1	1	1	1	1	1	1,78E+07	384875	1	1
[11349] 3-hydroxyflavone [21.139]	1	1	1	410694	1	1	13129,37	16069,1	27815,5	15327,9	1	14536
[94220] lactamide 2 [8.394]	1	1	1	1	1	1	1	1	9270676	1	1	1
[33032] L-glutamic acid 3 (dehydrated) [13.232]	1	1	1	1	1	1	1	929515	1761914	1	1	1
[150923] 3-methyloxyindole 2 [13.348]	1	1	1	1	1	1	1	1	198765	1	1	101648
ethylene-5-(2,5-Dioxotetrahydrofuran-3-YL)-6-OXO--10, 10-Dimethylbicyclo[7:2:0]Undec	1	1	1	187358	1	1	1	715387	198067	1	1	107302
[171161] N-gamma-acetyl-N-2-formyl-5-methoxykynurenamine 2 [21.593]	1	1	742027	1	1	1	1	1	487768	1	1	842472
[1136] 4-methyl-5-thiazoleethanol [11.256]	603858,56	1	1,42E+07	637390	1625631	1	1	1	1562612	1	1	1,87E+07
[2901] cycloleucine 2 [11.282]	1	1	1	1	114080	1	1	1	2731720	1	1	1
[444972] fumaric acid [10.94]	1	1	1	1	1	1	1	1	677409	1	1	1
[439742] beta-cyano-L-alanine [11.288]	1	1	1	1	1	1	1	1	414644	1	1	1
[8066] 2-butyne-1,4-diol [9.446]	1	1	2,72E+07	920805	1	1	134215,66	1	6,71E+07	1209895	1	2569778
[73064] beta-glutamic acid [13.279]	1	1	2,09E+07	253749	3454073	1	1	1	2,23E+07	1	1	1
[3015189] Avocadyne [21.805]	925970,75	1	266934	1	1	1	1	1	3373192	1	1	1
[7418] m-toluic acid [11.006]	1	274020,78	240235	204180	1	446832,84	1	157387	290612	237800	1	1
[10820] 4-isopropylbenzoic acid [13.247]	1	1	2665963	1	254867	1	1	21685,7	2366089	1	1	6154236

[11983] 2-indanone [21.732]	1	2153100,5	1	1	1	65329,92	1	1	158639	1	1	1
[3744] indole 3-propionic acid 1 [18.758]	1	1	339412	1	1	1	1	341923	1,18E+07	1	1	9850876
[119] gamma-aminobutyric acid (GABA) [13.326]	1	1367287,4	1	6078079	244880	1	1	1	3049362	1	1	1
[439280] 5-hydroxy-L-tryptophan 2 [22.328]	1	1	1	1	1	1	1	1	304623	1	1	1
[128869] galactonic acid 1 [17.346]	1	1	1	1	1	1	1	1	1872756	1	1	1
[24135] 4-O-Methylphloracetophenone 1 [15.588]	1	1	383965	1	1	1	667806,06	243610	22095,4	1	1	1
[33032] L-glutamic acid 1 [13.338]	1	1	1	1	1	1	1	1	1617262	1	1	192892
[5984] fructose 2 [17.288]	1	1	1	1	1	1	1	1	1417277	1	1	1
[440917] limonene [6.621]	1	1	174725	1	1	1	55454,9	1	91608,9	1	1	1
[753] glycerol [9.941]	1	1	6187260	1,06E+07	7511810	1,03E+07	1	1	9545954	2015984	1	3429366
[7463] p-cymene [6.529]	1	256369,69	148935	1	120092	1	1	90037,7	1,34E+07	1	1	72719,2
[31404] 2,6-ditert-butyl-4-methylphenol 2 [15.189]	1	1	1	1	1	1	1	1	120908	1	1	1
[1549095] coniferyl alcohol [17.849]	1	1	1	1	1	1	1	1	9723,34	1	1	1
[316542] N-ethylglycine 2 [8.773]	1	1	1	1	2092379	1	1	1	2774294	1	1	1
[3037582] mucic acid [18.907]	1	1	110821	1	1	1	1	1	1751647	1	1	1
[6038] 2-hydroxyquinoline 2 [15.5613]	1	1	1	1	1	1	1	1	69169	1	1	1
[243] benzoic acid [9.594]	397720,88	1606826,1	1108997	8365,72	1	210894,12	1	1	863763	1	1	1
[71034] 2-Methoxyxanthone [19.691]	1	1	1	1	1	1	1	1	204305	1	1	1
[18986] 5-methoxy-3-indoleacetic acid 1 [19.743]	1	1	1	1	1	1	1	1	825228	1	1	1
[7472] N,N-dimethyl-1,4-phenylenediamine 1 [11.209]	1	1	1	1	1	1	1	1	3984177	1	1	1749553
[69602] N-omega-acetylhistamine 1 [16.804]	1	1	1	1	131821	1	1	1	685609	1	1	1
[5280335] D-sphingosine 1 [22.326]	1	1	1	3674042	1	8292846	1	487404	2,12E+07	1	1	1
[268779] N-methylglutamic acid 2 [13.38]	1	1	1	1	1	1	1	1	1	1	1	605176
[n/a] L-glutamic acid-2,3,3,4,4-d5 3 (dehydrated) [13.208]	1	1	1	1	1	1	1	1	1	1	1	4,75E+07
[5789] thymidine [21.96]	1	1	1	1	1	1	3376668,8	1	1	1	1	2008039
[994] Phenylalanine 1 [13.545]	1	1	1	1	1	1	1	1	1	1	1	7,71E+07
[5367146] 2-hydroxychalcone 2 [20.305]	525276,56	1	1	277139	1	333352,88	1	1	1	1	1	296790
[4180364] 1,3-dihydroxyacetone [9.662]	1	1	1	1	1	1	1	1	1	1	1	3641205
[995] phenanthrene [16.541]	1	1	1	1	1	7053,43	312071,6	21966,7	1	1	1	19119,8
[92904] 3-indolelactic acid 1 [19.811]	1	1	1	1	1	1	1	1	1	1	1	3,13E+07
[RTL] Myristic Acid d27 [16.727]	1	2366234,2	4620763	5206961	4688308	1	7729748,5	220492	1	1	1	2,88E+07
[8512] 1-hydroxyanthraquinone [20.965]	1	1	100682	1	1	1	1	165014	1	1	1	837634
[72924] 6-hydroxynicotinic acid [13.827]	1	1	1	1	12120,3	1	1	1	1	1	1	262066
[8742] shikimic acid [16.433]	1	1	1	1	1	1	1	1	1	1	1	2563673
[255720] 2-amino-3-methoxybenzoic acid 2 [16.5]	1	1	1	1	1	1	1	1	1	1	1	59941,3
[760] glyoxylic acid [10.813]	1	83131,71	1	1	1	1	1	1	1	1	1	243661
[70] 2-ketoisocaproic acid 2 [9.041]	1	1	1	1	1	1	1	1	1	1	1	9325108
[931] naphthalene [8.87]	1	1	1	1	1	1	1	1	1	1	1	5073945
[8697] 2-ethylhexanoic acid [8.407]	1	1	1	1	1	1	1	1	1	1	1	3085129
[93556] 5,6-dihydro-5-methyluracil 1 [11.637]	1	1	1	1	1	1	1	1	1	1	1	307176
[601] D-Ala-D-Ala3 [16.898]	1	1	1	1	1	1	1	1	1	1	1	2129738
[C8] Methyl Caprylate [7.812]	1	1	3349655	1	1	1	1	1	1	1	1	1267446
[12298] valeramide 1 [7.029]	19857,5	1	1	1	2,51E+07	1	1	8883223	1	1	1	1,94E+07
[10758] mandelonitrile [11.038]	1	1	1	1	1	1	1	1	1	1	1	1,13E+07
[62453] 4-vinylphenol 1 [10.051]	302874,25	171848,67	210126	136734	22245,5	216117,23	40559,08	102782	1	1	1	278890
[326] 4-isopropylbenzaldehyde [11.452]	1	1	1	1	1	1	1	1	1	1	1	375513
[10241] 9-fluorenone [17.583]	855660,2	1	170193	1	165458	291577,8	1	131707	1	1	1	695782
[998] phenylacetaldehyde 2 [8.708]	1	1	1	1	1	1	1	1	1	1	1	2030134
[10836] Methamphetamine 2 [11.387]	1	1	1	1	1	1	1	1	1	1	1	9794359
[1287] epigallocatechin gallate [34.36]	1	1	1	1	1	1	1	1	1	1	1	219330
[21236] L-norleucine 1 [8.945]	1	3548754,8	1,10E+07	1	1	1	1	1	1	1	1	1,89E+07
[5280335] D-sphingosine 3 [22.527]	1	1	1	1	1	1	1	1	1	1	1	453682
[5897] N-2-fluorenylacetamide 2 [22.128]	1	1	1	1	1	59862,99	1	1	1	1	1	222825
[5288725] N-methylalanine [8.43]	1	1	1	1	1	1	1	1	1	1	1	1,13E+07
[4737] Pentobarbital [16.366]	1	1	166610	1	1	1	1	1	1	1	1	364660
[637511] cinnamaldehyde 1 [11.669]	1	1	1	1	1	1	5462702	1	1	1	1	1,27E+07
[39] dihydro-4,4-dimethyl-2,3-furandione 2 [9.671]	1	1	1	1	1	1	1	1	1	1	1	216485
[6724] acenaphthenequinone 1 [18.99]	1	1	1	1	1	1	1	1	1	1	1	76390,1
[13006] 1,2-cyclohexanedione 1 [10.83]	1	1	1	8680,82	1	1	1	1	1	1	1	80524,7
[6998] salicylaldehyde [11.979]	1	1	1	1	212853	1	1	1	1	1	1	232779
[338] salicylic acid [13.075]	1	41375,45	32103,7	1	1	1	337177,38	1	1	1	1	623905
[22819] 1-indanol [11.038]	27985,69	1	1	2568459	1	1	1	1	1	1	1	2821595
[736228] 3-Methylorsellinic Acid 1 [12.918]	439283,53	1	39773,7	190826	1	143756,56	539899,8	1	1	1	1	166242
[441032] D (+)altrose 2 [17.46]	1	1	1	1	2207198	1	1	1	1	1	1	1
[1531] 2-amino-2-methyl-1,3-propanediol 2 [10.56]	1	1	1	1	89181,4	535559,5	1	1	1	1	1	1
[4623424] sophorose 2 [25.189]	1	1	1	1	67150,9	1	1	1	1	1	1	1
[637520] methyl cinnamate [11.58]	1	1	1	1	5194160	1	1	1	1	2292281	1	1
[3848] 3-phenyllactic acid [13.981]	1	1	1	54460,4	17362,5	1	1	1	1	548580	1	1
[1110] succinic acid [10.509]	1	1	1025633	1	290987	3014949,5	1	1	1	1	1	1
[637517] elaidic acid [20.508]	1	1	1	333418	401873	1	1	1	1	1	1	1
[24154] galactosamine 4 [17.797]	1	3,58E+07	1	1,63E+07	5,15E+07	4,47E+07	1	1	1	1	1	1
[2346] benzyl isothiocyanate [11.361]	1	1	1	1	108654	9662,58	1	1	1	1	1	1
[750] glycine [10.456]	1	1	1	1	1,80E+07	3,16E+07	1	1	1	1	1	1
[10393] 4-(2-hydroxyethyl)phenol (tyrosol) [13.862]	1	1	1	1	16839,6	1	1	1	1	182250	1	1
[440294] cis-1,2-dihydro-1,2-naphthalenediol [14.877]	1	1	1	1	283305	1	64937,12	280087	1	521295	1	1
[5826] d-Amphetamine [10.263]	1	1,68E+07	1	1	1,50E+07	1	2568610,5	1	1	1	1	1
[649] 5,6-dihydrouracil 1 [12.314]	1	1	1	1	8980092	1	1	1	1	1	1	1
[94214] methyl-beta-D-galactopyranoside [16.935]	1	1	1	1	4896045	1	1	1	1	1	1	1
[660] dihydrocoumarin 4 [15.666]	1	1	1	1	385731	551364,5	657614,6	595567	1	1	1	1
[643801] methyl palmitoleate [17.466]	1	1	1	1	215255	1	1	1	1	1	1	1
[6912] xylitol [15.376]	1	1	1	1	4245874	1	1	1	1	1	1	1
[3126] DL-dihydrosphingosine 2 [22.602]	1	599318,2	1	1	2461563	1	1,38E+07	668264	1	1	1	1
[12647] L-homoserine 2 [12.359]	1	1	1	1	754247	1	1	1	1	1	1	1
[7478] p-anisic acid [13.2267]	1	111101,35	1	15251,3	16929,8	1	1	17812,7	1	1	1	1
[124925] 8-oxo-2'-deoxyadenosine [23.464]	1	1	1	1	26922,2	1	1	1	1	1	1	1
[n/a] 3-amino-3-(4-hydroxy-phenyl)-propionic acid 1 [17.14]	1	1	1	1	15672,2	1	1	1	1	1	1	1
[31404] 2,6-ditert-butyl-4-methylphenol 1 [13.049]	1	1	1	308228	3153890	570278,75	476449,1	1	1	1	1	1
[4771] Phentermine 2 [11.286]	1	1	1	1	2,45E+07	1	5128651,5	6863676	1	1	1	1
[439626] cellotetraose [30.626]	1	1	1	1	191643	1	1	1	1	1	1	1
[92907] N-alpha-acetyl-L-lysine 2 [17.813]	1	1	1	1	17460	1	1	1	1	1	1	1
[487] methylmalonic acid [9.088]	1	1	1	1	1533361	1	1	1	1	1	1	1
[19] 2,3-dihydroxybenzoic acid [15.698]	1	1	1	1	127695	1	1	1	1	1	1	1
[1101] L- sorbose 1 [17.187]	1	1	1	1	3474811	1	1	1	1	1	1	1
[11266] 2-hydroxybutyric acid [7.852]	1	1	1	584100	143632	1	5117862,5	1	1	1	1	1
[9958] 4-methylcatechol [11.51]	682730,6	1	1	1	574511	1	611363,06	289663	1	1	1	1
[24154] galactosamine 3 [17.523]	1	1	1	1	1,65E+07	1	1	1	1	1	1	1
[608] L-galactono-gamma-lactone 1 [17.331]	1	1	1	1	1136582	1	1	1	1	1	1	1
[79784] tricine 1 [16.048]	1	1	1	1	6813233	1	1	1	1	1	1	1
[3625615] maltotriitol [31.801]	1	1	1	1	17865,6	1	1	1	1	1	1	1
[16217112] D-glucose-C-d7 1 [17.411]	1332271,5	1	447988	1	317568	1396889,1	350063,94	277452	1	174159	1	1
[7817] glycine anhydride 1 [13.52]	1	1	1	1	1237191	1	1	1	1	1	1	1
[9750] citrulline 3 [17.912]	1	1	1	1	189428	1	1	1	1	1	1	1
[403] 4-aminophenol 1 [11.046]	1	1	1	1	12774,5	1	1	1	1	1	1	1
[5280335] D-sphingosine 2 [22.36]	1	1	1	1	76209,1	1	1	1	1	1	1	1
[913] halostachine 1 [11.202]	1	1	1	176642	1	1	1	1	1	1	1	1
[115288] 2-amino-2-norbornanecarboxylic acid 3 [13.389]	1	1	1	147769	1	1	1	1	1	1	1	1
[64956] DL-3-aminoisobutyric acid 1 [9.066]	1	1	1	219173	1	717976,75	1	234884	1	1	1	1
[11970] 2-hydroxyphenylacetic acid [13.786]	1	1	1	110199	1	1	1	1	1	1	1	1

[439352] 1,4-dithioerythritol [17.119]	1	1	1	1,49E+07	1	1	1	1	1	1	1	1
[] L-Ascorbic Acid-13C6 4 [17.73]	1	1	1	4491290	1	1	1	1	1	1	1	1
[351795] 3-indoleacetonitrile [17.214]	1	733424,4	696585	1651229	1	1	1	1	1	1	1	1
[638129] citraconic acid [10.792]	1	1	1	59489,2	1	1	1	1	1	1	1	1
[5275520] geranic acid [12.354]	19823,44	1	1	145517	1	1	1	1	1	1	1	1
[10918] L-carnitine 1 [15.426]	120065,62	222380,3	1	90466,5	1	1	1	1	1	1	1	1
[10256] indole-3-carbaldehyde 1 [17.215]	1	1	1	13772,1	1	1	1	1	1	1	1	1
[5801] 2-aminophenol 2 [12.039]	781911,4	553306,06	137130	216434	1	1	1	1	1	610678	1	1
[68152] 3-hydroxypropanoic acid 3 [18.459]	1	1,11E+07	270784	2414378	1	6104492,5	1	1	1	1	1	1
[11848] 2,3-dimethylsuccinic acid [11.134]	1	1	1	784177	1	1	1	1	1	1	1	1
[2519] caffeine [16.964]	1	1	1	7397,76	1	1	1	1	1	1	1	1
[8174] 1-decanol (decyl alcohol) [11.344]	1	1	1	8226765	1	1	1	1	1	1	1	1
[379] caprylic acid [9.81]	1	2929605	1	5765116	1	1613972,2	1	1	1	1	1	1
[5280441] vitexin 2 [32.988]	1	1	1	1023059	1	1	1	1	1	1	1	1
[12511] 1,4-cyclohexanedione 1 [10.212]	1	1	1	9971,37	1	1	1	1	1	1	1	1
[9316] methyl linolenate [19.432]	1	1	1	112436	1	1	1	1	1	1	1	1
[989] pantolactone [9.05]	1	1	1	452573	1	1	1	1	1	1	1	1
[159664] 2-ketocaproic acid [9.707]	1	1	1	381530	1	1	1	1	1	1	1	1
[97856] guanidinosuccinic acid 1 [17.108]	1	1	1	192635	1	1	1	1	1	1	1	1
[8299] acetol 4 [15.498]	1	1	198012	1	1	1	1	1	1	1	1	1
[997] phenylpyruvate [13.964]	245930,55	1	1,70E+07	1	1	1	1	37365,7	1	1	1	1
[1738] homovanillic acid (HVA) [16.076]	1	1	134356	1	1	1	79947,34	1	1	1	1	1
[275] L-canavanine 1 [9.22]	1	1	5585412	1	1	1	1	1	1	1	1	1
[7911] malonamide 1 [11.636]	1	1	5,49E+07	1	1	1	1	1	1	1	1	1
[359] phloroglucinol [14.621]	1	1	64187,2	1	1	1	1	1	1	17125,9	1	1
[2801] clomipramine [22.582]	1	1	20632,1	1	1	1	1	1	1	1	1	1
[1178] urocanic acid 1 [17.468]	1	1	27194,5	1	1	1	1	1	1	1	1	1
[5960] aspartic acid 2 [13.207]	1	1	11890,3	1	1	1	1	1	1	1	1	1
[1549026] neryl acetate 2 [11.461]	1	1	110296	1	1	1	1	1	1	1	1	1
[1135] thymine [11.599]	1	1	7842,59	1	1	1	1	1	1	1	1	1
[10918] L-carnitine 2 [15.735]	1	1	20418,9	1	1	1	1	1	1	1	1	1
[500] 4-guanidinobutyric acid 2 [13.348]	1	1	975008	1	1	1	1	1	1	1	1	1
[72924] 6-hydroxynicotinic acid [13.845]	1	1	6657,93	1	1	1	1	1	1	1	1	1
[16553] atrazin-2-hydroxy 1 [16.511]	1	1	5493,05	1	1	1	1	1	1	1	1	1
[8163] 2-undecanone 1 [11.323]	1	11975,92	4650908	1	1	1	1	1	1	1	1	1
[439215] galacturonic acid 1 [17.917]	1	1	43137,8	1	1	1	1	1	1	1	1	1
[439176] 5'-deoxy-5'-(methylthio)adenosine 1 [24.627]	1	1	587106	1	1	1	1	1	1	1	1	1
[167685] 22-hydroxycholesterol [28.36]	1	6095524,5	1	1	1	1	1	1	1	1	1	1
[6919] 2-furoic acid [8.073]	1	35515,08	1	1	1	1	1	5430,52	1	1	1	1
[11915] benzoylformic acid 2 [13.386]	795374,94	210556,98	1	1	1	1	600518,4	1	1	1	1	1
[258531] digitoxose 1 [14.22]	1	107018,7	1	1	1	1	1	1	1	1	1	1
[31253] beta-myrcene [6.012]	1	28618,09	1	1	1	1	1	1	1	1	1	1
[2526] beta-glycerolphosphate [15.645]	1	29889,36	1	1	1	1	1	1	1	1	1	1
[101612] Asarinin (-) [27.465]	1	341655,8	1	1	1	1	1	1	1	1	1	1
[443163] (-)-dihydrocarveol 2 [10.205]	1	48389,31	1	1	1	1	1	1	1	1	1	1
[1000] 2-amino-1-phenylethanol [15.668]	1	646252,2	1	1	1	1	1	1	1	1	1	1
[93556] 5,6-dihydro-5-methyluracil 2 [12.524]	1	43818,38	1	1	1	1	1	1	1	1	1	1
[65124] 3-nitro-L-tyrosine 2 [20.658]	1	619040,3	1	1	1	1	1	1	1	1	1	1
[751] DL-glyceraldehyde 2 [9.186]	1	1940476,8	1	1	1	1	1	1	1	1	1	1
[649] 5,6-dihydrouracil 2 [12.773]	1	87983,55	1	1	1	1	1	1	1	1	1	1
[12205373] L-alanine-2,3,3,3-d4 [7.449]	1	1731750,1	1	1	1	1	821909,7	1	1	1	1	1
[n/a] L-glutamic acid-2,3,3,4,4-d5 1 [13.329]	1	28701,72	1	1	1	1	1	1	1	1	1	1
[440294] (1R,2S)-cis-1,2-dihydro-1,2-naphthalenediol [14.922]	1	294442,16	1	1	1	1	1	1	1	1	1	1
[8406] 2-carboxybenzaldehyde 2 [14.282]	1	2,43E+07	1	1	1	1	1	1	1	1	1	1
[1548943] capsaicin [22.788]	613354	238356,05	1	1	1	1	1	139739	1	1	1	1
[763] guanidinoacetic acid 1 [13.855]	1	5912331	1	1	1	1	1	1	1	1	1	1
[9679] 5-aminoimidazole-4-carboxamide 1 [14.616]	1	65330,46	1	1	1	41989,93	1	1	1	1	1	1
[99289] L-allothreonine 1 [10.212]	1	1668752,9	1	1	1	950730,9	1	1	1	1	1	1
[12460] Phendimetrazine 1 [14.38]	1	47240,14	1	1	1	1	1	1	1	1	1	1
[5280802] trans-3,5-dimethoxy-4-hydroxycinnamaldehyde [19.433]	1	202999,31	1	1	1	1	1	1	1	1	1	1
[119054] conduritol epoxide 1 [17.751]	1	1344651,9	1	1	1	1	1	1	1	1	1	1
[8299] acetol 2 [15.293]	1	1	1	1	1	3673823	1	1	1	1	1	1
[751] DL-glyceraldehyde 1 [8.974]	1	1	1	1	1	3,66E+07	1	3265798	1	1	1	1
[439204] xylulose [15.077]	1	1	1	1	1	1506466,9	1	1	1	1	1	1
[439782] glucuronolactone 1 [16.97]	1	1	1	1	1	81039,26	1	1	1	1	1	1
[11321] acetylisatin 6 [17.361]	1	1	1	1	1	327539	1	1	1	1	1	1
[6058] 2-aminoethanethiol 2 [21.574]	1	1	1	1	1	1175406,5	1	1	1	1	1	1
[5143] saccharin 1 [16.694]	1	1	1	1	1	36699,48	1	1	1	1	1	1
[5988] Sucrose [23.988]	1	1	1	1	1	15950,78	1	1	1	1	1	1
[289] catechol [10.524]	733972,75	1	1	1	1	414004,56	1	44146,6	1	1	1	1
[440473] L-mimosine 1 [8.863]	1	1	1	1	1	3421225,5	1	1	1	1	1	1
[171161] N-gamma-acetyl-N-2-formyl-5-methoxykynurenamine 1 [21.074]	1	1	1	1	1	34280,08	1	1	1	1	1	1
[5280598] farnesal 2 [16.331]	1	1	1	1	1	109870,35	1	1	1	1	1	1
[10787] benzene-1,2,4-triol [14.164]	1	1	1	1	1	32528,88	1	1	1	1	1	1
[637511] cinnamaldehyde 2 [11.814]	1	1	1	1	1	8379065,5	1	1	1	1	1	1
[19844] methyl 4-hydroxy-3-methoxybenzoate [14.744]	1	1	1	1	1	67939,81	1	1	1	132863	1	1
[936] nicotinamide 1 [11.656]	1	1	1	1	1	30674,51	1	1	1	1	1	1
[5960] aspartic acid 1 [12.002]	1	1	1	1	1	1	1	1780196	1	1	1	1
[65098] norvaline 1 [7.582]	1	1	1	1	1	1	1	388434	1	1	1	1
[64969] 3-methyl-L-histidine [16.423]	1	1	1	1	1	1	1	16444,5	1	1	1	1
[638011] citral 2 [10.912]	1	1	1	1	1	1	1	20743,3	1	1	1	1
[8400] benzoin 2 [17.102]	1	1	1	1	1	1	1	29377,1	1	1	1	1
[676293] 6,3'-Dimethoxyflavone [24.691]	1	1	1	1	1	1	1	196093	1	1	1	1
[3337] Fenfluramine [9.3575]	1	1	1	1	1	1	1	7299,97	1	1	1	1
[228398] L-theanine 2 [16.171]	1	1	1	1	1	1	1	35664,7	1	1	1	1
[C24] Methyl Linocerate [24.603]	1	1	1	1	1	1	1	291655	1	1	1	1
[1017] phthalic acid [15.218]	1	1	1	1	1	1	1	18800,2	1	1	1	1
[660] dihydrocoumarin 3 [15.092]	1	1	1	1	1	1	1	1087769	1	705135	1	1
[440575] trans-3-hydroxy-L-proline 2 [12.536]	1	1	1	1	1	1	1	86797,3	1	1	1	1
[637566] geraniol [11.181]	1	1	1	1	1	1	1	276923	1	1	1	1
[5280450] linoleic acid [20.399]	1	1	1	1	1	1	1	2132752	1	1	1	1
[863] lipoamide 1 [16.384]	1	1	1	1	1	1	1	5537,65	1	1	1	1
[6854] carbazole 1 [17.044]	1	1	1	1	1	1	1	10369,7	1	1	1	1
[7618] triethanolamine [14.464]	1	1	1	1	1	1	5760299	1	1	1	1	1
[5778] 6-methylmercaptopurine 2 [17.874]	1	1	1	1	1	1	4316,86	1	1	1	1	1
[717531] 3,4-Dimethoxycinnamic Acid 1 [16.984]	1	1	1	1	1	1	112327,42	1	1	1	1	1
[439665] threose 1 [12.251]	970809,8	1	1	1	1	1	2784330,5	1	1	1	1	1
[42953] diglycerol 3 [15.989]	1	1	1	1	1	1	5908919	1	1	1	1	1
[8914] 1-nonanol [10.014]	1	1	1	1	1	1	552381,6	1	1	1	1	1
[328] DL-4-hydroxymandelic acid [16.126]	1	1	1	1	1	1	84885,72	1	1	1	1	1
[5459862] D-erythrose-4-phosphate 1 [17.508]	1	1	1	1	1	1	180354,53	1	1	1	1	1
[597] cytosine 2 [13.255]	1	1	1	1	1	1	11711,54	1	1	1	1	1
[614] L-proline 2 [10.341]	1	1	1	1	1	1	181512,73	1	1	1	1	1
[4771] Phentermine 1 [8.357]	28944,95	1	1	1	1	1	14552,9	1	1	1	1	1
[9750] citrulline 2 [16.691]	1	1	1	1	1	1	13429,75	1	1	1	1	1
[1178] urocanic acid 2 [18.533]	1	1	1	1	1	1	134500,19	1	1	1	1	1
[68499] nicotinoylglycine [17.348]	1	1	1	1	1	1	559618,4	1	1	1	1	1
[97143] 3-Hydroxy-3',4'-Dimethoxyflavone [24.584]	1	1	1	1	1	1	1	1	1	11337,4	1	1

[676159] 1-methyl-L-tryptophan 1 [19.523]	1	1	1	1	1	1	1	1	1	7231663	1	1
[7705] butylbenzene [6.985]	1	1	1	1	1	1	1	1	1	32485,1	1	1
[4762] Phenmetrazine [14.774]	1	1	1	1	1	1	1	1	1	2778498	1	1
[273260] N-acetyl-L-histidine 2 [19.507]	1	1	1	1	1	1	1	1	1	92841,4	1	1
[5351896] trans-3-hexenedioic acid [13.08]	1	1	1	1	1	1	1	1	1	8020662	1	1
[1088] sarcosine [8.032]	1	1	1	1	1	1	1	1	1	54656,4	1	1
[835] dehydroascorbic acid 3 [17.49]	1	1	1	1	1	1	1	1	1	751626	1	1
[6262] L-ornithine 1 [14.349]	1	1	1	1	1	1	1	1	1	78404,4	1	1
[873] 3-(2-hydroxyphenyl)propanoic acid [15.087]	1	1	1	1	1	1	1	1	1	197220	1	1
[428] 1,3-diaminopropane 1 [14.708]	1	1	1	1	1	1	1	1	1	140505	1	1
[904] acetanilide 2 [11.346]	1	1	1	1	1	1	1	1	1	23412,8	1	1
[4303260] Anhydrobrazilic Acid [20.7505]	1	1	1	1	1	1	1	1	1	1099840	1	1
[2879] p-cresol [8.211]	1	1	1	1	1	1	1	1	1	9133,28	1	1
[978] 4-aminobenzoic acid [16.732]	1	1	1	1	1	1	1	1	1	242351	1	1
[36143] 4-hydroxyphenylglycine 1 [16.094]	29672,72	1	1	1	1	1	1	1	1	1	1	1
[446220] Cocaine [20.605]	17806,27	1	1	1	1	1	1	1	1	1	1	1
[5280887] 15-keto-prostaglandin F2alpha [24.939]	975179,9	1	1	1	1	1	1	1	1	1	1	1
[369312] (-)-perillyl alcohol [11.693]	401695,97	1	1	1	1	1	1	1	1	1	1	1
[12460] Phendimetrazine [12.585]	9366,39	1	1	1	1	1	1	1	1	1	1	1
[7680] 2-phenylacetamide 1 [11.591]	8713,98	1	1	1	1	1	1	1	1	1	1	1
[58] 2-ketobutyric acid [7.427]	104853,52	1	1	1	1	1	1	1	1	1	1	1
[121805] 2-Methoxyresorcinol [11.936]	301777,03	1	1	1	1	1	1	1	1	1	1	1
[12122] 3-hydroxyphenylacetic acid [14.264]	834823,06	1	1	1	1	1	1	1	1	1	1	1
[135] 4-hydroxybenzoic acid [14.505]	559925,5	1	1	1	1	1	1	1	1	1	1	1
[8419] 3,4-dimethoxybenzaldehyde [13.9]	727191,1	1	1	1	1	1	1	1	1	1	1	1

B

	control			Fe-deficiency			S-deficincy			Fe+S-deficiency		
Compound	exud_1-A	exud_2-A	exud_3-A	exud_4-A	exud_5-A	exud_6-A	exud_7-A	exud_8-A	exud_9-A	exud_10-A	exud_11-A	exud_12-A
6-Prenylnaringenin	1494587	1469769	1741803	357838	1	524810	1557643	1534968	561419	1619208	947182	574926
Myristic acid	438731	266340	1	790545	247063	1	926058	1	532740	551872	927455	929777
[6]-Gingerol	1748458	1775674	2243122	1571049	1452560	1518071	1585377	1821062	2677551	2083466	2434154	2988430
L-tryptophan	64297	58443	58115	26366	46261	27685	59369	44140	79568	1	256123	27365
L-histidine	75087	93106	63453	41200	209880	31142	22377	279942	363691	29231	73888	50329
Neodiosmin	150520	180377	179232	190251	154541	180626	150506	142474	250095	184620	298147	160249
deoxymugineic acid	79068	63870	80461	40778	42723	17402	1	70300	108111	20675	15745	13334
5-Caffeoylquinic acid	57730	1	28206	38759	28260	27827	78345	1	36653	43323	58485	60076
ıethyl-3-(3-hydroxyphenyl)propionat	273712	428362	358900	485172	247070	195584	295052	341972	375397	415482	264180	330224
Vanillic acid	1	1	1	1	1	1	1	1	1	1	1	74943
Lauric acid	1	87404	121721	100823	81850	1	127514	1	296187	1	196497	107449
7-Oxomatairesinol	1	214335	1	350995	308844	302337	1	74396	1	1	262639	160181
Schottenol ferulate	2464290	1	2379654	1	599111	1	1694941	1	1	1	1237069	356937
Avenanthramide 2c	26179	1	38239	72807	325085	1063408	141278	93201	41404	106089	77429	69071
Cyanidin 3-O-glucosyl-rutinoside	66946	105514	105033	113208	87622	117778	123956	99247	79434	104447	120007	119311
Dihydrocaffeic acid	154793	131595	150438	118988	148949	147952	152607	92860	116995	124902	1	125947
1-Caffeoylquinic acid	57730	1	28206	38759	28260	27827	78345	1	36653	43323	58485	60076
24-Methylcholesterol ferulate	1031537	2113849	1	2357892	871909	238621	1284324	1631779	741630	45980	2692301	43376
citramalic acid	1	1	1	1	1	1	1	1	1	1	1	158938
Arachidic acid	257541	193425	355611	302866	174441	1	394723	421619	1	259472	460733	485013
3,5-Dicaffeoylquinic acid	1	652108	678790	383144	1	623737	716997	719055	1	754349	747644	760838
4-Vinylguaiacol	21695	3253153	4364452	1	58844	77402	4267172	3566953	1	2188311	3831017	1747773
5-Heptadecylresorcinol	69138	62484	69006	66297	63845	55261	66928	64780	55646	68506	73549	71756
Avenanthramide 2p	1	1	1	1	325085	1063408	141278	93201	41404	106089	77429	69071
Palmitic acid	184375	160775	165653	124405	58530	86101	194704	153558	427518	242643	1	297105
Thymol	953517	408288	1833433	229355	890524	1015030	1320822	1147569	1097188	1333596	473366	185070
7-Hydroxymatairesinol	1	107882	1	1	279675	57021	1	80261	1	1	221946	61094
Lignoceric acid	199649	201690	259695	112460	262558	181022	256683	292589	137847	271850	510464	238789
Benzoic acid	1195719	1127005	2126188	1326020	1517047	90141	1197776	1197624	1160438	1168788	171345	177759
8-Prenylnaringenin	1494587	1469769	1741803	357838	1	524810	1557643	1534968	561419	1619208	947182	574926
Naringenin 7-O-glucoside	305459	247137	324606	326030	260660	274671	287820	274058	342951	1	337562	374517
L-glutamate	99623	190134	38857	45084	76088	89083	84968	200993	242369	49632	142043	19917
Kaempferol 3-O-galactoside	758185	494381	800859	1	678596	639034	667875	795978	751966	786682	779846	809925
p-Coumaroyl glycolic acid	1	1	1	1	1	1	1	1	1	1	1	74943
glucose/fructose	389095	50101	33391	12146	619779	1	10090	354604	385538	1	139799	16320
Malvidin 3-O-(6''-acetyl-galactoside)	802816	749292	770335	797623	716506	735390	775478	803008	806904	882182	845585	898904
Epirosmanol	1	1	1	1	1	1	1	1	1	36104	1	40543
m-Coumaric acid	154793	131595	150438	118988	148842	147952	152607	92860	116995	119703	1	125947
Petunidin 3-O-(6''-acetyl-galactoside)	1543652	1665877	1701905	1396270	458283	163799	1649310	1694048	1682679	1821010	1816877	1923351
Malvidin 3-O-(6''-acetyl-glucoside)	802816	749292	770335	797623	716506	735390	775478	803008	806904	882182	845585	898904
Methoxyphenylacetic acid	319669	339402	150054	407863	1	338274	344087	293037	267012	112224	310503	202330
Sinapic acid	213115	109236	70527	40866	97812	40179	36570	113593	147336	1	72375	59601
Sitosterol ferulate	2464290	1	2379654	1	599111	1	1694941	1	1	1	1237069	356937
3-Caffeoylquinic acid	57730	1	28206	38759	28260	27827	78345	1	36653	43323	58485	60076
3,4-Dihydroxyphenylacetic acid	1	1	1	1	1	1	1	1	1	1	1	74943
Caprylic acid	1	1	1	1	1	1	1	1	1	1	594073	72185
L-glutamine	61590	68493	25022	29069	340768	150292	53872	100465	201826	65173	1	19532
L-citrulline	85816	14187	1	44521	51749	47244	1	105635	145713	28831	113698	19674
Isoferulic acid	553213	1	824858	758469	399154	649895	473285	332868	453897	636916	654051	571320
1,5-Dicaffeoylquinic acid	688203	652108	678790	383144	1	623737	716997	719055	1	754349	747644	760838
Syringaldehyde	154793	131595	150438	118988	148949	147952	152607	92860	116995	124902	1	125947
Homovanillic acid	154793	131595	150438	118988	148949	147952	152607	92860	116995	124902	1	125947
Quercetin 3-O-rhamnoside	758185	494381	800859	1	678596	639034	667875	795978	751966	786682	779846	809925

Sesamol	70091	1	1	98432	1	1	99694	116125	72581	1	1	54819
Neohesperidin	134596	177267	173456	171210	132714	129112	119598	79675	194194	142640	168765	66732
Sitostanyl ferulate	2499375	1	2379654	1	599111	1	1694941	1	1	1	1237069	360192
4-Vinylsyringol	273712	428362	358900	485172	247070	195584	295052	341972	375397	415482	264180	330224
5-Tricosylresorcinol	4022472	3785382	3935954	4043314	3942656	3961271	3914001	4052906	4084376	4186832	4243962	4244739
4-Hydroxycoumarin	403177	413248	1	511558	1	390191	470893	576732	498785	579132	532330	624086
succinate	446330	439804	444925	441169	429671	465464	334772	363104	325347	308998	345893	286917
Syringaresinol	58120	25103	30484	21168	75650	47171	71066	37543	80041	84000	48166	54829
4-Ethylphenol	1	305760	353300	576826	635188	424386	280381	512036	504891	289929	330266	433176
L-lysine	165582	184599	1	74729	1	185908	1	1	1	173452	1	88490
Kaempferol 7-O-glucoside	758185	494381	800859	1	678596	639034	667875	795978	751966	786682	779846	809925
Isohydroxymatairesinol	1	107882	1	1	279675	57021	1	80261	1	1	221946	61094
Ferulic acid	553213	1	824858	758469	399154	649895	473285	332868	453897	636916	654051	571320
Resveratrol	1	1423551	1	1	1	1	1	66368	183419	368402	76647	293853
Caffeic acid ethyl ester	25452	1	1	1	20368	53930	1	18970	58821	83072	1	62375
5-Pentacosenylresorcinol	4444017	4446023	4384315	4410139	4299235	4582405	4738288	4817370	4812238	4786786	4953116	4759139
1,3-Dicaffeoylquinic acid	688203	652108	678790	383144	1	623737	716997	719055	1	754349	747644	760838
6''-O-Malonyldaidzin	1	271559	248616	1435755	1194625	73815	1406366	1459979	1405079	1510061	1553708	1091901
Umbelliferone	403177	413248	1	511558	1	390191	470893	576732	498785	579132	532330	624086
Nortrachelogenin	1	107882	1	1	279675	57021	1	80261	1	1	221946	61094
l-dihydroxyphenyl-2-oxypropanoic a	403928	386581	389702	508079	1	409673	1	544762	515924	550344	516195	601772
Phytofluene	79505	52325	46623	48089	31128	15354	33122	106412	113782	1	44260	35023
Hesperidin	134596	177267	173456	171210	132714	129112	119598	79675	194194	142640	168765	66732
Xanthohumol	67963	1	104304	129090	87846	1	64528	156104	172311	1	136611	133540
4-Caffeoylquinic acid	57730	1	28206	38759	28260	27827	78345	1	36653	43323	58485	60076
Peonidin 3-O-rutinoside	157093	180377	194357	190251	160287	183501	150506	142474	261192	199027	301782	160249
Cerotic acid	247899	253131	292643	165196	261890	132133	291015	283789	324698	156352	181388	354556
Caffeic acid	403928	386581	389702	508079	1	409673	1	544762	515924	550344	516195	601772
Carnosic acid	211707	177366	221700	170906	1	656528	211184	141832	181690	167569	195627	188422
Capric acid	1877062	1678348	1683648	2215958	1477266	1832916	1512330	1957329	1	1953936	1815137	1502315
Cyanidin	430502	394667	377473	334887	272127	257392	257355	256039	231046	265507	268607	219597
Zeaxanthin	48845	1	43896	44287	48384	46205	1	73908	38775	59195	1	29139
4-Vinylphenol	65939	109973	1	85782	105891	1	61862	1	1	1	1	77906
Petunidin 3-O-(6''-acetyl-glucoside)	1543652	1665877	1701905	1396270	458283	163799	1649310	1694048	1682679	1821010	1816877	1923351
o-Coumaric acid	154793	131595	150438	118988	148842	147952	152607	92860	116995	119703	1	125947
3-Methoxyacetophenone	21695	3253153	4364452	1	58844	77402	4267172	3566953	1	2188311	3831017	1747773
Cirsimaritin	600051	511011	399935	288302	272192	119689	42853	347000	644416	85889	126992	55264
p-Coumaric acid ethyl ester	109861	250315	66865	51581	205537	114066	180115	1	157576	89952	1	64576
p-Coumaric acid	154793	131595	150438	118988	148842	147952	152607	92860	116995	119703	1	125947
Luteolin 6-C-glucoside	758185	494381	800859	1	678596	639034	667875	795978	751966	786682	779846	809925
Conidendrin	1	246158	1	117971	279675	1	151336	82884	1	126060	1	65157
Behenic acid	316871	206171	303576	367574	336073	211006	254672	113303	393124	440571	519931	278119
Phytoene	120649	85744	79882	67786	70172	88672	100648	148880	137183	34568	200345	138727
Dihydroquercetin	357767	251814	498078	193779	204318	193852	222352	188117	434230	298734	117197	301806
Kaempferol 3-O-glucoside	758185	494381	800859	1	678596	639034	667875	795978	751966	786682	779846	809925
Ferulic acid 4-O-glucoside	1	22614	1	1	1	1	1	1	1	1	79266	130040
Cinnamic acid	263108	272930	230536	354922	207612	263965	324181	173107	221435	263696	243185	168352
5-Heneicosenylresorcinol	112286	97174	149442	135335	180153	1	181827	151383	164679	168916	185817	197790
Dicaffeoylquinic acid	688203	652108	678790	383144	1	623737	716997	719055	1	754349	747644	760838
Phlorin	1	1	1	1	1	1	1	1	1	1	158226	145728
6-Hydroxyluteolin 7-O-rhamnoside	758185	494381	800859	1	678596	639034	667875	795978	751966	786682	779846	809925
Luteolin 7-O-glucoside	758185	494381	800859	1	678596	639034	667875	795978	751966	786682	779846	809925
Dimethylmatairesinol	1918267	1928837	2020529	2929658	2667688	2061438	2035529	2259967	2470753	1578533	1847114	1864992
7-Hydroxysecoisolariciresinol	1	1	1	73165	53651	1	24271	47513	1	1	1	50089
npferol 3-O-glucosyl-rhamnosyl-gluc	59049	77247	74222	76214	61570	84073	93512	75639	71787	87771	89797	96863
Carvacrol	953517	408288	1833433	229355	890524	1015030	1320822	1147569	1097188	1333596	473366	185070
Feruloyl glucose	1	22614	1	1	1	1	1	1	1	1	79266	130040
Cinnamoyl glucose	130935	109414	147365	155153	100236	1	1	138971	1	49806	89934	38222
4,5-Dicaffeoylquinic acid	688203	652108	678790	383144	1	623737	716997	719055	1	754349	747644	760838
Campesteryl ferulate	4305491	4408798	4314725	4694750	4284994	4429214	4761247	4954320	5083339	5204168	5128123	5420476
Estragole	245091	175590	173032	209206	1	200909	113316	151894	192073	183367	170759	156510
Isoxanthohumol	67963	1	104304	129090	87846	1	64528	156104	172311	1	136611	133540
p-Coumaroyl tyrosine	138320	38635	108882	144997	55186	1	1	95562	174661	38648	35454	27406
Diosmin	150520	180377	179232	190251	154541	180626	150506	142474	250095	184620	298147	160249
methylthiopropyl-desulfoglucosinola	148599	46750	136391	132024	62914	240329	162089	116400	73956	229489	91196	66675
Dihydro-p-coumaric acid	319669	339402	150054	407863	1	338274	344087	293037	267012	112224	310503	202330
Lutein	48845	1	43896	44287	48384	46205	1	73908	38775	59195	1	29139
pyroglutamate	99623	190134	38857	45084	76088	89083	84968	200993	239149	49632	138201	19917
pferol 3-O-glucosyl-rhamnosyl-galact	59049	77247	74222	76214	61570	84073	93512	75639	71787	87771	89797	96863
2-Hydroxybenzoic acid	70091	1	1	98432	1	1	99694	116125	72581	1	1	54819
3,4-Dicaffeoylquinic acid	688203	652108	678790	383144	225221	623737	716997	719055	1	754349	747644	760838
5-Tricosenylresorcinol	1	46954	40476	1	34742	1	1	50455	1	37208	42575	46410
Coumarin	101999	30018	138953	119964	93748	35434	29566	110544	161561	97058	370488	19256
Anethole	245091	175590	173032	209206	1	200909	113316	151894	192073	183367	170759	156510
cetin 3-O-rhamnosyl-rhamnosyl-gluc	59049	77247	74222	76214	61570	84073	93512	75639	71787	87771	89797	96863

1-Sinapoyl-2,2'-diferuloylgentiobiose	1	30902	1	44328	33760	1	33996	32776	18628	38925	41053	37686
3-Hydroxybenzoic acid	1	1	1	1	1	1	1	1	1	1	1	1
avenacin A1	1	1	1	1	1	1	1	124392	57449	1	1	1
3-Methoxysinensetin	1	1	1	1	161222	567414	18152	1	1	1	69510	1
6-Geranylnaringenin	1	1	100104	54407	1	33269	40333	66854	85627	141734	46441	1
4-Hydroxybenzoic acid 4-O-glucoside	1	1	1	1	108670	514202	1	1	1	1	62982	1
Trachelogenin	1	1	1	1	156210	564114	1	1	1	1	55388	1
Kaempferol	349928	248807	1	201720	200914	1	1	1	1	322868	147788	1
3-p-Coumaroylquinic acid	1	22650	1	1	1	1	1	1	1	102378	80863	1
2-Methoxy-5-prop-1-enylphenol	1	1	1	91529	1	408729	1	1	36427	1	1	1
Indol	1	1	1	1	86796	215699	22661	1	1	1	56849	1
Vanillin	36528	40320	56829	1	11915	1	1	52349	69185	1	1	1
Phloretin	26278	1	28350	22633	1	12427	1	29500	43481	1	1	1
Punicalagin	1	1	1	1	60931	1	140622	1	1	99265	330320	1
avenacin B1	296027	32746	26066	1	74897	21110	21868	380926	489236	1	105531	1
Protocatechuic acid 4-O-glucoside	37676	45119	30057	17204	18616	1	1	26287	53668	1	1	1
4-Hydroxyphenylacetic acid	36528	40320	56829	1	11915	1	1	52349	69185	1	1	1
4-Feruloylquinic acid	117035	1	1	1	37316	1	1	112507	175124	1	40212	1
Tetramethylscutellarein	195634	1	1	1	267276	1	875142	889459	1	1050573	1	1
benzoxazinone	1	1	1	1	50483	27649	1	1	1	1	1	1
Pinosylvin	1	1	1	1	62878	211818	1	1	1	1	32865	1
Scutellarein	349928	248807	1	201720	200914	1	1	1	1	322868	147788	1
Nobiletin	1	1	1	1	161222	567414	18152	1	1	1	69510	1
Quercetin 3-O-acetyl-rhamnoside	1	1	1	1	1	169832	1	1	1	1	1	1
5-p-Coumaroylquinic acid	1	22650	1	1	1	1	1	1	1	102378	80863	1
Arctigenin	1	1	1	1	1	1	1	1	1	81025	105847	1
p-Coumaroyl malic acid	1	1	1	1	79477	110674	1	1	1	1	1	1
4-Ethylguaiacol	1	88794	92757	1	105665	1	1	185542	1	1	78847	1
3-Feruloylquinic acid	117035	1	1	1	37316	1	1	112507	175124	1	40212	1
L-valine	1	1	1	1	1004518	857213	1	1	1	1	1666606	1
1,4-Naphtoquinone	1	1	1	1	1	1	1	1	1	1	1	1
5-Feruloylquinic acid	117035	1	1	1	37316	1	1	111593	175124	1	40212	1
Medioresinol	1	1	1	1	156210	564114	1	1	1	1	55388	1
Hydroxycaffeic acid	16308	1	1	1	330377	1	1	58351	41832	1	174977	1
isosakuranetin	62633	10660	1	1	17993	1	1	83831	98206	1	33699	1
Stearic acid	61636	1	270552	394802	130071	1	234720	340222	356253	212434	200836	1
Quercetin 4'-O-glucoside	1	1	1	1	161222	567414	18152	1	1	1	69510	1
1,2-Disinapoylgentiobiose	1	32662	1	40434	1	44299	44770	45862	1	1	1	1
sorgolactone	595863	1	1	1	1	1	1	49949	34402	1	1	1
L-proline	139306	108146	107438	1	1	130994	119142	1	1	1	1	1
3-hydroxymugineic acid	23651	1	1	1	1	1	1	1	1	47681	1	1
p-Coumaroylquinic acid	1	22650	1	1	1	1	1	1	1	102378	80863	1
4-p-Coumaroylquinic acid	1	22650	1	1	1	1	1	1	1	102378	80863	1
Daidzin	310658	261033	339370	328786	260660	274671	287820	273767	345594	360119	371136	1
Luteolin	349928	248807	1	201720	200914	1	1	1	1	322868	147788	1
24-Methyllathosterol ferulate	1031537	2113849	1	2357892	871909	238621	1284324	1631779	741630	1	1	1
Eugenol	1	1	1	91529	1	408729	1	1	36427	1	1	1
L-arginine	62168	1	1	29360	1	25325	1	34315	120143	1	1	1
4-Ethylcatechol	65939	112751	1	106205	104872	1	1	1	1	1	1	1
maltose/sucrose	811260	141322	158153	1	258552	101662	149941	782927	1183489	1	373682	1
benzyl-desulfoglucosinolate	85397	74461	30776	1	27286	1	1	137916	43572	1	1	1
1,2,2'-Triferuloylgentiobiose	36126	36602	35138	46891	40629	53156	47349	56795	39469	51627	44800	1
4-Hydroxybenzoic acid	70091	1	1	98432	1	1	99694	116125	72581	1	1	1
Formononetin	1	1	1	198914	79806	106463	182041	164483	118421	1	100073	1
-methylthiohexyldesulfoglucosinolat	1	1	1	1	1	61409	27807	46455	26083	74178	67069	1

Supplementary Table 4. Fold-change analysis of metabolites obtained through LC-MS in the root exudates of plants exposed to the different nutritional conditions

Supplementary Table 5. Metabolites resulting down-accumulated or up-accumulated in the root exudates of plants exposed to the different nutritional conditions. Tanimoto substructure chemical similarity coefficients through Chemical Similarity Enrichment Analysis tool were used to cluster metabolites into chemical groups.

Class	Compound	FC Fe deficiency	FC S deficiency	FC Fe + S deficiency
Acetoacetates	acetoacetate	-1.7	-11	-8.7
Acids, Carbocyclic	diethyl phthalate	3.3	-9.5	-1.3
	Dihydro-p-coumaric acid	-5.4	0.19	-0.54
	Methoxyphenylacetic acid	-5.4	0.19	-0.54
	mono(2-ethylhexyl)phthalate	15	16	14
Alkaloids	trigonelline	0.13	1	-17
Alkanes	eicosane	-15	-15	1.8
Alkenes	1-octadecene	-	1.4	13
Amides	adipamide	24	-	15
Amino Acids	L-allothreonine	4.1	-3.1	-8.9
	Beta- alanine	-0.35	-7.8	-8
	DL-3-aminoisobutyric acid	19	18	-
	DL-isoleucine	-1.3	-9.4	-7.4
	glycine	25	-	-
	L-citrulline	5.7	1.2	5.1
	L-glutamine	1.5	1.1	-5.6
	L-homoserine	-1.1	-10	-20
	L-serine	20	19	11
	N-acetyl-ornithine	19	-	11
	indole 3-propionic acid	-18	-5.6	4.9
	L-proline	-11	-11	-17
	L-tryptophan	-0.66	-0.078	-5.1
Anisoles	3-Methoxyacetophenone	-8.4	-4.8	1.7
	Anethole	-5.6	-0.45	-0.34
	Estragole	-5.6	-0.45	-0.34
Ascorbic Acid	L-Ascorbic Acid	-3.4	-2.3	0.51
Benzaldehydes	3-hydroxybenzaldehyde	0.36	-5.6	0.73
	4-hydroxybenzaldehyde	-2.3	-2.3	-13
	benzaldehyde	-0.034	-0.71	-5.8
	Syringaldehyde	0.16	-0.35	-6
	Vanillin	-11	-4.9	-16
Benzene Derivatives	1,2,4,5-tetramethylbenzene	4.8	-6.1	3.9
	biphenyl	-15	-3.4	-15
	p-cymene	-0.7	-5.7	-1.4
Benzimidazoles	5,6 - dimethylbenzimidazole	-6.6	-9.2	-21
	5,6 - dimethylbenzimidazole	-20	-20	-6.4
Benzoates	4-isopropylbenzoic acid	-3.4	-12	1.2

	m-toluic acid	0.24	-8.5	-0.11
	benzoic acid	-4.4	-16	0.31
Benzodiazepinones	Flurazepam	-0.23	-2.2	-7.1
Benzothiazoles	benzothiazole	-5.4	-2.6	-4.7
Benzyl Alcohols	2-hydroxybenzyl alcohol	-3.1	-18	-8.3
	4-isopropylbenzyl alcohol	2.2	-6.6	-7.8
	benzyl alcohol	-16	-16	-7.4
Butyrates	gamma-aminobutyric acid	-0.16	-15	-20
	2-hydroxybutyric acid	18	22	-
	4-acetamidobutyric acid	-	22	13
	L-(+) lactic acid	1.8	-14	-5.3
Caffeic Acids	1,3-Dicaffeoylquinic acid	-6.5	-6.4	0.026
	4-Caffeoylquinic acid	5	0.22	5.4
	5-Caffeoylquinic acid	5	0.22	5.4
	Caffeic acid	-5.8	-6	0.36
	Dicaffeoylquinic acid	-6.5	-6.4	0.026
	Dihydrocaffeic acid	0.16	-0.35	-6
	Hydroxycaffeic acid	-7.5	-3.5	-8.2
Carbamates	carbamic acid ethyl ester (urethane)	0.15	-4.1	-8.3
Carotenoids	Lutein	5.4	0.083	-0.24
	Phytofluene	-0.79	0.29	-5.8
	Zeaxanthin	5.4	0.083	-0.24
Ceramides	DL-dihydrosphingosine	2	2.3	-19
Cinnamates	1,5-Dicaffeoylquinic acid	-6.5	-6.4	0.026
	1-Caffeoylquinic acid	5	0.22	5.4
	3,4-Dicaffeoylquinic acid	-0.6	-6.4	0.026
	3,5-Dicaffeoylquinic acid	-0.062	0.017	6.5
	3-Caffeoylquinic acid	5	0.22	5.4
	Isoferulic acid	6.5	5.7	6.2
Coumaric Acids	1,2-Disinapoylgentiobiose	5.5	10	-5.1
	24-Methylcholesterol ferulate	6.2	6.4	3.6
	4-Vinylguaiacol	-8.4	-4.8	1.7
	Ferulic acid	6.5	5.7	6.2
	m-Coumaric acid	0.16	-0.35	-6
	o-Coumaric acid	0.16	-0.35	-6
	p-Coumaric acid	0.16	-0.35	-6
	p-Coumaroyl glycolic acid	-0.075	-0.09	16
	Sinapic acid	-0.88	-0.53	-6.3
	Sitostanyl ferulate	-7.5	-7.3	-1.4
	Sitosterol ferulate	-7.5	-7.3	-1.4
Coumarins	xanthotoxin	6.2	-17	-4.6
	12a-Hydroxy-9-Demethylmunduserone-8-Carboxylic Acid	-0.33	-8.7	-9.3
	4-Hydroxycoumarin	0.32	6.5	6.6

	dihydrocoumarin 4	19	19	-
	Umbelliferone	0.32	6.5	6.6
Cyclitols	conduritol epoxide	21	11	19
Cyclohexenes	limonene	-17	-9.5	-17
Deoxyadenosines	2', 5'-Dideoxyadenosine	-0.57	-16	1
Dicarboxylic Acids	succinic acid	-0.13	-20	-20
	3-hydroxypropanoic acid	1.1	-2.7	-2.7
	malonic acid	25	8.3	14
	oxalic acid	0.6	-10	-8.1
Diterpenes, Abietane	Carnosic acid	-5.2	-0.26	-0.28
Ethanol	phenylethyl alcohol	17	-	11
Ethanolamines	D-sphingosine	22	13	-
	ethanolamine	21	-	11
Flavones	3,4',5,6,7-Pentamethoxyflavone	1.5	2.6	-13
	Acacetin	-0.16	-8.9	-0.34
	Cirsimaritin	-1	-1.3	-2.7
	Luteolin 6-C-glucoside	-6.2	0.082	0.1
	Luteolin 7-O-glucoside	-6.2	0.082	0.1
	Quercetin 3-O-rhamnoside	-6.2	0.082	0.1
Flavonoids	3,7-Dimethoxyflavone	18	8.6	-
	2-hydroxychalcone	-0.79	-19	-0.82
	3-hydroxyflavone	19	8.7	14
	6-Geranylnaringenin	4.9	10	5.2
	6-Prenylnaringenin	-7.9	-0.56	-0.84
	8-Prenylnaringenin	-7.9	-0.56	-0.84
	Isoxanthohumol	0.46	5.9	0.32
	Xanthohumol	0.46	5.9	0.32
Glutamates	beta-glutamic acid	-4.5	-16	-24
	L-glutamic acid	-	12	-
Glycols	1,3-propanediol	-	21	12
	2,3-butanediol	-0.92	-14	-7.8
	2-amino-2-methyl-1,3-propanediol	-0.41	-8.6	-6.6
	2-butyne-1,4-diol	-4.9	-11	-3.9
Hexosamines	galactosamine	-0.096	-25	-25
Hexoses	fructose	7	-8.8	-6.4
Hydantoins	1-methylhydantoin	3	2.5	-2.3
Hydroxamic Acids	acetohydroxamic acid	-0.89	-5.7	-5.1
Hydroxybenzoates	2-Hydroxybenzoic acid	1.1	0.53	-11
	4-Hydroxybenzoic acid	1.1	0.53	-16
	p-anisic acid	-2.8	-2.6	-17
	salicylic acid	-0.18	3.2	4.1
	Vanillic acid	-0.075	-0.09	16
Hydroxyquinolines	4-hydroxyquinoline	-4.9	-8.5	1.3

Imino Acids	iminodiacetic acid	-26	-26	-11
	N-(2-hydroxyethyl)iminodiacetic acid	22	8.7	12
Isoflavones	6''-O-Malonyldaidzin	7.2	8.4	8.3
	Daidzin	0.16	-0.061	-6
	Formononetin	17	17	16
Isothiocyanates	benzyl isothiocyanate	15	-	-
Kaempferols	Kaempferol 3-O-glucoside	-6.2	0.082	0.1
	Kaempferol 7-O-glucoside	-6.2	0.082	0.1
Keto Acids	3-methyl-2-oxobutanoic acid	18	-	17
Ketones	2-undecanone	-4.3	-4.3	-4.3
	4-O-Methylphloracetophenone	-19	-6.8	-19
	6-methyl-5-hepten-2-one	0.79	-7.8	-15
Lactates	3-phenyllactic acid	15	-	19
Methamphetamine	Benzphetamine	17	3.8	13
Nicotinic Acids	nicotinic acid	16	1.9	10
Nitriles	3-aminopropionitrile	0.95	-25	-18
OH-FA_17_-1_1	Avocadyne	-0.9	-14	-0.9
Organic Chemicals	urea	2.2	-7	-9.2
ortho-Aminobenzoates	Avenanthramide 2c	8.4	6.3	6.2
	Avenanthramide 2p	13	16	16
Oxaloacetates	oxalacetic acid	0	3.4	15
Peptides	L-leucine	-0.55	-13	-0.24
Phenols	2,3-dihydroxybiphenyl	-3.2	1.4	-17
	2-aminophenol	-	-	14
	3,5-dihydroxyphenylglycine	-2	-3.2	-18
	2,6-ditert-butyl-4-methylphenol	20	19	-
	4-Ethylphenol	7.1	6.4	6
	4-methylcatechol	-0.25	-0.7	-19
	4-vinylphenol	17	18	13
	5-Heneicosenylresorcinol	-5.1	0.44	0.5
	orcinol	1.5	-7.8	-16
	p-Coumaric acid ethyl ester	0.032	-5.4	-6.2
	Resveratrol	-6.6	4.3	11
	Sesamol	1.1	0.53	-11
	thymol	-0.42	-7.5	-8.1
Phenylacetates	3,4-Dihydroxyphenylacetic acid	-0.075	-0.09	16
	4-Hydroxyphenylacetic acid	-11	-4.9	-16
	Homovanillic acid	0.16	-0.35	-6
Phenylpyruvic Acids	phenylpyruvate	-3.1	-5.8	-3.1
Pipecolic Acids	pipecolic acid	-17	-17	-5.8
Polycyclic Aromatic Hydrocarbons	cis-1,2-dihydro-1,2-naphthalenediol	18	17	19

	9-hydroxyfluorene	-0.0005	-3.7	-8.8
	fluorene	-3.8	-4.5	-11
	phenanthrene	13	16	14
Polymers	phosphoric acid	23	8.6	13
Pyridines	4-hydroxypyridine	0	-	8
Saturated FA	2-ethylcaproic acid	-0.12	-5	0.11
	Arachidic acid	-5.9	-5.6	0.43
	azelaic acid	19	4	-
	behenic acid	-0.32	-0.044	-20
	Capric acid	0.29	-7	-0.14
	caprylic acid	0.058	-21	-21
	Myristic acid	0.48	0.64	7.2
	palmitic acid	-	17	23
	stearic acid	0.77	6.8	18
Sugar Alcohols	allo-inositol	-19	-7.2	-15
	diglycerol	0.93	-22	-10
	glycerol	0.6	-16	-1.2
	L-dithiothreito	-24	-11	-1.6
Thiazoles	4-methyl-5-thiazoleethanol	-1.5	-17	2.7
Thioglycolates	thioglycolic acid	-	15	25
UnSaturated FA	elaidic acid	18	-	-
Valerates	beta-hydroxyisovalerate	0.24	-6.4	-8.2
	valeramide	-25	-11	-25
Other compounds	phytosphingosine	2.9	-0.43	-13
	2-Methylene-5-(2,5-Dioxotetrahydrofuran-3-YL)-6-OXO--10, 10-Dimethylbicyclo[7:2:0]Undecane 1	18	10	17
	benzoxazinone	15	0.02	-0.059
	benzyl-desulfoglucosinolate	-11	-5.1	-16

Acknowledgements

The research was carried out in the frame of the MIUR (Ministry for education, University and Research) initiative “Department of excellence” (Law 232/2016).

Author Contribution

SA conceived the idea. SA, YP and LL planned the experimental approach. SV, SC and EC performed the biochemical characterization of tomato plants and the collection of root exudates. YP performed gene expression and relative statistical analyses. LL, BMM and SV performed untargeted metabolomic analysis of root exudates. SA, YP, LL, TM and StC discussed the data. SA, BMM and YP wrote the manuscript with the critical revision of LL, TM, MT and StC to the various drafts.

References

[1]Scherr, S.J. Soil degradation: A threat to developing country food security by 2020? *2020 Vision Discussion Papers*, **1999**, *58*, 1–51.

[2]White, P.J.; Brown, P.H. Plant nutrition for sustainable development and global health. *Ann. Bot.* **2010**, *105*, 1073–1080.

[3]Tilman, D.; Cassman, K.G.; Matson, P.; Naylor, R.; Polasky, S. Agricultural sustainability and intensive production practices. *Nat.* **2002**, *418*, 671–7.

[4]Taiz, L. Agriculture, plant physiology, and human population growth : past , present , and future. *Theor. Exp. Plant. Physiol.* **2013,** *25*, 167–181.

[5]Goucher, L.; Bruce, R.; Cameron, D.D.; Lenny Koh, S.C.; Horton, P. The environmental impact of fertilizer embodied in a wheat-to-bread supply chain. *Nat. Plants* **2017**, *3*, 1-5.

[6]Sambo, P. ; Nicoletto, C.; Giro, A.; Pii, Y.; Valentinuzzi, F.; Mimmo, T.; Lugli, P.; Orzes, G.; Mazzetto, F.; Astolfi, S.; Terzano, R.; Cesco, S. Hydroponic Solutions for Soilless Production Systems: Issues and Opportunities in a Smart Agriculture Perspective. *Front. Plant Sci*. **2019**, *10*, 923.

[7]Tomasi, N.; Mimmo, T.; Terzano, R.; Alfeld, M.; Janssens, K.; Zanin, L.; Pinton, R.; Varanini, Z.; Cesco, S. Nutrient accumulation in leaves of Fe-deficient cucumber plants treated with natural Fe complexes. *Bio.l Fertil. Soils* **2014**, *50***,** 973–982.

[8]Pii, Y.; Cesco, S.; Mimmo, T. Shoot ionome to predict the synergism and antagonism between nutrients as affected by substrate and physiological status. *Plant Physiol. Biochem*. **2014**, *94*, 48–56.

[9]Marastoni, L,; Sandri, M.; Pii, Y.; Valentinuzzi, F.; Brunetto, G.; Cesco, S.; Mimmo, T. Synergism and antagonisms between nutrients induced by copper toxicity in grapevine rootstocks: Monocropping vs. intercropping. *Chemosphere* **2019** *214*, 563–578.

[10]Marastoni, L,; Sandri, M.; Pii, Y.; Valentinuzzi, F.; Cesco, S.; Mimmo, T. Morphological Root Responses and Molecular Regulation of Cation Transporters Are Differently Affected by Copper Toxicity and Cropping System Depending on the Grapevine Rootstock Genotype. *Front. Plant Sci*. **2019**, *10*, 946.

[11]Forieri, I.; Wirtz, M. and Hell R. Towards new perspectives on the interaction of iron and sulfur metabolism in plants. *Front. Plant Sci*. **2013**, *4*, 357.

[12]Zuchi, S.; Watanabe, M.; Hubberten, H.M.; Bromke, M.; Osorio, S.; Fernie, A.R.; Celletti, S.; Paolacci, A.R.; Catarcione, G.; Ciaffi, M.; Hoefgen, R.; Astolfi, S. The interplay between sulfur and iron nutrition in tomato. *Plant Physiol*. **2015**, *169*, 2624–2639.

[13]Zamboni, A.; Celletti, S.; Zenoni, S., Astolfi, S.; Varanini Z. Root physiological and transcriptional response to single and combined S and Fe deficiency in durum wheat. *Env. Exp. Bot*. **2017**, *143*, 172–184.

[14]Vigani, G.; Pii, Y.; Celletti, S., Maver, M.; Mimmo, T.; Cesco, S.; Astolfi, S. Mitochondria dysfunctions under Fe and S deficiency: Is citric acid involved in the regulation of adaptive responses? *Plant. Physiol. Biochem.* **2018**, *126*, 86-96.

[15]Coppa, E.; Celletti, S., Pii, Y.; Mimmo, T.; Cesco, S.; Astolfi, S. Revisiting Fe/S interplay in tomato: A split-root approach to study the systemic and local responses. *Plant Sci*. **2018**, *276*, 134–142.

[16]Astolfi, S; Pii, Y.; Terzano, R.; Mimmo, T.; Celletti, S.; Allegretta, I.; Lafiandra, D.; Cesco S.Does Fe accumulation in durum wheat seeds benefit from improved whole-plant sulfur nutrition? *J. Cereal Sci.* **2018**, *83*, 74–82.

[17]Schnug, E.; Evans, E. J. Monitoring of the sulfur supply of agricultural crops in northern Europe. *Phyton* **1992**, *32(03)*, 119-122

[18]Colombo, C.; Palumbo, G.; He, J. Z.; Pinton, R.; Cesco, S. Review on iron availability in soil: interaction of Fe minerals, plants, and microbes. *J Soils Sediments* **2014**, *14(3)*, 1–11.

[19]Mimmo, T.; Del Buono, D.; Terzano, R.; Tomasi, N.; Vigani, G.; Crecchio, C.; Pinton, R.; Zocchi, G.; Cesco, S. Rhizospheric organic compounds in the soil-microorganism-plant system: their role in iron availability. *Eur. J. Soil. Sci.* **2014**, *65*, 629–642.

[20]Dakora, F.D.; Phillips, D.A. Root exudates as mediators of mineral acquisition in low-nutrient environments. *Plant Soil* **2002,** *245*, 35–47.

[21]Walker, T.S.; Bais, H.P.; Grotewold, E.; Vivanco, J.M.Root exudation and rhizosphere biology. *Plant Physiol.* **2003**, *132*, 44–51.

[22]Badri, D. V.; Vivanco, J.M. Regulation and function of root exudates. *Plant Cell Environ.* **2009**, *32*, 666–681.

[23]Canarini, A.; Kaiser, C.; Merchant, A.; Richter, A.; Wanek, W. Root exudation of primary metabolites: Mechanisms and their roles in plant responses to environmental stimuli. *Front. Plant Sci*. **2019**, *10*, 157.

[24]Rengel, Z.; Marschner, P. Nutrient availability and management in the rhizosphere: Exploiting genotypic differences. *New Phytol*. **2005**, *168*, 305–312.

[25]Houmani, H.; Rabhi, M.; Abdelly, C.; Debez, A. Implication of rhizosphere acidification in nutrient uptake by plants: Cases of potassium (K), phosphorus (P), and iron (Fe). In *Crop Production and Global Environmental Issues*. Hakeem, K. Eds.; Springer, Cham, Switzerland 2015; pp. 103-122.

[26]Terzano, R.; Cesco, S.; Mimmo, T. Dynamics, thermodynamics and kinetics of exudates: crucial issues in understanding rhizosphere processes. *Plant Soil* **2015**, *386*, 399–406.

[27]Terzano, R.; Cuccovillo, G.; Gattullo, C.E.; Medici, L.; Tomasi, N.; Pinton, R.; Mimmo, T.; Cesco, S. Combined effect of organic acids and flavonoids on the mobilization of major and trace elements from soil. *Biol. Fert. Soils* **2015**, *51*, 685–695.

[28]Gattullo, C.E.; Pii, Y.; Allegretta, I.; Medici, L.; Cesco, S.; Mimmo, T.; Terzano, R. Iron mobilization and mineralogical alterations induced by iron-deficient cucumber (*Cucumis sativus* L.) plants in a calcareous soil. *Pedosphere* **2018**, *28*, 59–69.

[29]Pii, Y.; Mimmo, T.; Tomasi, N.; Terzano, R.; Cesco, S.; Crecchio, C. Microbial interactions in the rhizosphere: beneficial influences of plant growth-promoting rhizobacteria on nutrient acquisition process. A review. *Biol. Fert. Soils* **2015**, *51*, 403–415.

[30]Alegria Terrazas, R.; Giles, C.; Paterson, E., Robertson-Albertyn, S.; Cesco, S.; Mimmo, T.; Pii, Y.; Bulgarelli, D. Plant-microbiota interactions as a driver of the mineral turnover in the rhizosphere. *Adv. App, Microbiol*. **2016**, *95*, 1–67.

[31]Kobayashi, T.; Nishizawa, N. K. Iron uptake, translocation, and regulation in higher plants. *Annu. Rev. Plant Biol.* **2012**, *63*, 131-152.

[32]Bocchini, M.; Bartucca, M. L.; Ciancaleoni, S.; Mimmo, T.; Cesco, S.; Pii, Y.; Albertini, E.; Del Buono, D. Iron deficiency in barley plants: phytosiderophore release, iron translocation, and DNA methylation. *Frontiers in plant science* **2015** *6*, 514**.**

[33]Pii, Y.; Penn, A.; Terzano, R.; Crecchio, C.; Mimmo, T.; Cesco, S. Plant-microorganism-soil interactions influence the Fe availability in the rhizosphere of cucumber plants. *Plant Physiol. Biochem.* **2015**, *87*, 45-52.

[34]Valentinuzzi, F.; Pii, Y.; Vigani, G.; Lehmann, M.; Cesco, S.; Mimmo, T. Phosphorus and iron deficiencies induce a metabolic reprogramming and affect the exudation traits of the woody plant *Fragaria × ananassa*. *J. Exp. Bot.* **2015**, *66*, 6483–6495.

[35]Celletti, S.; Pii, Y.; Mimmo, T.; Cesco, S.; Astolfi, S.. The characterization of the adaptive responses of durum wheat to different Fe availability highlights an optimum Fe requirement threshold. *Plant Physiol. Biochem*. **2016**,*109*, 300–307.

[36]Valentinuzzi, F.; Cesco, S.; Tomasi, N.; Mimmo, T. Influence of different trap solutions on the determination of root exudates in *Lupinus albus* L. *Biol.Fert. Soils* **2015**, *51*, 757–765.

[37]Barupal, D.K.; Fiehn, O. Chemical Similarity Enrichment Analysis (ChemRICH) as alternative to biochemical pathway mapping for metabolomic datasets. *Sci. Rep.* **2017**, *7*, 1-11.

[38]Altschul, S.F; Madden, T.L.; Schäffer, A,A; Zhang, J.; Zhang, Z; Miller, W.; Lipman, D.J. Gapped BLAST and PSI-BLAST: a new generation of protein database search programs. *Nucleic Acids Res*. **1997**, *25*, 3389–3402.

[39]Xiong, H.; Kakei, Y.; Kobayashi, T.; Guo, X.; Nakazono, M.; Takahashi, H.; Nakanishi, H.; Shen, H.; Zhang, F.; Nishizawa, N.K; Zuo, Y. Molecular evidence for phytosiderophore-induced improvement of iron nutrition of peanut intercropped with maize in calcareous soil. *Plant Cell Environ*. **2013**, *36*, 1888–902.

[40]Marschner, P. *Marschner's mineral nutrition of higher plants*, 3rd ed.; Academic press, London, 2012.

[41]Scherer, H.W. Sulphur in crop production — invited paper. *Eur. J. Agron.* **2001**, *14*, 81–111.

[42]Hesse, H.; Hoefgen, R. Molecular aspects of methionine biosynthesis. *Trends Plant Sci*, **2003**, *8*, 259–262.

[43]Kobayashi, T.; Nozoye, T.; Nishizawa, N.K. Iron transport and its regulation in plants. ***Free.*** *Radic. Biol. Med.* **2019**, *133*, 11–20.

[44]Zuchi, S.; Cesco, S.; Varanini, Z.; Pinton, R.; Astolfi, S. Sulphur deprivation limits Fe deficiency responses in tomato plants. *Planta* **2009**, *230*, 85–94.

[45]Celletti, S.; Paolacci, A.R.; Mimmo, T.; Pii, Y.; Cesco, S., Ciaffi, M.; Astolfi S. The effect of excess sulfate supply on iron accumulation in three graminaceous plants at the early vegetative phase. *Environ. Exp. Bot*. **2016,** *128*, 31-38.

[46]Nikiforova, V.J.; Gakière, B.; Kempa, S.; Adamik, M.; Willmitzer, L.; Hesse, H. Hoefgen, R. Towards dissecting nutrient metabolism in plants: A systems biology case study on sulphur metabolism. *J. Exp. Bot*. **2004**, *55*, 1861–1870.

[47] Rellán-Álvarez, R.; Andaluz, S.S.; Rodríguez-Celma, J.; Wohlgemuth, G.; Zocchi, G.; Álvarez-Fernández, A.; Fiehn, O.; López-Millán, A.F.; Abadía, J. Changes in the proteomic and metabolic profiles of *Beta vulgaris* root tips in response to iron deficiency and resupply. *BMC Plant Biol.* **2010**, *10*, 120.

[48]Carvalhais, L.C.; Dennis, P.G.; Fedoseyenko, D.; Hajirezaei, M.R.; Borriss, R.; von Wirén, N. Root exudation of sugars, amino acids, and organic acids by maize as affected by nitrogen, phosphorus, potassium, and iron deficiency. *J. Plant Nut. Soil Sci*. **2011**, *174*, 3–11.

[49]Astolfi, S.; Cesco, S.; Zuchi, S.; Neumann, G.; Roemheld, V. Sulfur starvation reduces phytosiderophores release by iron-deficient barley plants. *Soil Sci.Plant Nut*. **2006**, *52*, 43–48.

[50]Watanabe, M.; Hubberten, H.M.; Saito, K.; Hoefgen, R. General regulatory patterns of plant mineral nutrient depletion as revealed by serat quadruple mutants disturbed in cysteine synthesis. *Mol. Plant* **2010**, *3*, 438–66.

[51]Watanabe, M.; Hubberten, H.M.; Hoefgen, R. Plant Response to Mineral Ion Availability: Transcriptome Responses to Sulfate, Selenium and Iron. In *Sulfur Metabolism in Plants: Mechanisms and Applications to Food Security and Responses to Climate Change*. De Kok, L. J.; Tabe, L.; Tausz, M.; Hawkesford, M. J.; Hoefgen, R.; McManus, M. T.; Norton, R.; Rennenberg, H.; Saito, K. Eds.; Springer, Dordrecht, Netherlands, 2012, 1, pp. 123–134.

[52]El-Baz, F.K.; Mohamed, A.A.; Aboul-Enein, A.M.; Salama, Z.A. Alteration in root exudates level during Fe deficiency in two cucumber cultivars. *Int. J. Agric. Biol.* **2004**, *6*, 45–48

[53]Tomasi, N.; Weisskopf, L.; Renella, G.; Landi, L.; Pinton, R.; Varanini, Z.; Nannipieri, P.; Torrent, J.; Martinoia, E.; Cesco, S. Flavonoids of white lupin roots participate in phosphorus mobilization from soil. *Soil Biol. Biochem.* **2008**, *40*, 1971–1974.

[54]Chen, Y.T.; Wang, Y.; Yeh, K.C. Role of root exudates in metal acquisition and tolerance. *Curr. Opin. Plant Biol.* **2017**, *39*, 66–72.

[55]Schmidt, M.A.; Halvorson, J.J.; Hagerman, A.E.; Gonzalez, J.M. Macronutrients and metals released from soils by solutions of naturally occurring phenols. *J.Plant Nutr. Soil Sci.* **2017**, *180*, 544–553.

[56]Cesco, S.; Neumann, G.; Tomasi, N.; Pinton, R.; Weisskopf, L. Release of plant-borne flavonoids into the rhizosphere and their role in plant nutrition. *Plant Soil* **2010**, *329*, 1–25.

[57]Yang, T.J.W.; Lin, W.D.; Schmidt, W. Transcriptional profiling of the Arabidopsis iron deficiency response reveals conserved transition metal homeostasis networks. *Plant Physiol*. **2010**, *152*, 2130–2141.

[58]Rodríguez-Celma, J.; Lin, W.D.; Fu, G.M.; Abadía, J.; López-Millán, A.F.; Schmidt, W. Mutually exclusive alterations in secondary metabolism are critical for the uptake of insoluble iron compounds by arabidopsis and Medicago truncatula. *Plant Physiol*. **2013**, *162*, 1473–1485.

[59]Fourcroy, P.; Sisó-Terraza, P.; Sudre, D.; Savirón, M.; Reyt, G.; Gaymard, F.; Abadía, A.; Abadia, J.; Álvarez-Fernández, A. Briat, J.F. Involvement of the ABCG37 transporter in secretion of scopoletin and derivatives by Arabidopsis roots in response to iron deficiency. *New Phytol.* **2014**, *201*, 155–167.

[60]Fourcroy, P.; Tissot, N.; Gaymard, F.; Briat, J.F.; Dubos, C. Facilitated Fe Nutrition by Phenolic Compounds Excreted by the Arabidopsis ABCG37/PDR9 Transporter Requires the IRT1/FRO2 High-Affinity Root Fe^{2+} Transport System. *Mol. Plant* **2016**, *9*, 485–488.

[61]Schmid, N.B.; Giehl, R.F.H.; Döll, S.; Mock, H.P.; Strehmel, N.; Scheel, D.; Kong X.; Hider, R.C., von Wirén, N. Feruloyl-CoA 6′-Hydroxylase1-Dependent Coumarins Mediate Iron Acquisition from Alkaline Substrates in Arabidopsis. *Plant Physiol.* **2014**, *164*, 160–172.

[62]Schmidt, H.; Günther, C.; Weber, M.; Spörlein, C.; Loscher, S.; Böttcher, C.; Schobert, R.; Clemens, S. Metabolome Analysis of Arabidopsis thaliana Roots Identifies a Key Metabolic Pathway for Iron Acquisition. *PLoS ONE* **2014,** *9*, e102444.

[63]Sisó-Terraza, P.; Luis-Villarroya, A.; Fourcroy, P.; Briat, J.F.; Abadía, A.; Gaymard, F.; Abadía, J.; Álvarez-Fernández, A. Accumulation and secretion of coumarinolignans and other coumarins in Arabidopsis thaliana roots in response to iron deficiency at high pH. *Front. Plant Sci*. **2016**, *7*. 1711.

[64]Siwinska, J.; Siatkowska, K.; Olry, A.; Grosjean, J.; Hehn, A.; Bourgaud, F.; Meharg, A.A.; Carey, M.; Lojkowska, E.; Ihnatowicz, A. Scopoletin 8-hydroxylase, A novel enzyme involved in coumarin biosynthesis and iron-deficiency responses in Arabidopsis. *J. Exp. Bot*. **2018**, *69*, 1735–1748.

[65]Rajniak, J.; Giehl, RFH.; Chang, E.; Murgia, I.; von Wirén, N.; Sattely, E.S. (2018). Biosynthesis of redox-active metabolites in response to iron deficiency in plants. *Nat. Chem. Biol*. **2018**, *14*, 442–450.

[66]Tsai, H.H.; Rodríguez-Celma, J.; Lan, P.; Wu, Y.C.; Vélez-Bermúdez, I.C.; Schmidt, W. Scopoletin 8-Hydroxylase-Mediated Fraxetin Production Is Crucial for Iron Mobilization. *Plant Physiol*. **2018**, 177, 194–207.

[67]Tawaraya, K.; Horie, R.; Saito, S.; Wagatsuma, T.; Saito, K.; Oikawa, A. Metabolite Profiling of Root Exudates of Common Bean under Phosphorus Deficiency. *Metabolites* **2014**, *4*, 599–611.

[68]Barbour, W.M.; Hattermann, D.R.; Stacey, G. Chemotaxis of Bradyrhizobium japonicum to soybean exudates. *Appl. Environ. Microbiol.* **1991**, *57*, 2635–2639.

[69]Pii, Y.; Borruso, L.; Brusetti, L.; Crecchio, C.; Cesco, S.; Mimmo, T. The interaction between iron nutrition, plant species and soil type shapes the rhizosphere microbiome. *Plant Physiol. Biochem.* **2016**, *99*, 39–48.

[70]Mimmo, T.; Ghizzi, M.; Marzadori, C.; Gessa, C.E. Organic acid extraction from rhizosphere soil: Effect of field-moist, dried and frozen samples. *Plant Soil* **2008**, *312*, 175–184.

[71]Grillet, L.; Schmidt, W. Iron acquisition strategies in land plants: not so different after all. New Phytol. **2019**, *224*, 11-18.

[72]Nozoye, T.; Nagasaka, S.; Kobayashi, T.; Takahashi, M.; Sato, Y.Y.; Uozumi, N.; Nakanishi, H.; Nishizawa, N.K. Phytosiderophore efflux transporters are crucial for iron acquisition in graminaceous plants. *J. Biol. Chem.* **2011**, *286*, 5446–54.

[73]Zhang, F.S.; Römheld, V.; Marschner, H. Role of the root apoplasm for iron acquisition by wheat plants. *Plant Physiol.* **1991**, *97*, 1302–1305.

[74]Kumar, P.; Lucini, L.; Rouphael, Y., Cardarelli, M.; Kalunke, R.M.; Colla, G. Insight into the role of grafting and arbuscular mycorrhiza on cadmium stress tolerance in tomato. *Front. Plant Sci.* **2015**, *6*, 477.

[75]Lucini, L.; Borgognone, D.; Rouphael, Y.; Cardarelli, M.; Bernardi, J.; Colla, G. Mild potassium chloride stress alters the mineral composition, hormone network, and phenolic profile in artichoke leaves. *Front. Plant Sci.* **2016**, *7*, 948.

[76]Lucini, L.; Colla, G.; Miras Moreno, M.B.; Bernardo, L.; Cardarelli, M.; Terzi, V.; Bonini, P.; Rouphael, Y. Inoculation of Rhizoglomus irregulare or Trichoderma atroviride differentially modulates metabolite profiling of wheat root exudates. *Phytochemistry* **2019**, *157*, 158–167.

[77]Lisec, J.; Schauer, N.; Kopka, J.; Willmitzer, L.; Fernie, A.R. Gas chromatography mass spectrometry-based metabolite profiling in plants. *Nat.Protoc*. **2006**, *1*, 387–396.

[78]Ramakers, C.; Ruijter, J.M.; Deprez, R.H.L.; Moorman, A.F.M. Assumption-free analysis of quantitative real-time polymerase chain reaction (PCR) data. *Neurosci. Lett.* **2003**, *339*, 62–66.

[79]Pfaffl, M.W.; Horgan, G.W.; Dempfle, L. Relative expression software tool (REST©) for group-wise comparison and statistical analysis of relative expression results in real-time PCR. *Nucleic. Acids. Res.* **2002**, *30*, e36–e36.

Chapter 3

Revisiting Fe/S interplay in tomato: A split-root approach to study the systemic and local responses.

Published in Plant Science (2018) 276, 134-142 as "*Revisiting Fe/S interplay in tomato: A split-root approach to study the systemic and local responses*", E.Coppa, S. Celletti, Y. Pii, T. Mimmo, S. Cesco, S.Astolfi.

Abstract

Based on our previous studies demonstrating an intriguing interplay between sulfur (S) and iron (Fe), a split-root experiment was performed to determine whether plant S status and/or S external concentration could modify plant capability to take up and accumulate Fe. This split-root system allowed the roots of each tomato plant to grow in two different compartments, both Fe-deficient, but one S-sufficient, and the other one S-free. Although S was freely available to half root system and thus plant S status was preserved, S-deficient part of root apparatus exhibited a decrease of total S, thiols and protein content, an enhanced activity of both ATPsulfurylase and *O*-acetylserine(thiol)lyase, and a higher expression of *SlST1.1*, as occurring under S deficiency. The side of the root apparatus exposed to combined S and Fe deficiency, showed an over induction of the FeIII-reducing capacity (+40%) and of the expression levels of the gene codifying for this protein (*SlFRO1*), with respect to the Fe-deficient part of the root system. Interestingly, the regulation pattern of the *bHLH* transcription factor *SlFER*, controlling the expression of both *SlFRO1* and *SlIRT1* genes, was very close to that of *SlFRO1*. *SlIRT1* expression levels appeared unaffected by S supply, suggesting distinct regulatory processes targeting *SlFRO1* and *SlIRT1*.

Keywords: Iron-deficiency; Solanum lycopersicum; Split-root; Strategy I; Sulfur.

3.1 Introduction

The lower Fe accumulation in leaves of S-deficient maize plants was the first clear indication of an intriguing relation between sulfur (S) and iron (Fe) acquisition in plants [1] and triggered a quite intense scientific production in the following years on this topic. It is interesting to note that the same response was recorded in other crops such as barley [2], durum wheat [3] and tomato [4], regardless of which mechanism is employed by plants to cope with Fe deficiency (*i.e.* Strategy I, or FeIII-reduction based mechanism, or Strategy II, or FeIII-chelation based mechanism) [5]. It

should be highlighted that at the field scale multiple nutrient depletions are more common than single nutritional deficiencies and the response of plants to a combined deficiency is completely different when compared to the single one, at both physiological and molecular level [6,7]. The comprehension of the mechanisms underlying the responses to the combined deficiency are still mostly lacking, even if some theories have been postulated. In particular, it has been suggested that in grasses (Strategy II plants) the reduced Fe accumulation in plant tissues induced by S deficiency could be ascribed to a decrease in the production and release of phytosiderophores (PS) [2], whereas in tomato (a Strategy I plant) the effect was rather due to an impaired ethylene and nicotianamine (NA) production [4]. In addition, the involvement of sulfate in transcriptional regulation of cellular Fe homeostasis was described in both barley, in which *HvYS1* expression changed in response to S external supply [8], and tomato, in which S deficiency virtually abolished the expression of the NA synthase (*LeNAS*) gene and limited the expression of both *LeIRT1* and *LeFRO1* gene [4]. According to this theory, limited Fe availability results in a further sulfate demand that becomes the driving force which leading to an increased sulfate uptake and assimilation rate [6,9]. Interestingly, PS, ethylene and NA share a common precursor, namely S-adenosylmethionine (SAM), whose synthesis depends on the availability of methionine (Met) [10]. Furthermore, it has been shown in plants that Fe is normally linked with S when it is bound in Fe-S proteins suggesting that Fe-S clusters are the biggest sink for Fe within the plant [11]. However, higher S need to sustain the activation of Strategy I and II machinery cannot fully account for the observed link between the flow of these two essential nutrients in plant tissues, but also likely reflect a direct interference of Fe with the signal transduction pathway involved in S metabolism (and *vice versa*) and with the activation of different acquisition strategies. In this regard, evidences have been provided by using transcriptome [7] and metabolome-wide [6] approaches that Fe and S metabolism need to be coordinated to a certain extent, as *e.g.* maintenance of Fe-S-cluster formation and, on the other hand, being sulfur metabolism additionally involved in multiple processes of primary and secondary metabolism, they need also to be independently modulated. According to this model, an intensive overlap, as well as distinct responses by comparing the transcriptome and the metabolome of single and combined S and Fe starved plants has been observed [6,7,12]. Finally, only recently citrate has shown to represent a key role in the regulation of some Fe- and S-responsive genes, demonstrating the mitochondria involvement in the regulation of Fe and S interplay in plants [13].

In addition, an uneven nutrient distribution in soil is further complicating the understanding of what is happening at the soil/root interface. In this respect, all these studies have been carried out by exposing the whole root system to a single (Fe or S) or combined (Fe and S) nutritional stress, conditions that do not completely represent the heterogeneous availability of nutrients often present at the rhizosphere level. This aspect is of particular relevance also in relation to the extent, and the relative efficacy, of the root responses to nutritional deficiency. The aim of this study was to assess whether the S-nutritional state of the plant (systemic effect) and/or the S availability in a restricted part of the root system (local effect) could modify the plant capability to take up Fe and, then, to allocate it at the shoot level.

Therefore, a split-root hydroponic system was developed to allow the root system of each single tomato plant to grow in two different and independent compartments, both Fe-free, but half of the root apparatus was in a S-starved condition and the other one received S (1.2 mM sulfate). After one-week treatment, the root capability to cope with Fe deficiency was evaluated by analysing the FeIII-reducing activity and the expression of the *SlFRO1*, *SlIRT1* and *SlFER* genes. Changes in plant sulfate uptake and assimilation rate were investigated by analysing the expression of a high affinity sulfate transporter gene, *SlST1.1*, and the activity of ATPsulfurylase (ATPS) and *O*-acetylserine(thiol)lyase (OASTL), two S pathway-related enzymes.

2.2 Materials and methods

2.2.1 Plant growth conditions

Tomato (*Solanum lycopersicum* L., cv. Marmande) seeds were germinated in the dark at room temperature for five days and then seedlings were grown hydroponically in plastic pots containing 2.2 L of complete nutrient solution (NS) [14], being exposed to 1.2 mM sulfate and 40 μM FeIII-EDTA [4]. After two weeks, seedlings having root system of sufficient length and approximately equal size were chosen for planting in split-root (SR) containers filled with NS (Fig. 1). Each container consisted of two equal compartments, where each half of the tomato root system was allowed to grow separately being exposed to two different treatments: sole Fe deficiency (F, 1.2 mM sulfate and 0 μM FeIII-EDTA) and combined Fe and S deficiency (D, 0 mM sulfate and 0 μM FeIII-EDTA). The plants were grown an additional week in order to induce nutrient deficiency responses and then shoot and root samples were harvested (21 days after sowing).

As control conditions, whole (W) tomato plants were also grown hydroponically being exposed to sole Fe deficiency (F condition, WF) and combined Fe and S deficiency (D condition, WD). Nutrient solution was continuously aerated and renewed every 3 days. Plants were grown in a growth chamber under 200 µmol photons m^{-2} s^{-1} photosynthetic photon flux, with 16/8 h photoperiod (27 °C/20 °C day/night temperature cycling and 80% relative humidity.

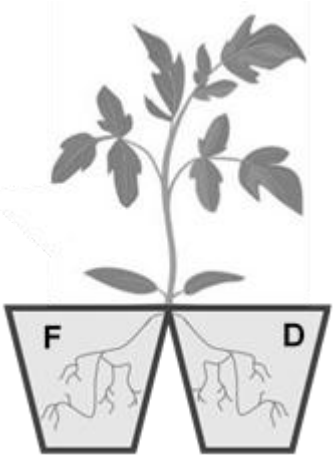

Fig. 1. Design of the split-root system. The terms used to describe the various parts of split-root plants are indicated in the text. F indicates condition where the Fe-deficient compartment (1.2mM sulfate and 0 µMFeIII-EDTA), D condition of the dual deficient compartment (0mM sulfate and 0 µMFeIII-EDTA).

2.2.2 Determination of ferric chelate reductase activity

Root capability to reduce FeIII-EDTA was measured *in vivo* by using the bathophenanthrolinedisulfonate (BPDS) reagent [4]. Briefly, roots were carefully washed with deionized water, transferred to an assay solution containing 0.5 mM $CaSO_4$, 0.25 mM FeIII-EDTA, 0.6 mM BPDS, 10 mM Mes at pH 5.5 adjusted by 1 M KOH, and incubated in the dark at 25 °C for 20 min, continuously aerated. The absorbance of the assay solution was recorded at 535 nm and the amount of reduced FeIII was calculated by the concentration of the FeII-$BPDS_3$ complex using an extinction coefficient of 22.1 mM^{-1} cm^{-1}.

2.2.3 Extraction of total RNA and qRT-PCR analysis

Total RNA extraction from F and D roots was performed by using Spectrum Plant Total RNA Kit (Sigma-Aldrich Co. LLC) according to the manufacturer's instructions.

One mg of DNase-treated RNA was reverse-transcribed by ImProm-II Reverse Transcription System kit (Promega, Madison, WI, USA) according to the manufacturer's protocol. The expression of genes involved in Fe homeostasis (*SlFER, SlFRO1, SlIRT1)* and coding for a high affinity sulfate transporter (ST) of group 1 (*SlST1.1)* were analyzed by qRT–PCR as described in Zuchi et al. [6].

Nevertheless, the identity of each amplicon was determined by sequencing. The amplification efficiency was calculated from raw data using LinRegPCR software [15]. The expression of genes was normalized using two housekeeping transcripts, namely Tomato *LeEF-1* mRNA for elongation factor 1 alpha (X14449.1) and Tomato *Ubi3* gene for ubiquitin (X58253.1), previously described [13]. The relative expression ratio value was calculated for treated samples relative to the corresponding untreated sample at the same time-point according to the Pfaffl equation [16]. Standard error values were calculated according to Pfaffl et al. [17].

2.2.4 Total sulfur and non-protein thiols extraction and determination

For the determination of total S concentration, 1 g of each shoot and root sample was first oven-dried at 105 °C and then ashed in a muffle furnace at 600 °C. After complete mineralization, the ashes were dissolved in 10 mL of 3 N HCl and filtered through Whatman No. 42 papers. In contact with $BaCl_2$, a $BaSO_4$ precipitate was formed, which was determined according to the turbidimetric method described by Bardsley and Lancaster [18].

Thiols extract was prepared from shoot and root tissues of plants grown as described above. Briefly, one g of frozen plant tissue was homogenized in a solution containing 80 mM trichloroacetic acid, 1 mM ethylenediaminetetraacetic acid, 0.15% (w/v) ascorbic acid and 10% (w/v) polyvinylpyrrolidone (PVP), in a ratio of 1:5 (w/v). After a centrifugation step of 30 min at 4000 g and 4 °C, the supernatants were collected, and the concentrations of DTNB-reactive compounds were detected by VIS absorption at 415 nm.

2.2.5 Enzyme extraction and assay

Shoot and root tissues (1 g fresh weight) were powdered in a pre-chilled mortar with liquid N_2 and extraction steps were performed according to the method described by Celletti et al. [18]. Briefly, extraction buffer contained 50 mM HEPES-KOH (pH 7.4), 5 mM $MgCl_2$, 1 mM EDTA, 10% (v/v) glycerol, 0.1% (v/v) Triton X-100, 5 mM dithiothreitol (DTT), 1 mM phenylmethylsulphonyl fluoride (PMSF), and 1% (w/v) polyvinylpyrrolidone (PVP) and was added in a ratio of 1:7 and

1:3 (w/v) for shoots and roots, respectively. The activity of ATP sulphurylase (ATPS; EC 2.7.7.4) and *O*-acetylserine(thiol) lyase (OASTL; EC 4.2.99.8) activity was determined by the bioluminescence technique and by detecting cysteine production, respectively, as described by Celletti et al. [19]. Protein concentration in the extracts of plant tissues was determined according to the dye-binding method of Bradford [20] using BSA as standard.

2.2.6 Citric acid extraction

Shoot and root tissues were powdered in a mortar with liquid N_2 and extracted with 10 mM H_2SO_4 using a ratio of 1:10 (w/v). The determination of the concentration of citric acid was performed by HPLC using a cation exchange column Aminex 87-H column (300 × 7.8 mm, 9 mm, Bio-Rad) using an isocratic elution with 10 mM H_2SO_4 as mobile phase at a flow rate of 0.6 mL min^{-1}. Citric acid was detected at 210 nm with a Waters 2998 photodiode array detector (Waters Spa, Italy). Standard acid was prepared as individual stock solutions and then prepared to give diluted reference standards. Citric acid was identified by comparing retention times of the unknown to the pure compound. Standards were purchased from Sigma–Aldrich (St. Louis, MO, United States).

2.2.7 Other measurements and statistics

The measurements of chlorophyll content per unit area was determined in the youngest fully expanded leaves by the SPAD porFaig apparatus (Minolta Co., Osaka, Japan) and presented as SPAD units.

Each reported value represents the mean ± SD of measurements carried out in triplicate and obtained from four independent experiments. All the data were statistically analysed using ANOVA and data from each treatment was then compared with the control treatment using Tukey's post hoc test at $P < 0.01$ by using the GraphPad InStat Program (version 3.06).

2.3 Results

2.3.1 Plant growth

Stimulation of root growth, and following reduction of shoot:root ratio, is one of the earliest and distinct symptoms of plant S deficiency [3,19]. When the performance of hydroponically grown split-root plants was evaluated, no difference in root growth was observed between the two portions of the split root system, one part subjected only to Fe deficiency (F) and the other grown under dual deficiency of Fe and S (D) condition (Fig. 1A). Interestingly, there was no difference in the

root system development also considering not-split (whole, W) plants between roots of plants exposed only to the Fe deficiency (WF) or to the combined Fe and S shortages (WD) (Fig. 2A, insert). On the other hand, shoots of tomato seedlings exhibited obvious changes in phenotype, showing different total fresh biomass and chlorophyll levels depending on the nutrient regime and the growing system. In fact, the shoots of split-root plants displayed a reduced growth as compared to both shoots from not-split plants (WF and WD) (Fig. 2B) and leaf chlorosis when compared to shoots from Fe-deficient not-split plants (WF) (insert in Fig. 2B). The highest shoot fresh matter production was observed when tomato seedlings were cultivated without Fe and with S (WF condition). The reduction of biomass accumulation was greater in shoots from split-root plants than in those from whole plants grown in D condition (WD). Accordingly, the latter were reduced by 30%, whereas the former by 44% when compared to Fe-deficient shoots (WD) (Fig. 2B). The same result occurred with the chlorophyll level, which was highest in WF seedlings, but in this case no significant difference in chlorophyll content was observed between shoots from split-root plants and those from whole plants grown in D condition (WD) (insert in Fig. 2B).

2.3.2 Accumulations of total S and thiols and activities of enzymes involved in S metabolism

As might be expected, in roots (insert in Fig. 3A and C) and shoots (Fig. 3B and D) from not-split plants under dual deficiency (WD) the concentration of both total S and thiols was significantly lower (approximately 80 and 30%, respectively) compared to that of the Fe-deficient plants (WF). Interestingly, in split root plants the different availability of sulfate in the two root compartments caused a different content of both total S (Fig. 3A) and thiols (Fig. 3C) between the two sides of root system, in spite of belonging to the same plant. As expected, the lowest levels of total S and thiols concentrations (-80% and -40%, respectively) were measured in the portion of the root system exposed to combined S and Fe deficiency (D) (Fig. 3B and D). It is worth to notice that in the shoot tissue of split-root plants the levels of the two parameters (total S and thiols concentrations) were significantly higher than those measured in the not-split-root plants exposed to the double deficiency (WD) (Fig. 3B and D).

To understand why total S and thiols concentration changed under single (F) and combined deficiency (D) stress we monitored the sulfate uptake and assimilation steps.

First, we investigated the modulation of the mechanisms underlying the S uptake process determining the transcript levels of the gene *SlST1.1* codifying for a high affinity sulfate transporter, whose expression is known to be modulated by the S availability.

Indeed, transcript levels of *SlST1.1* in the roots were much higher for dual deficient (WD) plants than that of the Fe-deficient (WF) (insert in Fig. 4). Interestingly, *SlST1.1* expression was up-regulated also in the D portion of the root apparatus of split-root plants (Fig. 4). In particular, the level of *SlST1.1* transcripts in D roots of split-root plants was three-fold higher than in F half root system (Fig. 4). Next, we monitored the activities of enzymes involved in S metabolism: ATPS and OASTL (the first and the last enzyme involved in the S assimilatory pathway, respectively). the activity of both ATPS and OASTL was significantly increased (+25%) in the root portion exposed to S shortage (D condition) with respect to that only Fe-deficient (F condition) (Fig. 5A and C). On the other hand, we found that when not split-root plants were treated with dual deficiency (WD), only the root ATPS activity was increased (+45%, insert in Fig. 5A), whereas OASTL activity was significantly decreased (−27%, insert Fig. 5C) with respect to only Fe-deficient plants (WF). In shoots, the activity of OASTL was not significantly affected by different nutritional conditions (Fig. 5D), whereas the levels of ATPS activity was significantly augmented only in the shoots of split plants (+60% and +53% when compared with both WF and WD shoots, respectively) (Fig. 5B).

2.3.3 Iron homeostasis

Iron deficiency stress, sole or in combination with S starvation, affected the transcript levels of genes involved in Fe homeostasis.

Changes in expression of *SlFER*, *SlFRO1* and *SlIRT1* were diverse. The expression levels of both *SlFER*, the ortholog in tomato of FIT (FE DEFICIENCY-INDUCED TRANSCRIPTION FACTOR) and *SlFRO1* (FERRIC REDUCTASE OXIDASE 1) were strongly up-regulated (to 60 and 2 folds, respectively) in the portion of the root system exposed to the dual deficiency (D side) with respect to the root portion only subjected to the Fe shortage (F side) (Fig. 6A and B). On the other hand, *SlIRT1* expression did not change between the two distinct portions of the root system (Fig. 6C).

In addition, we analyzed the root specific expression of the same key genes involved in Fe homeostasis also in not split-root plants. Surprisingly, no difference in the expression level of the *SlFER* and *SlFRO1* genes was measured in roots of not split-root plants between the treatment of sole Fe- (WF) and dual- (WD) deficiency (inserts in Fig. 6A and B). On the contrary, a higher amount of *SlIRT1* transcripts was measured in WD roots in comparison to WF ones (1.5-fold increase, insert in Fig. 6).

Having observed changes in expression of *SlFRO1* which encode for the FeIII-chelate reductase, we evaluated also the root FeIII-reducing capacity. We found a significant increase in *in vivo* assayed FeIII reducing capacity in D roots of split-root plants with respect to F ones (+40%) (Fig. 7). It has to be pointed out that this response pattern was very contrasting to that displayed by roots of not split-root plants exposed to combined Fe and S deficiency (WD), which indeed showed a strong reduction of the activity of this enzyme (−25%) (insert in Fig. 7).

It is well known that Fe deficiency induces production of organic acids (citric acid, malic acid) in plants [5] and it has been recently suggested that citric acid could also have a role as an important player in the regulation of adaptive responses to the combined S/Fe deficiency [13], in addition to the well-known role for the long-distance transport of Fe in plants [5].

Results here reported showed a strong increase of citrate concentration in D portion of the root system (+47%, with respect to F one) (Fig. 8A). In contrast, in not split-root plants citrate accumulation was significantly reduced in roots exposed to dual deficiency (WD) (−55%, with respect to WF roots) (insert in Fig. 8A). It is interesting to note that the citrate concentration was significantly but only slightly decreased (6%) in the shoots of WD plants with respect to WF ones (Fig. 8B), whereas in the shoots of split-root plants the concentration of this organic acid was more than halved (−55%) in comparison to the one measured in both WF and WD shoots of not split-root plants (Fig. 8B).

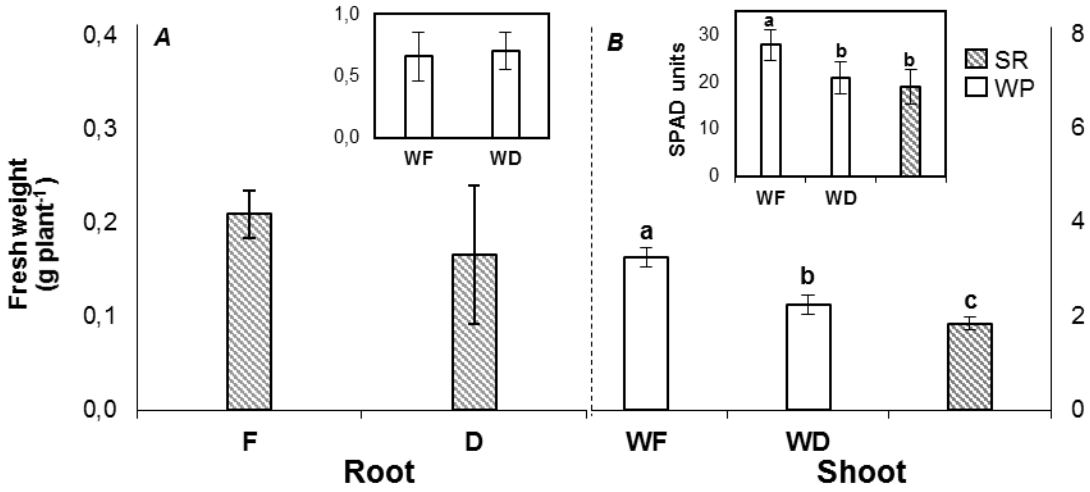

Fig. 2. Fresh weight of roots (A) and shoots (B) from split-root (SR) (lined bars) or not split-root (whole, W) (white bars) tomato plants grown under sole Fe deficiency (F and WF, 1.2mM sulfate and 0 µMFeIII-EDTA) and under combined S and Fe deficiency (D and WD, 0mM sulfate and 0 µMFeIII-EDTA). Insert in A: Fresh weight of roots from not split-root plants under Fe deficiency (WF) or dual deficiency (WD). Insert in B: Chlorophyll content, measured by SPAD meter, in leaf of split- and not split-root tomato plants. Data are means ± SD of four independent replications run in triplicate. Significant differences between samples are indicated by different letters ($P < 0.01$) (n=4). Stars indicate significant differences between F and D (or WF and WD) samples of both split and not split-root tomato plants (* $P < 0.05$, ** $P < 0.01$, *** $P < 0.005$ and **** $P < 0.001$).

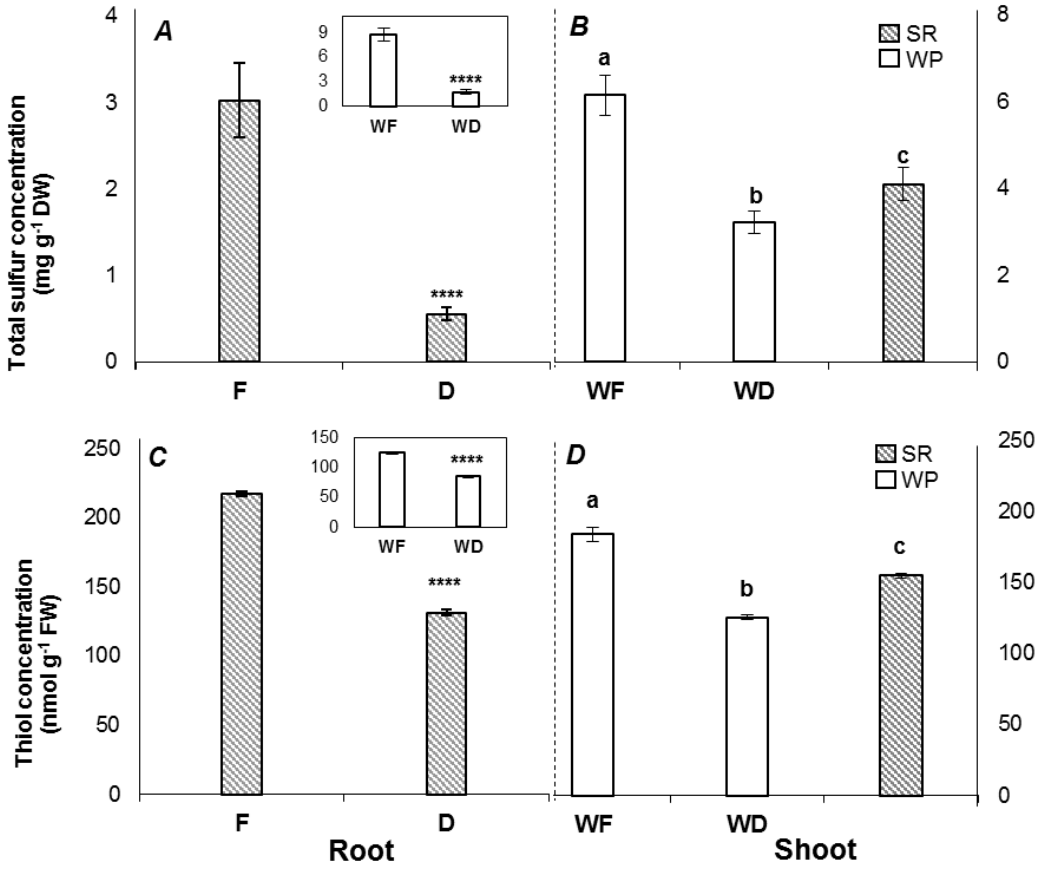

Fig. 3. Total sulfur (A and B) and thiol (C and D) concentration in roots and shoots of split- and not split-root tomato plants. Terms, treatments and statistics as in Fig. 2.

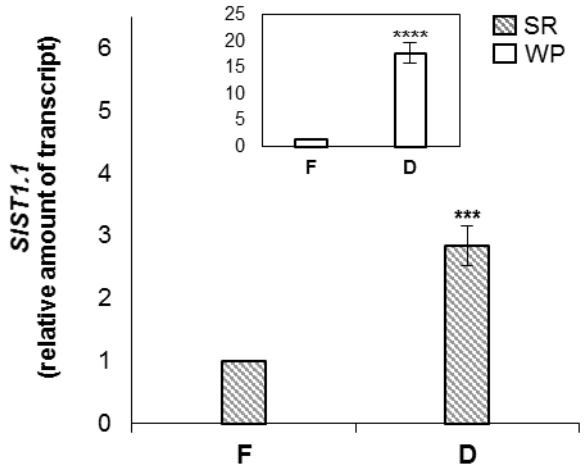

Fig. 4. Relative amount of transcript by qRT-PCR of *SlST1.1* gene in roots from split- and not split-root tomato plants. Terms, treatments and statistics as in Fig.2.

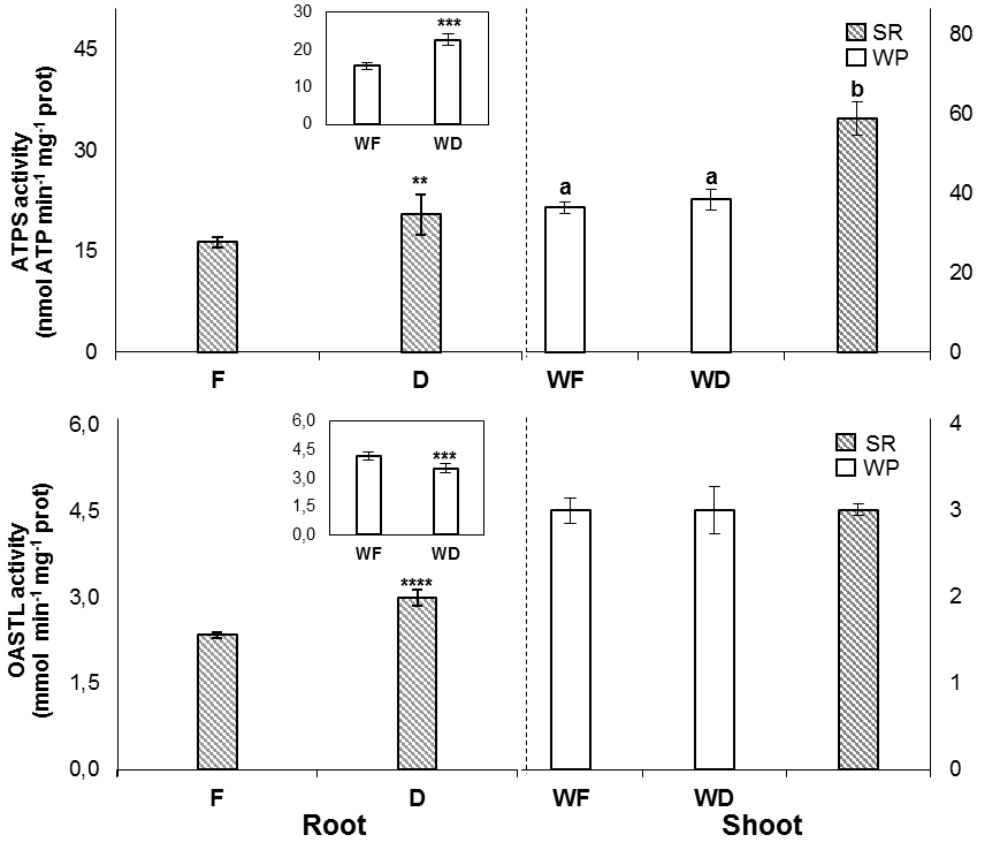

Fig. 5. ATPS (A and B) and OASTL (C and D) activity in roots and shoots of split- and not split-root tomato plants. Terms, treatments and statistics as in Fig. 2.

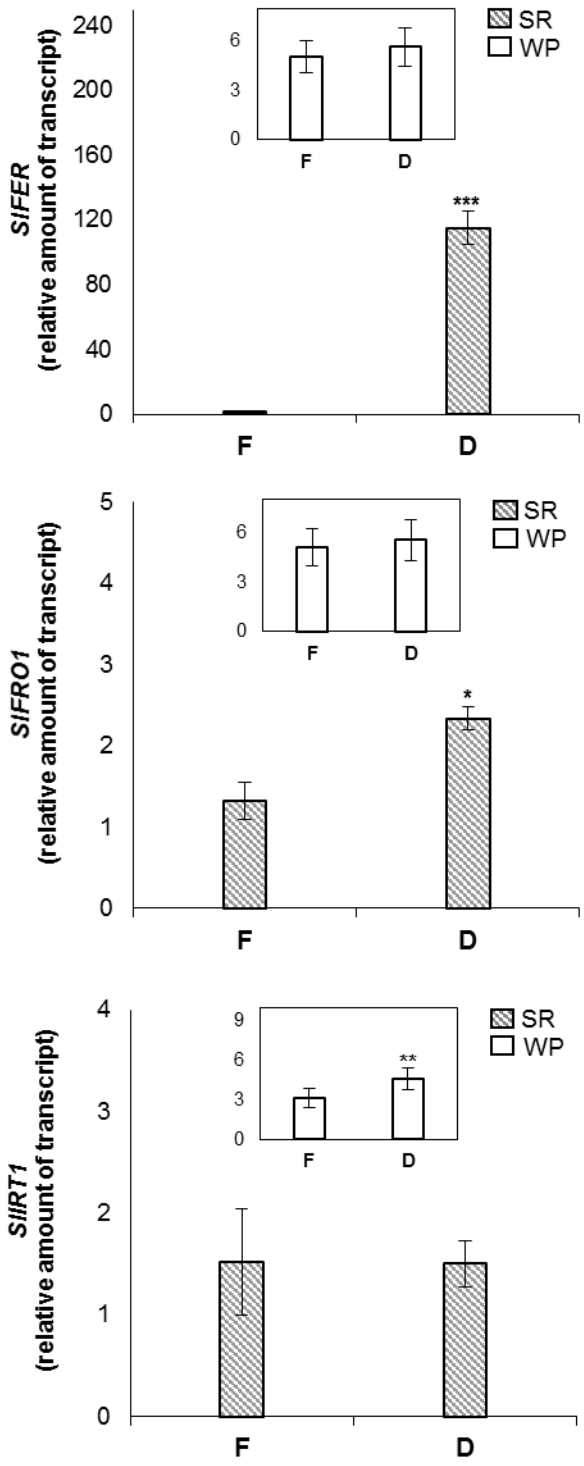

Fig. 6. Relative amount of transcript by qRT-PCR of *SlFER* (A), *SlFRO1* (B) and *SlIRT1* (C) genes in roots of split- and not split-root tomato plants. Terms, treatments and statistics as in Fig. 2.

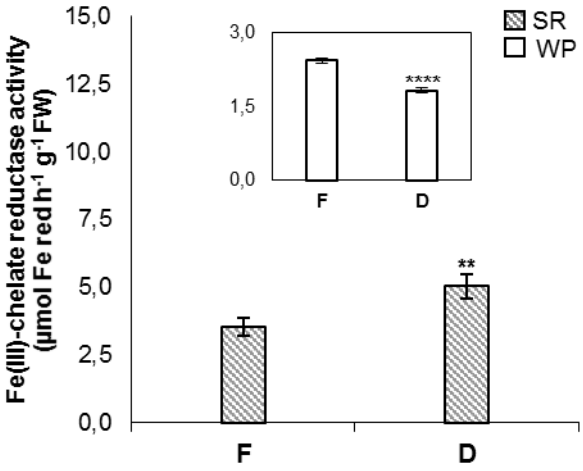

Fig. 7. FeIII-chelate reductase activity in roots of split- and not split-root tomato plants. Terms, treatments and statistics as in Fig. 2.

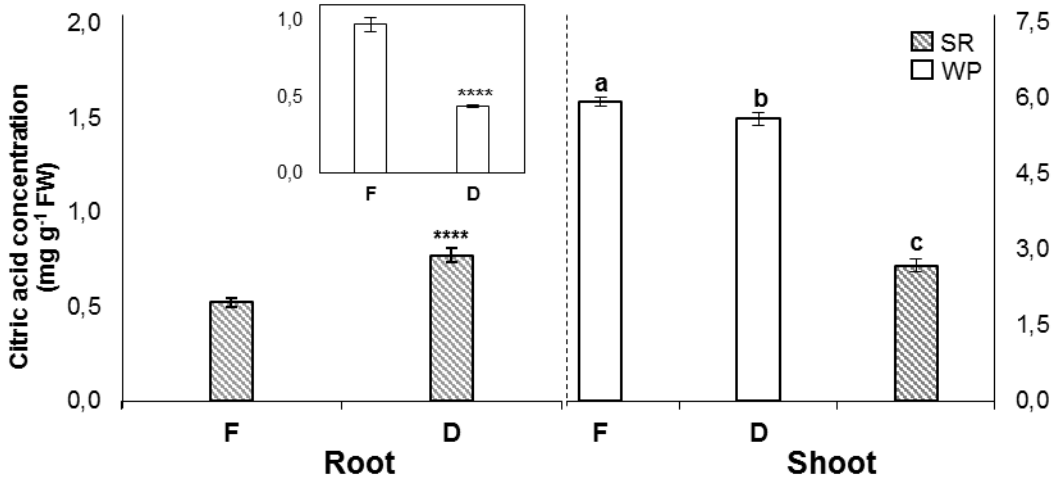

Fig. 8. Citric acid concentration in roots and shoots of split- and not split-root tomato plants. Terms, treatments and statistics as in Fig. 2.

2.4 Discussion

It has been demonstrated that the enhanced sulfate uptake and assimilation rate are crucial to allow the onset of the typical responses to Fe deficiency in dicots (Strategy I) [4]. Contrariwise, the capability of these plants to cope with the Fe nutritional disorder is seriously hampered by the simultaneous imposition of S deficiency [4]. Following up on these previous findings, this work was addressed at studying the development of the typical root responses to Fe deficiency when the availability of S is not guaranteed homogeneously on the entire root system. In parallel, the mechanisms underlying S homeostasis necessary for the Fe shortage responses in plants sensing the S deficiency only in a specific root area but containing an adequate S content in the whole plant tissues, were also considered in order to decipher the long- or short-distance signaling triggering the onset of the plant response to the nutritional stresses. To this purpose, a split-root hydroponics system was used to grow the root system of each single tomato plant in two separated and independent compartments, both Fe-free, but only one root half was starved (combined S and Fe deficiency, D) while the other root half was supplied with sulfate (single Fe deficiency, F).

Stimulation of root growth, and following reduction of shoot:root ratio, is one of the earliest and distinct symptoms of plant S deficiency [3,19]. When the performance of hydroponically grown split-root plants was evaluated, no difference in root growth was observed between the two portions of the split root system, one part subjected only to Fe deficiency (F) and the other grown under dual deficiency of Fe and S (D) condition (Fig. 2A). In other words, the uneven S availability did not cause a different developmental rate of the root tissue. Interestingly, there was no difference in root system development also considering not-split (whole) plants between roots of plants exposed only to the Fe deficiency (WF) or to the combined Fe and S shortages (WD) (Fig. 2A, insert). On the other hand, shoot biomass production changed depending on the nutrient regime and the growing system. In fact, the shoots of split-root plants displayed a reduced growth as compared to both shoots from not-split plants (WF and WD) (Fig. 2B) and leaf chlorosis when compared to shoots from Fe-deficient not-split plants (WF) (insert in Fig. 2B).

The reduction of biomass accumulation was greater in shoots from split-root plants than in those from whole plants grown in D condition (WD). On the other hand, no significant difference in chlorophyll content was observed between shoots from split-root plants and those from whole plants grown in D condition (WD) (Fig. 3).

As might be expected, S starvation induced a significant reduction of both total S and thiols concentrations in roots and shoots from not-split plants (Fig. 3). Interestingly, the same response (*i.e.* the lowest levels of total S and thiols concentrations) was found in split root plants in the portion of the root system exposed to combined S and Fe deficiency (D) (Fig. 3). It is worth to notice that in the shoot tissue of split-root plants the levels of the two parameters (total S and thiols concentrations) were significantly higher than those measured in the not-split-root plants exposed to the double deficiencies (WD) (Fig. 3B and D). This result clearly indicates that the supply of S, even if localized at only one side of the root, is likely to contribute to the nutritional S state of the aerial part of the plant. However, given that the levels of both parameters in shoots of split-root plants were significantly lower than those measured in not split-root plants exposed only to Fe deficiency (WF), it provides clear evidence that the localized application of sulfate was not able to adequately match S nutritional level similar to that of plants provided with sulfate uniformly available for the whole root system.

It is quite reasonable to expect that the reduced accumulation of total S and thiols in D side of root system of split-root plants could be most likely correlated with changes in S uptake and assimilation rate. Therefore, we investigated the modulation of the mechanisms underlying the S uptake process determining the transcript levels of the gene *SlST1.1* codifying for a high affinity sulfate transporter, whose expression is known to be modulated by the S availability [21,22,23].

The increased transcript levels of *SlST1.1* found in root tissues of not split-root plants exposed to the dual deficiency (WD) is a typical response to S deficiency. It is interesting to note that *SlST1.1* expression was up-regulated also in the D portion of the root apparatus of split-root plants (Fig. 4), suggesting a localized increased sulfate uptake capacity. On the other hand, withdrawal of S locally applied to one root portion (D) did not alter that *SlST1.1* expression, and thus S uptake capability, in the S-sufficient root portion (F) of the split-root system, as previously reported [24,25]. However, the increase in transcript abundance of *SlST1.1* in the roots under S deficiency was much higher for WD plants than that of the D side of split root plants (Fig. 4). It is possible that sulfate provision by the Fe deficient root half or the shoot mentioned above may be partly responsible for the inhibition of *SlST1.1* expression. Therefore, it remains a challenge to determine how plants sense changing environment and manage their different uptake rates of sulfate.

The activity of ATPS and OASTL (the first and the last enzyme involved in the S assimilatory pathway, respectively) has been used as an indicator to evaluate changes of the S assimilation rate

(Fig. 5). According to what has been described for the levels of *SlST1.1* transcripts, also the activity of both ATPS and OASTL was significantly increased in the root portion exposed to S shortage (D condition) with respect to that only Fe-deficient (F condition) (Fig. 5A and C). On the other hand, we found that when not split-root plants were treated with dual deficiency (WD), only the root ATPS activity was increased (insert in Fig. 5A), whereas OASTL activity was significantly decreased (insert Fig. 5C) with respect to only Fe-deficient plants (WF). Interestingly, the modulation of the two enzymes at the shoot level ascribable to the treatments appeared quite different: only ATPS activity was significantly augmented in the shoots of split plants (+60% and +53% when compared with both WF and WD shoots, respectively), whereas OASTL activity did not change irrespective of different nutritional conditions (Fig. 5B and D).

It is well known that the uptake and assimilation of most major nutrients including sulfate is governed by the nutritional status of the plant [23]. Accordingly, sulfate influx in roots, the expression of genes encoding different sulfate transporters and many enzymes involved in sulfur metabolism, as well as their activity, are regulated by signals that respond to the nutrient status of the plants [26].

The results of this work clearly show that the uneven distribution of a nutrient along the root system, does not only differently affect the response of the plant to the nutritional stress linked with the availability of this specific element, but can also affect the efficiency of the response to the shortage of other elements. It was found a positive modulation of the mechanisms underlying both the uptake and the assimilation of sulfate took anyway place in the S-deficient portion of root system (D side), although S was supplied to a portion of the root system (F side) thus reasonably guaranteeing the S-nutritional status of the whole plant. Accordingly, the higher accumulation of total S and thiols in shoots of split-root plants (+25% for both parameters) with respect to those from not-split root plants exposed to dual deficiency (WD) is most likely the result of both the S acquisition by the part of root supplied with the nutrient (F) and the satisfaction of the plant S nutritional needs (Fig. 4, Fig. 5).

These findings suggest that S uptake, assimilation and accumulation are closely regulated in response to the local nutrient availability in the growth medium rather than as a consequence of the plant S nutritional status, since in split-root system, half root apparatus is in a S-deprived condition (D side) whereas the other receives S (F side), providing adequate amounts of the nutrient in the shoots. Thus, the increased S demand to cope with Fe starvation condition [4,6] might, at least in part, explain the phenomenon. For this reason, the modulation of the mechanism underlying the

acquisition of Fe has been also evaluated in these growing conditions focusing on Fe deficiency-induced gene expression patterns.

It is well known that Strategy I plants cope with Fe deficiency *via* the rhizosphere acidification and the reduction of sparingly soluble FeIII [27,28,29,30]. These steps involve two enzymatic activities located at the root surface, the plasma membrane (PM) H^+ATPase which catalyzes the active extrusion of protons in the rhizosphere and the FeIII -chelate reductase (FRO1) mediating the reduction of soil Fe^{3+} to soluble Fe^{2+}. Once reduced, Fe^{2+} is then taken up into root cells *via* the high-affinity Fe^{2+} transporter (IRT1) [31]. It has been also demonstrated that Fe shortage induces the ethylene production of roots playing an important role in the modulation of the FeIII-reducing capacity [32,33].

Our earlier work showed that S-deficient tomato plants were quite unable to cope with Fe deficiency [4], since increases in both ethylene production and FeIII-chelate reductase activity were prevented. Moreover, the transcript levels of *LeFRO1* and *LeIRT1* genes, codifying for the reductase and for the Fe^{2+} transporter, respectively, were severely affected by the imposition of the dual (S and Fe) deficiency [4].

The variation of expression of Fe deficiency marker genes (*SlFER*, *SlFRO1*, *SlIRT1***)** after quantitative RT-PCR analysis are summarized in the graphs given in Fig. 6. Both *SlFER*, the ortholog in tomato of FIT (FE DEFICIENCY-INDUCED TRANSCRIPTION FACTOR) and *SlFRO1* (FERRIC REDUCTASE OXIDASE 1) were strongly up-regulated in the D portion of the root system with respect to the root portion only subjected to the Fe shortage (F side) (Fig. 6A and B), whereas *SlIRT1* expression did not change between the two distinct portions of the root system (Fig. 6C).

Surprisingly, no difference in the expression level of the *SlFER* and *SlFRO1* genes was measured in roots of not split-root plants between the treatment of sole Fe- (WF) and dual- (WD) deficiency (inserts in Fig. 6A and B). On the contrary, a higher amount of *SlIRT1* transcripts was measured in WD roots in comparison to WF ones (insert in Fig. 6C). Furthermore, the up-regulation of *SlFRO1* expression was associated by significant increase in *in vivo* assayed FeIII reducing capacity found in D roots of split-root plants with respect to F ones (Fig. 7). Thus, these results seem to indicate that, in split-root plants, unexpectedly, a more efficient response to the Fe deficiency is taking place in the portion of the root system subjected to the combined deficiency (D side, Fig. 7). It has to be pointed out that this response pattern was very contrasting to that displayed by roots of not split-root plants exposed to combined Fe and S deficiency (WD), which

indeed showed a strong reduction of the activity of this enzyme (−25%) (insert in Fig. 7), as was observed in previous experiences [4]. The expression patterns of Fe deficiency marker genes (*SlFER, SlFRO1, SlIRT1***)** led us to suggest that the two different steps of Strategy I mechanism (uptake and reduction) could be regulated by different mechanisms among which Fe deficiency is not the sole regulating factor. In particular, it is likely that *SlIRT1* might be controlled by regulatory mechanisms more complex with respect to *SlFRO1*.

The strong induction of transcription of *SlFRO1* gene followed by a significant increase of the enzyme activity observed in the portion of root system exposed to the dual deficiency (D) makes plausible to argue the intervention of other signal mechanisms regulating the development of the adaptive responses, mediating the expression of genes and consequently the activity of enzymes.

Indeed, very recently it has been hypothesized that intracellular citrate could act as a signaling molecule affecting the expression level of several genes [13].

It is well known that Fe and S closely interact for the building of Fe–S clusters, whose assembly takes place mainly in the mitochondria [11]. Therefore, mitochondria might play a pivotal role in the regulation of Fe and S interaction. The Fe deficiency-induced alteration in the synthesis of mitochondria-derived carboxylic acids, such as citric acid [6], and the evidence that such molecules have already been identified as important players of metabolite signalling in several organisms, further support this hypothesis [34,35,36,37]. Thus, it is possible this also occurred in our study: the increased citrate accumulation in D portion of the root system (Fig. 8) was found to be positively correlated with Fe(III) reducing capacity (Fig. 7), as well as reduction in citrate accumulation in roots of not split root plants exposed to dual deficiency (WD) (insert in Fig. 8) correlated with lower Fe(III) reducing capacity in the same plants (insert in Fig. 7). However, it cannot be ruled out the possibility that the changes in citrate concentration could be attributed to a redistribution of the Fe tissue concentration. Further studies are required and are ongoing in order to fully elucidate the mechanisms behind such differential accumulation of citrate between WD and D plants.

In conclusion, the split-root system developed in this work also integrates a better knowledge of how and to what extent the root system is able to adjust nutrient acquisition capacity to meet variations in shoot demand or in external nutrient availability, an aspect that requires special attention in the frame of plant mineral nutrition.

However, it remains a challenge to determine how the interplay between S and Fe is regulated and how plants sense environmental nutrient fluctuations and manage their different uptake,

translocation, assimilation, and signaling. Indeed, although it is well known that Fe deficiency response can be hampered by S starvation [4], results of the present work indicated that the supply of S in specific portion of the root system (F side) can allow the onset of the Fe deficiency response also in those root zones not adequately supplied with S (D side). More importantly, being the Fe response over-activated in such root zones, where, on the contrary, it should be limited on the basis of what described in literature [4] this phenomenon suggests that a local response signal can be ruled out.

Therefore, the interaction S/Fe must include a complex signaling pathways to be further studied. However, the results led us to conclude that this may be partly related to the role of citric acid in the cross talk of signalling pathways required for the adaptation of the plants to combined deficiency, as recently hypothesized [13].

Acknowledgements

The research was carried out in the frame of the MIUR (Ministry for education, University and Research) initiative "Department of excellence" (Law 232/2016).

References

[1] S. Astolfi, S. Zuchi, C. Passera, S. Cesco, Does the sulfur assimilation pathway play a role in the response to Fe deficiency in maize (Zea mays L.) plants? J. Plant Nutr. 26 (2003) 2111–2121.

[2] S. Astolfi, S. Cesco, S. Zuchi, G. Neumann, V. Römheld, Sulfur starvation reduces phytosiderophores release by iron-deficient barley plants, Soil Sci. Plant Nutr. 52 (2006) 43–48.

[3] S. Zuchi, S. Cesco, S. Astolfi, High S supply improves Fe accumulation in durum wheat plants grown under Fe limitation, Environ. Exp. Bot. 77 (2012) 25–32.

[4]S. Zuchi, S. Cesco, Z. Varanini, R. Pinton, S. Astolfi, Sulphur deprivation limits Fedeficiency responses in tomato plants, Planta 230 (2009) 85–94.

[5]H. Marschner, Mineral Nutrition of Higher Plants, 2nd ed., Academic press, 1995.

[6]S. Zuchi, M. Watanabe, H.M. Hubberten, M. Bromk, S. Osorio, A.R. Fernie, S. Celletti, A.R. Paolacci, G. Catarcione, M. Ciaffi, R. Hoefgen, S. Astolfi, The interplay between sulfur and iron nutrition in tomato, Plant Physiol. 169 (2015) 2624–2639.

[7]A. Zamboni, S. Celletti, S. Zenoni, S. Astolfi, Z. Varanini, Root physiological and transcriptional response to single and combined S and Fe deficiency in durum wheat, Environ. Exp. Bot. 143 (2017) 172–184.

[8]S. Astolfi, S. Zuchi, H.M. Hubberten, R. Pinton, R. Hoefgen, Supply of sulphur to Sdeficient young barley seedlings restores their capability to cope with iron shortage, J. Exp. Bot. 61 (2010) 799–806.

[9]A.R. Paolacci, S. Celletti, G. Catarcione, M.J. Hawkesford, S. Astolfi, M. Ciaffi, Iron deprivation results in a rapid but not sustained increase of the expression of genes involved in iron metabolism and sulfate uptake in tomato (Solanum lycopersicum L.) seedlings, J. Integr. Plant Biol. 56 (2014) 88–100.

[10]H. Hesse, R. Hoefgen, Molecular aspects of methionine biosynthesis, Trends Plant Sci. 8 (2003) 259–262.

[11]J. Balk, M. Pilon, Ancient and essential: the assembly of iron–sulfur clusters in plants, Trends Plant Sci. 16 (2011) 218–226.

[12]I. Forieri, C. Sticht, M. Reichelt, N. Gretz, M.J. Hawkesford, M. Malagoli, M. Wirtz, R. Hell, System analysis of metabolism and the transcriptome in Arabidopsis thaliana roots reveals differential co-regulation upon iron, sulfur and potassium deficiency, Plant Cell Environ. 40 (2017) 95–107.

[13]G. Vigani, Y. Pii, S. Celletti, M. Maver, T. Mimmo, S. Cesco, S. Astolfi, Mitochondria dysfunctions under Fe and S deficiency: is citric acid involved in the regulation of adaptive responses? Plant Physiol. Biochem. 126 (2018) 86–96.

[14]F.S. Zhang, V. Römheld, H. Marschner, Role of the root apoplasm for iron acquisition by wheat plants, Plant Physiol. 97 (1991) 1302–1305.

[15]C. Ramakers, J.M. Ruijter, R.H.L. Deprez, A.F.M. Moorman, Assumption-free analysis of quantitative real-time polymerase chain reaction (PCR) data, Neurosci. Lett. 339 (2003) 62–66.

[16]M.W. Pfaffl, A new mathematical model for relative quantification in real-time RT–PCR, Nucleic Acids Res. 29 (2001) 45.

[17]M.W. Pfaffl, G.W. Horgan, L. Dempfle, Relative expression software tool (REST) for group-wise comparison and statistical analysis of relative expression results in realtime PCR, Nucleic Acids Res. 30 (2002) 36.

[18]C.E. Bardsley, J.D. Lancaster, Determination of reserve sulphur and soluble sulphate in soils, Soil Sci. Soc. Am. Proc. 24 (1962) 265–268.

[19]S. Celletti, Y. Pii, T. Mimmo, S. Cesco, S. Astolfi, The characterization of the adaptive responses of durum wheat to different Fe availability highlights an optimum Fe requirement threshold, Plant Physiol. Biochem. 109 (2016) 300–307.

[20]M.M. Bradford, A rapid and sensitive method for quantitation of microgram quantities of protein utilizing the principle of protein-dye binding, Anal. Biochem. 72 (1976) 248–254.

[21]L. Hopkins, S. Parmar, D.L. Bouranis, J.R. Howarth, M.J. Hawkesford, Coordinated expression of sulfate uptake and components of the sulfate assimilatory pathway in maize, Plant Biol. 6 (2004) 408–414.

[22]M. Lewandowska, A. Sirko, Recent advances in understanding plant response to sulfur-deficiency stress, Acta Biochim. Pol. 55 (2008) 457–471.

[23]H. Takahashi, S. Kopriva, M. Giordano, K. Saito, R. Hell, Sulfur assimilation in photosynthetic organisms: molecular functions and regulations of transporters and assimilatory enzymes, Ann. Rev. Plant Biol. 62 (2011) 157–184.

[24]H. Rouached, D. Secco, A.B. Arpat, Getting the most sulfate from soil: regulation of sulfate uptake transporters in Arabidopsis, J. Plant Physiol. 166 (2009) 893–902.

[25]H.M. Hubberten, A. Drozd, B.V. Tran, H. Hesse, R. Hoefgen, Local and systemic regulation of sulfur homeostasis in roots of Arabidopsis thaliana, Plant J. 72 (2012) 625–635.

[26]H. Hesse, V. Nikiforova, B. Gakiere, R. Hoefgen, Molecular analysis and control of cysteine biosynthesis: integration of nitrogen and sulphur metabolism, J. Exp. Bot. 55 (2004) 1283–1292.

[27]M. Dell'Orto, S. Santi, P. De Nisi, S. Cesco, Z. Varanini, G. Zocchi, R. Pinton, Development of Fe deficiency responses in cucumber (Cucumis sativus L.) roots: involvement of plasma membrane H+-ATPase activity, J. Exp. Bot. 51 (2000) 695–701.

[28]S. Santi, S. Cesco, Z. Varanini, R. Pinton, Two plasma membrane H+-ATPase genes are differentially expressed in iron-deficient cucumber plants, Plant Physiol. 43 (2005) 287–292.

[29]S.A. Kim, M.L. Guerinot, Mining iron: iron uptake and transport in plants, FEBS Lett. 81 (2007) 2273–2280.

[30]J. Morrissey, M.L. Guerinot, Iron uptake and transport in plants: the good, the bad, and the ionome, Chem. Rev. 109 (2009) 4553–4567.

[31]C. Curie, J.F. Briat, Iron transport and signalling in plants, Ann. Rev. Plant Biol. 54 (2003) 183–206.

[32]F.J. Romera, E. Alcántara, Iron-deficiency stress responses in cucumber (Cucumis sativus L.) roots. A possible role for ethylene? Plant Physiol. 105 (1994) 1133–1138.

[33]F.J. Romera, E. Alcántara, M.D. De la Guardia, Ethylene production by Fe-deficient roots and its involvement in the regulation of Fe deficiency stress responses by Strategy I plants, Ann. Bot. 83 (1999) 51–55.

Chapter 4

Iron and sulfur deficiency differentially affect Target of Rapamycin (TOR) activity in tomato plants

In submission to Plant Science as "*Iron and sulfur deficiency differentially affect Target of Rapamycin (TOR) activity in tomato plants?*", E. Coppa, G. Vigani, R. Aref, M. Wirtz, R. Hell, S. Astolfi.

Abstract

During their lifetime, plants have to cope with simultaneous nutrient deficiencies. Over the past few decades, a close relationship between S and Fe was clearly demonstrated in tomato. However, till date, very little is known about the regulatory mechanisms underlying the responses to the combined S and Fe deficiency. The first and main hypothesis on the reason for Fe/S interplay was the amino acid methionine, being the precursor of S-adenosine methionine, the common precursor of nicotianamine and ethylene, both involved in plant response to Fe starvation. The second link has been ascribed to the involvement of both nutrients in Fe-S cluster assembly. However, obtained results did not fully account the initial hypotheses, suggesting the involvement of unknown and complex regulation/signalling mechanisms. Recently, the potential role of citric acid in plant adaptation to Fe deficiency and combined S and Fe deficiency has been described. It is well known that an impaired organic acid metabolism may stimulate a retrograde signal and that response is involved in the regulation of many different processes within the plant. Moreover, it has been proved that the retrograde response is linked to Target of Rapamycin (TOR) signaling in yeast and in animal cells, even if this link has not been resolved. Recent reports provide evidence that TOR may play an integrative role in modulating sulfur nutrient sensing in plants. This intriguing suggestion prompted us to investigate whether TOR may play a role in the cross talk of signaling pathway occurring during plant adaptation to combined deficiency of Fe and S. Our results revealed that Fe deficiency elicited an increase of TOR activity in shoots associated to enhanced accumulation of citrate in the same tissue, whereas S deficiency resulted in decreased TOR activity and citrate accumulation. In addition, we found that citrate accumulated in shoots of plants exposed to combined S/Fe deficiency assumed values between those found in F and S plants, as well as TOR activity.

In conclusion, this work suggests a new mechanism for nutritional stress perception, in which citrate could play a relevant role as TOR inducer, at least in tomato.

Keywords: TOR; Iron deficiency; Sulfur deficiency, citric acid; nutrient interaction.

4.1 Introduction

In the last few decades, a close relationship between S and Fe was clearly established in tomato: S deficiency significantly impairs plant capability to cope with Fe deficiency (Zuchi et al 2009), whereas Fe deficiency induces a significant increase of S uptake and assimilation rate, (Paolacci et al., 2014). These results were ascribed to methionine, being well known as the common precursor of both ethylene and nicotianamine (NA) (Hesse and Hoefgen 2003).

Ethylene has been suggested to play a role in the regulation mechanisms of Fe deficiency responses (Lucena et al. 2006; Garcia et al. 2010), whereas NA is involved in Fe transport within the plant via xylem or phloem (Rudolph et al., 1985; Douchkov et al., 2002).

As revealed by Zuchi et al. (2009) in Fe-deficient tomato plants, S deficiency prevented ET production at root level and the induction of Fe(III)-chelate reductase activity and severely limited the expression of NA synthase (*LeNAS*), *LeFRO1* (FERRIC REDUCTASE OXIDASE 1) and *LeIRT1* (IRON-REGULATED TRANSPORTER 1) genes, suggesting that the lower Fe accumulation in tomato shoots could be attributed to missed activation of Strategy I (ethylene) as well as impaired Fe translocation to the shoot (NA). Thus, it has been suggested that increased demand of reduced S under Fe deficiency could be functional to allow proper methionine availability to sustain ethylene and NA biosynthesis (Zuchi et al., 2009; Paolacci et al., 2014; Zuchi et al., 2015).

However, higher S needs to sustain the activation of *Strategy I* mechanism cannot fully account for the observed link between the flow of these two essential nutrients in plant, as demonstrated by using a metabolomic approach, which showed an intensive overlap, but also distinct responses (Zuchi et al., 2015). On the other hand, the multi-faceted effects of combined S and Fe deficiency on plant metabolome cannot even be explained by the need to maintain Fe-S cluster synthesis (Balk and Pilon, 2011). This latest link could indeed only account for the reduced Fe accumulation under

S deficiency, since Fe and S need to be clearly coordinated for the maintenance of Fe-S-cluster formation, but not for increased S uptake and assimilation under Fe deficiency.

Evidently, there must be many interacting factors and complex mechanisms that can likely include a direct interference of Fe with the signal transduction pathway involved in S metabolism and *vice versa*.

Intriguingly, mitochondria represent an important cellular site for the assembly of Fe-S clusters (Balk and Pilon, 2011). Furthermore, mitochondria are the power house of the cell providing energy as well as a plethora of compounds, such as carboxylic acids, necessary for the whole metabolism. Among these compounds, citric acid has been shown to play a role as metabolite signal in several organisms (Schwarzländer et al., 2012; Finkemeier et al., 2013; Ostaszewska et al., 2014; Vigani and Briat, 2016). Recently, changes in intracellular citrate have been shown to correlate with some Fe- and S- responsive genes (Vigani et al., 2018). Moreover, it was found a positive feedback between root citric acid concentration and plant ability to cope with Fe starvation, in terms of increased Fe(III)-chelate reductase activity and both *SlFRO1* and *SlFER* expression (Coppa et al., 2018). Overall, these data were interpreted to suggest that citrate may be involved in plant's adaptation to the combined deficiency of Fe and S in tomato (Vigani et al., 2018; Coppa et al., 2018).

It is well known that an impaired organic acid metabolism (TCA cycle) in cells may stimulate a retrograde signal (from mitochondria to the nucleus) and that response is involved in the regulation of many different processes within the plant (Butow and Avadhani, 2004). Moreover, it has been proved that the retrograde response is linked to Target of Rapamycin (TOR) signaling in yeast and in animal cells, but this link has not been resolved (Butow and Avadhani, 2004).

TOR is a strongly conserved kinase that is widely present in all eukaryote organisms. Several metabolic compound like sugars, amino acids, hormones, and energy stimulate TOR activity in order to to promote nutrient assimilation and protein production. TOR activity induction results in activation mRNA translation and in turn, cell growth and division. Furthermore, TOR represses catabolic processes such as autophagy or protein degradation (Forzani et al., 2018 and references therein). Recent evidence gathered in plants supports its role as "regulatory-hub" in a wide range of processes such as cell metabolism, biogenesis, organ growth, and development transitions in response to nutrient availability, energy, hormone, and environmental signals (Wullschleger et al., 2006; Loewith and Hall, 2011; Yan et al., 2012; Dobrelen et al., 2016; Pu et al., 2017; Wu et al., 2019).

Some available evidence indicates that TOR may play an integrative role in modulating sulfur nutrient sensing in plants (Wu et al., 2019; Fu et al., 2020). In particular, in *Arabidopsis* S deficiency results in reduced TOR activity, monitored by phosphorylation of its target, S6K protein (Dong et.al 2017). In addition, TOR protein kinase has been demonstrated to be activated by glucose (Wu et al., 2019).

This intriguing suggestion prompted us to investigate whether TOR may play a role in the cross talk of signaling pathway occurring during plant adaptation to combined deficiency of Fe and S.

To disentangle this relation, we characterized changes in TOR activity in roots and shoots of tomato plants grown under single and combined deficiency of S and Fe. Results revealed that the TOR activity correlated with citric acid content, rather than glucose content, suggesting that citrate might be involved in establishing a link between plant response to combined S/Fe deficiency and the TOR network.

4.2 Materials and methods

4.2.1 Plant growth conditions

Tomato (*Solanum lycopersicum* L., cv. Marmande) plants were grown hydroponically in plastic pots containing 2.2 L of complete nutrient solution (NS), containing 1.2 mM sulfate and 40 µM FeIII-EDTA) (Zuchi et al., 2009). After two weeks, half of the plants were transferred in a S-free NS and half of the plants deriving from the two S growth conditions were transferred to a Fe-free NS to obtain four different treatments defined as control (C, 1.2 mM sulfate and 40 µM FeIII-EDTA), Fe-deficient (F, 1.2 mM sulfate and 0 µM FeIII-EDTA), S-deficient (S, 0 mM sulfate and 40 µM FeIII-EDTA) and dual deficient (D, 0 mM sulfate and 0 µM FeIII-EDTA). Plants were grown in a growth chamber under 200 µmol photons m^{-2} s^{-1} photosynthetic photon flux, with 16/8 h photoperiod (27°C/20°C day/night temperature cycling and 80% relative humidity.

4.2.2 Immunological assay

Immunological detection of S6K-p and S6K1/2 was performed as described by Dong et al. (2017), with minor modifications. Total soluble proteins were extracted from 50 µg of root and shoot tissues by adding in a ratio 1:5 (w/v) 2x Laemmli Buffer supplemented with 3% of phosphatase inhibitor cocktail 2 (Sigma). Proteins were denatured for 7 min at 95 °C. For the immunological detection of S6K-p proteins were separated on 10% SDS-PAGE, while for the immunological detection of S6K1/2 proteins were separated on 15% SDS-PAGE supplemented with 8 M urea, and

then for both, S6K-p and S6K1/2 detection, proteins were transferred on PVDF membrane. The blocking solution was supplemented with Twin 0.1% only for S6K1/2 detection. Membranes were incubated with the primary antibodies overnight at 4°C: anti-S6K1-p (abcam, phospho T449 ab 207399, 1:2500) anti-S6K1/2 (Agrisera, Ribosomal S6 kinase 1/2 AS12 1855, 1:3000). The primary antibodies were detected using the HRP-conjugated secondary antibody (1:20000). The bands intensity was quantified by Image Quant LAS4000 version 1.21 and normalized by the loading control.

4.2.3 TCA cycle enzyme activity

Mitochondrial enhriched fraction was collected by tomato root according to Vigani et al. (2018). Citrate synthase, succinate dehydrogenase, aconitase activity were performed according to Vigani et al. (2009).

4.2.4 Other measurements and Statistics

The concentration of glucose in root and shoot tissues of tomato plants was determined by Glucose Colorimetric/Fluorometric Assay Kit (Sigma Aldrich). Glucose is oxidized to generate a colorimetric (570 nm) product, proportional to the amount of glucose present in plant tissues.

Citric acid concentration in root and shoot samples of tomato plants was determined by Citrate Assay Kit (Sigma Aldrich). Citrate concentration is determined by a coupled enzyme assay, which results in a colorimetric (570 nm) product, proportional to the citrate present in plant tissues.

Each reported value represents the mean ± SD of data from four independent experiments on three biological replicates per experiment. Statistical analyses of data were carried out by ANOVA tests with the GraphPad InStat Program (version 3.06). Significant differences were established by posthoc comparisons (HSD test of Tukey) at $P < 0.001$ or $P < 0.01$.

4.3 Results

4.3.1 Differential modulation of TOR Activity under single or combined Fe and S deficiency

TOR activity was determined by the ratio S6K-p/S6K1/2 in shoots and roots of tomato plants (Fig. 1 A, B). Tomato plants exposed to S deficiency (S) showed a strongly decreased TOR activity (-38%, with respect to the control) at shoot level (Fig. 1A), whereas TOR activity in roots was similar to that of control plants (Fig. 1B).

The withdrawal of Fe from NS significantly increased TOR activity in both shoots and roots (+ 89% and +68% compared to control, respectively).

Finally, when plants were treated with combined deficiency (D), TOR activity showed values similar to those of control plants (Fig. 1A, B). However significant differences were observed between D and S plants as well as between D and F plants. As reported in Fig.1, D plants had about 50% and 20% lower TOR activity in their shoots and roots, respectively, than F plants. Additionally, D plants had about 50% and 60% higher TOR activity in their roots and leaves, respectively, than S plants (Fig. 1A, B).

4.3.2 Glucose and amino acids content

Regulation of plant TOR by glucose was previously reported (Xiong et al., 2013) and later research supported a role of the glucose-TOR signaling under sulfur deprivation (Dong et al., 2017).

Our results showed that all starvation treatments significantly increased shoot glucose concentration, but to a different extent (Fig. 2A). In particular, glucose concentration increased by 24%, 15% and 30% in F, S and D plants, respectively, relative to the control (Fig. 2A).

On the other hand, there was no difference in root glucose concentration among the four different treatments (Fig. 2B).

No correlation was found between glucose concentration and TOR activity in both shoots and roots of the tomato plants under the four nutritional conditions (Fig. 3A, B).

A further aspect affecting TOR activity is linked to the N metabolism in particular to the amino acid content. By reanalysing metabolic data obtained from tomato plant grown under single and combined Fe and S deficiency (Zuchi et al., 2015), a general decrease of AA can be observed in both leaves (Fig. 4A) and root (Fig. 4B) of Fe deficient plants, while S deficiency, either in single or in combination with Fe deficiency, leads to a general accumulation of AA both in leaves and roots tissues.

4.3.3 Citric acid concentration

In our experiment, citrate concentration in tomato shoots was not affected by Fe deficiency, whereas when the external supply of sulfate was limited (both S and D condition), citrate concentrations are significantly lower (-23% in both cases) than those in the shoots of control plants (Fig. 5A).

The concentration of citrate in roots followed closely the pattern of TOR activity (Fig. 5B). The highest value for citrate concentration were found in roots of plants exposed to Fe deficiency (F) and was more than threefold higher than those found in control roots (Fig. 5B). In roots of plants exposed to single S deficiency (S), the concentration of citrate was similar to that of control plants (Fig. 5B). However, combined deficiency treatment (D) caused a 55% increase in citrate concentration in roots relative to the control (Fig. 5B). Citric acid accumulation in roots is related to the changing activity of TCA cycle related enzymes (Fig. 6). Under Fe deficiency, the higher induction of citrate synthase along with the slowing down of succinate dehydrogenase and aconistase results in citrate accumulation in root cells.

These data raises the question of a possible impact of different citrate concentrations on TOR activity and actually a positive correlation was observed between the two parameters in both shoots (Fig. 7 A) and roots (Fig. 7 B) which can be described by the following linear functions (Fig. 7):

Shoot: $y = 1{,}4303x + 3{,}4556$ ($R^2 = 0{,}7091$)

Root: $y = 5{,}3144x - 1{,}8249$ ($R^2 = 0{,}8201$)

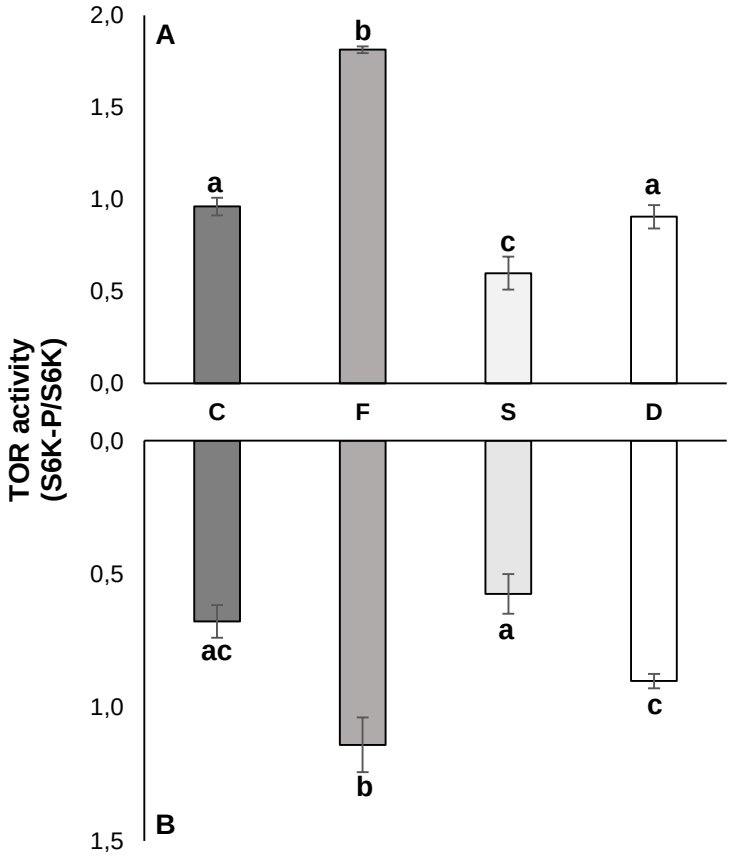

Fig. 1 TOR activity in shoot (A) and root (B) of tomato plants grown with different availability of iron (Fe) and sulfur (S): C, control; F, Fe deficiency; S, S deficiency; D, double deficiency of Fe and S. Data are means ± SD of three independent replications run in triplicate. The statistical significance was tested by means of ANOVA with Tukey post-test. Different letters indicate statistically different values ($P < 0.01$).

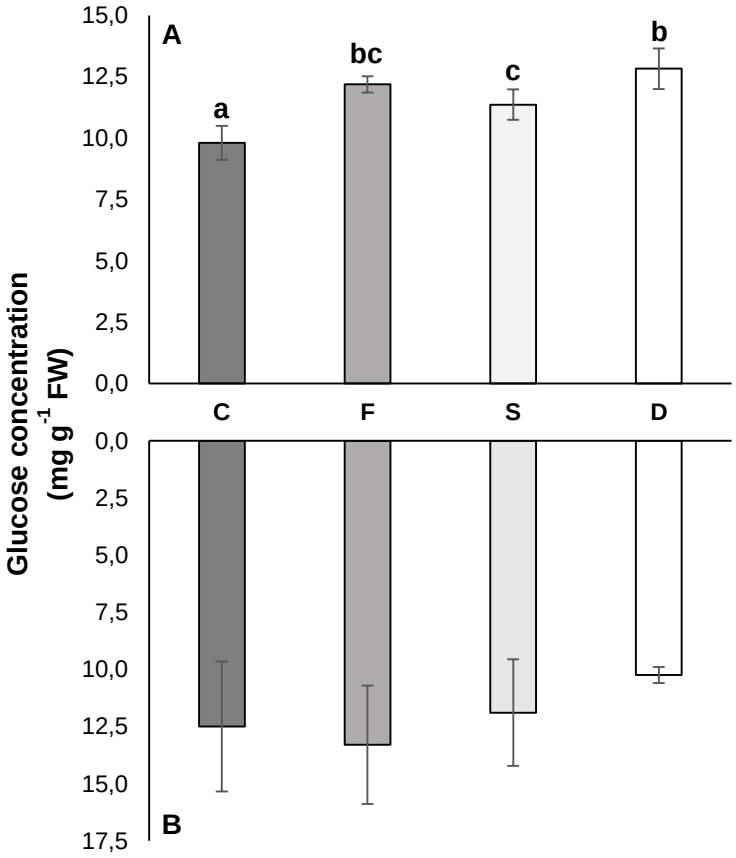

Fig. 2 Glucose concentration in shoot (A) and root (B) of tomato plants. Treatments and statistics as in Fig. 1.

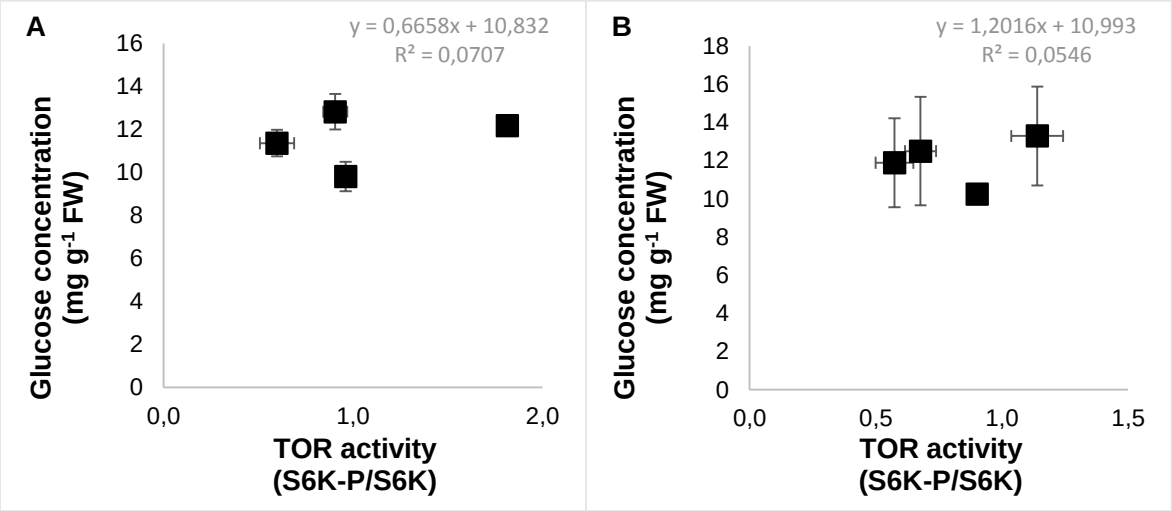

Fig. 3 Glucose concentration measured in shoot (A) and root (B) of tomato plants according to TOR activity in the same tissue.

Leaves

Aminoacids	F	S	D
Alanine	0,78	2,17	3,65
Valine	0,87	3,68	10,79
Isoleucine	0,91	3,85	12,48
Glycine	1,42	21,43	19,65
Proline	0,65	0,97	1,09
Serine	0,87	3,42	5,78
Threonine	1,00	2,90	6,26
Alanine, beta-	0,67	2,40	3,46
Serine, O-acetyl-	0,84	17,40	75,76
Proline, 4-hydroxy	1,15	5,04	14,32
Aspartic acid	0,56	0,56	0,49
Methionine	0,75	0,44	0,64
Glutamic acid	0,79	0,89	0,69
Phenylalanine	0,78	4,77	10,69
Asparagine	0,43	3,55	14,65
Glutamine	0,52	6,43	8,65
Arginine	0,61	8,22	25,11
Lysine	1,04	11,44	44,36
Glutamine	0,52	6,43	8,65
Arginine	0,61	8,22	25,11
Lysine	1,04	11,44	44,36
Ornithine	0,73	11,16	39,28
Tryptophan	0,61	4,11	12,59
Tyrosine	0,66	4,08	19,17

Roots

Aminoacids	F	S	D
Alanine, DL- (2TMS)	1,17	2,57	1,72
Valine, DL- (2TMS)	0,79	2,23	3,62
Isoleucine, L- (2TMS)	0,54	1,75	3,42
Proline, L- (2TMS)	0,80	1,22	1,69
Serine, DL- (3TMS)	0,89	1,68	1,32
Threonine, DL- (3TMS)	0,85	1,88	3,38
Alanine, beta- (3TMS)	0,82	2,11	1,45
Serine, O-acetyl-, DL- (2TMS)	0,95	17,98	15,64
GABA	1,09	1,50	1,45
Aspartic acid, L- (3TMS)	0,79	1,49	1,03
Methionine, DL- (2TMS)	0,52	0,52	0,52
Ornithine, DL- (4TMS)	1,02	3,90	7,60
Asparagine, DL- (3TMS)	0,58	6,43	22,79
Arginine	0,55	6,90	15,39
Lysine, L- (4TMS)	0,63	2,29	6,02
Glutamine, DL- (3TMS)	0,81	5,90	10,61
Tyrosine, DL- (3TMS)	0,53	2,00	2,49
Tryptophan, L- (2TMS)	0,45	1,06	2,10

Fig. 4 Changes in the aminoacid levels in leaves and roots of tomato plants. Treatments as in Fig. 1.

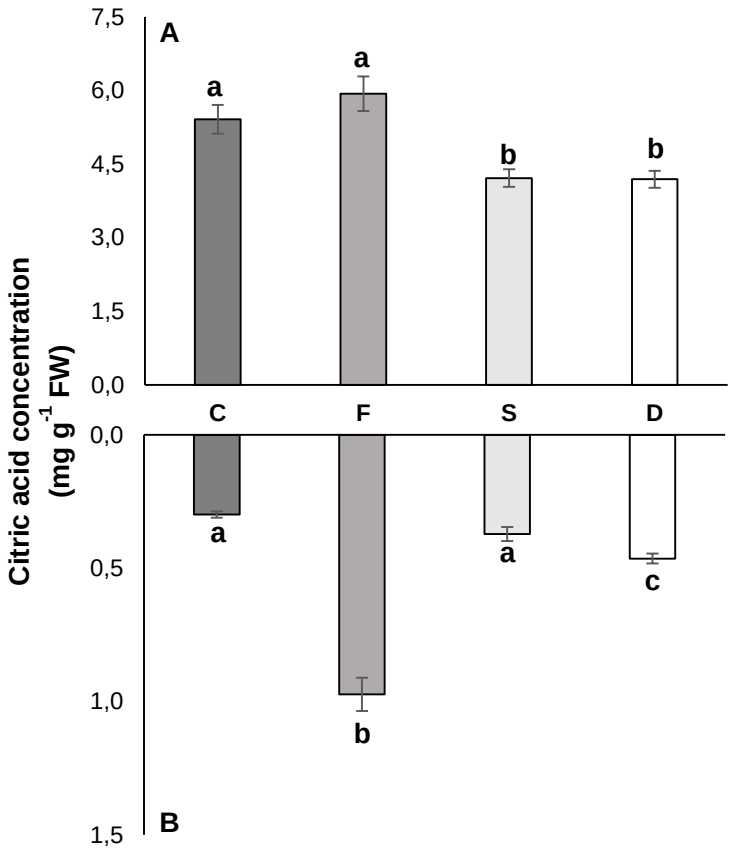

Fig. 5 Citric acid concentration in shoot (A) and root (B) of tomato plants. Treatments and statistics as in Fig. 1.

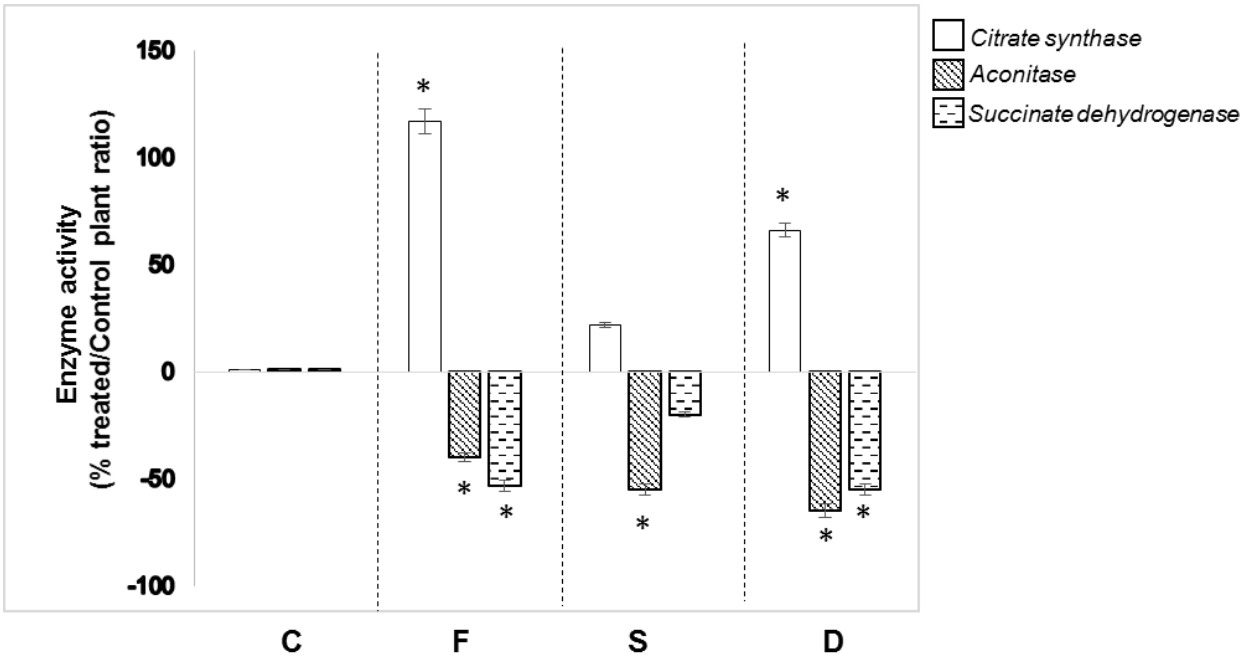

Fig. 6 Citrate synthase, aconitase and succinate dehydrogenase activities on purified mitochondria from roots of tomato plants. Treatments and statistics as in Fig. 1.

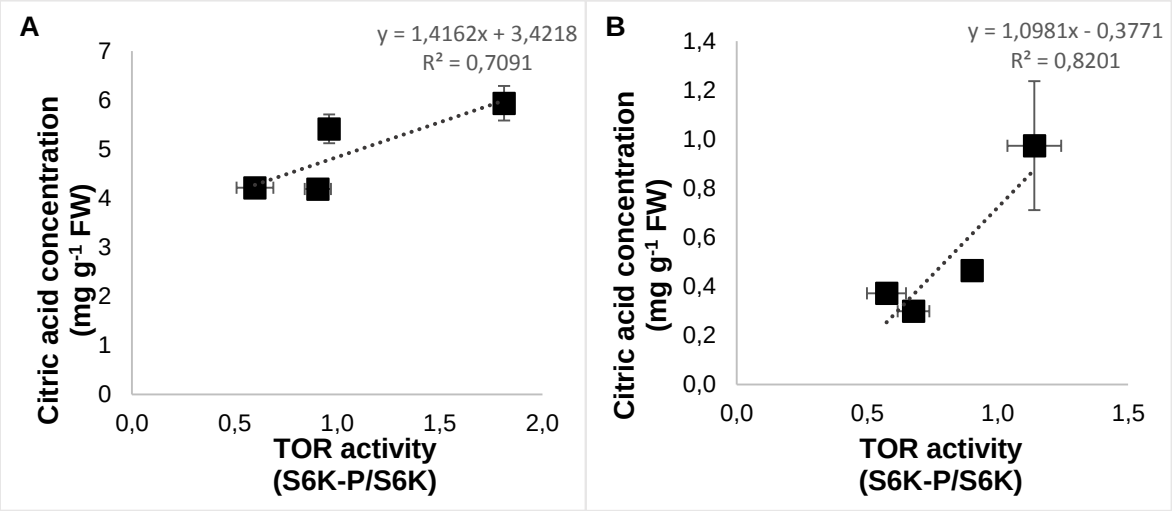

Fig.7 Citric acid concentration measured in shoot (A) and root (B) of tomato plants according to TOR activity in the same tissue.

4.4 **Discussion**

The existence of a close relationship between S and Fe has been clearly demonstrated in plants (Forieri *et al.*, 2013; Zuchi *et al.*, 2015; Zamboni *et al.*, 2017; Vigani *et al.*, 2018; Coppa *et al.*, 2018).

The relation was firstly attributed to methionine, being well known as the common precursor of both ethylene and nicotianamine (NA) (Hesse and Hoefgen 2003), and later to Fe-S cluster synthesis. However, neither of them fully accounts for the observed link between the flow of these two essential nutrients in plant, but it seems associated with many and complex mechanisms that can likely include a direct interference of Fe with the signal transduction pathway involved in S metabolism and *vice versa* (Zuchi et al., 2015).

It has been recently demonstrated a role for TOR in the adaptation responses to S deficiency in *Arabidopsis* (Dong et al., 2017; Wu et al., 2019; Fu et al., 2020).

Thus, putting all these in context, we hypothesized that TOR might play a role in the cross talk of signaling pathway occurring during plant adaptation to combined deficiency of Fe and S.

The inhibition of TOR activity observed in shoots of tomato plants exposed to single S deficiency (Fig. 1A) is consistent with that reported in literature. For instance, Dong et al. (2017) demonstrated that TOR activity strongly decreased in *Arabidopsis* shoots, without phosphorylation of S6K protein, under S starvation condition. This response has been ascribed to autophagy in shoot induced by decreased TOR activity, resulting in the remobilization of the internal resources under S deficiency condition (Dong et al., 2017). This could be considered a general response of plants to S stress and probably a protective response against it. However, this hypothesis needs further experimental substantiation in tomato. Furthermore, the reduction in TOR activity due to S starvation has been associated with the reduction of the glucose concentration in *Arabidopsis* (Dong et al., 2017).

This report is in contrast with our results, which have shown that all starvation treatments, including S deficiency, significantly increased shoot glucose concentration (Fig. 2A). On the other hand, our data showed that plants exposed to single Fe deficiency accumulated significantly more glucose in their shoots (Fig. 2A), while showing significantly increased TOR activity (Fig. 1A). Interestingly, combined deficiency (D) resulted in an intermediate pattern of TOR activity, assuming values similar to those of control plants, but significantly different from those of F and S plants (lower and higher, respectively) (Fig. 1A), once again associated to an increased glucose accumulation

(Fig. 2A). Indeed, no positive correlation was found between glucose accumulation and TOR activity in both root and shoot (Fig. 3A, B). Such findings would indicate that no relation can be established between decrease in TOR activity and decrease in glucose production in tomato during S deficiency.

However, sugar accumulation has been observed under several abiotic stresses [Signorelli et al. 2019]. Recently, Rodriguez et al. (2019) provided possible explanations that might link sugar content and TOR activity: i) the TOR kinase is activated above a given threshold of sugars; ii) the hexose-to-Suc ratio alteration or a different subcellular localization of sugars and the TOR complex prevent kinase activation and iii) an active TOR kinase is needed for the plant stress response. Yokawa and Baluška (2016) suggested that TOR could be activated by reactive oxygen species (ROS) as an escape strategy to avoid the stress situation.

Therefore, several cellular metabolic aspect affect TOR activity, and, since our results showed that S starvation resulted in an inhibition of TOR activity (Fig. 1) without a reduction in glucose concentration (Fig. 2), we could suggest that other mechanisms than glucose could be responsible for S-starvation-induced inhibition of TOR activity observed in our tomato plants. However, the induction of TOR in Fe-deficienct leaf seem to be linked to the glucose accumulation, indicating that a Glu-TOR signalling pathway might be involved in Fe deficient leaves, even an opposite way respect S deficiency.

It has been stated that TOR senses sulfur limitation via a decrease in sulfite reduction to sulfide in the plastids through a decline in glucose and sucrose concentrations. Despite, the mechanistic link between sulfite/sulfide and sugar metabolism remains to be uncovered, it has been suggested that plastidic sulfide or sulfite levels may be the signal connecting sulfur assimilation and growth through sugar regulated changes in TOR kinase activity. In our system sulfide content is strongly affected by both Fe and S deficiency, with a strong decrease under low S availability (S and D treatments) (Zuchi et al., 2015), indicating that the differential modulation of TOR activity under F and S treatments might be linked to other processes.

The TOR kinase pathway is a master regulator of eukaryotic carbon metabolism, where its activation generally serves to promote anabolic metabolism and inhibit catabolic metabolism (Dobrenel et al., 2016). Amino acids have been considered one of the primary signals activating the TOR pathway in other eukaryotes (Jewell et al., 2013). Recently, O'Leary et al (2020) demonstrated that amino acids play a role in the regulation of TOR activity in plants. They provided evidence that TOR activity is influences by amino acids levels leading to downstream effect on the

use of respiratory substrates. Particularly, O'Leary and coworkers suggested that accumulation of amino acids as well as TCA cycle organic acids might occur after impairment of TOR signaling pathway in plants.

Single or combined S and Fe deficiency differentially affect amino acid content both in leaves and roots (Fig. 4A, B). Overall, low Fe (F treatment) leads a decrease of amino acids contents, while low S (S and D) leads to an increase of amino acids contents. Therefore, the differential TOR activity in tomato plants, might linked to the different impact of Fe and S deficiency in amino acids metabolism, although, not clear relations can be obtained at this stage. It has been demonstrated that the GCN2 (general control non-derepressible 2) act as amino acid sensors in plants (Dong et al., 2017) and it is involved in the formation of pre-initiation complex for ribosome biogenesis by the phosphorylation of the eukaryotic initiation factor (eIF2α). GCN2 is selectively stimulated by amino acid depletion in plants and other organisms (Luna et al.,2014). Therefore, in our system Fe deficiency seems to stimulate cell division and growth by promoting TOR and likely GCN2. Unlikely, a Glc-TOR signaling pathway is involved in the repression of TOR under S deficiency in tomato.

Concerning TCA cycle intermediated, inhibition of TOR leads to opposite responses in plant and animal cells: organic acid levels increase and decrease in plant and animal cells, respectively, in line with changes in respiration rate (Ramanathan and Schreiber, 2009; Caldana et al., 2013).

Among others, citric acid plays a central role in the plant responses to nutrient starvations. It has been recently suggested that citric acid could be involved in the adaptation mechanisms to the combined deficiency of S and Fe in tomato (Vigani et al., 2018; Coppa et al., 2018). As reported in literature, Fe deficiency commonly increases citrate production (Marschner, 1995). Consistently with this pattern, the roots of tomato plants deprived of Fe exhibited increased levels of citrate accumulation (Fig. 5B), which however resulted unchanged in shoots compared to control plants (Fig. 5A). Interestingly, it has been recently demonstrated that increased citric acid levels correlate with the expression of some Fe deficiency induced genes, such as *SlFRO1* gene (Coppa et al., 2018). More importantly, it was found a significant positive relation between increase of citric acid concentration and TOR activity in both shoots (R^2 = 0,7063) and roots (R^2 = 0,8191) of tomato plants (Fig. 7A, B).

These findings reasonably suggest that accumulation of citrate might be a linked to of the modulation of TOR activity under Fe deficiency, supporting the hypothesis of TOR involvement in the activation of Fe deficiency response in tomato.

Given that citrate levels have been shown to be correlated also with the expression of some S deficiency induced genes in tomato plants (Coppa et al., 2018), it is informative to examine whether S deficiency response could be mediated by the inhibition of TOR activity resulting by decreased citrate accumulation.

In the present study, we found that single and combined S deficiency (S and D condition, respectively) induced an inhibition of TOR activity. More importantly, we found that the decrease of TOR activity was associated to a decrease in citrate accumulation (Fig. 1, 5 and 7). These observations corroborate the hypothesis that changes in citrate accumulation might underlie the S deficiency-induced inhibition of TOR activity.

In conclusion, this work suggests a new mechanism for nutritional stress perception in tomato, supporting a relevant role for citrate, being positively correlated with TOR activity. It has been demonstrated that Fe deficiency elicited an increase of TOR activity in shoots associated to enhanced accumulation of citrate in the same tissue, whereas S deficiency resulted in decreased TOR activity and citrate accumulation. In addition, we found that citrate accumulated in shoots of plants exposed to combined S/Fe deficiency assumed values between those found in F and S plants, a well as TOR activity.

Our data seem to rule out the prediction about the importance of glucose as TOR inducer, at least in tomato, confirming that distinct differences occur between the Arabidopsis model system and tomato (Zuchi et al., 2015). Such discrepancy might be linked to the different threshold level of S deficiency perceived by plants or a different mechanisms operating in tomato respect to Arabidposis.

Furthermore, considering that the regulatory properties of the plant TOR pathway are likely different between tissues and developmental stages (Xiong and Sheen, 2014), it will be also important to spend efforts by performing specific studies addressing the role of TOR in leaf and root under nutrient starvations

References

Balk, J., Pilon, M. (2011). Ancient and essential: the assembly of iron–sulfur clusters in plants. *Trends in plant science*, *16*(4), 218-226.

Barbet, N. C., Schneider, U., Helliwell, S. B., Stansfield, I., Tuite, M. F., Hall, M. N. (1996). TOR controls translation initiation and early G1 progression in yeast. *Molecular biology of the cell*, *7*(1), 25-42.

Butow, R. A., Avadhani, N. G. (2004). Mitochondrial signaling: the retrograde response. *Molecular cell*, *14*(1), 1-15.

Caldana, C., Li, Y., Leisse, A., Zhang, Y., Bartholomaeus, L., Fernie, A. R., Willmitzer, L., Giavalisco, P. (2013). Systemic analysis of inducible target of rapamycin mutants reveal a general metabolic switch controlling growth in Arabidopsis thaliana. *The Plant Journal*, *73*(6), 897-909.

Coppa, E., Celletti, S., Pii, Y., Mimmo, T., Cesco, S., Astolfi, S. (2018). Revisiting Fe/S interplay in tomato: A split-root approach to study the systemic and local responses. *Plant science*, *276*, 134-142.

Dobrenel, T., Caldana, C., Hanson, J., Robaglia, C., Vincentz, M., Veit, B., Meyer, C. (2016). TOR signaling and nutrient sensing. *Annual review of plant biology*, *67*, 261-285.

Dobrenel, T., Caldana, C., Hanson, J., Robaglia, C., Vincentz, M., Veit, B., Meyer, C. (2016). TOR signaling and nutrient sensing. *Annual review of plant biology*, *67*, 261-285.

Dong, Y., Silbermann, M., Speiser, A., Forieri, I., Linster, E., Poschet, G., Allboje Samami, A., Wanatabe, M., Sticht, C., Teleman, A. A. , Deragon J. M., Saito K., Hell R., Wirtz M. (2017). Sulfur availability regulates plant growth via glucose-TOR signaling. *Nat. Commun*. 8, 1174.

Douchkov, D., Herbik, A., Koch, G., Mock, H. P., Melzer, M., Stephan, U. W., Bäumlein, H. (2002). Nicotianamine synthase: gene isolation, gene transfer and application for the manipulation of plant iron assimilation. *Plant and soil*, *241*(1), 115-119.

Finkemeier, I., König, A. C., Heard, W., Nunes-Nesi, A., Pham, P. A., Leister, D., Fernie, A. R & Sweetlove, L. J. (2013). Transcriptomic analysis of the role of carboxylic acids in metabolite signaling in Arabidopsis leaves. *Plant physiology*, *162*(1), 239-253.

Forieri I, Wirtz M, Hell R. 2013. Towards new perspectives on the interaction of iron and sulfur metabolism in plants . Frontiers in Plant Science

Fu, L., Wang, P., Xiong, Y. (2020). Target of Rapamycin signaling in plant stress responses. *Plant Physiology*, *182*(4), 1613-1623.

García, M. J., Lucena, C., Romera, F. J., Alcántara, E., Pérez-Vicente, R. (2010). Ethylene and nitric oxide involvement in the up-regulation of key genes related to iron acquisition and homeostasis in Arabidopsis. *Journal of Experimental Botany*, *61*(14), 3885-3899.

Glucose-TOR signalling reprograms the transcriptome and activates meristems. Nature 496, 181–186 (2013).

Hall, M. N. (2008, December). mTOR—what does it do?. In *Transplantation proceedings* (Vol. 40, No. 10, pp. S5-S8). Elsevier.

Hesse, H., Hoefgen, R. (2003). Molecular aspects of methionine biosynthesis. *Trends in plant science*, *8*(6), 259-262.

Jewell, J. L., Russell, R. C., Guan, K. L. (2013). Amino acid signalling upstream of mTOR. *Nature reviews Molecular cell biology*, *14*(3), 133-139.

Kobayashi, T., & Nishizawa, N. K. (2012). Iron uptake, translocation, and regulation in higher plants. *Annual review of plant biology*, *63*, 131-152.

Loewith, R., & Hall, M. N. (2011). Target of rapamycin (TOR) in nutrient signaling and growth control. *Genetics*, *189*(4), 1177-1201.

Lucena, C., Waters, B. M., Romera, F. J., García, M. J., Morales, M., Alcántara, E., & Pérez-Vicente, R. (2006). Ethylene could influence ferric reductase, iron transporter, and H+-ATPase gene expression by affecting FER (or FER-like) gene activity. *Journal of Experimental Botany*, *57*(15), 4145-4154.

Luna, E., Van Hulten, M., Zhang, Y., Berkowitz, O., López, A., Pétriacq, P., Sellwood, M. A., Chen, B., Burrel, M., van de Meene, A., Pieterse, C. M. J., Flors, V., Ton, J. (2014). Plant perception of β-aminobutyric acid is mediated by an aspartyl-tRNA synthetase. *Nature chemical biology*, *10*(6), 450.

Marschner H. (1995) Mineral nutrition of higher plants. 2nd edn. AcademicPress, San Diego.

McGrath SP, Zhao FJ (1995) A risk assessment of sulphur defciency in cereals using soil and atmospheric deposition data. Soil Use Manag 11:110–114

McGrath SP, Zhao FJ, Whiters PJA (1996) Development of sulphur defciency in crops and its treatment. In: Proceedings of the fertilisers society, No. 379. The Fertilisers Society, Peterborough, UK.

O'Leary, B. M., Oh, G. G. K., Lee, C. P., Millar, A. H. (2020). Metabolite regulatory interactions control plant respiratory metabolism via Target of Rapamycin (TOR) kinase activation. *The Plant Cell*, *32*(3), 666-682.

Ostaszewska, M., Juszczuk, I. M., Kołodziejek, I., Rychter, A. M. (2014). Long-term sulphur starvation of Arabidopsis thaliana modifies mitochondrial ultrastructure and activity and changes tissue energy and redox status. *Journal of plant physiology*, *171*(7), 549-558.

Paolacci, A. R., Celletti, S., Catarcione, G., Hawkesford, M. J., Astolfi, S., & Ciaffi, M. (2014). Iron deprivation results in a rapid but not sustained increase of the expression of genes involved in iron metabolism and sulfate uptake in tomato (Solanum lycopersicum L.) seedlings. *Journal of integrative plant biology*, *56*(1), 88-100.

Pu, Y., Luo, X., & Bassham, D. C. (2017). TOR-dependent and-independent pathways regulate autophagy in Arabidopsis thaliana. *Frontiers in plant science*, *8*, 1204.

Ramanathan, A., Schreiber, S. L. (2009). Direct control of mitochondrial function by mTOR. *Proceedings of the National Academy of Sciences*, *106*(52), 22229-22232.

Rodriguez, M., Parola, R., Andreola, S., Pereyra, C., Martínez-Noël, G. (2019). TOR and SnRK1 signaling pathways in plant response to abiotic stresses: do they always act according to the" yin-yang" model? *Plant Science*, 110220.

Romera, F. J., Alcantara, E., De La Guardia, M. D. (1999). Ethylene production by Fe-deficient roots and its involvement in the regulation of Fe deficiency stress responses by strategy I plants. *Annals of Botany*, *83*(1), 51-55.

Rudolph, A., Becker, R., Scholz, G., Procházka, Ž., Toman, J., Macek, T., Herout, V. (1985). The occurrence of the amino acid nicotianamine in plants and microorganisms. A reinvestigation. *Biochemie und Physiologie der Pflanzen*, *180*(8), 557-563.

Schwarzländer, M., König, A. C., Sweetlove, L. J., & Finkemeier, I. (2012). The impact of impaired mitochondrial function on retrograde signalling: a meta-analysis of transcriptomic responses. *Journal of experimental botany*, *63*(4), 1735-1750.

Signorelli, S., Tarkowski, Ł. P., Van den Ende, W., Bassham, D. C. (2019). Linking autophagy to abiotic and biotic stress responses. *Trends in plant science*.

Vigani G, Pii Y, Celletti S, Maver M, Mimmo T, Cesco S, Astolfi S (2018) Mitochondria dysfunctions under Fe and S deficiency: Is citric acid involved in the regulation of adaptive responses? Plant Physiol Biochem 126:86-96.

Vigani, G., & Briat, J. F. (2016). Impairment of respiratory chain under nutrient deficiency in plants: does it play a role in the regulation of iron and sulfur responsive genes?. *Frontiers in plant science*, *6*, 1185.

Vigani, G., Maffi, D., Zocchi, G. (2009). Iron availability affects the function of mitochondria in cucumber roots. *New Phytologist*, *182*(1), 127-136.

Wu, Y., Shi, L., Li, L., Fu, L., Liu, Y., Xiong, Y., & Sheen, J. (2019). Integration of nutrient, energy, light, and hormone signalling via TOR in plants. *Journal of experimental botany*, *70*(8), 2227-2238.

Wullschleger, S., Loewith, R., & Hall, M. N. (2006). TOR signaling in growth and metabolism. *Cell*, *124*(3), 471-484.

Xiong, Y., Sheen, J. (2014). The role of target of rapamycin signaling networks in plant growth and metabolism. *Plant physiology*, *164*(2), 499-512.

Yan, G., Lai, Y., & Jiang, Y. (2012). The TOR complex 1 is a direct target of Rho1 GTPase. *Molecular cell*, *45*(6), 743-753.

Yokawa, K., Baluška, F. (2016). The TOR complex: an emergency switch for root behavior. *Plant and Cell Physiology*, *57*(1), 14-18.

Zamboni, A., Celletti, S., Zenoni, S., Astolfi, S.,Varanini, Z. (2017). Root physiological and transcriptional response to single and combined S and Fe deficiency in durum wheat. *Environmental and Experimental Botany*, *143*, 172-184..

Zuchi, S., Cesco, S., Varanini, Z., Pinton, R., Astolfi, S. (2009). Sulphur deprivation limits Fe deficiency responses in tomato plants. *Planta 230*, 85–94.

Zuchi, S., Watanabe, M., Hubberten, H.M., Bromke, M., Osorio, S., Fernie, A.R., Celletti, S., Paolacci, A.R., Catarcione, G., Ciaffi, M., Hoefgen, R., Astolfi, S. (2015). The interplay between sulfur and iron nutrition in tomato *Plant Physiology*, *169*(4), 2624-2639.

Chapter 5

Evaluating the potential use of Cu-contaminated soils for giant reed (*Arundo donax*, L.) cultivation as a biomass crop

Published in Environmental Science and Pollution Research (2020) 27, 8662–8672 as "*Evaluating the potential use of Cu-contaminated soils for giant reed (Arundo donax, L.) cultivation as a biomass crop*", E. Coppa, S. Astolfi, C. Beni, M. Carnevale, D. Colarossi, F. Gallucci, E. Santangelo.

A**bstract**

Over the past decades, the important topic of environmental sustainability, impact, and security of the fossil fuel supply has stimulated interest in using lignocellulosic feedstocks as biofuel to partially cover energy demands. Among energy no-food crops, giant reed (*Arundo donax*, L.), a perennial rhizomatous grass has been identified as a leading candidate crop for lignocellulosic feedstock, due to its positive energy balance, and low ecological/agro-management demands. The aim of the present study was to characterize the physiological response of *Arundo donax* (L.) to artificial soil contamination with three different Cu levels (200, 400, and 800 ppm), and to assess the relationship between plant Cu tolerance and S assimilation rate. The present study not only confirms the ability of *Arundo donax* L. to cope with Cu stress and therefore to grow in marginal, degraded lands abandoned by mainstream agricultural, but also shows that plant performance might be likely ascribed to a modulation of sulfate metabolism resulting in increased thiols content.

Keywords: *Arundo donax* L.. Bioenergy. Copper. Energy crops. Sulfur.

4.1 Introduction

Well-established and widespread agricultural practices, such as the excessive use of fertilizers, the agronomic use of farm effluents, urban sewage sludge, and the uncontrolled distribution of pesticides have worsened the quality of soils. The pollution caused by the presence of heavy metals in soil poses a threat to agricultural productivity, but also to food security and human health (Toth et al. 2016a). The presence of contaminated areas embraces most European regions, differently affected by the specific contaminant and the level of contamination (Lado et al. 2008; Toth et al. 2016a, b).

Inorganic copper (Cu) is used as a broad-spectrum fungicide and bactericide as it combines efficiency and low cost. The widespread use of copper-based plant protection products in vineyards, orchards, and also organic farming has led to a progressive and worrisome accumulation of this metal in the upper layer (0–20 cm) of the soils of the Mediterranean countries (France, Italy, Portugal and Spain). Copper has a low mobility in soil and relatively small variations in the total content of the soil profiles. In Italy, the total Cu concentration of the soil was reported between 2 and 375 mg kg^{-1} (Toselli et al. 2009; La Torre et al. 2018), but Cicchella et al. (2015) observed values above 800 mg kg^{-1} in the Vesuvian area.

Currently, EC legislation 473/2002 limits the annual dose of Cu applied to 6 kg Cu ha^{-1}, which corresponds to an annual accumulation of about 5 mg of Cu per kilogram of soil in the first 10 cm (Ruyters et al. 2013). For copper, a regulatory review process is underway as the substance has been included among the candidates for substitution due to the long persistence in the soil and toxicity on aquatic and telluric organisms (Armentano 2017).

Cu is an essential micronutrient for plants, playing a very important role in their growth and development (Brunetto et al. 2016). It acts as an acceptor of electrons in numerous enzymatic systems, some of which are involved in antioxidative processes. Cu, as a component of plastocyanin, involved in electron transport, both at mitochondrial level and in chloroplasts (Wintz and Vulpe 2002). However, at high concentrations, Cu negatively influences plant growth and development (La Torre et al. 2018). Its toxic effects affect different biochemical and physiological processes producing oxidative stress, leading to profound alterations in plant metabolism associated with growth reductions, nutrient uptake, chlorophyll content, and leaf expansion (Miotto et al. 2014; Shiyab 2018; Marzilli et al. 2018). However, the copper concentration causing a damage to plants cannot be easily established because it depends on the bioavailability of the element (Ruyters et al. 2013; Brunetto et al. 2016; La Torre et al. 2018).

The use of energy crops for the removal of heavy metals in contaminated sites (phytoremediation) has been proposed as a sustainable technology able to couple the environmental concerns with the sustain of income farmer (Marchiol and Fellet 2011; Nsanganwimana et al. 2014; Fernando et al. 2016). To be suitable for phytoremediation, beside the ability to detoxify the pollutant the plant species must possess some other characteristics associated to biomass production (high amount in short time), its handling (adoption of known farming practices, ease of biomass collection, and clear destination), and the possibility to produce a feedstock for no-food uses (Marchiol and Fellet

2011; Fernando et al. 2016; Tripathi et al. 2016). Among the perennial crops, the giant reed (*Arundo donax*, L.) is deemed to match the ideotype requested to assure a cost-effective removal of heavy metals in soil (Nsanganwimana et al. 2014; Fernando et al. 2016). In the last 10 years, the studies appeared about its ability in phytoremediation have concerns the growth responses, the accumulation capacity, and the uptake of nutrients when grown in the presence of different elements such as As, Cd, Cr, Cu, Ni, Pb, Se, and Zn (Papazoglou et al. 2007; Mirza et al. 2011; Kausar et al. 2012; Barbosa et al. 2015; Elhawat et al. 2015; Domokos-Szabolcsy et al. 2018; Shaheen et al. 2018). A study on Arundo tolerance to copper has been carried out by Elhawat et al. (2014, 2015) using plantlets regenerated by somaticembryos of two genotypes grown on increasing amount of Cu (0–26 mg L^{-1}) in the medium. The plantlets showed an appreciable level of tolerance growing on Cu-contaminated soil up to 10 mg L−1 without significant foliar symptoms. Moreover, high levels of bioaccumulation and translocation factor revealed the great potential of the species for Cu removal.

The aim of the present work was to evaluate the adaptive capacity of *Arundo* in soils artificially contaminated with different concentrations of Cu (200, 400, and 800 ppm), higher than the thresholds set in the Italian legislation for residential (120 mg kg^{-1}) and industrial (600 mg kg^{-1}) areas. The work linked the effect on plant growth with specific physiological response, associated with the enzymatic machinery activated during the stress.

4.2 Materials and methods

4.2.1 Plant growth

The *Arundo* cuttings were prepared from a 6-year-old plantation grown in the experimental farm of CREA-IT in Monterotondo (42° 03′ N 12° 37′ E) accordingly to Castelli and Ceotto (2016) with minor modifications. Briefly, the auxiliary stems growing on culms of 2 years were immerged in a plastic tank of 0.46 m^3 (0.80 × 0.50 × 1.16 m) filled up with two-thirds of water (about 300 L) and containing a structure of 120 plastic tubes (80 cm high). One cutting per hole was inserted and left immersed up to 20–25 cm. The tank has been placed inside a not heated protected structure. After 3 months, the cuttings had abundantly rooted.

In May, 28 rooted plants were transplanted in plastic wells of 0.125 m^3 (0.5 × 0.5 × 0.5 m) containing 40 kg of soil. The soil was a clay-loam soil (USDA classification), with subalkaline pH and low organic matter content (Table 1). The substrate had a medium-high content of nutrients and a good CeC. From July to October, the plants were watered two times a week with an amount

required to fill soil up to 15% of field capacity in the 0–40-cmsoil depth, where most of the roots are expected to grow in *Arundo*. During the winter, the irrigation was suspended, relying on the natural precipitations.

Table 1 Chemical and physical characterization of the soil used as substrate for the growth of the plants

Parameter	**U.M.**	**Valore**
Sand	%	24.4
Silt	%	47.6
Clay	%	28.0
pH		7.6
Organic matter	%	1.79
Nitrogen	%	0.12
P Olsen	mg kg^{-1}	25.20
P_2O_5	mg kg^{-1}	58.40
K_2O	mg kg^{-1}	598.14
Cation-exchange capacity (CEC)	meq $100g^{-1}$	29.51
Field capacity	wt%	
Ca	meq $100g^{-1}$	24.33
Mg	meq $100g^{-1}$	3.21
K	meq $100g^{-1}$	1.27
Na	meq $100g^{-1}$	0.70

4.2.2 Treatment with Cu

In mid-July, the soil was contaminated with copper. The experimental design was a completely randomized design. Treatments included four concentrations of Cu (0, 200, 400, and 800 ppm of Cu ion) with 6 replicates (single plant) for each treatment. The remaining four plastic wells were left without plants but filled with soil and treated with the scheduled doses of copper.

The hardening of rooted cuttings lasted for 1 month. Then, they were contaminated using a commercial product (Manica S.p.a.) containing 99% of $CuSO_4$ $5H_2O$. The doses of the product

were calculated considering the concentration of copper ion presents into the salt, dissolved inwater, and applied to the plants.

On each plant, the following traits were measured at 30 (August), 90 (October), and 120 (January) days after the contamination (DAC): height of the main stem, number of stems, chlorophyll content. The latter was measured using a SPAD- 502 Plus (Konica Minolta, Japan) on the penultimate leaf of each plant. On each leaf were taken three readings.

Leaf samples collected after 6 months from contamination (January) at the end of growth period were used for ICP-MS analysis, and biochemical and enzymatic assays.

4.2.3 ICP-MS analysis

The Cu content of macro and micro element was analyzed at the laboratory LAS-ER-B of CREA-IT (Monterotondo). Leaf samples were dried at 105 °C for 24 h and homogenized to have a uniform distribution of the elements. At the end, about 0.5 g of each sample was weighed and placed into amicrowave Milestone START D with the addition of 6 ± 0.1 ml of HNO_3 65% and 3 ± 0.1 ml of H_2O_2 30%. The digestion was accomplished at a 180 °C, 650Wfor 42 min. At the end, the samples were filtered and diluted with deionized water. Every sample was analyzed in triplicate and with a blank. The content of microelements was measured with ICP-MS (Agilent 7700).

4.2.4 Determination of malondialdehyde content

The level of lipid peroxidation was expressed as determination of malondialdehyde (MDA) content and was determined as TBA reactive metabolites according to (Astolfi et al. 2005).

Briefly, fresh apical leaf tissues (0.2 g) were homogenized in 10 ml of 0.25% TBA made in 10% TCA. Extract was heated at 95 °C for 30 min and then quickly cooled on ice. After centrifugation at 10,000×g for 10 min, the absorbance of the supernatant was measured at 532 nm. Correction of nonspecific turbidity was made by subtracting the absorbance value taken at 600 nm. The level of lipid peroxidation was expressed as μmol g^{-1} fresh weight by using an extinction coefficient of 155 mM cm^{-1}.

4.2.5 Enzyme extraction and assay

Apical leaves (ca. 1 g FW) of plants grown in control condition or treated with four concentrations of Cu (0, 200, 400, and 800 ppm of Cu ion) were powdered in a pre-chilled mortar under liquid nitrogen and then homogenized in 3 mL of a cold extraction buffer (pH 7.4), prepared with 50 mM

HEPES-KOH, 5 mM $MgCl_2$, 1 mM EDTA, 10% (v/v) glycerol, 0.1% (v/v) Triton X-100, 5 mM DTT, 1 mM PMSF, and 1% (w/v) PVPP. The homogenate was filtered and then centrifuged at 4 °C for 5 min at 1000g. The supernatant was desalted at 4 °C on a Sephadex G-25 column (PD-10, Pharmacia, Uppsala, Sweden) pre-equilibrated with the extraction buffer without Triton X-100. The desalted extract was centrifuged at 4 °C for 5 min at 30,000g, and the resulting supernatant was frozen in liquid nitrogen and stored by freezing (− 80 °C) until use for in vitro enzyme assays. The extractable ATPS (EC 2.7.7.4) activity was determined by the bioluminescence technique, as described in Celletti et al. (2016). Briefly, the ATP production during the enzyme reaction is coupled to the light producing reaction catalyzed by firefly luciferase (E.C. 1.13.12.7). The reactionmixture contained in a total volume of 0.25 ml: 16 mM Tris-Acetate buffer pH 7.75, 8 mM APS, 68 mM $Na_4P_2O_7$, 40 ml of firefly luciferase (ATP Monitoring Reagent, ThermoLabSystems), and 5 ml of sample. Light emission was measured with LKB 1250 luminometer.

OASTL (EC 4.2.99.8) activity was assayed by detecting cysteine production (Celletti et al. 2016). Reaction medium (pH 7.5) contained 50 mM Tris-HCl, 1 mM DTT, 10 mM *O*-acetyl-Ser, and 2.5 mM Na_2S.

Quantitative protein determination of the root extracts was estimated by the protein-binding Coomassie brilliant blue G-250 dye method, using bovine serum albumin (BSA) as standard (Bradford 1976).

4.2.6 Statistics

For the morphological traits, the differences among treatments were analyzed by one-way ANOVA of the PAST software version 2.15 (https://folk.uio.no/ohammer/past/). The analyses were carried out after checking the normality. Different means were separated by Tuckey's HSD test. For biochemical measurements, each reported value represents the mean ± SD of measurements carried out in triplicate and obtained from four independent experiments. All the data were statistically analyzed using ANOVA with the GraphPad InStat Program (version 3.06). Significant differences were established by posthoc comparisons (Tukey test) at $P < 0.01$. The Past 3.25 statistical software package was used for principal component analysis (PCA).

4.3 Results

4.3.1 Plant growth as a function of Cu application

Increasing the Cu concentration in soil from 200 to 800 ppm did not significantly affect the plant growth, in terms of both height of the main stem and number of shoots during the first 6 months (Table 2). A significant reduction in chlorophyll content was observed just 30 days after the treatment with the highest Cu concentration (Table 2). In particular, plants grown with 800 ppm Cu showed 29% less chlorophyll level than the control (Table 2). However, in the following months, the leaves of the plants grown on 800 ppm recovered gradually and the chlorophyll content increased from 71 to 92% of the control (Table 2).

4.3.2 Cu, Fe, and Zn concentration as a function of Cu application

The increase in Cu concentration supplied to the soil was followed by a significant increase in Cu accumulation in *Arundo* leaves, which can be described by the following linear function (Fig. 1):

$$y = 0{,}1458x + 1{,}4463 \ (R2 = 0{,}9833)$$

In particular, the leaves of plants treated with 200, 400, and 800 ppm contained 5-fold, 10-fold, and 22-fold higher Cu, respectively, than the control (Figs. 1 and 2).

In the present study, we found that exposure of *Arundo* plants to increasing concentrations of Cu did not significantly affect Zn content in leaves, but the content of Fe in the same plants was enhanced when challenged with both 400 and 800 ppm (twofold and 30% higher than the control, respectively (Fig. 2). On the other hand, the lowest Cu concentration treatment level (200 ppm) did not cause a significant change in leaf Fe content (Fig. 2).

4.3.3 Lipid peroxidation as a function of Cu application

Plants suffering from Cu toxicity often exhibit symptoms associated with oxidative stress and membrane peroxidation as evidenced by enhanced accumulation of malondialdehyde (MDA), a highly toxic by-product generated by lipid peroxidation and commonly used as biomarkers for the assessment of membrane damage (Pätsikkä et al. 2002;Miotto et al. 2014;Adrees et al. 2015). In the present study, leaf MDA content was not significantly affected by the treatment with the lowest Cu concentration (200 ppm). By contrast, MDA levels in leaves of plants exposed to the higher Cu

concentration showed a significant increase relative to control leaves (28 and 51%, respectively) (Fig. 3).

4.3.4 Thiol pools as a function of Cu application

Changes in thiols accumulation in plant tissues can be explained by their role in the protection against oxidative damage (Foyer and Noctor 2011; Brunetto et al. 2016).

In plants that had been exposed to 200 ppm Cu, a 32% depletion in leaf thiols concentration was observed (Fig. 4). On the other hand, when grown with 400 and 800 ppm Cu, plants exhibited a 46% and 54% increase in thiols accumulation, respectively, relative to the control (Fig. 4).

4.3.5 Protein concentration as a function of Cu application

In leaves of exposed plants, the concentration of protein was slightly higher than that of control plants, with increases ranging from 7 to 10% (Fig. 5).

4.3.6 Sulfur assimilation rate as a function of Cu application

Changes in thiols accumulation in response to Cu exposure would be expected to modulate sulfate assimilation through the adjustment of the activity of enzymes involved in the S metabolism. Therefore, changes of ATPS and OASTL activity, the first and the last enzyme of the S assimilatory pathway, respectively, were evaluated in leaves of *Arundo* plants in response to increasing levels of Cu application (Figs. 6 and 7).

Results showed that Cu application stimulated the foliar ATPS activity and the metal effects on ATPS activity were greater when plants were exposed to the lowest and the highest Cu concentration (+ 163 and + 170% with respect to the control) (Fig. 6). Application of 400 ppm Cu also induced ATPS activity, but to a lesser extent (+ 65%with respect to the control) (Fig. 6).

On the other hand, OASTL activity in leaf of treated plants was similar to that of control plants when Cu was added at 200 and 400 ppm, whereas the application of the highest concentration (800 ppm) resulted in a significant increase of the enzyme activity (+ 46% with respect to the control) (Fig. 7).

4.3.7 Principal component analysis

Following detailed point-by-point comparison of the different treatments, a more detailed statistical comparison of the combined data sets (herein, micronutrients, MDA levels, thiol compounds, and enzyme activities) was performed to verify which variables contributed to the separation of treatment. The principal component analysis (PCA) was used to achieve this goal, and all treatments were clearly separated (Fig. 7).

The PCA carried out on the dataset previously described, extracted three components having an eigenvalue higher than 1 (4.09, 2.04, and 1.05, respectively) and describing 79.74% of the total variance. The first two components used to build both the scatter and loading plots (Fig. 8a–c respectively) accounted for 68.11% of the total variance. The first principal component (PC1) explained 45.45% of the variation separating the treatments on the basis of the Cu treatment level (Fig. 8a). The respective PCA loading displays that the main variables driving this separation are Cu, MDA level, thiols content, and OASTL activity (Fig. 8b).

The second principal component (PC2) explained 22.66% of the total variation, with a high positive loading for ATPS activity and a negative loading for Fe (Fig. 8c). Along PC1, treatments are separated based on Cu treatment level concentration, with the highest treatments, such as 800 and 400 ppm, clustering on the upper and lower right side of the plot, respectively, and the lowest treatments, such as 0 (control) and 200 ppm, clustering in the upper and lower left quadrant, respectively (Fig. 8a).

The PC2 differentiated treatments with high and low Fe content and ATPS activity (Fig. 8a). Treatments showing higher ATPS activity and lower Fe content (200 and 800 ppm) clustered in the upper part of the PCA (left and right quadrant, respectively), while treatments showing lower ATPS activity and higher Fe content (control and 400 ppm), clustered in the lower part (left and right quadrant, respectively) (Fig. 8a).

Tab. 2 Main morphological traits of the plants after 30, 90 and 180 days after the treatment. When present, different letters represent significant differences between the treatments (P<0.01) within each column

Treatment (ppm)	Days after contamination (n)		
	30	**90**	**180**
Height of the main stem (cm)			
Control	73.3	101.7	93.0
200	76.5	102.5	97.2
400	76.3	105.7	98.5
800	76.0	111.2	105.3
Number of stems (n)			
Control	9.7	9.7	9.2
200	8.7	9.3	8.8
400	8.2	8.2	7.5
800	7.8	8.5	7.5
Chorophyll content (SPAD units)[1]			
Control	39.7 a	32.4	33.4
200	40.4 a	31.4	27.1
400	38.2 a	31.7	30.0
800	28.4 b	30.0	31.0

[1]Measured at 30, 90 and 150 days from contamination

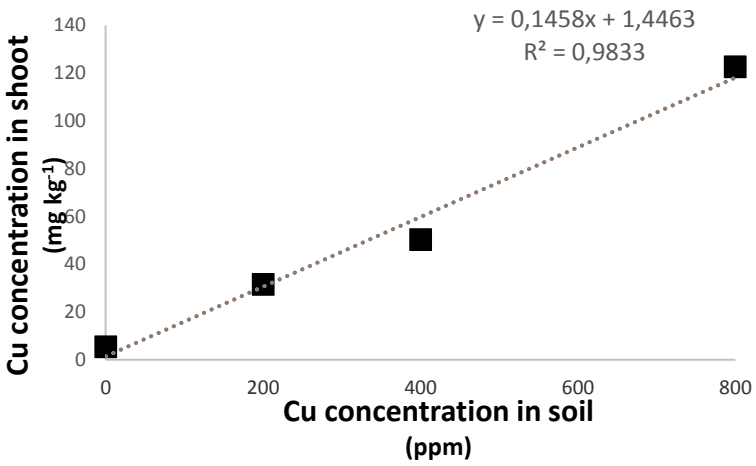

Fig. 1 Copper concentration measured in *Arundo* shoots according to the concentration of Cu in the external medium. Shoot content of Cu can be modelled by the function: [Cu] in shoots (mg kg^{-1} DW) = 0.1458 [ppm Cu] in soil + 1.4463 *(R^2=0.9833)*

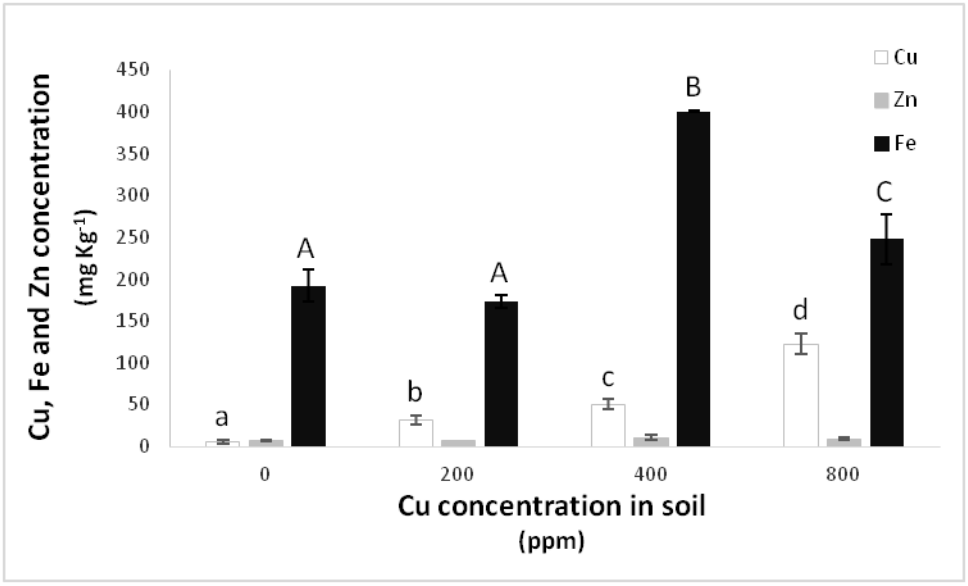

Fig. 2 Cu, Fe and Zn concentration in leaves of Arundo plants grown being exposed to different Cu levels (from 0 to 800 ppm). Data are means ± SD of three independent replications run in triplicate. The statistical significance was tested by means of ANOVA with Tukey post-test. Different letters indicate statistically different values ($P<0.01$).

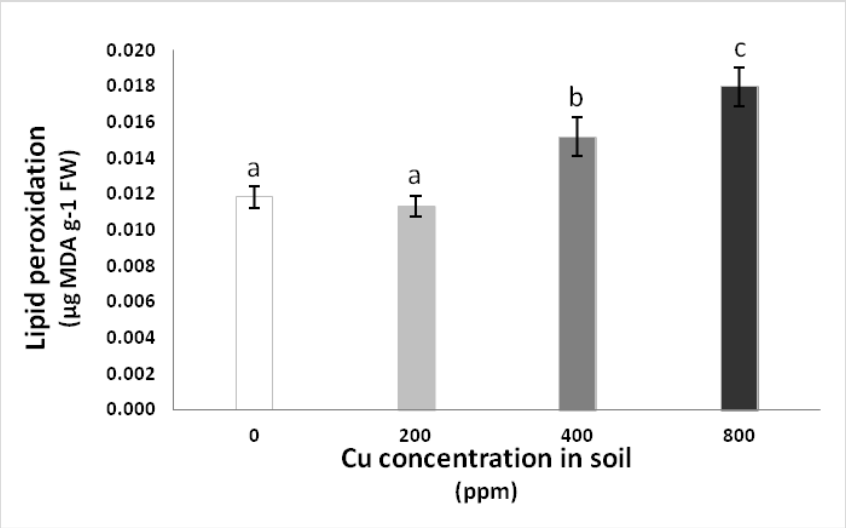

Fig. 3 MDA levels in shoots of *Arundo donax* plants. Treatments and statistics as in Fig. 2.

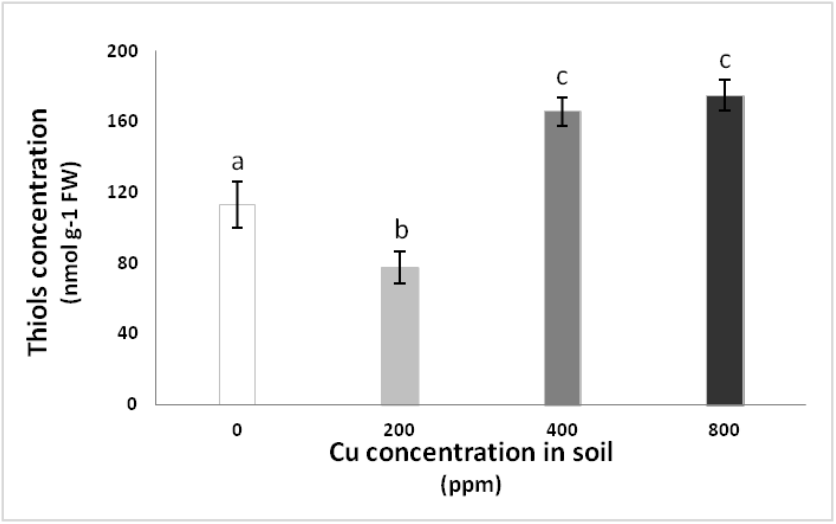

Fig. 4 Thiols concentration in shoots of *Arundo donax* plants. Treatments and statistics as in Fig. 2.

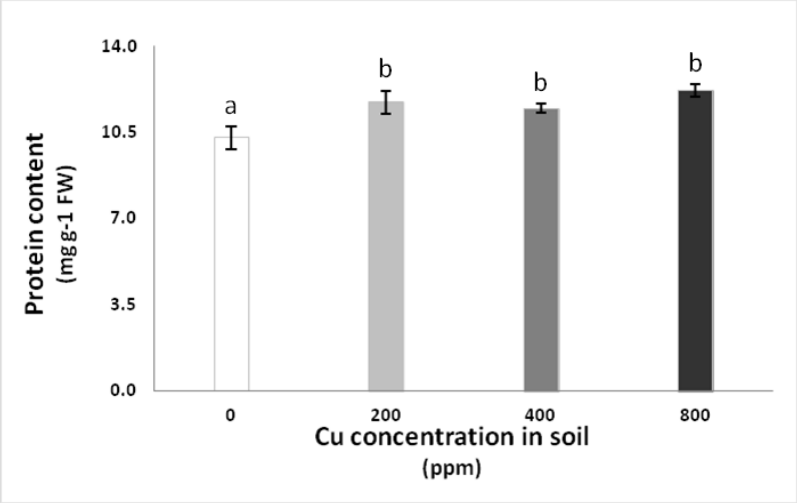

Fig. 5 Protein content in shoots of Arundo donax plants. Treatments and statistics as in Fig. 2.

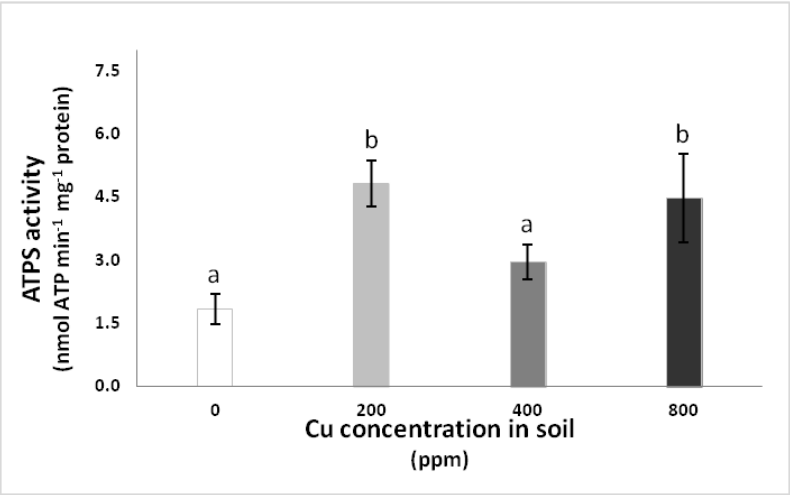

Fig. 6 ATPS activity in shoots of *Arundo donax* plants. Treatments and statistics as in Fig. 2.

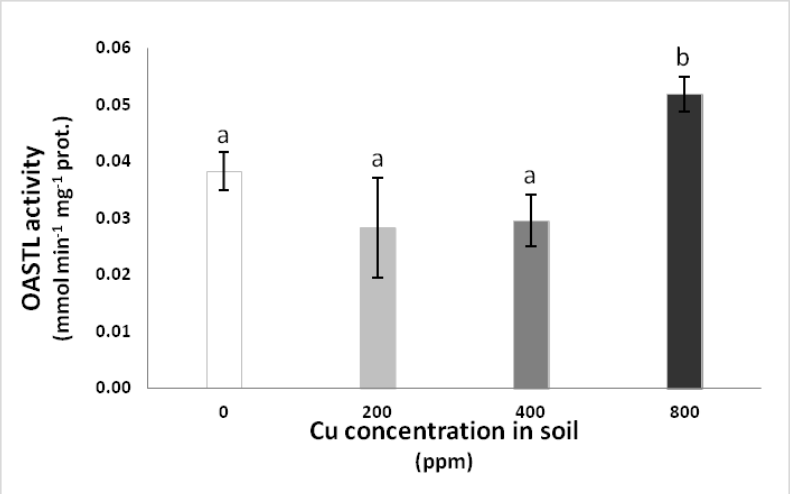

Fig. 7 OASTL activity in shoots of *Arundo donax* plants. Treatments and statistics as in Fig. 2.

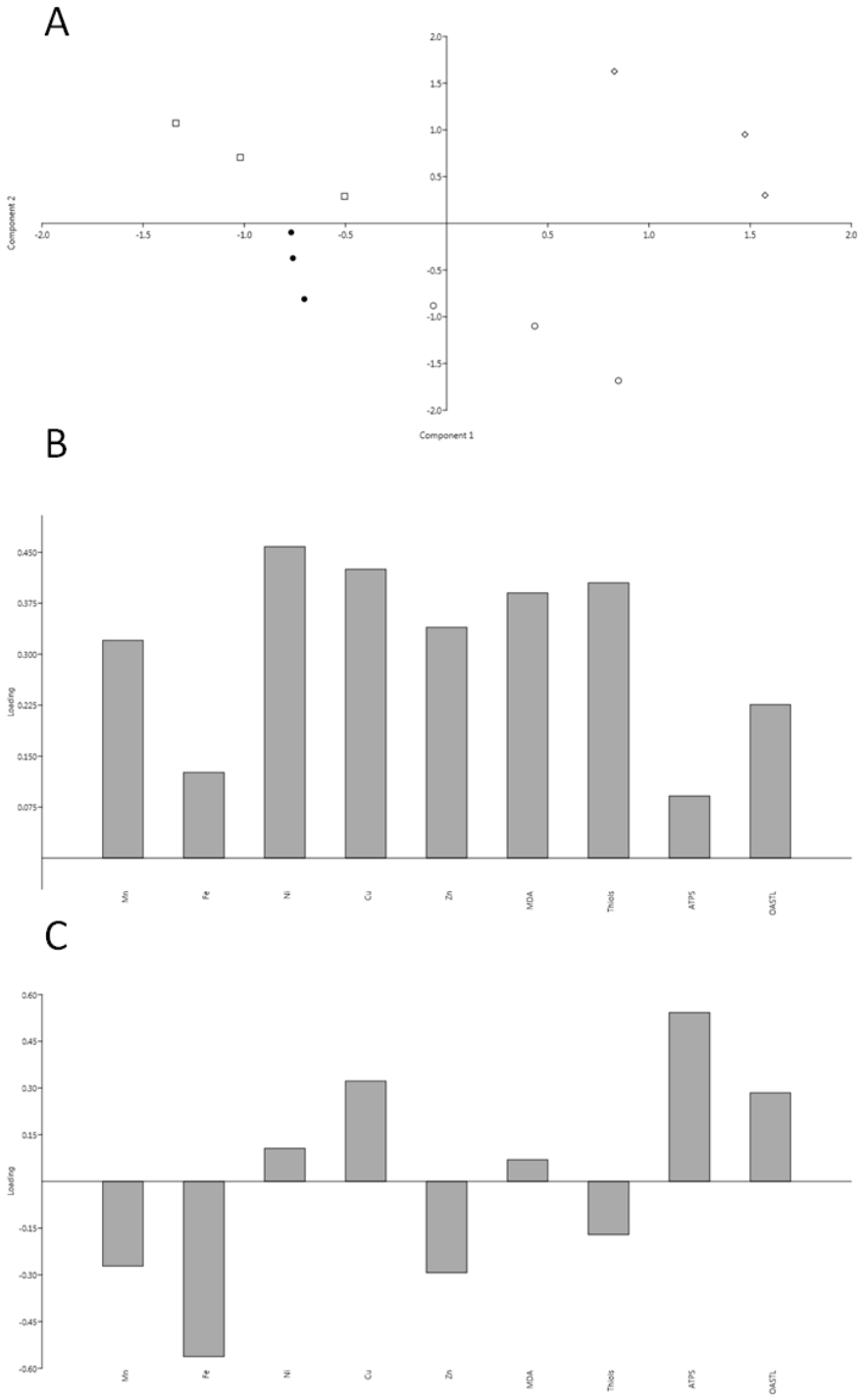

Fig. 8 (A) Scatterplot representing the four clusters as a function of Cu application levels (●= control, □=200 ppm, o=400 ppm, ◊=800 ppm). The analysis was performed as defined in the Materials and Methods. Growth conditions as in Fig. 2. Principle Component 1 (PC1) contributed with 45.45% and Principle Component 2 (PC2) with 22.66% to the separation. (B) Major PC1 loadings were Cu content, MDA level, thiols content and OASTL activity. (C) Major PC2 loadings were ATPS activity (positive loading) and Fe (negative loading).

5.4 Discussion

Arundo donax (L.) possesses some key attributes required to energy crops (Ceotto and Di Candilo 2010). It has a perennial habit, a fast growth, a high biomass production, a low susceptibility to pests and diseases, and it is adaptable to a wide range of ecological conditions that range from the most fertile soils to the saline up to the marginal soils. Such characteristics make *Arundo* a valid candidate for phytoremediation systems.

This study describes a short-term Cu treatment to investigate the phytoextraction potential of *Arundo*. Plants were exposed to Cu concentrations from 200 to 800 ppm. Such values comprised and overcome the limits set by the Italian law (DL 152/06) for Cu contamination for both residential (120 mg kg^{-1}) and industrial (600 mg kg^{-1}) soils. Furthermore, the Cu treatments included the wide range of concentrations (from 200 to above 800 mg kg^{-1}) observed in the Italian soils with particular reference to vineyard or volcanic soils (Deluisa et al. 2007; Ruyters et al. 2013; Cicchella et al. 2015; La Torre et al. 2018).

Plants exposed to heavy metal stress often exhibit symptoms associated with growth reduction of both root and shoot (Wang and Zhou 2005). In the present study, we found that exposure of *Arundo* plants to Cu concentrations from 200 to 800 ppm did not limit stem development (Tab. 2). Our finding is consistent with that reported in the literature. For instance, Papazoglou et al. (2007) demonstrated that in *Arundo*, the height of the plants and the average number of branches were not significantly affected by high dosages of cadmium and nickel.

This observation can be explained by the fact that different factors can affect the degree of Cu toxicity, including plant species, metal concentration, exposure time, and soil properties (Yruela 2009). A reduced toxicity may result fromthe reduction of Cu uptake, its partitioning in less-sensitive tissues, systems of chelation or binding to cell walls (Adrees et al. 2015), and the activation of an efficient antioxidant machinery.

Chlorophyll concentration rapidly dropped to 71% of control during the first month when Cu was applied at highest concentration (800 ppm) but increased again to control values in the following 2 months as indicated by chlorophyll measurements reported in Table 2. Previous studies have shown that young grapevine plantlets exposed to Cu concentration ranging from 25 to 165 mg kg^{-1} showed a decrease of leaf chlorophyll a and b by 32 and 44%, respectively, between the lowest and the highest Cu dose (Ambrosini et al. 2018). However, the study lasted 53 days, and no indications are available about a recovery of chlorophyll content. In our study, the dramatic recovery of chlorophyll concentration of *Arundo* indicates a high capability to tolerate high Cu levels.

Furthermore, analysis of protein data evidenced that the protein content in leaves was increased by increasing Cu concentration in soil (Fig. 5). This unexpected result might be explained considering that the oxidative stress imposed to the plants upon copper exposure requires the stimulation of the synthesis of proteins having a protective role (antioxidant enzymes).

Leaf Cu accumulation by *Arundo* plants appeared to be dose dependent, with a positive relationship clearly existing between the Cu concentrations in the soil solution and in plant tissues (Fig. 1).

On the basis of metal uptake rate in relation to the substrate concentrations, higher plants are classified into three basic groups: excluder, indicator, and accumulator (Baker and Walker 1990). Results of the present study showing that Cu concentration in the leaves were enhanced by increasing Cu application to soil, suggest that *Arundo* performance is more consistent with the indicator group (Baker and Walker 1990).

It is well known that the first negative effect caused by presence of heavy metals, such as Cu, is related to nutrient uptake, since these metals compete for the same nutrient uptake transporters as Fe, Mn, and Zn (Clemens 2006). The alteration of the ion balance generally leads to the so-called "inducible deficiency" (Astolfi et al. 2005; Astolfi et al. 2014) which, together with the metal toxicity effects, can seriously inhibit the development of plants and then compromise the phytoextraction of metals.

The absorption of Cu by the roots is essentially mediated by the COPT1 transporter (Sancenón et al. 2003), even if transporters belonging to the ZIP family, such as the iron transporter (IRT1) (Korshunova et al. 1999), also play an important role in Cu homeostasis in plants (Wintz et al. 2003). Accordingly, it cannot be ruled out a direct competition of Cu with other essential elements, such as Fe and Zn during uptake (Monni et al. 2000; Astolfi et al. 2014).

However, in *Arundo* plants, high external concentrations of Cu did not cause a decrease in the tissue concentrations of both Zn and Fe (Fig. 2). Rather, it might be proposed that the better nutritional status of Cu-treated plants can alleviate the effects of Cu toxicity thus contributing to the plant tolerance to the metal (Yang et al. 2002). This finding is consistent with that reported in the literature. For instance, Marzilli et al. (2018) demonstrated that tissue concentration of Fe was increased by two- and fourfold after exposure of micropropagated poplar plantlets to 250 and 500 mM Cu, respectively.

An increased production and accumulation of reactive oxygen species (ROS), such as superoxide radical (O_2^-) and hydrogen peroxide (H_2O_2), is commonly observed on exposure of plants to Cu (Noriega et al. 2012). Cells generate ROS as part of their metabolism, but the increase in ROS

levels in response to various external stress factors can potentially result toxic by causing significant damage to biomolecules and cell structures. In particular, excessive ROS production can lead to lipid peroxidation evidenced by enhanced accumulation of malondialdehyde (MDA), used as biomarkers for the assessment of membrane damage.

In the present study, we found that exposure of *Arundo* plants to 400 and 800 ppm Cu significantly increased MDA contents in shoots by 28 and 51%, respectively (Fig. 3).

This pattern is consistent with previous studies showing increased MDA levels in *Arundo* plants grown in hydroponic system in presence of cadmium (Shaheen et al. 2018). In particular, the production of MDA, as well as of some enzymatic antioxidants such as superoxide dismutases and catalases, followed a dose-dependent pattern and, at the highest Cd concentration the MDA level was about tenfold higher than that found in control plants. Interestingly, our results showed as at the lowest dose of Cu (200 ppm), the level of MDA was comparable with the control thus indicating that the specie could cope with a mild oxidative stress.

Besides enzymatic antioxidants, also antioxidant compounds, such as glutathione (GSH), play an important role in alleviating heavy metals-induced oxidative damage (Hernández et al. 2015). The tripeptide glutathione is the most abundant soluble S-containing metabolite and not only plays a role as major antioxidant and redox buffer in plant metabolism (Foyer and Noctor 2011), but also as precursor of phytochelatins (PCs), cysteine-rich peptides peptides that limit the free ion cellular concentration of heavy metals (Cobbett and Goldsbrough 2002).

Therefore, suppressing ROS production or enhancing the capacity for ROS scavenging it is expected to result in increased rate of synthesis of total non-protein thiols by tightly regulation of the sulfur assimilation pathway (Rausch and Wachter 2005).

Our results support this hypothesis, as the significant increase in MDA levels found in plants under Cu stress was significantly positively correlated ($R = 0.928^{***}$) with total non-protein thiols (Fig. 4). Furthermore, this study evidenced the modulation of the activity of ATPS and OASTL, the first and the last enzyme of S assimilation pathway in plants upon Cu exposure (Figs. 6 and 7). In particular, the pattern of thiols production correlated well with the OASTL activity ($R = 0.585^{*}$), suggesting that both contribute toward the activation of the plant defense response to cope with oxidative stress induced by Cu uptake. It is interesting to note that OASTL directly catalyzes the cysteine biosynthesis (Wirtz and Hell 2006), and some investigations have already demonstrated the responsiveness of OASTL activity in plants exposed to toxic metals (Astolfi et al. 2004; Pajuelo et al. 2007).

Summarizing all these findings by the PCA analysis computed with the complete dataset comprising the leaf, micronutrients content, MDA and thiols levels, and enzyme activities (Fig. 8) appeared a clear clustering along the first component (describing 45.45% of the total variance) on the basis of Cu dose application and along the second one (describing 22.66% of the total variance), with a high positive loading for ATPS activity and a negative loading for Fe. This distribution indicates that in *Arundo* the activation of defense response against Cu toxicity is not only dose dependent, but also rely on the regulation of plant nutritional status and, more importantly, on the modulation of S assimilation pathway.

In conclusion, this study allowed for the characterization of the Cu phytoextraction potential of *Arundo donax* and importantly demonstrated that plants responded to Cu application by the induction of defense responses having different impact in terms of plant metabolic costs, but without detrimental consequences on biomass accumulation.

Funding information This work was supported by the ItalianMinistry of Agricultural, Food and Forestry Policies (MiPAAF) under the AGROENER project (D.D. n. 26329, 1 April 2016)-http://agroener.crea.gov.it/. The research was carried out in the frame of the MIUR (Ministry for education, University and Research) initiative “Department of excellence” (Law 232/2016).

References

Adrees M, Ali S, Rizwan M, Ibrahim M, Abbas F, Farid M, Zia-Ur-Rehman M, Irshad MK, Bharwana SA (2015) The effect of excess copper on growth and physiology of important food crops: a review. Environ Sci Pollut Res 22(11):8148–8162.

Ambrosini VG et al (2018) High copper content in vineyard soils promotes modifications in photosynthetic parameters and morphological changes in the root system of “Red Niagara” plantlets. Plant Physiol Biochem. Elsevier 128(May):89–98.

Armentano G (2017) Rame, si va verso una riduzione delle dosi annue. L’Informatore Agrario 25:8.

Astolfi S et al (2004) Influence of iron nutrition on sulphur uptake and metabolism in maize (Zea mays L.) roots. Soil Sci Plant Nutr 50(7):1079–1083.

Astolfi S, Zuchi S, Passera C (2005) Effect of cadmium on H+ATPase activity of plasma membrane vesicles isolated from roots of different S-supplied maize (Zea mays L.) plants. Plant Sci 169(2):361–368

Astolfi S, Ortolani MR, Catarcione G, Paolacci AR, Cesco S, Pinton R, Ciaffi M (2014) Cadmium exposure affects iron acquisition in barley (Hordeum vulgare) seedlings. Physiol Plant 152(4):646–659.

Baker AJM, Walker PL (1990) Ecophysiology of metal uptake by tolerant plants. In: Shaw AJ (ed) Heavy metal tolerance in plants: evolutionary aspects. CRC Press, Boca Raton, pp 155–177.

Barbosa B et al (2015) Phytoremediation of heavy metal-contaminated soils using the perennial energy crops Miscanthus spp. and Arundo donax L. Bioenergy Res 8(4):1500–1511.

Bradford M (1976) A rapid and sensitive method for the quantitation of microgram quantities of protein utilizing the principle of protein-dye binding. Anal Biochem 72:248–254.

Brunetto G, Bastos de Melo GW, Terzano R, del Buono D, Astolfi S, Tomasi N, Pii Y, Mimmo T, Cesco S (2016) Copper accumulation in vineyard soils: rhizosphere processes and agronomic practices to limit its toxicity. Chemosphere 162:293–307.

Castelli F, Ceotto E (2016) The float system for producing giant reed (Arundo donax L.) transplants. In: 24th European biomass conference and exhibition, 6–9 June 2016, Amsterdam, The Netherlands, pp 305–308

Celletti S et al (2016) The characterization of the adaptive responses of durum wheat to different Fe availability highlights an optimum Fe requirement threshold. Plant Physiol Biochem 109:300–307

Ceotto E, Di Candilo M (2010) Shoot cuttings propagation of giant reed (Arundo donax L.) in water and moist soil: the path forward? Biomass Bioenergy. Elsevier Ltd 34(11):1614–1623

Cicchella D et al (2015) GEMAS: spatial distribution of chemical elements in agricultural and grazing land soil of Italy. J Geochem Explor. Elsevier B.V. 154:129–142.

Clemens S (2006) Toxic metal accumulation, responses to exposure and mechanisms of tolerance in plants. Biochimie 88(11):1707–1719

Cobbett C, Goldsbrough P (2002) Phytochelatins and metallothioneins: roles in heavy metal detoxification and homeostasis. Annu Rev Plant Biol 53(1):159–182.

Deluisa A, et al (2007) Il rame nei vigneti biologici, Notiziario ERSA, 4(Inserto speciale), pp 43–49.

Domokos-Szabolcsy É, Fári M, Márton L, Czakó M, Veres S, Elhawat N, Antal G, el-Ramady H, Zsíros O, Garab G, Alshaal T (2018) Selenate tolerance and selenium hyperaccumulation in the monocot giant reed (Arundo donax), a biomass crop plant with phytoremediation potential. Environ Sci Pollut Res 25(31):31368–31380.

Elhawat N, Alshaal T, Domokos-Szabolcsy É, el-Ramady H, Márton L, Czakó M, Kátai J, Balogh P, Sztrik A, Molnár M, Popp J, Fári MG (2014) Phytoaccumulation potentials of two biotechnologically propagated ecotypes of Arundo donax in copper-contaminated synthetic wastewater. Environ Sci Pollut Res 21(12):7773–7780

Elhawat N, Alshaal T, Domokos-Szabolcsy É, el-Ramady H, Antal G, Márton L, Czakó M, Balogh P, Fári M (2015) Copper uptake efficiency and its distribution within bioenergy grass giant reed. Bull Environ Contam Toxicol 95(4):452–458.

Fernando AL et al (2016) Giant reed (Arundo donax L.): a multipurpose crop bridging phytoremediation with sustainable bioeconomy. Bioremediation Bioeconomy. Elsevier Inc.

Foyer CH, Noctor G (2011) Ascorbate and glutathione: the heart of the redox hub. Plant Physiol 155(1):2–18. Hernández LE, Sobrino-Plata J, Montero-Palmero MB, Carrasco-Gil S, Flores-Cáceres ML, Ortega-Villasante C, Escobar C (2015) Contribution of glutathione to the control of cellular redox homeostasis under toxic metal and metalloid stress. J Exp Bot 66(10):2901–2911. Kausar S et al (2012) Potential of Arundo donax to treat chromium contamination. Ecol Eng. Elsevier B.V. 42:256–259.

Korshunova YO et al (1999) The IRT1 protein from Arabidopsis thaliana is a metal transporter with broad specificity. Plant Mol Biol 40(1):37–44.

La Torre A, Iovino V, Caradonia F (2018) Copper in plant protection: current situation and prospects. Phytopathol Mediterr 57(2):201–236.

Lado LR, Hengl T, Reuter HI (2008) Heavy metals in European soils: a geostatistical analysis of the FOREGS Geochemical database. Geoderma. Elsevier B.V. 148(2):189–199.

Marchiol L, Fellet G (2011) Agronomy towards the green economy. Optimization of metal phytoextraction. Ital J Agron 6(3):189–197.

Marzilli M et al (2018) Cd and Cu accumulation, translocation and tolerance in Populus alba clone (Villafranca) in autotrophic in vitro screening, Environmental Science and Pollution Research. Environ Sci Pollut Res 25(10):10058–10068.

Miotto A et al (2014) Copper uptake, accumulation and physiological changes in adult grapevines in response to excess copper in soil. Plant Soil 374(1–2):593–610.

Mirza N et al (2011) Ecological restoration of arsenic contaminated soil by Arundo donax L. Ecol Eng. Elsevier B.V. 37(12):1949–1956.

Monni S, Salemaa M, White C, Tuittila E, Huopalainen M (2000) Copper resistance of Calluna vulgaris originating from the pollution gradient of a Cu-Ni smelter, in Southwest Finland. Environ Pollut 109(2):211–219.

Noriega G, Cruz DS, Battle A et al. (2012) Heme oxygenase is involved in the Protection Exerted by Jasmonic Acid Against Cadmium Stress in Soybean Roots. J Plant Growth Regul 31:79–89.

Nsanganwimana F et al (2014) Arundo donax L., a candidate for phytomanaging water and soils contaminated by trace elements and producing plant-based feedstock. A review. Int J Phytoremediation 16(10):982–1017.

Pajuelo E, Carrasco JA, Romero LC, Chamber MA, Gotor C (2007) Evaluation of the metal phytoextraction potential of crop legumes. Regulation of the expression of O-acetylserine (thiol)lyase under metal stress. Plant Biol 9(5):672–681

Papazoglou EG, Serelis KG, Bouranis DL (2007) Impact of high cadmium and nickel soil concentration on selected physiological parameters of Arundo donax L. Eur J Soil Biol 43(4):207–215

Pätsikkä E, Kairavuo M, Sersen F, Aro EM, Tyystjärvi E (2002) Excess copper predisposes photosystem II to photoinhibition in vivo by outcompeting Iron and causing decrease in leaf chlorophyll. Plant Physiol 129:1359–1367.

Rausch T, Wachter A (2005) Sulfur metabolism: a versatile platform for launching defence operations. Trends Plant Sci 10(10):503–509.

Ruyters S et al (2013) Copper toxicity in soils under established vineyards in Europe: a survey. Sci Total Environ, The Elsevier B.V. 443:470–477.

Sancenón V et al (2003) Identification of a copper transporter family in *Arabidopsis thaliana*. Plant Mol Biol 51(4):577–587.

Shaheen S et al (2018) Physiology and selected genes expression under cadmium stress in Arundo donax L. International Journal of Phytoremediation. Taylor & Francis 20(11):1162–1167.

Shiyab S (2018) Phytoaccumulation of copper from irrigation water and its effect on the internal structure of lettuce. Agriculture 8(2).

Toselli M et al (2009) The accumulation of copper in soils of the Italian region Emilia-Romagna. Plant Soil Environ 55(2):74–79.

Toth G, Hermann T, Da Silva M et al (2016a) Heavy metals in agricultural soils of the European Union with implications for food safety. Environ Int. The Authors 88:299–309.

Toth G, Hermann T, Szatmári G et al (2016b) Maps of heavy metals in the soils of the European Union and proposed priority areas for detailed assessment. Sci Total Environ. The Authors 565:1054–1062.

Tripathi V, Edrisi SA, Abhilash PC (2016) Towards the coupling of phytoremediation with bioenergy production. Renew Sust Energ Rev 57:1386–1389.

Wang M, Zhou Q (2005) Single and joint toxicity of chlorimuron-ethyl, cadmium and copper acting on wheat Triticum aestivum. Ecotoxicol Environ Saf 60:169–175.

Wintz H, Vulpe C (2002) Plant copper chaperons. Biochem Soc Trans 30:732–735.

Wintz H, Fox T, Wu YY, Feng V, Chen W, Chang HS, Zhu T, Vulpe C (2003) Expression profiles of Arabidopsis thaliana in mineral deficiencies reveal novel transporters involved in metal homeostasis. J Biol Chem 278(48):47644–47653

Wirtz M, Hell R (2006) Functional analysis of the cysteine synthase protein complex from plants: structural, biochemical and regulatory properties. J Plant Physiol 163(3):273–286.

Yang MJ, Yang XE, Roemheld V (2002) Growth and nutrient composition of Elsholtzia splendens nakai under copper toxicity. Journal of Plant Nutrition 25(7):1359–1375.

Yruela I (2009) Copper in plants: acquisition, transport and interactions. Funct Plant Biol 36:409–430.

Chapter 6

Sensitivity of olive (*Olea europaea* L.) to saline stress is mediated by the modulation of sulfur metabolim

In submission to Environmental and Experimental Botany as "*Sensitivity of olive (Olea europaea L.) to saline stress is mediated by the modulation of sulfur metabolim*", M. Ajmal Bashir, C. Silvestri, E. Coppa, V. Cristofori, E. Rugini, B. Ruggiero, T. Ahmad, I. A. Hafiz, N. A. Abbasi, S. Astolfi.

Abstract

Global warming has two dangerous global consequences for agriculture: drought, due to water scarcity, and salinization, due to the prolonged use of water containing high concentrations of salts. Since global climate is projected to continue to change over this century and beyond, choosing salt-tolerant plants could represent a potential paramount last resort for exploiting the secondary saline soils. Olive is considered moderately resistant to soil salinity as compared to other fruit trees, and in the present study we investigated the influence of NaCl solutions (ranging from 0 to 200 mM) in a salt-tolerant (cv. Canino) and two its transgenic lines (Canino *At17-1* and Canino *At17-2*), overexpressing tobacco osmotin gene, and in a salt-sensitive (cv. Sirole) olive cultivar. After four weeks, most of the shoots of both Canino and Sirole plants showed stunted growth and ultimate leaf drop by exposure to salt-enriched media, contrary to transgenic lines, that did not show injuries and exhibited a normal growth rate. Malondialdehyde (MDA) content was also measured as an indicator of the lipid peroxidation level. To evaluate the role of S assimilatory pathway in alleviating the adverse effects of salt stress, thiols levels as well as extractable activities of ATPS and OASTL, the first and the last enzyme of S assimilation pathway, respectively, have been estimated. The results have clearly depicted that both transgenic lines overexpressing osmotin gene coped with increasing levels of NaCl by the induction of S metabolism, and particularly increase in OASTL activity closely paralleled changes of NaCl concentration. Linear correlation between salt stress and OASTL activity provides evidence that S assimilation pathway plays a key role in adaptive response of olive plants under salt stress conditions.

Keywords: olive, osmotin, salinity, sulfur assimilation, transgenesis

6.1 Introduction

Global warming has two dangerous global consequences for agriculture: drought, due to water scarcity, and salinization, due to the prolonged use of water containing high concentrations of salts. Thus, it is important to identify plants able to cope with drought and salt stress to increase crop resilience under climate change. Olive (*Olea europaea* L.) belongs to family Oleaceae is one of the most popular specie of the genus Olea which is used for food purpose (Rugini et al., 2016, Hashmi et al., 2015).

Olive is widely grown all over the world, with a great potential for expansion due to its ability to cope with unfavorable conditions (Ghanbari et al., 2012; Uylaser and Yildiz, 2014). However, most olive production (about 98%) comes from Mediterranean basin (Rugini et al., 2016). As a consequence, climate change will have a strong impact on olive cultivation as this area has warmed up 20% faster than the world average.

Olive is known as a glycophytic species presenting medium tolerance to salts (Gucci and Tattini, 1997) with marked differences among cultivars (Mousavi et al., 2019; Bracci et al., 2009; Chartzoulakis, 2005).

One of the major effects of salt stress is oxidative stress, resulting in increased levels of reactive oxygen species (ROS) (Zhu et al. 2007). Reactive oxygen species have the potential to interfere with many cellular components, causing cell membrane and other cellular structures damage, metabolic disorders, inhibited photosynthesis and impaired nutrient uptake (Hasegawa et al., 2000). To face increased ROS production, plants have developed defensive strategies, including enzymatic and non-enzymatic antioxidant systems.

Thiol compounds, and in particular glutathione (GSH) (Rennenberg, 1984), act as antioxidants that protect plants against the damaging effects of increased ROS levels due to salt stress (Foyer and Noctor, 2005).

Furthermore, plant responses to salinity include the synthesis of harmonious osmolytes, and stimulation of phytohormones production (Parida and Das, 2005). The molecular mechanism involves the overexpression of particular genes triggering different stress-related proteins and play a pivotal role in stress adaptation mechanisms (Subramanyam et al. 2011).

Among the several stress-related proteins, osmotin is known to be induced in response to both biotic and abiotic stresses in plants (Parkhi et al., 2009). Osmotin is a cationic protein belonging to the PR5 family proteins (Singh et al. 1985). It has been suggested that osmotin confers the tolerance

to salinity stress by increasing the accumulation of osmolytes, such as proline and glycine betaine (Barthakur et al. 2001a; Singh et al. 1987; Husaini and Abdin 2008; Subramanyam et al. 2011).

Aim of this study was to investigate the contribution of osmotin in olive response to salinity by using a salt-tolerant (cv. Canino) and two its transgenic lines (Canino *At17-1* and Canino *At17-2),* overexpressing tobacco osmotin gene, and a salt-sensitive (cv. Sirole) olive cultivar, exposed to NaCl solutions (ranging from 0 to 200 mM). In particular, we investigated whether the presence of *osmotin* gene triggered changes in proline accumulation and on lipid peroxidation (as an estimate of oxidative damage).

Furthermore, since GSH plays an active role in the process of response to salinity, we tested the hypothesis that a close relationship might exist between salt tolerance and S assimilation rate. Thus, changes in thiols levels as well as in extractable activities of ATPS and OASTL, the first and the last enzyme of S assimilation pathway, respectively, have been estimated in plants exposed to salt stress.

6.2 Materials and methods

6.2.1 Plant material and growing conditions

Shoot culture derived from *in vitro* propagation of a salt-tolerant (cv. Canino) and two its transgenic lines (Canino *At17-1* and Canino *At17-2*), and a salt-sensitive (cv. Sirole) olive cultivar were studied.

The transgenic lines (Canino *At17-1* and Canino *At17-2*) expressing tobacco osmotin gene were obtained by *A. tumefaciens*-mediated transformation of olive somatic embryos (Rugini and Caricato, 1995, Rugini and Silvestri, 2016; Rugini et al., 2016).

The shoots were subcultured a four-week intervals on OM medium (Rugini, 1984) containing mannitol 3,6 g/L, L-glutamine 2,2 g/L and zeatin 1 mg/L (added filter-sterilized after autoclave) and plant agar (Duchefa, NL) 0.6%. The pH of the medium was adjusted to 5.8 before autoclaving. Three 250 ml jars, containing ten single node explants, were sub-cultured, as above described, in 50 ml proliferation medium supplemented with four different NaCl concentrations NaCl (0, 50, 100 and 200 mM), corresponding to the electrical conductivity reported in Table 1. Explants were kept under controlled conditions in a growth chamber with a day/night cycle of 16/8 h at 24±1 °C air temperature, 80% relative humidity, and 40 mmol m^{-2} s^{-1} light intensity. Data collection were

performed after 28 days in culture. Plant tissues were collected and stored for following analyses at -80°C until use.

6.2.2 Test for Transgenosis

Shoots of transgenic olive lines (Canino *AT17-1* and Canino *AT17-2*) were preventively tested for kanamycin resistance, by using a kanamiycin-enriched media (150 mg L^{-1}), and the presence of the transgenic genes in their DNA were ascertained. Olive genomic DNA was extracted from young leaves (150 mg of fresh tissue) using a based CTAB (cetyl-trimethyl-ammonium bromide) method (Doyle and Doyle 1990). DNA concentration and quality were determined by 1% agarose gel electrophoresis and using a Nanodrop Bioanalyzer ND1000 (ThermoScientific). Then, the transformant were screened for the transgene by polymerase chain reaction (PCR) using the osmotin-specific primers Osm-F (5'- CCAACAACCCAACTTGTTAAAA- 3') and Osm-R (5'- CGACAGAATAATTTGACCAAAAG- 3'). The PCR conditions were: 95°C for 5 min; 35 cycles of 94°C for 30 s, 60°C for 45 s, and 72°C for 80 s, and final extension at 72°C for 10 min. The reaction products were separated electrophoretically on 1,5% (w/v) agarose gel, stained with ethidium bromide, and photographed (Figure 1).

6.2.3 Growth analysis

The Relative Growth Rate (RGR) index was calculated after 4 weeks of culture as described by (Gatti et al., 2017).

Mckinney index (MKI) and tolerance index (TI) were calculated in order to evaluate the damage caused by salinity stress and data was recorded on the basis of a rating scale by dividing each shoot into ten classes using MKI (Table 2), as reported by Di Cori et al. (2013).

The estimation of (TI) was performed on the basis of chlorophyll content by using the formula described by Köhl and Lösch (2004).

6.2.4 Photosynthetic pigments

To determine pigment concentration, 100 mg of fresh leaves were collected in 15 mL tubes and 4 mL of methanol 100% were added for the extraction. The tubes were heated at 65°C for 10 minutes and then stored at 4°C for 24 hrs. The values of total chlorophyll content, chlorophyll a, chlorophyll b and carotenoid content were determined after centrifugation at 5000 rpm for 5 minutes, using a

spectrophotometer (model EVO 60, made: Thermo Fisher Scientific Inc.) by following the methods described by Lichtenthaler (1987). Furthermore, Chla/Chlb ratio has been calculated.

6.2.5 Proline accumulation

Freshly harvested leaf tissues (100 mg of fresh weight) were collected and proline concentration was determined spectrophotometrically, by reaction with ninhydrin, according to Bates et al. (1973). Briefly, a 1:1:1 solution of proline, ninhydrin acid and glacial acetic acid was incubated at 100°C for 1 hour. The reaction was arrested in an iced bath and the cromophore was extracted with 4 mL toluene and the absorbance at 520 nm was determined with a spectrophotometer EVO 60 (Thermo Fischer Scientific Inc.).

6.2.6 Determination of MDA

The lipid peroxidation was estimated as malondialdehyde (MDA) content by following the methods described by (Astolfi et al., 2005). Briefly, shoot tissues (0.2 g) were mixed in 10 ml of 0.25% TBA buffer prepared in 10% TCA. Extracts were then heated at 95°C for 30 minutes and then quickly cooled in ice. After a centrifugation step at 10000 rpm for 10 min, the absorbance of the supernatant was measured at 532 nm absorbance in spectrophotometer EVO 60 (Thermo Fischer Scientific Inc.). The correction of non-specific turbidity was done by subtracting the absorbance values taken at 600 nm absorbance. The level of lipid peroxidation was presented as mmol g^{-1} fresh weight by using coefficient of 155 mM cm^{-1}.

6.2.7 Non-protein thiols extraction and determination

Water soluble non-protein thiol compounds were determined colorimetrically with 5,5′ dithio-bis-(2-nitrobenzoic acid) (DTNB), following the procedure reported by Celletti et al. (2016). Briefly, shoots samples (1 g fresh weight) were ground in liquid N_2 and extracted in 3 mL of a solution composed of 80 mM trichloroacetic acid (TCA), 1mM ethylenediaminetetraacetic acid (EDTA), 0.15% (w/v) ascorbic acid, and 10% (w/v) polyvinylpolypyrrolidone (PVP). After a centrifugation step (30 min at 4000 g and 4 °C), the supernatants were collected and the concentrations of DTNB-reactive compounds were measured spectrophotometrically by reading the A415.

6.2.8 Determination of ATPs and OASTL

Shoot tissues (1 g fresh weight) were powdered in a pre-chilled mortar with liquid N2. Cold extraction buffer, containing 50 mM HEPES-KOH (pH 7.4), 5 mM MgCl2, 1 mM EDTA, 10% (v/v) glycerol, 0.1% (v/v) Triton X-100, 5 mM dithiothreitol (DTT), 1 mM phenylmethylsulphonyl fluoride (PMSF), and 1% (w/v) polyvinylpyrrolidone (PVP), was added in a ratio of 1:7 and 1:3 (w/v) for shoots and roots, respectively. Following extraction steps were performed according to the method described by Celletti et al. (2016).

The activity of ATP sulphurylase (ATPS; EC 2.7.7.4) and O-acetylserine(thiol) lyase (OASTL; EC 4.2.99.8) activity was determined by the bioluminescence technique and by detecting cysteine production, respectively, as described by Celletti et al. (2016). Protein content were recorded by following the protocols described by (Bradford, 1976).

6.2.9 Statistical analysis

The effects of NaCl, genotyps and interaction between them were evaluated at three levels of significance: $p<0.05$ (*), $p<0.01$ (**) and $p<0.001$ (***). A Fisher's test was used for mean separation and to provide homogeneous groups for the means (at $p \leq 0.01$).

All data were process in XLSTAT, a user-friendly statistical software for Microsoft Excel.

Table 1: Electrical conductivity (Ec), expressed in (µS/cm) of the proliferation media enriched with different concentrations of NaCl (50, 100, 200 mM and 0 as control).

mM NaCl	Ec (µS/cm)
0	7,653 ± 15
50	13,764 ± 12
100	19,905 ± 75
200	40,002 ± 62,5

Table 2: Rating scale consisting of ten classes with the numeric values for McKinney Index (MKI)

Class	Symptoms
0	0 injuries
1	Browning at basal sections of the stem
2	0 to 20% chlorotic symptoms
3	20-50% chlorotic symptoms
4	Up to 10% browning on stem or over 50% chlorotic symptoms
5	10-30% browning of the stem
6	Necrosis on apical leaves
7	30-50% necrosis of the stem
8	50% necrotic symptoms on stem
9	Restricted growth or necrosis on whole stem
10	Necrosis of the whole explant

6.3 Results

6.3.1 Effect of NaCl on in vitro shoot growth performance

Statistical analysis showed significant interaction between relative growth rate at different concentrations of NaCl for both *wt* genotypes (Canino and Sirole) and transgenic lines (Canino *AT17-1* and Canino *AT17-2*). In particular, positive interaction between each genotype and treatment with 50 mM NaCl has been observed, as showed in Table 3.

The *in vitro* shoot growth was significantly influenced by NaCl concentration in the growing media (Figure 2). The highest relative growth rate (RGR) has been observed in Canino shoots in medium enriched with 50 mM NaCl, followed by Sirole at the same salt concentration. However, both cultivars showed a significantly reduced RGR at higher NaCl concentrations (100 and 200 mM), compared to the transgenic lines, Canino *AT17-1* and Canino *AT17-2*, that showed a RGR of 3.92 and 3.72 at 100mM NaCl, and 2.55 and 1.77 at 200 mM NaCl, respectively (Table 3).

McKinney Index (MKI) and Tolerance Index (TI) were calculated in order to evaluate the level of shoot chlorosis and necrosis resulting from NaCl treatment. Our results showed that MKI was positively correlated with increasing NaCl concentrations. However, values of MKI were higher in Canino and Sirole shoots, than in Canino *AT17-1* and Canino *AT17-2* ones (Table 4).

On the other hand, the exposure of shoots to increasing NaCl concentrations resulted in values for TI of 4.7, 16.5 and 23.4% for Canino, and 9.1, 18.2 and 20.5% for Sirole, at 50, 100 and 200 mM, respectively (Table 4). Interestingly, both transgenic lines (Canino *AT17-1* and Canino *AT17-2)* responded better to exogenous NaCl treatments, showing values for TI of 28.8, 46.4 and 47.9% and 14.3, 25.9 and 32.30%, at 50, 100 and 200 mM NaCl, respectively.

6.3.2 Effect of different levels of NaCl on photosynthetic pigments

After four weeks of exposure to salt stress, all genotypes showed typical toxicity symptoms, such as decreased chlorophyll content (Figure 3). Total chlorophyll concentration of Canino shoots slowly decreased with increasing NaCl concentration (7, 22 and 30%, at 50, 100 and 200 mM, respectively) (Figure 3). On the other hand, Sirole and both transgenic lines exhibited a worsen response to salt stress, resulting in more rapid and greater reduction of total chlorophyll concentration (Figure 3). The highest NaCl concentration (200 mM) resulted in 40, 57 and 48% lower chlorophyll content in Sirole, Canino *AT17-1* and Canino *AT17-2*, respectively (Figure 3).

Carotenoid concentration was approximately the same in both Canino and Sirole shoots in control condition (0 mM NaCl), whereas both transgenic lines showed higher carotenoid content (Figure 3).

In particular, Canino *AT17-1* showed an almost twofold increase from that of Canino *wt*, whereas in Canino *AT17-2* increased to a lesser extent (30% with respect to Canino *wt*) (Figure 3). Furthermore, while Canino *wt* maintained approximately the same carotenoid concentration irrespective of the NaCl in the growth medium, in Sirole and in both transgenic lines it significantly declined with increasing NaCl concentration (Figure 3). However, when growth medium was supplemented with 200 mM NaCl the highest values for carotenoid concentration were found in Canino *AT17-1*, showing values similar to Canino *wt*, followed by Canino *AT17-2* (Figure 3).

6.3.3 Effect of different levels of NaCl on proline accumulation

The proline accumulation in the salt-tolerant cv. (Canino) was significantly higher (36%) than in the and a salt-sensitive one (cv. Sirole) (Figure 4). but the same metabolite accumulated in even greater in the shoots of Canino *AT17-1* and Canino *AT17-2* (+75 e +20% compared to Canino wt in the control condition, respectively) (Table 6). In addition, both Canino and Sirole shoots resulted severely affected by 200 mM NaCl treatment, and showed a significative decrease of proline concentration (78 and 82%, respectively) (Figure 4). On the other hand, in both transgenic lines there was a consistent accumulation of proline in shoots on exposure to increasing NaCl concentrations (Figure 4). It is interesting to note that the increase of proline accumulation due to highest salt treatment (200 mM) in both Canino *AT17-1* and Canino *AT17-2* reached levels almost 7- and 9-fold higher, respectively, than those found in Canino wt in the same condition) (Figure 4).

6.3.4 Effect of different levels of NaCl on MDA content

Oxidative stress due to the presence of NaCl in the growth medium often results in lipid peroxidation which is generally evaluated by enhanced MDA content. However, our results showed that salt exposure did not increase MDA levels in the shoots of both *wt* and both transgenic lines irrespective of NaCl concentrations (Figure 5). On the other hand, it is interesting to note that the transgenic line *AT17-1* showed higher MDA concentration (+30%) than Canino wt in control condition (0 mM NaCl).

6.3.5 Effect of different levels of NaCl on non-protein thiol contents

It is well known that thiol compounds, and in particular GSH, act as antioxidants to counteract oxidative stress induced by NaCl toxicity (Astolfi and Zuchi, 2013). Our results show that non-protein thiols production and NaCl concentration in the growth medium significantly correlated in all four studied genotypes (Canino r^2= 0,8762; Sirole r^2=0,8193; Canino *AT17-1* r^2=0,6807; Canino *AT17-2* r^2=0,8259), even if at different extent) (Insert in Figure 6). In particular, as evidenced by the slope of the increase of thiols accumulation with increasing salt concentration, this response showed the following trend: Sirole > Canino > Canino *AT17-1*= Canino *At17-2*) (Insert in Figure 6).

6.3.6 Effect of different levels of NaCl on ATPS and OASTL activities

In order to evaluate if changes in thiols level required an adjustment in plant sulfur assimilation rate, the changes in ATPS and OASTL activity, the first and last enzyme of sulfur assimilation pathway, respectively, were measured) (Figure 7). A slight induction of ATPS activity was observed in response to the lowest NaCl concentration (50 mM) in Canino and Sirole cultivars, and in transgenic line Canino *AT17-1*, but the increase ranged between 15 and 20%. On the other hand, the same stress condition resulted in slightly decreased ATPS activity (-15%) in Canino *AT17-2*. No significant differences were observed in ATPS activity at 100 mM NaCl, relative to controls, in all four genotypes and, finally, when plants were treated with the highest salt concentration (200 mM) ATPS activity levels significantly decreased compared to control (decrease ranged from 25 to 30%), except for Canino which maintained approximately the same activity as in control condition(Figure 7)..

As for thiols, OASTL activity was positively correlated with salt concentration in the growth medium and, indeed, the correlation was very high in all four studied genotypes (Canino r^2= 0,9185; Sirole r^2= 0,7917; Canino *AT17-1* r^2=0,9451; Canino *AT17-2* r^2=0,8509) (Insert in Figure 7). However, distinct differences among genotypes were observed and, in particular, as evidenced by the slope of the increase of OASTL activity with increasing salt concentration, the induction showed the following trend: Sirole > Canino *AT17-1* > Canino *At17-2* > Canino) (Insert in Figure 7).

Table 3. Relative growht rate (RGR) of the salt-tolerant (cv. Canino) and two its transgenic lines (Canino *At17-1* and Canino *At17-2*), overexpressing tobacco osmotin gene, and the salt-sensitive (cv. Sirole) olive cultivar, exposed to NaCl solutions (ranging from 0 to 200 mM). Data are represented as mean ± SD. Different letters within the same colums indicating significant differences according to Fisher's test ($p<0.01$). Significant effect: *$p \leq 0.05$; **$p \leq 0.01$; ***$p \leq 0.001$; - not significant.

Genotype	mM NaCl	RGR
Canino	0	4.57 ± 0.27 **ab**
	50	5.59 ± 1.25 **a**
	100	4.65 ± 0.79 **ab**
	200	1.58 ± 0.30 **fg**
Sirole	0	3.88 ± 0.54 **a-d**
	50	4.48 ± 1.01 **ab**
	100	2.03 ± 0.19 **d-g**
	200	0.89 ± 0.22 **g**
Canino *AT17-1*	0	3.44 ± 1.02 **b-e**
	50	4.17 ± 0.76 **a-c**
	100	3.92 ± 0.26 **a-c**
	200	2.55 ± 0.90 **c-g**
Canino *AT17-2*	0	2.87 ± 1.36 **b-f**
	50	3.11 ± 0.51 **b-f**
	100	3.72 ± 0.72 **b-d**
	200	1.77 ± 0.53 **e-g**
Source of variation		
Genotype		***
NaCl concentration		***
Gen x NaCl		**

Table 4: McKinney Index (MKI) and Tolerance Index (TI) of the salt-tolerant (cv. Canino) and two its transgenic lines (Canino *At17-1* and Canino *At17-2*), overexpressing tobacco osmotin gene, and the salt-sensitive (cv. Sirole) olive cultivar, exposed to NaCl solutions (ranging from 0 to 200 mM).

Genotype	mM NaCl	MKI	TI
Canino	0	0	-
	50	0	4.7
	100	2.33	16.5
	200	8.87	23.4
Sirole	0	0	-
	50	0.25	9.1
	100	5	18.2
	200	9	20.5
Canino *AT17-1*	0	0	-
	50	0	28.8
	100	0.1	46.4
	200	4.45	47.9
Canino *AT17-2*	0	0	-
	50	0	14.3
	100	0.23	25.9
	200	5.1	32.3

Gene name	Primers	GenBank Accessions
a *nt_osm*	fwd: CCAACAACCCAACTTGTTAAAA rev: CGACAGAATAATTTGACCAAAAG	M29279

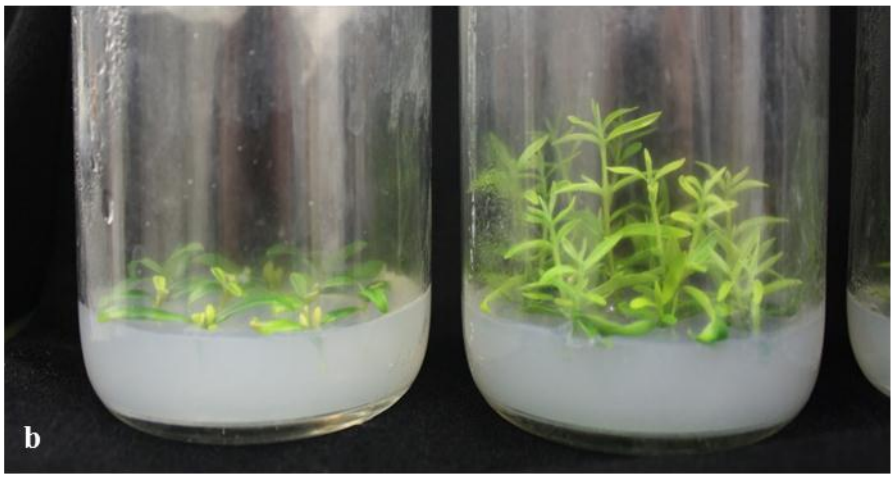

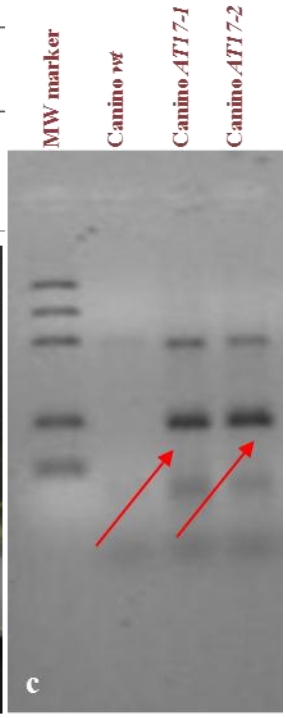

Figure 1: Tobacco osmotin gene with GenBank accession number and associated primers utilized in PCR (a), Canino wt (Control) and transgenic Canino *AT17-1* growing on selection medium enriched with kanamycin (150 mgL-1) (b), Analysis of tobacco osmotin gene integration in olive transgenic shoots: red arrows indicate the PCR products of the transgenic clones Canino *AT17-1* and Canino *AT17-2* (c).

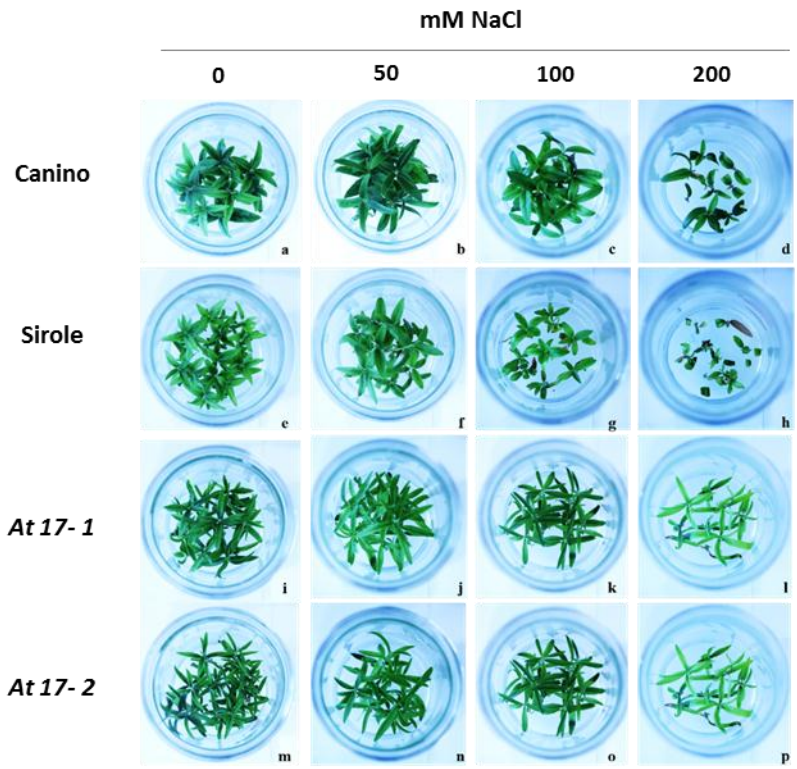

Figure 2: Effect of different concentrations of NaCl (0, 50, 100 and 200 mM) on a salt-tolerant (cv. Canino) and two its transgenic lines (Canino *At17-1* and Canino *At17-2),* overexpressing tobacco osmotin gene, and a salt-sensitive (cv. Sirole) olive cultivar.

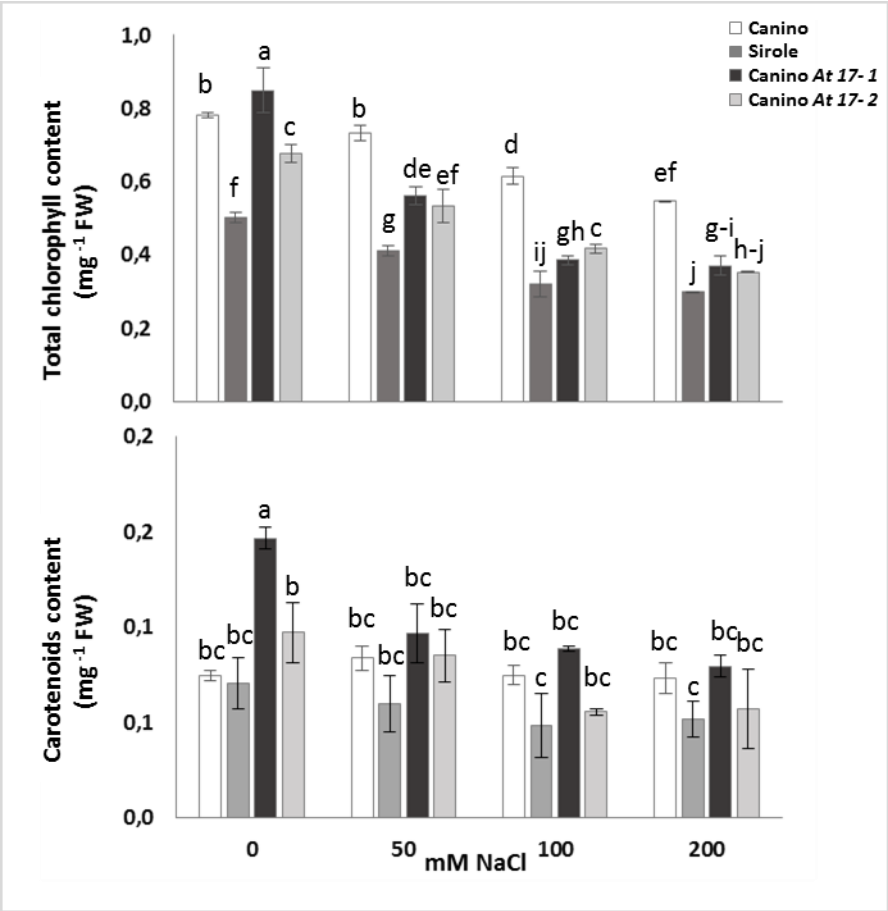

Figure 3: Total chlorophyll content and carotenoids content in shoots of the salt-tolerant (cv. Canino) and two its transgenic lines (Canino *At17-1* and Canino *At17-2),* overexpressing tobacco osmotin gene, and the salt-sensitive (cv. Sirole) olive cultivar, exposed to NaCl solutions (ranging from 0 to 200 mM). Different letters indicate significant differences according to Fisher's test ($p<0.01$).

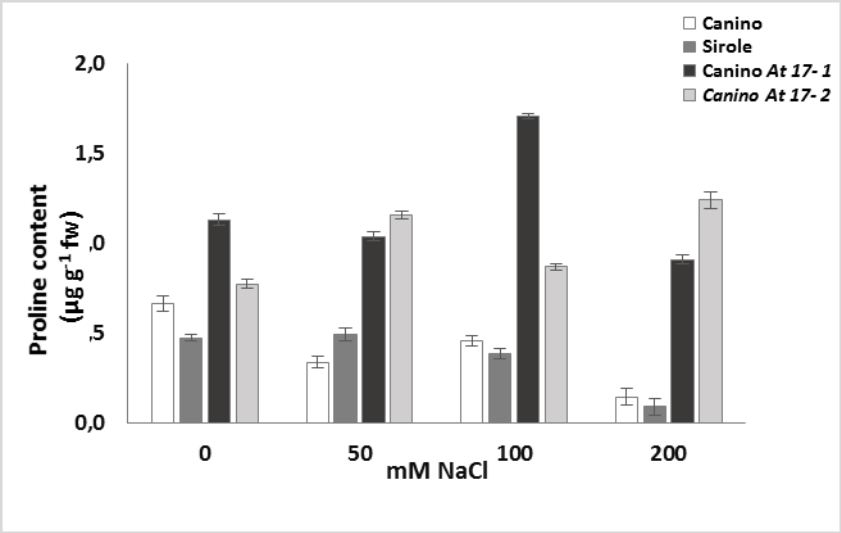

Figure 4: Proline content in shoots of the salt-tolerant (cv. Canino) and two its transgenic lines (Canino *At17-1* and Canino *At17-2)*, overexpressing tobacco osmotin gene, and the salt-sensitive (cv. Sirole) olive cultivar, exposed to NaCl solutions (ranging from 0 to 200 mM). Statistics as in Fig.3.

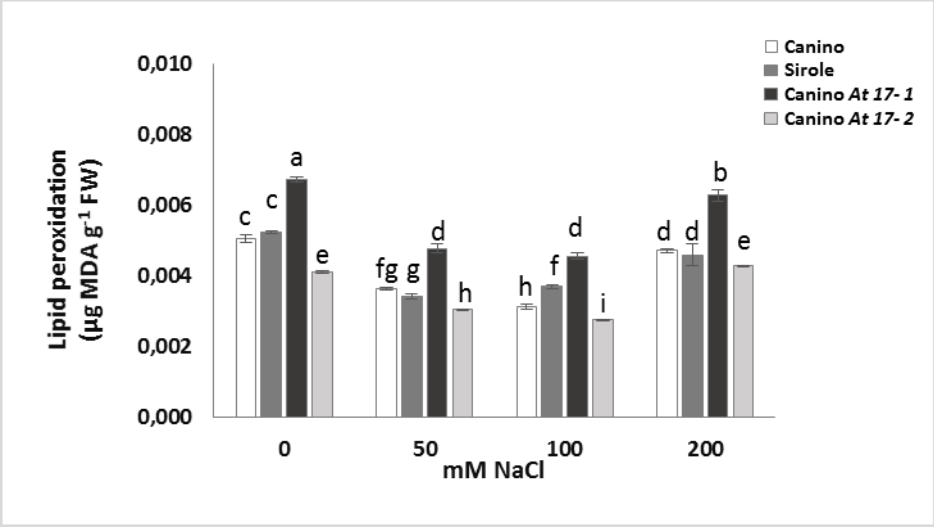

Figure 5: Changes in MDA content in shoots of the salt-tolerant (cv. Canino) and two its transgenic lines (Canino *At17-1* and Canino *At17-2),* overexpressing tobacco osmotin gene, and the salt-sensitive (cv. Sirole) olive cultivar, exposed to NaCl solutions (ranging from 0 to 200 mM). Statistics as in Fig.3.

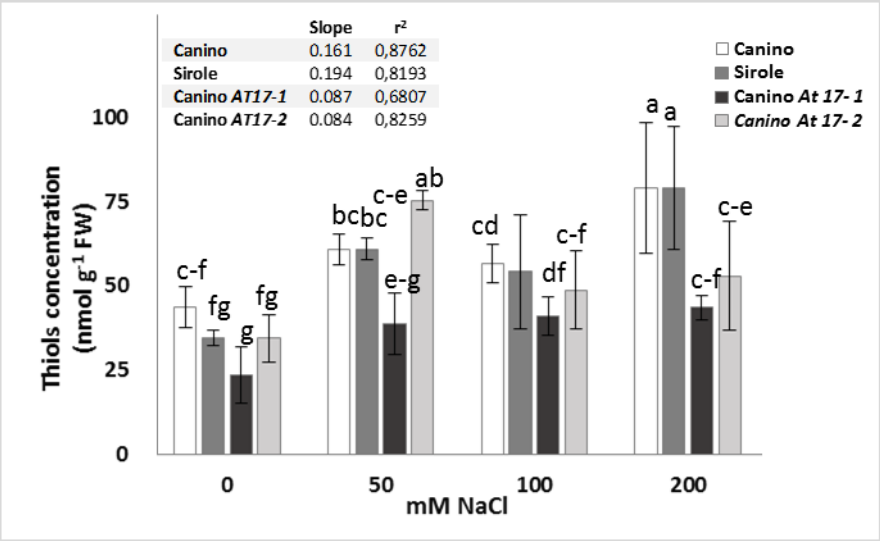

Figure 6: Thiols concentration in shoots of the salt-tolerant (cv. Canino) and two its transgenic lines (Canino *At17-1* and Canino *At17-2),* overexpressing tobacco osmotin gene, and the salt-sensitive (cv. Sirole) olive cultivar, exposed to NaCl solutions (ranging from 0 to 200 mM). The values for the slope of the increase in thiols accumulation and r^2 are indicated in the table. Statistics as in Fig.3.

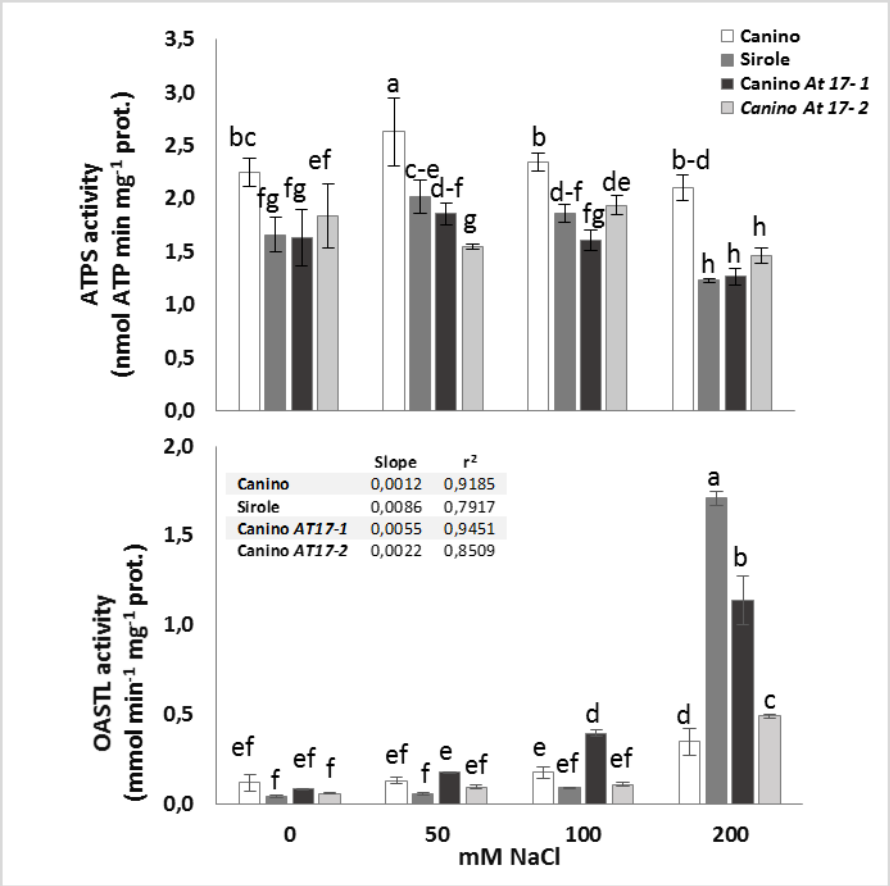

Figure 7: ATPS and OASTL activity in shoots of the salt-tolerant (cv. Canino) and two its transgenic lines (Canino *At17-1* and Canino *At17-2),* overexpressing tobacco osmotin gene, and the salt-sensitive (cv. Sirole) olive cultivar, exposed to NaCl solutions (ranging from 0 to 200 mM). The values for the slope of the increase in OASTL activity and r^2 are indicated in the table. Statistics as in Fig.3.

6.4 Discussion

Owing to their sessile lifestyle, plants are continuously challenged with a broad range of environmental stresses, among which salinity stress is recognized as one of the most negatively impacting stress on plant growth and crop yield (Suzuki et al., 2014). Plant response to stress commonly rely on expression of specific genes and synthesis of a large number of stress-related proteins, that plays a crucial role in stress adaptation (Subramanyam et al., 2012). Thus, the expression of genes involved in signaling and regulatory pathways could represent one of the most promising approach for improving stress tolerance in plants. In the past two decades, overexpression of osmotin gene in tobacco (Barthakur et al. 2001a; Sokhansanj, Noori, & Niknam, 2006), tomato (Sarad, Rathore, Singh, & Kumar, 2004), strawberry (Husaini & Abdin, 2008), and chilli pepper (Subramanyam et al., 2012) have been reported to enhance tolerance under NaCl-mediated salinity stress.

Olive (*Olea europaea* L.) is a typical crop of the Mediterranean basin, where soil salinization is projected to worsen as a consequence of global climate change climate.

In this study it has been investigated the contribution of osmotin in olive response to salinity by using four olive genotypes: a salt-tolerant (cv. Canino) and two its transgenic lines (Canino *At17-1* and Canino *At17-2),* overexpressing tobacco osmotin gene, and a salt-sensitive (cv. Sirole). Since one of the major effects of salt stress is oxidative stress, resulting in increased levels of reactive oxygen species (ROS) (Zhu et al. 2007), and being GSH actively involved as antioxidant in the process of response to salinity, we also tested the hypothesis that a close relationship might exist between salt tolerance and S assimilation rate.

By evaluating olive tolerance to salinity stress in terms of McKinney Index (MKI) and Tolerance Index (TI), indicating the level of shoot chlorosis and necrosis, respectively, we demonstrated that the lower effects of salt-induced stress were observed in both transgenic lines (Table 4). In particular, zero MKI values, corresponding to green leaves and stems, were observed in all tested genotypes grown in control condition (0 mM NaCl) until the end of the experiment. On the other hand, both Canino and Sirole showed significantly increased chlorosis with increasing salt concentration in the medium, while the transgenic lines showed normal growth even at highest salt stress level (Figure 2). This is a clear indication that both transgenic lines responded better to exogenous NaCl treatments, showing lower MKI values as well as higher TI values, than Canino and Sirole (Table 4).

These findings are consistent with previous study showing that *Myrtus communis* L. plants exposed to 150 and 250 mM NaCl showed high chlorosis levels, with highest MKI values found in shoots exposed to 250 mM NaCl for 30 days (Di Cori et al., 2013).

Nevertheless, this effect seemed not to be directly linked to total chlorophyll content. Indeed, in our experimental conditions, we observed that the treatment with NaCl was more negatively impacting on Sirole and both transgenic lines, which showed a higher rate of chlorophyll loss from shoots, than Canino (Figure 3).

It is well known that several abiotic stresses influence the accumulation of carotenoids, whose regulation is suggested to lead to stress tolerant phenotypes (Davison et al., 2002).

In our experimental conditions, we found that both transgenic lines showed higher carotenoid content than Canino and Sirole in control condition (0 mM NaCl), but Sirole and transgenic lines exhibited a net loss of carotenoids after NaCl treatment (Figure 3).

This result was consistent with those obtained by Bouvier et al. (1998), who showed that in pepper β-carotene content decreases under oxidative-induced stress.

The finding that salt stress resulted in similar decrease rate of carotenoids for genotypes with contrasted tolerance (Sirole and Canino transgenic lines), suggests that carotenoids metabolism is not directly involved in the stress tolerance mechanism, and changes in carotenoid accumulation are rather due to plant general metabolic modifications occurring during adaptation to stress condition.

Even if it has not been clearly demonstrated the mechanism by which osmotin improves plant response under abiotic stress, a few studies have shown that under salinity stress osmotin allows the reduction of Na^+ ions uptake into the cytoplasm though a Na^+/H^+ anti-porter (Le et al., 2017) and moreover that osmotin could be involved in osmotic adjustment of plants under stress either by facilitating the accumulation or compartmentation of different solutes in intracellular spaces (Barthakur et al., 2001b). As salinity results in water stress, plants have to accomplish an osmotic adjustment to maintain their metabolic activities. Osmotic adjustment is achieved by the accumulation of the compatible solutes such as free proline. It has been reported that stress tolerance increases with increasing proline accumulation (Wang et al., 2013) and, furthermore, that proline can induce the expression of several genes involved in stress tolerance (Ashraf and Foolad, 2007), suggesting a role for this metabolite not only to low water potential but also in plant protection from osmotic stress (Rejeb et al., 2014). Thus, the transgenic approach could represent a promisinig strategy to increase proline production and improve stress tolerance in plants.

Interestingly, our results showed that the salt-tolerant cv. (Canino) accumulated more proline than in the salt-sensitive one (cv. Sirole) (Figure 4), confirming previous study suggesting that proline accumulation is genotype-dependent (Regni et al., 2019).

More importantly, we found that shoots of both transgenic lines were able to increase poline accumulation with increasing NaCl concentrations in the medium and when they were exposed to the highest salt concentration (200 mM) proline content accumulated substantially (almost 7- and 9-fold higher in Canino *AT17-1* and Canino *AT17-2*, respectively, compred to those found in Canino wt in the same condition) (Figure 4). This result reasonably suggests that osmotin could play an important role in the regulation of the mechanism of proline accumulation under salt stress. Proline synthesis is commonly induced under stressed conditions through an intercellular signal pathway mediated by ROS accumulation (Rejeb et al., 2014). Indeed, in plants exposed to environmental constraints the accumulation of ROS is generally associated to proline accumulation (Rejeb et al., 2014).

Salt stress provokes an excessive ROS production resulting in oxidative damage leading to cell injury and death (Khan et al., 2014). Therefore, we compared the changes in MDA concentration (as an estimate of lipid peroxidation) to assess the degree of oxidative damage induced by NaCl treatment (Wang et al., 2009).

Our data showed that all tested genotypes were were able to maintain on average a lower MDA content than that found in control condition (Figure 5). This result might be explained by assuming a role of proline in modulating both ROS generation and scavenging of ions (Szabados and Savouré, 2010), but also to high efficiency of antioxidant system leading to an increased stress tolerance.

According to literature, plants possess some strategies to cope with oxidative stress, such as both enzymatic and non-enzymatic antioxidant systems. Non-enzymatic systems include thiol compounds such as glutathione and cysteine, playing an important role in improving the tolerance to oxidative stress induced by NaCl toxicity (Foyer and Noctor, 2011; Astolfi and Zuchi, 2013; Sharma et al., 2019).

Our results showed that non-protein thiols production and NaCl concentration in the growth medium were significantly positively correlated in all four studied genotypes (Canino r^2= 0,8762; Sirole r^2=0,8193; Canino *AT17-1* r^2=0,6807; Canino *AT17-2* r^2=0,8259) (Insert in Figure 6) and in particular, Sirole cv exhibited the highest slope of the increase of thiols accumulation with increasing salt concentration (Insert in Figure 6). It is noteworthy that in Sirole, being a salt-

sensitive cv, a large amount of ROS is produced following salt stress, leading to increased pressure on ROS scavenging activity and thus to increased amounts of antioxidant compounds to cope with stress condition. Moreover, this respose was well in line with the lowest proline content found in Sirole.

Changes in thiols production reasonably require an adjustment of sulfate assimilation rate under salt stress, thus the activities of ATPS and OASTL, the first and the last enzyme of S assimilation pathway, respectively, have been estimated in plants exposed to salt stress.

In this study, the increase of thiols production was parallel with that of OASTL activity, indicating that S assimilation pathway plays an important role in the regulation of plant response to salt stress. As for thiols, OASTL activity increased with increasing salt concentration in the growth medium and, indeed, the correlation was very high in all four studied genotypes (Canino r^2= 0,9185; Sirole r^2= 0,7917; Canino *AT17-1* r^2=0,9451; Canino *AT17-2* r^2=0,8509) (Insert in Figure 7), and as for thiols, the highest slope of the linear correlation was found in Sirole cv (Insert in Figure 7).

Interestingly, for both thiols and OASTL activity the lowest slope of the linear correlation was found in both transgenic lines (Insert in Figure 7).

The different pattern observed for ATPS and OASTL activity might be explained by assuming that OASTL directly catalyzes the biosynthesis of cysteine (Wirtz and Hell, 2006), the precursor for glutathione synthesis, and thus its activity could play a more important role in adaptation mechanisms to salt stress condition, than ATPS.

These results are well in line with previous studies showing ATPS activity increase (Khan et al. 2009a; Khan, et al., 2009b) as well as decrease (Gao et al., 2008) in response to salt treatment.

In conclusion our results suggested that both Canino *AT17-1* and Canino *AT17-2* transgenic lines had better salt tolerance ability than their relative wt (Canino). This positive effect could be associated to osmotin, which would play an important role in the regulation of proline accumulation, although the mechanism involved is still not fully understood. Enhanced proline accumulation would exert a protective role preventing or modulating ROS generation.

Furthermore, our data underlined the proposed interaction between salt stress and S metabolism: antioxidant response to scavenging excessive ROS requires the stimulation of S assimilation rate to sustain higher demand of reduced S.

Conflict of Interest

The authors declare that the research was conducted in the absence of any commercial or financial relationships that could be construed as a potential conflict of interest.

References

Astolfi, S., and Zuchi, S. (2013). Adequate S supply protects barley plants from adverse effects of salinity stress by increasing thiol contents. *Acta Physiol. Plant*. 35(1), 175-181.

Astolfi, S., Zuchi, S., and Passera, C. (2005). Effect of cadmium on H+ ATPase activity of plasma membrane vesicles isolated from roots of different S-supplied maize (*Zea mays* L.) plants. *Plant Sci.* 169(2), 361-368.

Barthakur, S. B. V. B., Babu, V., and Bansa, K. C. (2001). Over-expression of osmotin induces proline accumulation and confers tolerance to osmotic stress in transgenic tobacco. *J. Plant Biochem. Biotech. 10*(1), 31-37.

Bates, L. S., Waldren, R. P., and Teare, I. D. (1973). Rapid determination of free proline for water-stress studies. *Plant Soil, 39*(1), 205-207.

Bouvier, F., Backhaus, R. A., & Camara, B. (1998). Induction and control of chromoplast-specific carotenoid genes by oxidative stress. *Journal of Biological Chemistry*, *273*(46), 30651-30659.

Bracci, T., Sebastiani, L., Busconi, M., Fogher, C., Belaj, A., and Trujillo, I. (2009). SSR markers reveal the uniqueness of olive cultivars from the Italian region of Liguria. *Sci. Hortic. 122*(2), 209-215.

Bradford, M. M. (1976). A rapid and sensitive method for the quantitation of microgram quantities of protein utilizing the principle of protein-dye binding. *Analy. biochem., 72*(1-2), 248-254.

Celletti S., Pii Y., Mimmo T., Cesco S., Astolfi S. (2016) The characterization of the adaptive responses of durum wheat to different Fe availability highlights an optimum Fe requirement threshold. *Plant Physiology and Biochemistry* 109, 300-307.

Chartzoulakis, K. S. (2005). Salinity and olive: growth, salt tolerance, photosynthesis and yield. *Agric. Water Manag. 78*(1-2), 108-121.

Davison, P. A., Hunter, C. N., ans Horton, P. (2002). Overexpression of β-carotene hydroxylase enhances stress tolerance in Arabidopsis. *Nature*, *418*(6894), 203-206.

Di Cori, P., Lucioli, S., Frattarelli, A., Nota, P., Tel-Or, E., Benyamini, E, et al. (2013). Characterization of the response of in vitro cultured *Myrtus communis* L. plants to high concentrations of NaCl. *Plant physiol. Biochem. 73,* 420-426.

Foyer, C. H., and Noctor, G. (2005). Redox homeostasis and antioxidant signaling: a metabolic interface between stress perception and physiological responses. *Plant Cell*. 17:1866–1875.

Gatti, E., Sgarbi, E., Ozudogru, E. A., and Lambardi, M. (2017). The effect of Plantform™ bioreactor on micropropagation of *Quercus robur* in comparison to a conventional in vitro culture system on gelled medium, and assessment of the microenvironment influence on leaf structure. *Plant Biosys. 151*(6), 1129-1136.

Ghanbari, R., Anwar, F., Alkharfy, K. M., Gilani, A. H., and Saari, N. (2012). Valuable nutrients and functional bioactives in different parts of olive (*Olea europaea* L.), a review. *Int. J. Mol. Sci. 13*(3), 3291-3340.

Gucci, R., and Tattini, M. (1997). Salinity tolerance in olive. *Hortic. Rev. 21*, 177-214.

Hasegawa, M., Bressan, R., and Pardo, J. M. (2000). The dawn of plant salt tolerance genetics. *Trends in plant science*, *5*(8), 317-319.

Hashmi, M. A., Khan, A., Hanif, M., Farooq, U., and Perveen, S. (2015). Traditional uses, phytochemistry, and pharmacology of *Olea europaea* (Olive). *Evid. Based Complement. Alternat. Med.* 541591, 1-29.

Hesse, H., Nikiforova, V., Gakière, B., and Hoefgen, R. (2004). Molecular analysis and control of cysteine biosynthesis: integration of nitrogen and sulphur metabolism. *J. Exp. Bot. 55*(401), 1283-1292.

Husaini, A. M., and Abdin, M. Z. (2008). Overexpression of tobacco osmotin gene leads to salt stress tolerance in strawberry (*Fragaria× ananassa* Duch.) plants. *Indian J. Biotech., 7*: 465-471.

Khan, N. A., Anjum, N. A., Nazar, R., and Iqbal, N. (2009a). Increased activity of ATP-sulfurylase and increased contents of cysteine and glutathione reduce high cadmium-induced oxidative stress in mustard cultivar with high photosynthetic potential. *Russ. J. Plant Physiol., 56*(5), 670-677.

Khan, N. A., Nazar, R., and Anjum, N. A. (2009b). Growth, photosynthesis and antioxidant metabolism in mustard (*Brassica juncea* L.) cultivars differing in ATP-sulfurylase activity under salinity stress. *Sci. Hortic. 122*(3), 455-460.

Köhl, K. I., & Lösch, R. (2004). Experimental characterisation of metal tolerance. In: Heavy Metal Stress in Plants (pp. 434-454). Springer, Berlin, Heidelberg.

Larosa P. C., Chen, Z., Nelson, D. E., Singh, N. K., Hasegawa, P. M., and Bressan, R. A. (1992). Osmotin gene expression is post-transcriptionally regulated. *Plant Physiol*. 100:409–415.

Le, T. T., Williams, B., and Mundree, S., (2017). An osmotin from the resurrection plant *Tripogon loliiformis* (TlOsm) confers tolerance to multiple abiotic stresses in transgenic rice. *Physiol. Plant. 162*(1), 13-34.

Lichtenthaler, H. K. (1987). Chlorophylls and carotenoids: pigments of photosynthetic biomembranes. *Methods in enzymology, 148*,350-382.

Miller, G. A. D., Suzuki, N., Ciftci-Yilmaz, S., and Mittler, R. (2010). Reactive oxygen species homeostasis and signalling during drought and salinity stresses. *Plant Cell & Environ*. 33(4), 453-467.

Mousavi, S., Regni, L., Bocchini, M., Mariotti, R., Cultrera N.G.M., Mancuso, S., Googlani, J., Chakerolhosseini, M.R., Guerrero, C., Albertini, E., Baldoni, L., Proietti, P. (2019). Physiological, epigenetic and genetic regulation in some olive cultivars under salt stress. *Scientific Reports*. *9*(1) doi:10.1038/s41598-018-37496-5.

Parida, A. K., and Das, A. B. (2005). Salt tolerance and salinity effects on plants: a review. *Ecotox. Environ. Safe*. 60(3), 324-349.

Parkhi, V., Kumar, V., Sunilkumar, G., Campbell, LeAnne M., Singh, N. K., et al. (2009). Expression of apoplastically secreted tobacco osmotin in cotton confers drought tolerance. *Mol. Breeding. 23*(4), 625-639.

Raghothama, K. G., Maggio, A., Narasimhan, M. L., Kononowicz, A. K., Wang, G. L., Durzo, M. P., et al. (1997) Tissue-specific activation of the osmotin gene by ABA, C and NaCl involves the same promoter region. Plant Mol. Biol. 34:393–402.

Regni L, Del Pino AM, Mousavi S, Palmerini CA, Baldoni L, Mariotti R, Mairech H, Gardi T, D'Amato R and Proietti P (2019) Behavior of Four Olive Cultivars During Salt Stress. Front. Plant Sci. 10:867.doi: 10.3389/fpls.2019.00867

Reich, M., Aghajanzadeh, T., Helm, J., Parmar, S., Hawkesford, M. J., and De Kok, L. J. (2017). Chloride and sulfate salinity differently affect biomass, mineral nutrient composition and expression of sulfate transport and assimilation genes in *Brassica rapa*. *Plant & soil. 411*(1-2), 319-332.

Rejeb, K. B., Abdelly, C., & Savouré, A. (2014). How reactive oxygen species and proline face stress together. *Plant Physiology and Biochemistry*, *80*, 278-284.

Rennenberg, H. (1984). The fate of excess sulfur in higher plants. *Annu. Rev. Plant Physiol. 35*(1), 121-153.

Rugini, E. (1984). In vitro propagation of some olive (*Olea europaea* sativa L.) cultivars with different root-ability, and medium development using analytical data from developing shoots and embryos. *Sci. Hortic. 24*(2), 123-134.

Rugini, E., and Caricato, G. (1995). Somatic embryogenesis and plant recovery from mature tissues of olive cultivars (*Olea europaea* L.) "Canino" and "Moraiolo". *Plant Cell Rep. 14*(4), 257-260.

Rugini, E., and Silvestri, C. (2016). Somatic Embryogenesis in Olive (*Olea europaea* L. subsp. europaea var. sativa and var. sylvestris). *In Vitro Embryogen. Higher Plants*. *Springer*, 341-349.

Rugini, E., Silvestri, C., Ceccarelli, M., Muleo, R., and Cristofori, V. (2016). Mutagenesis and biotechnology techniques as tools for selecting new stable diploid and tetraploid olive genotypes and their dwarfing agronomical characterization. *Hort. Sci. 51*(7), 799-804.

Sarad, N., Rathore, M., Singh, N. K., & Kumar, N. (2004, September). Genetically engineered tomatoes: new vista for sustainable agriculture in high altitude regions. In: *Proceedings of the fourth international crop science congress*. Brisbane, Australia.

Szabados, L., & Savoure, A. (2010). Proline: a multifunctional amino acid. *Trends in plant science*, *15*(2), 89-97.

Singh NK, Nelson DE, Kuhn D, Hasegawa PM, Bressan RA (1989) Molecular cloning of osmotin and regulation of its expression by ABA and adaptation to low water potential. *Plant Physiol. 90*: 1096–1101.

Singh, N. K., Bracker, C. A., Hasegawa, P. M., Handa, A. K., Buckle, S., Hermodson, M. A., et al. (1987). Characterization of osmotin. *Plant Physiol. 85*:529–536.

Singh, N. K., Handa, A. K., Hasegawa, P. M., and Bressan, R. A. (1985). Proteins associated with adaptation of cultured tobacco cells to NaCl. *Plant Physiol. 79*:126–137.

Sokhansanj, A, Noori, S. A., and Niknam, V. (2006). Comparison of bacterial and plant genes participating in proline biosynthesis with osmotin gene, with respect to enhancing salinity tolerance of transgenic tobacco plants. *Russ. J. Plant Physiol. 53*(1), 110-115.

Subramanyam, K., Arun, M., Mariashibu, T., Salammal, T., Jeevaraj, R., Manoharan, S., et al. (2012). Overexpression of tobacco osmotin (*Tbosm*) in soybean conferred resistance to salinity stress and fungal infections. *Planta. 236*(6), 1909-1925.

Subramanyam, K., Sailaja, K. V., Subramanyam, K., Rao, D. M., and Lakshmidevi, K. (2011). Ectopic expression of an osmotin gene leads to enhanced salt tolerance in transgenic chilli pepper (*Capsicum annum* L.). *Plant Cell, Tiss. Org. Cult. 105*(2), 181-192.

Suzuki, N., Rivero, R. M., Shulaev, V., Blumwald, E., & Mittler, R. (2014). Abiotic and biotic stress combinations. *New Phytologist*. 203(1), 32-43. doi:10.1111/nph.12797

Uylaşer, V., and Yildiz, G. (2014). The historical development and nutritional importance of olive and olive oil constituted an important part of the Mediterranean diet. *Crit. Rev. Food Sci. Nutr. 54*(8), 1092-1101.

Wang, W., Kim, Y., Lee, H., Kim, K., Deng, X., and Kwak, S. (2009). Analysis of antioxidant enzyme activity during germination of alfalfa under salt and drought stresses. *Plant Physiol. Biochem. 47*(7), 570-577.

Youssefian, S., Nakamura, M., Orudgev, E., and Kondo, N. (2001). Increased cysteine biosynthesis capacity of transgenic tobacco overexpressing an O-acetylserine (thiol) lyase modifies plant responses to oxidative stress. *Plant Physiol.126*(3), 1001-1011.

Zhu, J., Fu, X., Koo, Y. D., Zhu, J. K., Jenney, F. E., Adams, M. W., et al. (2007). An enhancer mutant of Arabidopsis salt overly sensitive 3 mediates both ion homeostasis and the oxidative stress response. *Mol. Cell Biol. 27*:5214– 5224.

Zuchi, S., Cesco, S., and Astolfi, S. (2012). High S supply improves Fe accumulation in durum wheat plants grown under Fe limitation. *Environ. Exp. Bot. 77,* 25-32.

Chapter 7

Conclusions

Human world population is expected to increase to 9.7 billion by 2050 and 11.2 billion by 2100 (UN 2015), and a key challenge is to provide food and feed in an equitable, healthy, and sustainable manner (Beddington, 2010). Access to adequate and nutritious food is essential to human wellbeing, but to reach this objective global food production needs to increase by 70% by 2050. A healthy soil is the major factor for agriculture production, but soil resources are finite and non-renewable over the human time scale. Both natural forces and mostly anthropogenic activities (e.g., deforestation, drainage, tillage, ecc) led to soil degradation and consequently to limited access to high-quality soil for provisioning of essential ecosystem services. The scarcity of healthy soil to obtain the required food production will thus imply the exploitation of marginal agricultural land, characterized by depletion of organic matter and nutrients, elemental imbalance leading to deficiency or toxicity, salinization, water-air imbalance, ecc. (Scherr, 1999; Tilman et al, 2002).

Climate change will superimpose on these conditions in various regions of the world, including Europe, and in particular the Mediterranean area. Satisfying increased demands in agriculture with existing farming practices is likely to lead to more intense competition for natural resources, increased greenhouse gas emissions, and further deforestation and land degradation. This condition is even more dramatic by comparing agricultural productivity between high-income and low-income countries.

The dramatic climate changes have enhanced the agriculture challenges of increasing food production, mitigating climate change and restoring landscapes (Beddington, 2010).

Over the last 50 years, the combined outcome of significant reductions in S emission from industrial sources, use of mineral fertilizers without S, decreases in use of organic fertilizers, and changes in cropping systems including the use of high yielding commercial coupled with intensive management practices (Grant et al., 2012) have led to a widespread S deficiency in soils at the global scale (Blake-Kalff et al., 2001; McNeill et al., 2005). Until then, soils deficient in S were not historically known and consequently plant S nutrition was not commonly researched and discussed.

In the past two decades, much progress has been made in plant S nutrition research, and the knowledge of S metabolism has increased exponentially (Kopriva et al., 2019).

Most studies emphasized potential agronomical, ecological, and nutritional benefits of S, being crucial for many fundamental metabolic processes and to maintain crop production and quality. On the other hand, other important aspects have been recently highlighted, related to S exclusive

properties. Sulfur is indeed not only essential for optimal plant growth, development and crop productivity, but also for its contribution to the mitigation of stressful conditions in plants and, more importantly, for its integration with other nutrient uptake and metabolic pathways.
As a result, plant physiological responses to environmental stresses, such as nutrient deficiency or toxicity, could be modified and even hampered by S deficiency.
These evidences highlight the importance to discuss the interactions S has with other elements (essential or not) in the rhizosphere.
Depletion of nutrients, elemental toxicity and salinization represent common stress factors that plants commonly experience in their natural habitat and most important limiting factors for agricultural production.
Therefore, in this thesis, S implications on physiological responses to soil Fe deficiency, Cu pollution and Na accumulation were studied.

The study of the regulatory mechanisms underlying S and Fe interplay has allowed us to obtain highly innovative results. Through the analysis of exudation pattern in tomato roots, the presence of 3-hydroxymugineic acid, an organic compound belonging to the class of phytosiderophores (PS), has been clearly detected. It is well known that the secretion of PS is typical of Strategy II plants (only grasses). Thus, the presence of 3-hydroxymugineic acid in tomato root exudates (Strategy I) support the hypothesis that the distinction between the two mechanisms/strategies could not be so sharp (Grillet & Schmidt, 2019). Furthermore, new mechanisms of perception of nutritional stress were revealed. In particular, by using a split-root system it has been demonstrated that an endogenous variation in citric acid concentration might be involved in the regulation of Fe/S interaction, being citric acid produced in mitochondria, where the assembly of Fe–S clusters also occurs (Balk and Pilon, 2011).
Finally, obtained results revealed that citrate could play a relevant role as TOR inducer, at least in tomato. Indeed, Fe deficiency elicited an increase of Target of Rapamycin (TOR) activity in tomato shoots associated to enhanced accumulation of citrate in the same tissue, whereas S deficiency resulted in decreased TOR activity and citrate accumulation. In addition, we found that citrate accumulated in shoots of plants exposed to combined S/Fe deficiency assumed values between those found in F and S plants, as well as TOR activity.

By addressing Cu connections with sulfate assimilation, it has been demonstrated that Cu toxicity is not only dose dependent, but also rely on the regulation of plant nutritional status and, more importantly, on the modulation of S assimilation pathway.

By addressing Na connections with sulfate assimilation, it may be concluded that S metabolism is necessarily modulated for alleviating the adverse effects of salt stress. Linear correlation between salt stress and OASTL activity provides evidence that S assimilation pathway clearly plays a key role in adaptive response of olive plants under salt stress conditions.

Taken together these results could contribute to the development of crop management strategies which exploit the potential and sustainable use of S nutrition to improve plant adaptation to marginal lands, particularly vulnerable to climate change and characterized by natural resources limitation.

Results could specifically contribute to minimize Fe deficiency by modulating S supply without additional input of Fe fertilizers. The reduction of fertilizer amounts to be applied will allow a reduction of costs for farmers as well as reduction of environmental impact.

Furthermore, these results will positively impact on food security production. This could lead to a decrease, in the long term, of chemical inputs, getting healthier food and respecting the surrounding environment of the cultivated crops, as well as the health of the agricultural worker.

Finally, obtained results bring attention to the need to further investigate interactions among the various mineral elements in order to understand how the different sensing and signaling pathways activated in response to changes in availability of one element are coordinately integrated with those of other elements. A better knowledge of the mechanisms of nutrient interactions could provide a promising tool to face many challenges, including water quality, pollution remediation, food and fiber production.

References

Ali, A., Maggio, A., Bressan, R. A., Yun, D. J. (2019). Role and functional differences of HKT1-type transporters in plants under salt stress. *International journal of molecular sciences*, *20*(5), 1059.

Amir, R. (2010). Current understanding of the factors regulating methionine content in vegetative tissues of higher plants. *Amino acids*, *39*(4), 917-931.

Amtmann, A.,Sanders, D. (1999). Mechanisms of Na^+ uptake by plant cells. In *Advances in botanical research* (Vol. 29, pp. 75-112). Academic Press.

Angelini, L. G., Ceccarini, L., Bonari, E. (2005). Biomass yield and energy balance of giant reed (Arundo donax L.) cropped in central Italy as related to different management practices. *European journal of agronomy*, *22*(4), 375-389.

Ashfaque, F., Khan, M. I. R., Khan, N. A. (2014). Exogenously applied H_2O_2 promotes proline accumulation, water relations, photosynthetic efficiency and growth of wheat *(Triticum aestivum L.*) under salt stress. *Annual Research & Review in Biology*, 105-120.

Astolfi S., Cesco S., Zuchi S., Neumann G., Römheld V. (2006) Sulfur starvation reduces phytosiderophores release by iron-deficient barley plants. *Soil Science and Plant Nutrition* 52, 43-48.

Astolfi, S., Zuchi, S., Hubberten, H. M., Pinton, R., Hoefgen, R. (2010). Supply of sulphur to S-deficient young barley seedlings restores their capability to cope with iron shortage. *Journal of experimental botany*, 61(3), 799-806.

Baffes, J., T. Haniotis, 2010. *Placing the 2006/07 Commodity Price Boom into Perspective*, The World Bank Development Prospects Group, Working Per 5371, July.

Balk, J., Lobréaux, S. (2005). Biogenesis of iron–sulfur proteins in plants. *Trends in plant science*, *10*(7), 324-331.

Balk, J., Pilon, M. (2011). Ancient and essential: the assembly of iron–sulfur clusters in plants. *Trends in plant science*, *16*(4), 218-226.

Balk, J., Schaedler, T. A. (2014). Iron cofactor assembly in plants. *Annual review of plant biology*, *65*, 125-153.

Ballabio, C., Panagos, P., Lugato, E., Huang, J. H., Orgiazzi, A., Jones, A., Fernández-Ugalde, O., Borrelli, P., Montanarella, L. (2018). Copper distribution in European topsoils: An assessment based on LUCAS soil survey. *Science of the Total Environment*, *636*, 282-298.

Barker, A. V., & Pilbeam, D. J. (2007). Handbook of plant nutrition, CRC.

Barthakur, S. B. V. B., Babu, V., Bansa, K. C. (2001). Over-expression of osmotin induces proline accumulation and confers tolerance to osmotic stress in transgenic tobacco. *Journal of Plant Biochemistry and Biotechnology*, *10*(1), 31-37.

Beddington, J. (2010). Food security: contributions from science to a new and greener revolution. *Philosophical Transactions of the Royal Society B: Biological Sciences*, *365*(1537), 61-71.

Blake-Balff, M. M., Zhao, F. J., Hawkesford, M. J., McGrath, S. P. (2001). Using plant analysis to predict yield losses caused by sulphur deficiency. *Annals of Applied Biology*, 138(1), 123-127.

Blake-Kalff M.M.A., Zhao F.J., Hawkesford M.J., McGrath S.P. (2001). Using plant analysis to predict yield losses caused by sulphur deficiency. *Annals of Applied Biology*, *138*(1), 123-127.

Bocchini, M., Bartucca, M. L., Ciancaleoni, S., Mimmo, T., Cesco, S., Pii, Y., Albertini E., Del Buono, D. (2015). Iron deficiency in barley plants: phytosiderophore release, iron translocation, and DNA methylation. *Frontiers in plant science*, 6, 514.

Bouranis, D. L., Chorianopoulou, S. N., Protonotarios, V. E., Siyiannis, V. F., Hopkins, L., Hawkesford, M. J. (2003). Leaf Responses of Young Iron-Inefficient Maize Plants to Sulfur Deprivation. *Journal of plant nutrition*, *26*(6), 1189-1202.

Briat, J. F. (2009). Mechanisms of iron homeostasis in plants and their regulations.

Briat, J. F., Curie, C., Gaymard, F. (2007). Iron utilization and metabolism in plants. *Current opinion in plant biology*, *10*(3), 276-282.

Briat, J. F., Vert, G. (2004). Acquisition et gestion du fer par les plantes. *Cahiers agricultures*, *13*(2), 183-201.

Brunetto G., Wellington Bastos de Melo G., Terzano R., Del Buono D., Astolfi S., Tomasi N., Pii Y., Mimmo T., Cesco S. (2016). Copper accumulation in vineyard soils: Rhizosphere processes and agronomic practices to limit its toxicity. *Chemosphere*, *162*, 293-307.

Buchner, P., Takahashi, H., Hawkesford, M. J. (2004). Plant sulphate transporters: co-ordination of uptake, intracellular and long-distance transport. *Journal of experimental botany*, *55*(404), 1765-1773.

Bürstenbinder, K., Rzewuski, G., Wirtz, M., Hell, R., Sauter, M. (2007). The role of methionine recycling for ethylene synthesis in Arabidopsis. *The Plant Journal*, *49*(2), 238-249.

Butow, R. A., Avadhani, N. G. (2004). Mitochondrial signaling: the retrograde response. Molecular cell, 14(1), 1-15.

Cao, Z. H., & Hu, Z. Y. (2000). Copper contamination in paddy soils irrigated with wastewater. *Chemosphere*, *41*(1-2), 3-6.

Capaldi, F. R., Gratão, P. L., Reis, A. R., Lima, L. W., & Azevedo, R. A. (2015). Sulfur metabolism and stress defense responses in plants. *Tropical plant biology*, *8*(3-4), 60-73.

Celletti S, Pii Y, Mimmo T, Cesco S, Astolfi S. 2016b. The characterization of the adaptive responses of durum wheat to different Fe availability highlights an optimum Fe requirement threshold. Plant Physiology and Biochemistry 109: 300–307.

Cesco, S., Neumann, G., Tomasi, N., Pinton, R., Weisskopf, L. (2010). Release of plant-borne flavonoids into the rhizosphere and their role in plant nutrition. *Plant and Soil*, *329*(1-2), 1-25.

Chen, D., Shao, Q., Yin, L., Younis, A., Zheng, B. (2019). Polyamine function in plants: metabolism, regulation on development, and roles in abiotic stress responses. *Frontiers in plant science*, *9*, 1945.

Ciaffi, M., Paolacci, A. R., Celletti, S., Catarcione, G., Kopriva, S., Astolfi, S. (2013). Transcriptional and physiological changes in the S assimilation pathway due to single or combined S and Fe deprivation in durum wheat (Triticum durum L.) seedlings. *Journal of experimental botany*, *64*(6), 1663-1675.

Clarkson, D. T. (1993). Roots and the delivery of solutes to the xylem. *Philosophical Transactions of the Royal Society of London. Series B: Biological Sciences*, *341*(1295), 5-17.

Cobbett, C. S. (2000). Phytochelatins and their roles in heavy metal detoxification. *Plant physiology*, *123*(3), 825-832.

Coppa, E., Celletti, S., Pii, Y., Mimmo, T., Cesco, S., Astolfi, S. (2018). Revisiting Fe/S interplay in tomato: A split-root approach to study the systemic and local responses. *Plant science*, *276*, 134-142.

Crawford NM, Kahn M, Leustek T, Long SR (2000) Nitrogen and sulfur. In *Biochemistry and Molecular Biology of Plants*; Buchanan BB, Gruissem W, Jones RL, eds, pp 787-849. American Association of Plant Physiologists: Rockville, MD, US

Dakora, F. D., Phillips, D. A. (2002). Root exudates as mediators of mineral acquisition in low-nutrient environments. In *Food Security in Nutrient-Stressed Environments: Exploiting Plants' Genetic Capabilities* (pp. 201-213). Springer, Dordrecht.

Davidian, J. C., Kopriva, S. (2010). Regulation of sulfate uptake and assimilation—the same or not the same? *Molecular Plant*, 3(2), 314-325.

Demirevska-Kepova, K., Simova-Stoilova, L., Stoyanova, Z., Hölzer, R., Feller, U. (2004). Biochemical changes in barley plants after excessive supply of copper and manganese. *Environmental and Experimental Botany*, *52*(3), 253-266.

Directive 2009/28/EC of the European Parliament and of the Council of 23 April 2009 on the promotion of the use of energy from renewable sources and amending and subsequently repealing Directives 2001/77/EC and 2003/30/EC

Dong, Y., Silbermann, M., Speiser, A., Forieri, I., Linster, E., Poschet, G., Allboje Samami, A., Wanatabe, M., Sticht, C., Teleman, A. A. , Deragon J. M., Saito K., Hell R., Wirtz M. (2017). Sulfur availability regulates plant growth via glucose-TOR signaling. *Nature communications, 8(1), 1-10.*

Eckhardt, U., Marques, A. M., Buckhout, T. J. (2001). Two iron-regulated cation transporters from tomato complement metal uptake-deficient yeast mutants. *Plant molecular biology*, *45*(4), 437-448.

Eide, D., Broderius, M., Fett, J., Guerinot, M. L. (1996). A novel iron-regulated metal transporter from plants identified by functional expression in yeast. *Proceedings of the National Academy of Sciences*, *93*(11), 5624-5628.

El-Baz, F. K., Mohamed, A. A., Aboul-Enein, A. M., Salama, Z. A. (2004). Alteration in root exudates level during Fe deficiency in two cucumber cultivars. *International Journal of Agriculture and Biology*, *6*, 45-48.

Elhawat N., Alshaal T., Domokos-Szabolcsy É., el-Ramady H., Antal G., Márton L., Czakó M., Balogh P., Fári M. (2015). Copper uptake efficiency and its distribution within bioenergy grass giant reed. *Bulletin of environmental contamination and toxicology*, *95*(4), 452-458.

Elhawat N., Alshaal T., Domokos-Szabolcsy É., el-Ramady H., Márton L., Czakó M., Kátai J., Balogh P., Sztrik A., Molnár M., Popp J., Fári M.G. (2014). Phytoaccumulation potentials of two biotechnologically propagated ecotypes of *Arundo donax* in copper-contaminated synthetic wastewater. *Environmental Science and Pollution Research*, *21*(12), 7773-7780.

Eppendorfer, W. H., Eggum, B. O. (1992). Dietary fibre, sugar, starch and amino acid content of kale, ryegrass and seed of rape and field beans as influenced by S-and N-fertilization. *Plant foods for human nutrition*, *42*(4), 359-371..

Eppendorfer, W. H., Eggum, B. R. O. (1994). Dietary fibre, starch, amino acids and nutritive value of potatoes as affected by sulfur, nitrogen, phosphorus, potassium, calcium and water stress. *Acta Agriculturae Scandinavica B-Plant Soil Sciences*, *44*(2), 107-115.

Fageria, V. D. (2001). Nutrient interactions in crop plants. *Journal of plant nutrition*, *24*(8), 1269-1290.

Fagnano, M., Boccia L., Pindozzi S., Infascelli R., Faugno S. (2012). Aree potenzialmente convertibili a colture energetiche: caso studio della Regione Campania, in. *XLI Convegno Società Italiana di Agronomia*, Bari, September19–21, pp. 464-466.

FAO and ITPS. (2015). Status of the World's Soil Resources (SWSR) – Main Report. Food and Agriculture Organization of the United Nations and Intergovernmental Technical Panel on Soils, Rome, Italy

FAO. (2000). The State of Food and Agriculture Food and Agriculture Organization of the United Nations, Rome

FAO-UNESCO. (1974). Soil map of the world. Food and Agriculture Food and Agriculture Organization of the United Nations, Paris

Fatma, M., Asgher, M., Masood, A., Khan, N. A. (2014). Excess sulfur supplementation improves photosynthesis and growth in mustard under salt stress through increased production of glutathione. *Environmental and experimental botany*, *107*, 55-63.

Forieri, I., Wirtz, M., Hell, R. (2013). Toward new perspectives on the interaction of iron and sulfur metabolism in plants. *Frontiers in Plant Science*, *4*, 357.

Fourcroy P., Sisó-Terraza P., Sudre D., Savirón M., Reyt G., Gaymard F., Abadía A., Abadia J., Álvarez-Fernández A., Briat J-F. (2014). Involvement of the ABCG 37 transporter in

secretion of scopoletin and derivatives by *Arabidopsis* roots in response to iron deficiency. *New Phytologist*, *201*(1), 155-167

Foyer, C. H., Noctor, G. (2011). Ascorbate and glutathione: the heart of the redox hub. *Plant physiology*, *155*(1), 2-18.

Foyer, C. H., Noctor, G. (2009). Redox regulation in photosynthetic organisms: signaling, acclimation, and practical implications. *Antioxidants & redox signaling*, *11*(4), 861-905.

Freney, J. R., Williams, C. H. (1983). The sulfur cycle in soil. Chapter 3. Pages 129–201 In: Ivanov MV and Freney JR (ed) The global biogeochemical sulfur cycle, SCOPE 19.

García, M. J., Romera, F. J., Lucena, C., Alcántara, E., Pérez-Vicente, R. (2015). Ethylene and the regulation of physiological and morphological responses to nutrient deficiencies. *Plant physiology*, *169*(1), 51-60.

Germida, J. J., Wainwright, M. I. L. T. O. N., Gupta, V. V. S. R. (1992). Biochemistry of sulfur cycling in soil. *Soil biochemistry*, *7*, 1-53.

Gigolashvili, T., & Kopriva, S. (2014). Transporters in plant sulfur metabolism. *Frontiers in Plant Science*, *5*, 442.

Gilabel, A. P., Nogueirol, R. C., Garbo, A. I., Monteiro, F. A. (2014). The role of sulfur in increasing guinea grass tolerance of copper phytotoxicity. *Water, Air, & Soil Pollution*, *225*(1), 1806.

Giraud, E., Ho, L. H., Clifton, R., Carroll, A., Estavillo, G., Tan, Y. F., Howell .KA., Ivanova A., Pogson B.J., Millar A.H., Whelan, J. (2008). The absence of ALTERNATIVE OXIDASE1a in Arabidopsis results in acute sensitivity to combined light and drought stress. *Plant physiology*, *147*(2), 595-610.

Grant, C. A., Mahli, S. S., Karamanos, R. E. (2012). Sulfur management for rapeseed. *Field Crops Research*, *128*, 119-128.

Grillet, L., Schmidt, W. (2019). Iron acquisition strategies in land plants: not so different after all. *New Phytologist*, *224*(1), 11-18.

Guerinot, M. L., Yi, Y. (1994). Iron: nutritious, noxious, and not readily available. *Plant Physiology*, *104*(3), 815.

Haag, A.F., Kerscher, B., Dall'Angelo, S., Sani, M., Longhi, R., Baloban, M., Wilson, H.M., Mergaert, P., Zanda, M., and Ferguson, G.P. (2012). Role of cysteine residues and disulfide bonds in the activity of a legume root nodule-specific, cysteinerich peptide. *Journal of Biological Chemistry*. 287, 10791–10798.

Habtegebrial, K., Singh, B. R. (2006). Effects of timing of nitrogen and sulphur fertilizers on yield, nitrogen, and sulphur contents of Tef (Eragrostis tef (Zucc.) Trotter). *Nutrient cycling in agroecosystems*, *75*(1-3), 213-222.

Haneklaus S., Bloem E., Schnug E. (2008). History of sulfur deficiency in crops. Sulfur: A missing link between soils, crops, and nutrition, ed J Jez. Soil Science Society of America, Madison, WI, pp 45–58.

Haneklaus, S., Bloem, E., Schnug, E. (2007). Sulfur interactions in crop ecosystems. In *Sulfur in Plants An Ecological Perspective* (pp. 17-58). Springer, Dordrecht.

Haneklaus, S., Bloem, E., Schnug, E. (2000). Sulphur in agroecosystems. *Folia Universitatis Agriculturae Stetinensis, Agricultura*, (81), 17-31.

Hawkesford M.J., Kopriva S., De Kok L.J. (2014). Nutrient use efficiency in plants concepts and approaches. Springer International Publishing, Switzerland.

Hawkesford, M. J. (2000). Plant responses to sulphur deficiency and the genetic manipulation of sulphate transporters to improve S-utilization efficiency. *Journal of Experimental Botany*, *51*(342), 131-138.

Hawkesford, M. J. (2003). Transporter gene families in plants: the sulphate transporter gene family—redundancy or specialization? *Physiologia Plantarum*, *117*(2), 155-163.

Hawkesford, M. J. (2017). Sulfate Transport in Plants: A Personal Perspective. In *Sulfur Metabolism in Higher Plants-Fundamental, Environmental and Agricultural Aspects*, 3-12.

Hawkesford, M. J., De Kok, L. J. (2006). Managing sulphur metabolism in plants. *Plant, Cell & Environment*, *29*(3), 382-395

Hawkesford, Malcolm J., Luit J. De Kok. *Sulfur in plants*. Vol. 6. London: Springer, 2007.

He, Z. L., Fan, J. H., Yang, X. E., and Stoffella, P. J. (2009). Effect of copper contamination on soil quality and transport to the environment. In *Progress in Environmental Science and Technology*, Vol II, *PTS A and B*, eds S. C. Li, Y. J. Wang, F. X. Cao, P. Huang, and Y. Zhang (Marrickville: Science Press) 1892–1898

Heiss, S., Wachter, A., Bogs, J., Cobbett, C., Rausch, T. (2003). Phytochelatin synthase (PCS) protein is induced in Brassica juncea leaves after prolonged Cd exposure. *Journal of Experimental Botany*, *54*(389), 1833-1839.

Hell, R., Stephan, U. W. (2003). Iron uptake, trafficking and homeostasis in plants. *Planta*, *216*(4), 541-551.

Hesse, H., Hoefgen, R. (2003). Molecular aspects of methionine biosynthesis. *Trends in plant science*, *8*(6), 259-262

Hesse, H., Nikiforova, V., Gakière, B., Hoefgen, R. (2004). Molecular analysis and control of cysteine biosynthesis: integration of nitrogen and sulphur metabolism. *Journal of Experimental Botany*, *55*(401), 1283-1292.

Hoefgen, R., Hesse, H. (2007). Sulfur in plants as part of a metabolic network. In *Sulfur in Plants An Ecological Perspective* (pp. 107-142). Springer, Dordrecht.

Huang, Q., Wang, M., Xia, Z. (2018). The SULTR gene family in maize (Zea mays L.): gene cloning and expression analyses under sulfate starvation and abiotic stress. *Journal of plant physiology*, *220*, 24-33.

Husaini, A. M., Abdin, M. Z. (2008). Overexpression of tobacco osmotin gene leads to salt stress tolerance in strawberry (*Fragaria× ananassa* Duch.) plants. *Indian Journal of Biotechnology*, *7*: 465-471.

Kalmbacher, R. S., Ezenwa, I. V., Arthington, J. D., Martin, F. G. (2005). Sulfur fertilization of bahiagrass with varying levels of nitrogen fertilization on a Florida Spodosol. *Agronomy Journal*, 97(3), 661-667.

Kataoka, T., Watanabe-Takahashi, A., Hayashi, N., Ohnishi, M., Mimura, T., Buchner, P., Hawkesford, M. J., Yamaya, T., Takahashi, H. (2004). Vacuolar sulfate transporters are essential determinants controlling internal distribution of sulfate in Arabidopsis. *The Plant Cell*, *16*(10), 2693-2704..

Kawashima, C. G., Matthewman, C. A., Huang, S., Lee, B. R., Yoshimoto, N., Koprivova, A., Rubio-Somoza, I., Todesco, M., Rathjen, T., Saito, K., Takahashi, H., Dalmay, T., Kopriva, S. (2011). Interplay of SLIM1 and miR395 in the regulation of sulfate assimilation in Arabidopsis. *The Plant Journal*, *66*(5), 863-876.

Ke, W., Xiong, Z. T., Chen, S., Chen, J. (2007). Effects of copper and mineral nutrition on growth, copper accumulation and mineral element uptake in two Rumex japonicus populations from a copper mine and an uncontaminated field sites. *Environmental and Experimental Botany*, *59*(1), 59-67.

Khan, M. H., Panda, S. K. (2008). Alterations in root lipid peroxidation and antioxidative responses in two rice cultivars under NaCl-salinity stress. *Acta Physiologiae Plantarum*, *30*(1), 81.

Khan, N. A., Khan, M. I. R., Asgher, M., Fatma, M., Masood, A., Syeed, S. (2014). Salinity tolerance in plants: revisiting the role of sulfur metabolites. *Journal of Plant Biochemistry & Physiology*, *2*(120), 2.

Kim, S. A., Guerinot, M. L. (2007). Mining iron: iron uptake and transport in plants. *FEBS letters*, 581(12), 2273-2280.

Klein, M., & Papenbrock, J. (2004). The multi-protein family of Arabidopsis sulphotransferases and their relatives in other plant species. *Journal of experimental botany*, *55*(404), 1809-1820.

Kobayashi, T., Nishizawa, N. K. (2012). Iron uptake, translocation, and regulation in higher plants. *Annual review of plant biology*, *63*, 131-152

Kobayashi, T., Nozoye, T., Nishizawa, N. K. (2019). Iron transport and its regulation in plants. *Free Radical Biology and Medicine*, *133*, 11-20.

Kocsy, G., Szalai, G., Galiba, G. (2004). Effect of osmotic stress on glutathione and hydroxymethylglutathione accumulation in wheat. *Journal of plant physiology*, *161*(7), 785-794.

Komárek, M., Čadková, E., Chrastný, V., Bordas, F., Bollinger, J. C. (2010). Contamination of vineyard soils with fungicides: a review of environmental and toxicological aspects. *Environment international*, *36*(1), 138-151.

Kopriva, S. (2006). Regulation of sulfate assimilation in Arabidopsis and beyond. *Annals of botany*, *97*(4), 479-495.

Kopriva, S. (2017). Quo Vadis Sulfur Investigation?: 25 Years of Research into Plant Sulfate Reduction. In *Sulfur Metabolism in Higher Plants-Fundamental, Environmental and Agricultural Aspects* (pp. 13-30). Springer, Cham.

Kopriva, S., Malagoli, M., Takahashi, H. (2019). Sulfur nutrition: impacts on plant development, metabolism, and stress responses. *Journal of Experimental Botany, 70*, 4069–4073.

Kopriva, S., Mugford, S. G., Matthewman, C., Koprivova, A. (2009). Plant sulfate assimilation genes: redundancy versus specialization. *Plant cell reports*, *28*(12), 1769-1780.

Kopriva, S., Mugford, S. G., Matthewman, C., Koprivova, A. (2009). Plant sulfate assimilation genes: redundancy versus specialization. *Plant cell reports*, *28*(12), 1769-1780.

Koprivova, A., Suter, M., den Camp, R. O., Brunold, C., Kopriva, S. (2000). Regulation of sulfate assimilation by nitrogen in Arabidopsis. *Plant Physiology*, *122*(3), 737-746.

Kupper, H., Kroneck, P. M. (2005). Heavy metal uptake by plants and cyanobacteria. *Metal ions in biological systems*, *44*, 97.

Küpper, H., Küpper, F. C., Spiller, M. (2006). [Heavy metal]-chlorophylls formed in vivo during heavy metal stress and degradation products formed during digestion, extraction and storage of plant material. In *Chlorophylls and bacteriochlorophylls* (pp. 67-77). Springer, Dordrecht.

Lejay, L., Wirth, J., Pervent, M., Cross, J. M. F., Tillard, P., Gojon, A. (2008). Oxidative pentose phosphate pathway-dependent sugar sensing as a mechanism for regulation of root ion transporters by photosynthesis. *Plant physiology*, *146*(4), 2036-2053.

Leustek, T., Martin, M. N., Bick, J. A., Davies, J. P. (2000). Pathways and regulation of sulfur metabolism revealed through molecular and genetic studies. *Annual review of plant biology*, *51*(1), 141-165.

Lewandowska, M., Sirko, A. (2008). Recent advances in understanding plant response to sulfur-deficiency stress. *Acta Biochimica Polonica*, *55*(3), 457-471.

Li, L., Cheng, X., Ling, H. Q. (2004). Isolation and characterization of Fe (III)-chelate reductase gene LeFRO1 in tomato. *Plant molecular biology*, *54*(1), 125-136.

Li, X., Li, C. (2004). Is ethylene involved in regulation of root ferric reductase activity of dicotyledonous species under iron deficiency? *Plant and soil*, *261*(1-2), 147-153.

Lingam, S., Mohrbacher, J., Brumbarova, T., Potuschak, T., Fink-Straube, C., Blondet, E., Genschik, P., Bauer, P. (2011). Interaction between the bHLH transcription factor FIT and ETHYLENE INSENSITIVE3/ETHYLENE INSENSITIVE3-LIKE1 reveals molecular linkage

between the regulation of iron acquisition and ethylene signaling in Arabidopsis. *The Plant Cell*, *23*(5), 1815-1829.

Lobreaux, S., Briat, J. F. (1991). Ferritin accumulation and degradation in different organs of pea (Pisum sativum) during development. *Biochemical Journal*, *274*(2), 601-606.

López-Millán, A. F., Duy, D., Philippar, K. (2016). Chloroplast iron transport proteins–function and impact on plant physiology. *Frontiers in plant science*, *7*, 178.

Lucena, C., Romera, F. J., García, M. J., Alcántara, E., Pérez-Vicente, R. (2015). Ethylene participates in the regulation of Fe deficiency responses in Strategy I plants and in rice. *Frontiers in plant science*, *6*, 1056.

Luna, C. M., González, C. A., Trippi, V. S. (1994). Oxidative damage caused by an excess of copper in oat leaves. *Plant and Cell Physiology*, *35*(1), 11-15.

Maathuis, F. J. (2014). Sodium in plants: perception, signalling, and regulation of sodium fluxes. *Journal of Experimental Botany*, *65*(3), 849-858.

Mapolelo, D. T., Zhang, B., Randeniya, S., Albetel, A. N., Li, H., Couturier, J. E., Outten, C.E., Rouhier, N., Johnson, M. K. (2013). Monothiol glutaredoxins and A-type proteins: partners in Fe–S cluster trafficking. *Dalton transactions*, *42*(9), 3107-3115.

Marschner, H. (1995). Mineral nutrition of higher plants 2nd edition. *Academic, Great Britain*.

Marschner, H. (2012). Marschner's mineral nutrition of higher plants. Vol. 89.

Marschner, H., Romheld, V., Azarabadi, S. (1978). Iron stress response of efficient and inefficient plant species. *Plant nutrition*, 319-327.

Marschner, H., Römheld, V., Horst, W. J., Martin, P. (1986). Root-induced changes in the rhizosphere: Importance for the mineral nutrition of plants. *Zeitschrift für Pflanzenernährung und Bodenkunde*, *149*(4), 441-456.

Mathot, M., Mertens, J., Verlinden, G., Lambert, R. (2008). Positive effects of sulphur fertilisation on grasslands yields and quality in Belgium. *European Journal of Agronomy*, *28*(4), 655-658.

McFarlane, D. J., George, R. J., Barrett-Lennard, E. G., Gilfedder, M. (2016). Salinity in dryland agricultural systems: challenges and opportunities. In *Innovations in dryland agriculture* (pp. 521-547). Springer, Cham.

McGrath, S. P., & Zhao, F. J. (1995). A risk assessment of sulphur deficiency in cereals using soil and atmospheric deposition data. *Soil Use and Management*, *11*(3), 110-114.

McGrath, S. P., Zhao, F. J., & Withers, P. J. A. (1996). Development of sulphur deficiency in crops and its treatment. *Proceedings-Fertiliser Society (United Kingdom)*.

McNeill, A. M., Eriksen, J., Bergström, L., Smith, K. A., Marstorp, H., Kirchmann, H., & Nilsson, I. (2005). Nitrogen and sulphur management: challenges for organic sources in temperate agricultural systems. *Soil Use and Management*, *21*(1), 82-93.

Mengel, K. (1994). Iron availability in plant tissues-iron chlorosis on calcareous soils. *Plant and soil*, *165*(2), 275-283.

Mimmo et al., 2008; Mimmo, T., Ghizzi, M., Marzadori, C., Gessa, C. E. (2008). Organic acid extraction from rhizosphere soil: effect of field-moist, dried and frozen samples. *Plant and soil*, *312*(1-2), 175-184.

Molassiotis, A., Therios, I., Dimassi, K., Diamantidis, G., Chatzissavvidis, C. (2005). Induction of Fe (III)-chelate reductase activity by ethylene and salicylic acid in iron-deficient peach rootstock explants. *Journal of plant nutrition*, *28*(4), 669-682.

Mori, S., Nishizawa, N. (1987). Methionine as a dominant precursor of phytosiderophores in Graminaceae plants. *Plant and Cell Physiology*, 28(6), 1081-1092. ISO 690

Morrissey, J., Guerinot, M. L. (2009). Iron uptake and transport in plants: the good, the bad, and the ionome. *Chemical reviews*, *109*(10), 4553-4567

Nagajyoti, P. C., Lee, K. D., Sreekanth, T. V. M. (2010). Heavy metals, occurrence and toxicity for plants: a review. *Environmental chemistry letters*, *8*(3), 199-216.

Nazar, R., Umar, S., Khan, N. A., Sareer, O. (2015). Salicylic acid supplementation improves photosynthesis and growth in mustard through changes in proline accumulation and ethylene formation under drought stress. *South African Journal of Botany*, 98, 84-94.

Nielsen, H. D., Brownlee, C., Coelho, S. M., Brown, M. T. (2003). Inter-population differences in inherited copper tolerance involve photosynthetic adaptation and exclusion mechanisms in Fucus serratus. *New Phytologist*, *160*(1), 157-165..

Nikiforova, V. J., Gakiere, B., Kempa, S., Adamik, M., Willmitzer, L., Hesse, H., Hoefgen, R. (2004). Towards dissecting nutrient metabolism in plants: a systems biology case study on sulphur metabolism. *Journal of Experimental Botany*, *55*(404), 1861-1870.

Nikolic, M., Kastori, R. (2000). Effect of bicarbonate and Fe supply on Fe nutrition of grapevine. *Journal of Plant Nutrition*, *23*(11-12), 1619-1627.

Noctor, G. (2006). Metabolic signalling in defence and stress: the central roles of soluble redox couples. *Plant, Cell & Environment*, *29*(3), 409-425

Noctor, G., Arisi, A. C. M., Jouanin, L., Kunert, K. J., Rennenberg, H., Foyer, C. H. (1998). Glutathione: biosynthesis, metabolism and relationship to stress tolerance explored in transformed plants. *Journal of Experimental Botany*, *49*(321), 623-647.

North, K. A., & Kopriva, S. (2007). Sulfur in resistance to environmental stresses. In *Sulfur in Plants An Ecological Perspective* (pp. 143-168). Springer, Dordrecht.

Nozoye, T., Nagasaka, S., Kobayashi, T., Takahashi, M., Sato, Y., Sato, Y., Uozimi, N., Nakanishi, H., Nishizawa, N. K. (2011). Phytosiderophore efflux transporters are crucial for iron acquisition in graminaceous plants. *Journal of Biological Chemistry*, *286*(7), 5446-5454.

Ouzounidou, G., Čiamporová, M., Moustakas, M., Karataglis, S. (1995). Responses of maize (Zea mays L.) plants to copper stress—I. Growth, mineral content and ultrastructure of roots. *Environmental and Experimental Botany*, *35*(2), 167-176.

Pala, Z. R., Saxena, V., Saggu, G. S., Garg, S. (2018). Recent Advances in the [Fe–S] Cluster Biogenesis (SUF) Pathway Functional in the Apicoplast of Plasmodium. *Trends in parasitology*, *34*(9), 800-809.

Paolacci, A. R., Celletti, S., Catarcione, G., Hawkesford, M. J., Astolfi, S., Ciaffi, M. (2014). Iron deprivation results in a rapid but not sustained increase of the expression of genes involved in iron metabolism and sulfate uptake in tomato (Solanum lycopersicum L.) seedlings. *Journal of integrative plant biology*, *56*(1), 88-100.

Pietrzak, U., Uren, N. C. (2011). Remedial options for copper-contaminated vineyard soils. *Soil Research*, *49*(1), 44-55.

Pii, Y., Penn, A., Terzano, R., Crecchio, C., Mimmo, T., Cesco, S. (2015). Plant-microorganism-soil interactions influence the Fe availability in the rhizosphere of cucumber plants. *Plant Physiology and BiochemistryBiochemistry* 87: 45–52.

Printz, B., Lutts, S., Hausman, J. F., Sergeant, K. (2016). Copper trafficking in plants and its implication on cell wall dynamics. *Frontiers in plant science*, *7*, 601.

Puig, S. (2014). Function and regulation of the plant COPT family of high-affinity copper transport proteins. *Advances in Botany*, *2014*

Queval, G., Thominet, D., Vanacker, H., Miginiac-Maslow, M., Gakière, B., Noctor, G. (2009). H2O2-activated up-regulation of glutathione in Arabidopsis involves induction of genes encoding enzymes involved in cysteine synthesis in the chloroplast. *Molecular Plant*, *2*(2), 344-356.

Rahman, M. S., Di, L., Eugene, G. Y., Tang, J., Lin, L., Zhang, C, Zhiqi, Y., Gaigalas, J. (2018). Impact of Climate Change on Soil Salinity: A remote sensing based investigation in Coastal Bangladesh. In *2018 7th International Conference on Agro-geoinformatics (Agro-geoinformatics)* (pp. 1-5). IEEE.

Rausch, T., Wachter, A. (2005). Sulfur metabolism: a versatile platform for launching defence operations. *Trends in plant science*, *10*(10), 503-509.

Rauser, W. E. (1995). Phytochelatins and related peptides. Structure, biosynthesis, and function. *Plant physiology*, *109*(4), 1141.

Ravanel, S., Gakière, B., Job, D., Douce, R. (1998). The specific features of methionine biosynthesis and metabolism in plants. *Proceedings of the National Academy of Sciences*, *95*(13), 7805-7812.

Reich, M., Aghajanzadeh, T., Helm, J., Parmar, S., Hawkesford, M. J., De Kok, L. J. (2017). Chloride and sulfate salinity differently affect biomass, mineral nutrient composition and expression of sulfate transport and assimilation genes in *Brassica rapa*. *Plant and Soil*, *411*(1-2), 319-332.

Rennenberg, H. (1984). The fate of excess sulfur in higher plants. *Annual Review of Plant Physiology*, *35*(1), 121-153.

Report: EU agricultural outlook for the agricultural markets and income 2017-30

Robinson, N. J., Procter, C. M., Connolly, E. L., Guerinot, M. L. (1999). A ferric-chelate reductase for iron uptake from soils. *Nature*, *397*(6721), 694-697.

Rogers, E. E., Guerinot, M. L. (2002). FRD3, a member of the multidrug and toxin efflux family, controls iron deficiency responses in Arabidopsis. *The Plant Cell*, *14*(8), 1787-1799.

Romera, F. J., & Alcántara, E. (2004). Ethylene involvement in the regulation of Fe deficiency stress responses by Strategy I plants. *Functional Plant Biology*, 31(4), 315-328.

Romero, L. C., Domínguez-Solís, J. R., Gutiérrez-Alcalá, G., Gotor, C. (2001). Salt regulation of O-acetylserine (thiol) lyase in Arabidopsis thaliana and increased tolerance in yeast. *Plant Physiology and Biochemistry*, 39(7-8), 643-647.

Römheld V., Marschner H. (1986) Evidence for a specific uptake system for iron uptake system for iron phytosiderophores in root of grasses. Plant Physiology 80, 175-180.

Römheld, V. (1987). Different strategies for iron acquisition in higher plants. *Physiologia Plantarum*, *70*(2), 231-234.

Rouached, H., Wirtz, M., Alary, R., Hell, R., Arpat, A. B., Davidian, J. C., Fourcroy, P., Berthomieu, P. (2008). Differential regulation of the expression of two high-affinity sulfate transporters, *SULTR1. 1* and *SULTR1. 2*, in Arabidopsis. *Plant physiology*, *147*(2), 897-911.

Rout, G. R., Sahoo, S. (2015). Role of iron in plant growth and metabolism. *Reviews in Agricultural Science*, *3*, 1-24.

Rubio, F., Gassmann, W., Schroeder, J. I. (1995). Sodium-driven potassium uptake by the plant potassium transporter HKT1 and mutations conferring salt tolerance. *Science*, *270*(5242), 1660-1663.

Ruiz, J., Blumwald, E. (2002). Salinity-induced glutathione synthesis in Brassica napus. *Planta*, *214*(6), 965-969.

Saito, K. (2000). Regulation of sulfate transport and synthesis of sulfur-containing amino acids. *Current opinion in plant biology*, *3*(3), 188-195.

Salvagiotti, F., Castellarín, J. M., Miralles, D. J., Pedrol, H. M. (2009). Sulfur fertilization improves nitrogen use efficiency in wheat by increasing nitrogen uptake. *Field Crops Research*, *113*(2), 170-177.

Sancenón, V., Puig, S., Mira, H., Thiele, D. J., Peñarrubia, L. (2003). Identification of a copper transporter family in Arabidopsis thaliana. *Plant molecular biology*, 51(4), 577-587.

Santi S., Cesco S., Varanini Z., Pinton R. (2005) Two plasma membrane H^+- ATPase genes are differentially expressed in iron-deficient cucumber plants. Plant Physiology 43, 287-292.

Sasaki, J., & Nakashima, N. (2000). Methionine-independent initiation of translation in the capsid protein of an insect RNA virus. *Proceedings of the National Academy of Sciences*, *97*(4), 1512-1515.

Scherer, H. W. (2001). Sulphur in crop production. *European Journal of agronomy*, *14*(2), 81-111.

Scherer, H. W. (2009). Sulfur in soils. *Journal of Plant Nutrition and Soil Science*, *172*(3), 326-335.

Scherr, S. J. (1999). Soil degradation: a threat to developing-country food security by 2020? (Vol. 27). Intl Food Policy Res Inst.

Shahbaz, M., Tseng, M. H., Stuiver, C. E. E., Koralewska, A., Posthumus, F. S., Venema, J. H., Parmar, S., Schat, H., Hawkesford, M. J., De Kok, L. J. (2010). Copper exposure interferes with the regulation of the uptake, distribution and metabolism of sulfate in Chinese cabbage. *Journal of plant physiology*, *167*(6), 438-446.

Sharma, A., Kumar, V., Sidhu, G. P. S., Kumar, R., Kohli, S. K., Yadav, P., Kapoor, D., Bali, A.S., Shahzad, B., Khanna, K., Kumar, S., Thukral, A., Bhardwai, R. (2019). Abiotic Stress Management in Plants: Role of Ethylene. *Molecular Plant Abiotic Stress: Biology and Biotechnology*, 185-208.

Shen, Z., Zhang, F., Zhang, F. (1998). Toxicity of copper and zinc in seedlings of mung bean and inducing accumulation of polyamine. *Journal of plant nutrition*, *21*(6), 1153-1162.

Shibagaki, N., Rose, A., McDermott, J. P., Fujiwara, T., Hayashi, H., Yoneyama, T., & Davies, J. P. (2002). Selenate-resistant mutants of Arabidopsis thaliana identify Sultr1; 2, a sulfate transporter required for efficient transport of sulfate into roots. *The Plant Journal*, *29*(4), 475-486.

Singh, N. K., Bracker, C. A., Hasegawa, P. M., Handa, A. K., Buckel, S., Hermodson, M. A., Pfankoch, E., Regnier F. E., Ray A. Bressan, R. A. (1987). Characterization of osmotin: a thaumatin-like protein associated with osmotic adaptation in plant cells. *Plant physiology*, *85*(2), 529-536.

Smith, F. W., Ealing, P. M., Hawkesford, M. J., Clarkson, D. T. (1995). Plant members of a family of sulfate transporters reveal functional subtypes. *Proceedings of the National Academy of Sciences*, *92*(20), 9373-9377.

Soil Science Glossary Terms Committee, & Soil Science Society of America. (2008). *Glossary of soil science terms 2008*. ASA-CSSA-SSSA**.**

Stehling, O., Lill, R. (2013). The role of mitochondria in cellular iron–sulfur protein biogenesis: mechanisms, connected processes, and diseases. *Cold Spring Harbor perspectives in biology*, *5*(8), a011312.

Subbarao, G. V., Ito, O., Berry, W. L., Wheeler, R. M. (2003). Sodium—a functional plant nutrient. *Critical Reviews in Plant Sciences*, *22*(5), 391-416.

Subramanyam, K., Sailaja, K. V., Subramanyam, K., Rao, D. M., Lakshmidevi, K. (2011). Ectopic expression of an osmotin gene leads to enhanced salt tolerance in transgenic chilli pepper (Capsicum annum L.). *Plant Cell, Tissue and Organ Culture (PCTOC)*, *105*(2), 181-192.

Sugimoto, K., Tsuzuki, M., Sato, N. (2010). Regulation of synthesis and degradation of a sulfolipid under sulfur-starved conditions and its physiological significance in Chlamydomonas reinhardtii. *New phytologist*, *185*(3), 676-686.

Syeed, S., Anjum, N. A., Nazar, R., Iqbal, N., Masood, A., Khan, N. A. (2011). Salicylic acid-mediated changes in photosynthesis, nutrients content and antioxidant metabolism in two mustard (Brassica juncea L.) cultivars differing in salt tolerance. *Acta physiologiae plantarum*, *33*(3), 877-886.

Sytar, O., Kumar, A., Latowski, D., Kuczynska, P., Strzałka, K., Prasad, M. N. V. (2013). Heavy metal-induced oxidative damage, defense reactions, and detoxification mechanisms in plants. *Acta physiologiae plantarum*, *35*(4), 985-999.

Takahashi, H., Kopriva, S., Giordano, M., Saito, K., Hell, R. (2011). Sulfur assimilation in photosynthetic organisms: molecular functions and regulations of transporters and assimilatory enzymes. *Annual review of plant biology*, *62*, 157-184.

Takahashi, H., Watanabe-Takahashi, A., Smith, F. W., Blake-Kalff, M., Hawkesford, M. J., Saito, K. (2000). The roles of three functional sulphate transporters involved in uptake and translocation of sulphate in Arabidopsis thaliana. *The Plant Journal*, *23*(2), 171-182.

Tester, M., & Davenport, R. (2003). Na^+ tolerance and Na^+ transport in higher plants. *Annals of botany*, *91*(5), 503-527.

Tilman D, Cassman KG, Matson PA, Naylor R, Polasky S: Agricultural sustainability and intensive production practices (2002) Nature, 418: 671--677.

Tilman, D., Cassman, K. G., Matson, P. A., Naylor, R., Polasky, S. (2002). Agricultural sustainability and intensive production practices. *Nature*, *418*(6898), 671-677.

Valentinuzzi F, Pii Y, Vigani G, Lehmann M, Cesco S, Mimmo T. 2015. Phosphorus and iron deficiencies induce a metabolic reprogramming and affect the exudation traits of the woody plant *Fragaria* × *ananassa*. *Journal of Experimental Botany* 66: 6483–6495.

Van-Zwieten, L., Merrington, G., Van-Zwieten, M. (2004). Review of impacts on soil biota caused by copper residues from fungicide application. *SuperSoil*, *2004*, 3rd.

Vigani G, Pii Y, Celletti S, Maver M, Mimmo T, Cesco S, Astolfi S (2018) Mitochondria dysfunctions under Fe and S deficiency: Is citric acid involved in the regulation of adaptive responses? *Plant Physiol Biochem* 126:86-96.

Wang, H. Y., Klatte, M., Jakoby, M., Bäumlein, H., Weisshaar, B., Bauer, P. (2007). Iron deficiency-mediated stress regulation of four subgroup Ib BHLH genes in Arabidopsis thaliana. *Planta*, *226*(4), 897-908.

Wang, K. L. C., Li, H., Ecker, J. R. (2002). Ethylene biosynthesis and signaling networks. *The plant cell*, *14*(suppl 1), S131-S151.

Wawrzyńska, A., Sirko, A. (2014). To control and to be controlled: understanding the Arabidopsis SLIM1 function in sulfur deficiency through comprehensive investigation of the EIL protein family. *Frontiers in plant science*, *5*, 575.

White, P. J., Broadley, M. R. (2001). Chloride in soils and its uptake and movement within the plant: a review. *Annals of Botany*, *88*(6), 967-988.

Wintz, H., Fox, T., Wu, Y. Y., Feng, V., Chen, W., Chang, H. S., Zhu, T., Vulpe, C. (2003). Expression profiles of Arabidopsis thaliana in mineral deficiencies reveal novel transporters involved in metal homeostasis. *Journal of Biological Chemistry*, *278*(48), 47644-47653.

Wirtz, M., Droux, M., Hell, R. (2004). O-acetylserine (thiol) lyase: an enigmatic enzyme of plant cysteine biosynthesis revisited in Arabidopsis thaliana. *Journal of Experimental Botany*, *55*(404), 1785-1798.

Yang, J., Duan, G., Li, C., Liu, L., Han, G., Zhang, Y., Wang, C. (2019). The Crosstalks Between Jasmonic Acid and Other Plant Hormone Signaling Highlight the Involvement of Jasmonic Acid as a Core Component in Plant Response to Biotic and Abiotic Stresses. *Frontiers in plant science*, *10*.

Yoshimoto, N., Inoue, E., Saito, K., Yamaya, T., Takahashi, H. (2003). Phloem-localizing sulfate transporter, Sultr1; 3, mediates re-distribution of sulfur from source to sink organs in Arabidopsis. *Plant Physiology*, *131*(4), 1511-1517.

Yruela, I. (2005). Copper in plants. *Brazilian Journal of Plant Physiology*, *17*(1), 145-156.

Zamboni, A., Celletti, S., Zenoni, S., Astolfi, S., Varanini, Z. (2017). Root physiological and transcriptional response to single and combined S and Fe deficiency in durum wheat. *Environmental and Experimental Botany*, *143*, 172-184.

Zhang, F., Shen, J., Zhang, J., Zuo, Y., Li, L., Chen, X. (2010). Chapter one-rhizosphere processes and management for improving nutrient use efficiency and crop productivity: implications for China. *Advances in agronomy*, 107, 1-32

Zhang, M., He, Z., Calvert, D. V., Stoffella, P. J., Yang, X. (2003). Surface runoff losses of copper and zinc in sandy soils. *Journal of environmental quality*, *32*(3), 909-915.

Zhao FJ, Hawkesford MJ, McGrath SP (1999) Sulphur assimilation and effects on yield and quality of wheat. J Cereal Sci 30:1–17

Zhao, F. J., Withers, P. J. A., Evans, E. J., Monaghan, J., Salmon, S. E., Shewry, P. R., McGrath, S. P. (1997). Sulphur nutrition: an important factor for the quality of wheat and rapeseed. *Soil Science and Plant Nutrition*, *43*(sup1), 1137-1142

Zhu, J. K. (2001). Plant salt tolerance. *Trends in plant science*, *6*(2), 66-71.

Zuchi S, Cesco S, Astolfi S (2012) High S supply improves Fe accumulation in durum wheat plants grown under Fe limitation. Env Exp Bot 77: 25– 32

Zuchi S, Watanabe M, Hubberten HM, Bromke M, Osorio S, Fernie AR, Celletti S, Paolacci AR, Catarcione G, Ciaffi M, Hoefgen R, Astolfi S (2015) The interplay between sulfur and iron nutrition in tomato Plant Physiol 169:2624–2639.

Zuchi, S., Cesco, S., Varanini, Z., Pinton, R., Astolfi, S., 2009. Sulphur deprivation limits Fe deficiency responses in tomato plants. Planta 230, 85–94.

RINGRAZIAMENTI

Ringrazio di cuore la Prof.ssa Stefania Astolfi per il sostegno, la fiducia e gli insegnamenti ricevuti durante tutti questi anni. Sempre presente e disponibile sotto ogni punto di vista. Un punto di riferimento ineguagliabile. La ringrazio inoltre per avermi dato la possibilità di fare delle esperienze importanti durante questi anni di dottorato, esperienze che mi hanno permesso di crescere, delle quali porterò sempre un bellissimo ricordo.

Ringrazio vivamente la Prof.ssa Roberta Bernini attuale coordinatrice del corso di dottorato e la Prof.ssa Stefania Masci, coordinatrice per i primi due anni.

Ringrazio il Prof. Rüdiger Hell ed il Dott. Markus Wirtz (Centre for Organismal Studies, Heidelberg University) per avermi dato la possibilità di lavorare cinque mesi nel loro laboratorio per eseguire i saggi immunologici per la determinazione dell'attività della proteina chinasi TOR. Un ringraziamento speciale va alla Dott.ssa Rasha Aref con la quale ho condiviso tutto il periodo di lavoro in Germania. Il suo supporto tecnico e scientifico è stato fondamentale. Ringrazio di cuore anche la Dott.ssa Sara Haghani, con la quale ho condiviso gli ultimi mesi di lavoro in Germania ed una splendida amicizia che continua ancora oggi.

Ringrazio il Prof. Luigi Lucini (Università Cattolica del Sacro Cuore, sede di Piacenza) per avermi dato la possibilità di realizzare nel suo laboratorio le analisi metabolomiche per la caratterizzazione degli essudati radicali, ed il Prof. Stefano Cesco (Libera Università di Bolzano) per avermi dato la possibilità di realizzare nel suo laboratorio le analisi del profilo trascrizionale di geni chiave coinvolti nei meccanismi di risposta alla carenza di zolfo e di ferro.

Ringrazio tutti i tesisti ed i tirocinanti, ognuno di loro è stato parte fondamentale di questo percorso.

Ringrazio Luca, Alessandro, Chiara, Erika, Monica e Giulia compagni indiscussi di questi anni. Grazie per le risate, per il sostegno e per l'amicizia dimostratami. Senza di voi niente sarebbe stato uguale, siete stati la spensieratezza anche nei momenti più difficili!

Ringrazio le amiche di sempre, con loro ho condiviso tutti i momenti importanti della mia vita. Erika e Valeria, che nonostante la distanza e le difficoltà nel vederci, ci sono sempre; ed Elisa, che mi supporta, ma soprattutto sopporta tutti i giorni! Vi voglio bene!

Ringrazio i miei genitori, che hanno sempre fatto di tutto per assicurarmi il meglio. Grazie per ogni cosa, vi voglio bene!

Infine ringrazio il mio fidanzato, Marco. Grazie perché in te ho sempre trovato una mente brillante con cui confrontarmi, e perché sei sempre stato al mio fianco, sostenendo ogni mia scelta. Ti amo!